NEPRF TECHNICAL REPORT TR 83-03



NAVY TACTICAL APPLICATIONS GUIDE

# VOLUME 5
## PART 1
# INDIAN OCEAN
## Red Sea/Persian Gulf

# WEATHER ANALYSIS and FORECAST APPLICATIONS

## METEOROLOGICAL SATELLITE SYSTEMS







TACTICAL APPLICATIONS DEPARTMENT
NAVAL ENVIRONMENTAL PREDICTION RESEARCH FACILITY
MONTEREY, CALIFORNIA 93940

UNCLASSIFIED

SECURITY CLASSIFICATION OF THIS PAGE (When Data Entered)

# REPORT DOCUMENTATION PAGE

READ INSTRUCTIONS BEFORE COMPLETING FORM

| | | |
|---|---|---|
| 1. REPORT NUMBER NAVENVPREDRSCHFAC Technical Report 83-03 | 2. GOVT ACCESSION NO. A134412 | 3. RECIPIENT'S CATALOG NUMBER |
| 4. TITLE (and Subtitle) Navy Tactical Applications Guide. Volume 5. Part 1 Indian Ocean (Red Sea/Persian Gulf) Weather Analysis and Forecast Applications | | 5. TYPE OF REPORT & PERIOD COVERED |
| | | 6. PERFORMING ORG. REPORT NUMBER |
| 7. AUTHOR(s) Robert W. Fett, Walter A. Bohan, Ronald E. Englebretson | | 8. CONTRACT OR GRANT NUMBER(s) The Walter A. Bohan Company N00228-82-C-6222 |
| 9. PERFORMING ORGANIZATION NAME AND ADDRESS The Walter A. Bohan Company 2026 Oakton Street Park Ridge, IL 60068 | | 10. PROGRAM ELEMENT, PROJECT, TASK AREA & WORK UNIT NUMBERS 62759N. WF 59-553. NEPRF WU: 6.3-18 |
| 11. CONTROLLING OFFICE NAME AND ADDRESS Naval Air Systems Command Department of the Navy Washington, D.C. 20361 | | 12. REPORT DATE June 1983 |
| | | 13. NUMBER OF PAGES 91 |
| 14 MONITORING AGENCY NAME & ADDRESS(if different from Controlling Office) Naval Environmental Prediction Research Facility Monterey, California 93940 | | 15. SECURITY CLASS. (of this report) Unclassified |
| | | 15a. DECLASSIFICATION/DOWNGRADING SCHEDULE |

16. DISTRIBUTION STATEMENT (of this Report)

Approved for Public Release
Distribution Unlimited

17. DISTRIBUTION STATEMENT (of the abstract entered in Block 20, if different from Report)

DTIC

18. SUPPLEMENTARY NOTES

OCT 3 1 1983

19. KEY WORDS (Continue on reverse side if necessary and identify by block number)

Meteorological Satellite Systems
Analysis and Forecast Applications
Indian Ocean
Northeast Monsoon
Southwest Monsoon
Coastal Zone Phenomena
Ocean-Atmosphere Interaction

20 ABSTRACT (Continue on reverse side if necessary and identify by block number)

Case studies describing regional environmental analysis and forecast applications based on satellite data and conventional meteorological observations for the Indian Ocean area are presented Topics include Northeast Monsoon, Southwest Monsoon, coastal zone phenomena, and ocean-atmosphere interaction The studies provide insights into identifiable patterns of weather development that occur frequently, so that once the basic pattern is recognized at an early stage this information can be used for improved weather analysis and forecasting

NAVY TACTICAL APPLICATIONS GUIDE

# VOLUME 5
PART 1

# INDIAN OCEAN
## Red Sea/Persian Gulf
## WEATHER ANALYSIS AND FORECAST APPLICATIONS

METEOROLOGICAL
SATELLITE SYSTEMS


*Prepared under the direction of*
Robert W. Fett
Tactical Applications Department
Naval Environmental Prediction Research Facility

*Scientific Coordinator*
Walter A. Bohan
The Walter A. Bohan Company



1983





THE WALTER A. BOHAN COMPANY
2026 OAKTON STREET PARK RIDGE ILLINOIS 60068
APPLIED RESEARCH IN SATELLITE METEOROLOGY AND OCEANOGRAPHY

# *List of Contributors*


Robert W. Fett, Head
*Tactical Applications Department*
*Naval Environmental Prediction Research Facility*
*Monterey, California*

Walter A. Bohan, Certified Consulting Meteorologist
*The Walter A. Bohan Company*
*Park Ridge, Illinois*

Ronald J. Englebretson, Research Scientist
*Science Applications, Inc.*
*Monterey, California*

Sherree L. Tipton, Meteorologist
*The Walter A. Bohan Company*
*Park Ridge, Illinois*

## *Foreword*

Volume 5 of the Navy Tactical Applications Guide (NTAG) series is devoted to regional weather analysis and forecast applications in the northern Indian Ocean. Part 1 of Volume 5 is dedicated to operationally important weather phenomena affecting the region surrounding and including the Red Sea and Persian Gulf. Part 2 extends the area of interest to the Arabian Sea and Bay of Bengal. The case study technique of relating weather satellite imagery to concurrent conventional weather data and analyses from the surface to the upper troposphere, along with available numerical guidance products, is continued, focusing on the unique weather characteristics of the Indian Ocean region.

Whereas the topics of blocking and cyclogenesis were emphasized in previous volumes, it is the powerful monsoon influences of winter and summer that become the dominant interest in the Indian Ocean. Duststorm generation is a subject of major interest because of its effect on operations thoughout the northern portion of the Indian Ocean region. The ability to detect duststorms over land areas at the time of earliest inception in satellite data, and to forecast the areas most likely to be influenced by the dust, is given special attention.

The Indian Ocean volumes are intended as an evolving series which will be supplemented with additional material presently under development. The initial material is being distributed to the fleet to expedite access of completed work for operational use.

As with case studies developed for previous volumes, many of the principles derived for Indian Ocean weather analysis and forecasting are general in nature and equally applicable to similar weather events in other areas of the world.

It is anticipated that these guides will be useful supplements to other material available for the Indian Ocean region in their emphasis on new aspects of weather satellite interpretation for improved weather analysis and forecasts.

Kenneth L. Van Sickle

KENNETH L. VAN SICKLE
Captain, U.S. Navy
Commanding Officer, NEPRF

# *Acknowledgments*

This volume could not have been published without the devoted effort of the NEPRF Meteorological Laboratory personnel who obtained required documentation, and who spent many hours on the computer terminal entering information for the analyses utilized in the studies. Directed by AGCM D.M. Ales, the following personnel: AG2 J.V. Klimas, AG2 R.J. Bonaly, AG2 D.B. Elliott, AG3 J.L. Benvick, AG3 B.H. Kenthack, and AGAN J.M. Roy, did an outstanding job in supporting the work effort required for this volume.

PH1 A. Matthews and PH2 W.A. Anderson processed many of the original photos utilized. The correlative meteorological data were provided by the Fleet Numerical Oceanography Center, Monterey, CA, and the U.S. Naval Oceanographic Detachment, Asheville, N.C.

Additional satellite imagery was supplied by the National Environmental Satellite Data and Information Service (NESDIS) of the National Oceanic and Atmospheric Administration (NOAA).

The assistance of the staff of the Walter A. Bohan Company is again acknowledged; in particular, Lido A. Andreoni for design of the format of the publication and layout of the case studies. Gregory E. Terhune assisted in the preparation of case study graphics and preparation in the editing and formating of the text. The high quality of the reproduction of the satellite imagery used in the case studies and the excellent printing of the publication are due to the combined efforts of Peter M. Samorez and Michael E. Brock.

*This work was funded by the Naval Environmental Prediction Research Facility, Monterey, California, under Program Element 63207N, Project 2W0527, Remote Ocean Measuring System*

CONTENTS

# Contents

*List of Contributors* .................... iii
*Foreword* .................... v
*Introduction* .................... ix

## Section 1

*Red Sea/Persian Gulf*

1A Introduction (Under Development)

*Case Studies*

1B Autumn Transition (Under Development)
1C Winter .................... 1C-1
1D Spring Transition (Under Development)
1E Summer .................... 1E-1

# INTRODUCTION

# Introduction

## Seasonal Circulation Patterns of the Indian Ocean

The northern Indian Ocean is located within the world's most notorious monsoon regime. The term monsoon is a name for seasonal winds and is derived from the Arabic word *mausim*, meaning season. In general, the term describes a regime where there are highly persistent winds from nearly opposite directions in summer and winter and which are not the result of shifting migratory storm tracks. The basic cause of such a wind pattern is the differential heating and cooling of adjacent large land and sea areas. The land masses are warmer than the ocean areas in summer and cooler in winter, resulting in relatively lower pressure over the land in summer and higher in the winter. These pressure differences cause winds to blow primarily onshore (summer) and offshore (winter). The size, shape and orientation of the adjoining land/ocean areas play important roles in determining the specific monsoon characteristics of a given region.

The low-level circulation pattern for the Indian Ocean consists of southwest flow during the summer period and northeast flow during the winter period. When combined with the two intervening transitional periods it is convenient to use the mid-latitude convention of summer, autumn, winter, and spring season titles. It must by realized, however, that these terms applied to the tropics do not have the same connotations as when applied to the harsher extremes of mid latitudes. The approximate months of the four seasons are:

Autumn Transition—October through November
Winter Monsoon—December through March
Spring Transition—April through May
Summer Monsoon—June through September

SECTION 1

# Section 1

## Red Sea/Persian Gulf


### Introduction

*1A* (Under Development)

### Case Studies

*1B Autumn Transition* (Under Development)

*1C Winter*

*1 Red Sea Convergence Zone Cloud Band* .................. 1C-1
Passage of an Upper-level Disturbance
to the North of the Convergence
Zone Cloud Band
Red Sea, January 1980

*2 Red Sea Convergence Zone Cloud Band Displacement from Normal Winter Location* ............. 1C-9
Pronounced Northward Displacement of
the CZCB by a Low-pressure Development
in the Equatorial Trough (Sudan Low)
Red Sea, January 1980

*3 Subtropical Jet Streams and Surface Anticyclones* ........ 1C-25
Change in Intensity of a Surface Anticyclone
in Response to the Passage of a Jet Streak
Arabian Peninsula, December 1979

*4 Winter Storms over the Arabian Peninsula* ............. 1C-33
Squall line Development in Response to
Dynamics of a Merged Polar Jet and
Subtropical Jet
Arabian Peninsula, December 1979

*1D Spring Transition* (Under Development)

*1E Summer*

*1 Development of Convection in Southwest Monsoon Flow over the Southern Arabian Peninsula* .... 1E-1
Convective Buildups in the Southwest Monsoon Flow
Southern Arabian Peninsula, June 1979

*2 Red Sea Region Duststorms* ............................. 1E-5
Widespread Haboob Generated by Convective
Activity Associated with a Tropical Disturbance
Sudan/Red Sea Tokar Gap, June 1979

*3 Persian Gulf Duststorms* ................................ 1E-19
Large-scale Duststorms During the Summer Shamal
Persian Gulf, June 1979

This section is
under development
and will be forwarded
for inclusion in this volume.

This section is
under development
and will be forwarded
for inclusion in this volume.

*Passage of an Upper-level Disturbance to the North of the Convergence Zone Cloud Band*
*Red Sea*
*January 1980*

***Key Points***

1. *A persistent convergence zone cloud band (CZCB) is located over the south-central Red Sea during the winter months.*
2. *The location of the CZCB is not disrupted by the passage of a short-wave upper-level disturbance to the north.*
3. *Baroclinic-zone cloud patterns in satellite imagery provide observational data on the extent to which disturbances penetrate the Red Sea region.*

17 January

The early-morning DMSP picture (1C-2a) shows a typical convergence zone cloud band (CZCB) over the south-central Red Sea, extending from Port Sudan to Asmara. Fair weather conditions prevail, and the large-scale surface circulation features attending this convergence zone phenomenon are observed on the surface analysis (1C-3a and 3b), which shows the Sahara high, Sudan low, and Saudi Arabia high near their normal winter locations. (The Saudi Arabia high is an extension of the much larger Siberia high to the northeast.) Since the standard Northern Hemisphere NMC surface analysis provides only limited coverage of the Middle East, the NMC tropical surface streamline analysis (1C-3b) is included for more complete coverage of the area. Wind reports show light northerly winds directed toward the CZCB over the north-central basin, and light southerly winds over the southern basin. The streamline analysis over the Arabian Sea indicates a well-developed northeast monsoon, and the turning of a portion of this flow into the Red Sea, between the Sudan low and the Saudi Arabia high.

The surface analysis (1C-3b) shows that the CZCB consists primarily of stratocumulus, as reported at the coastal stations O1 and O2. In the satellite picture, broken stratocumulus is observed along the eastern shore, which becomes overcast with cumulus predominating along the western shore. The stratocumulus cloud deck extends inland south of Tokar, through a prominent break in the mountain barrier along the west coast called the Tokar gap. Inland, to the east of the CZCB, early morning convective clouds have developed along the higher elevations of the north-south Al Hijaz mountain range.

Convective cloud lines, funneling through the Bab al Mandab (1C-2a) into the Red Sea, provide an excellent pictorial display of the turning of the surface easterlies over the Gulf of Aden to southerly flow over the Red Sea. The surface report at Aden (1C-3b), on the southwest corner of Yemen, shows cumulus and stratocumulus with bases at different levels. The bright cloudy area (1C-2a) to the northwest of Aden is a dissipating stratocumulus deck banked up against the coastal mountains. To the west and east of Aden, fair weather cumulus is observed along the coastal plains bordering on the gulf, where moisture is advected inland by onshore flow. At Ash Shihr, local winds are light and offshore, and reflect the remnants of the nighttime land breeze circulation.

Over the warm waters of the Persian Gulf (1C-2a), cloud lines are also observed where cold polar air (5° C) reported at O3 and O4 is channeled southward between the Saudi Arabia high and the low over central Iran (1C-3a and 3b). The presence of anomalous gray shades surrounding the convective cloudiness over the Persian Gulf indicates high aerosol/moisture content of the low-level air and a corresponding decrease in surface visibility in these areas over the water.

In contrast to the fair weather conditions prevailing over the central Red Sea region (1C-2a), an extensive low overcast area, indicating poor weather conditions, is observed to the north of Sinai and along the eastern Mediterranean. The surface weather report (1C-3a) at Alexandria O5 shows overcast skies with openings, showers, and a temperature of 10° C. Intermittent light drizzle within the past hour and a temperature of 10° C is reported at Haifa O6. At Latakia O7, skies are overcast with low clouds, intermittent light rain is falling, and the temperature is 6° C. Nicosia O8, on the island of Cyprus, is also reporting overcast with openings, intermittent light rain, and a temperature of 12° C. These poor weather conditions are occurring in modified polar air which has had a westerly trajectory over the warm waters of the Mediterranean. The surface analysis shows that the westerly flow over the eastern Mediterranean is produced by the west-east oriented isobaric pattern between the polar low over Spain and the Sahara high over Africa.

The 500-mb analysis (1C-4b) shows that the cloudiness over the eastern Mediterranean (1C-5a) is associated with a short-wave trough passing to the north of the Red Sea. This trough has a small amplitude because it is moving over a ridge of high pressure to the south. The presence of the striated cloud band northwest of Alexandria, however, indicates that the baroclinic zone associated with this trough is strong and extends to lower levels.

At 200 mb (1C-4a), a broad band of subtropical westerlies is observed over northern Africa and Saudi Arabia. A double wind maxima structure is shown by a second wind maximum passing north of the Red Sea, over Saudi Arabia and the Persian Gulf. The long cirrus filaments (1C-5a) passing south of the Sinai and across Saudi Arabia reflect this double wind maxima structure.

*continued on page 1C-6*

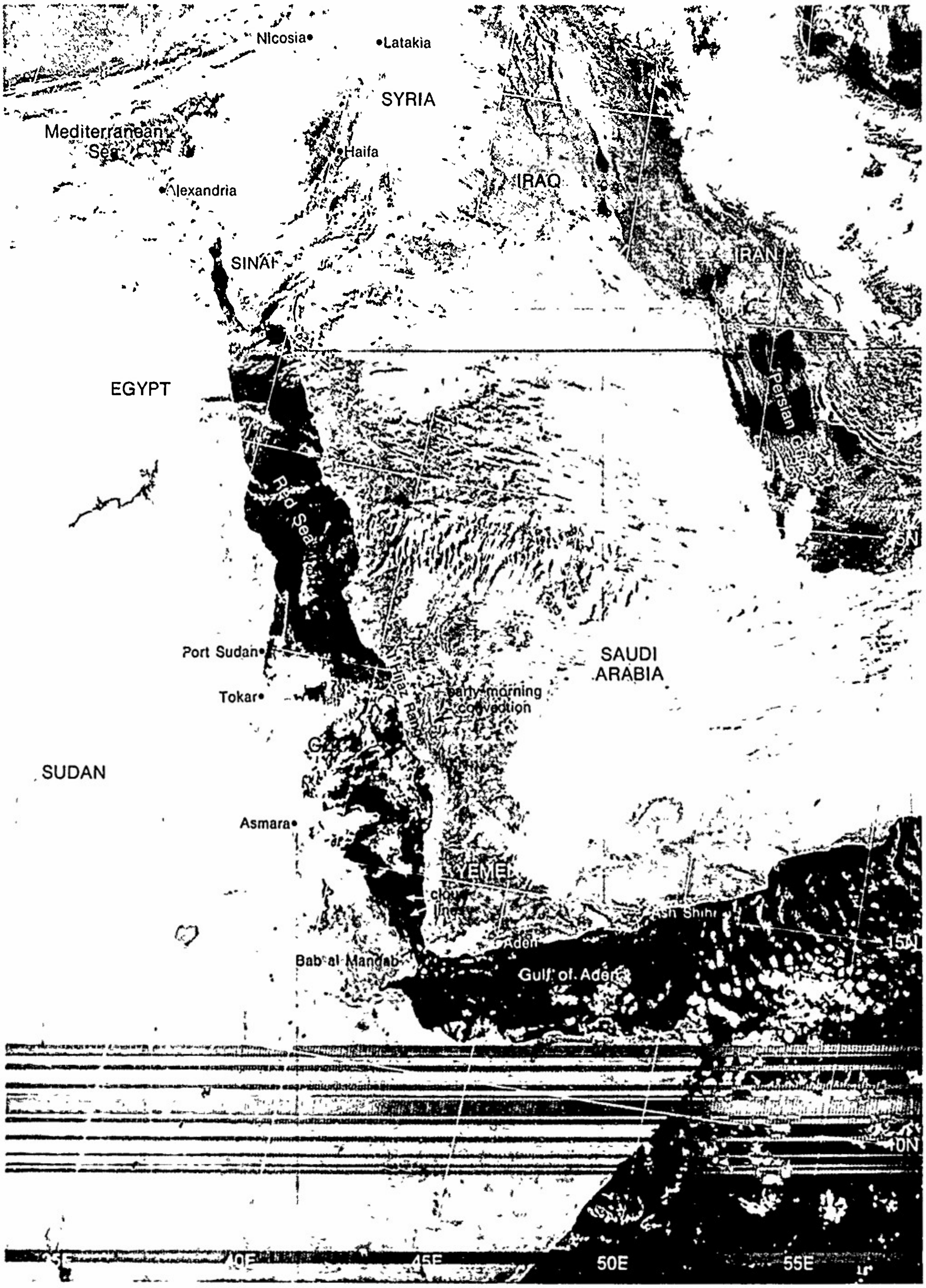


1C-2a. F-2. DMSP LF Log Enhancement. 0524 GMT 17 January 1980.

# Case 1 Red Sea/Persian Gulf—Winter

## Red Sea Convergence Zone Cloud Band

The Red Sea convergence zone cloud band (CZCB) is a persistent winter climatological feature over the Red Sea that is produced by large-scale circulation patterns. The cloud band forms along the convergence zone between northerly winds on the eastern periphery of the North African anticyclone over the Sahara, and southerly winds from the northeast monsoon over the Arabian Sea, which are turned northward between the surface anticyclone over Saudi Arabia and the equatorial trough over the Sudan (1C-1a).

The CZCB forms in the southern Red Sea in September and advances to about 18°-20°N in October where it generally remains until about February, when the convergence zone begins to retreat southward (NEPRF, 1980). During undisturbed weather conditions, day-to-day movements of the CZCB are small. However, when a synoptic-scale weather disturbance penetrates the Red Sea area, the CZCB may be temporarily displaced or completely disrupted until the weather event has passed and undisturbed weather conditions again prevail. The following case study is an example of the persistence of the CZCB during the passage of a short-wave disturbance across the northern region of the Red Sea.


**Reference**

NEPRF, 1980 Weather in the Indian Ocean to Latitude 30°S and Longitude 95°E including the Red Sea and Persian Gulf Vol 2, Part 1. NAVENVPREDRSCHFAC Technical Bulletin 80-02. Naval Environmental Prediction Research Facility, Monterey, Calif., 83 pp


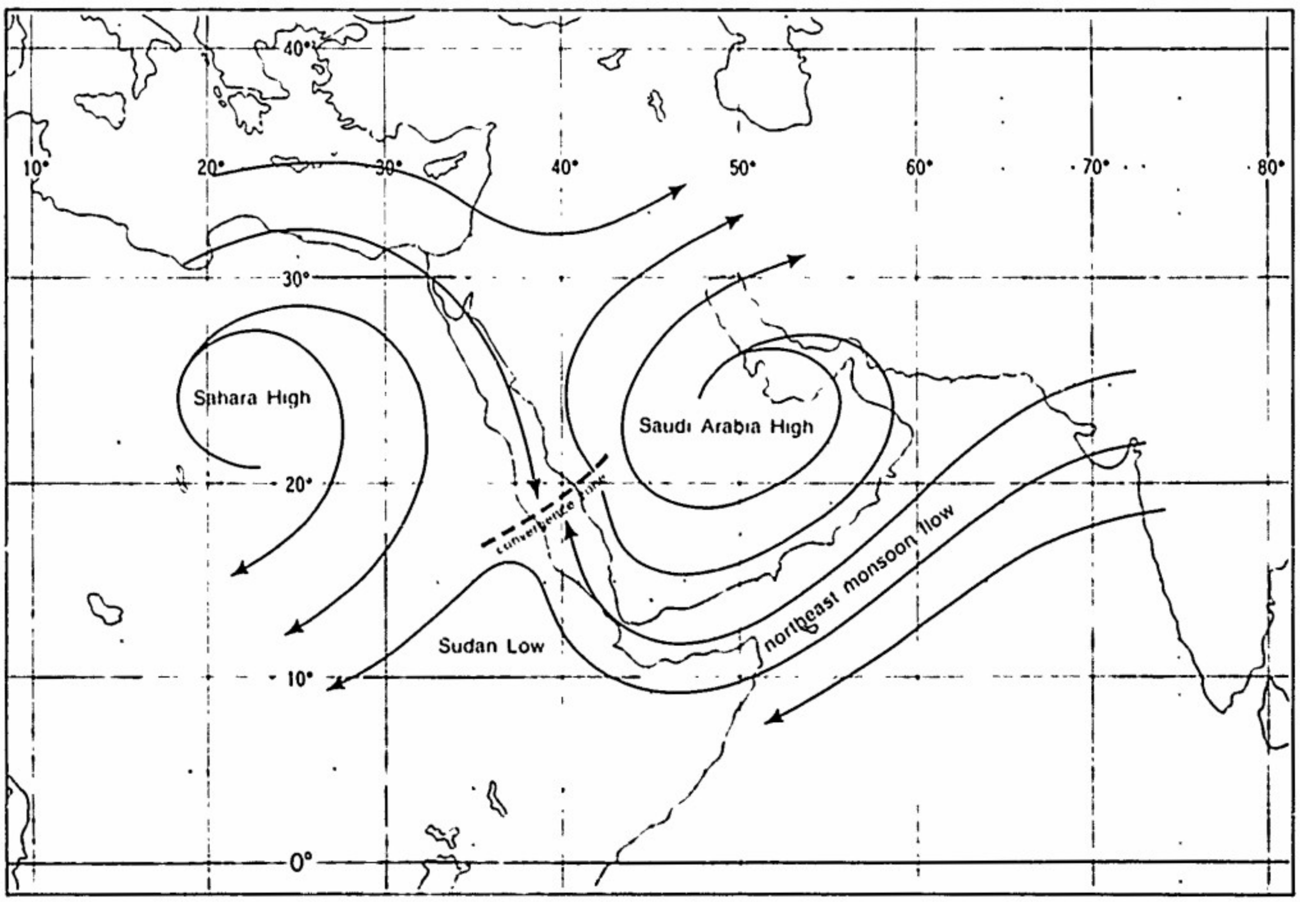


1C-1a. Typical Surface Streamline Map of January

surface

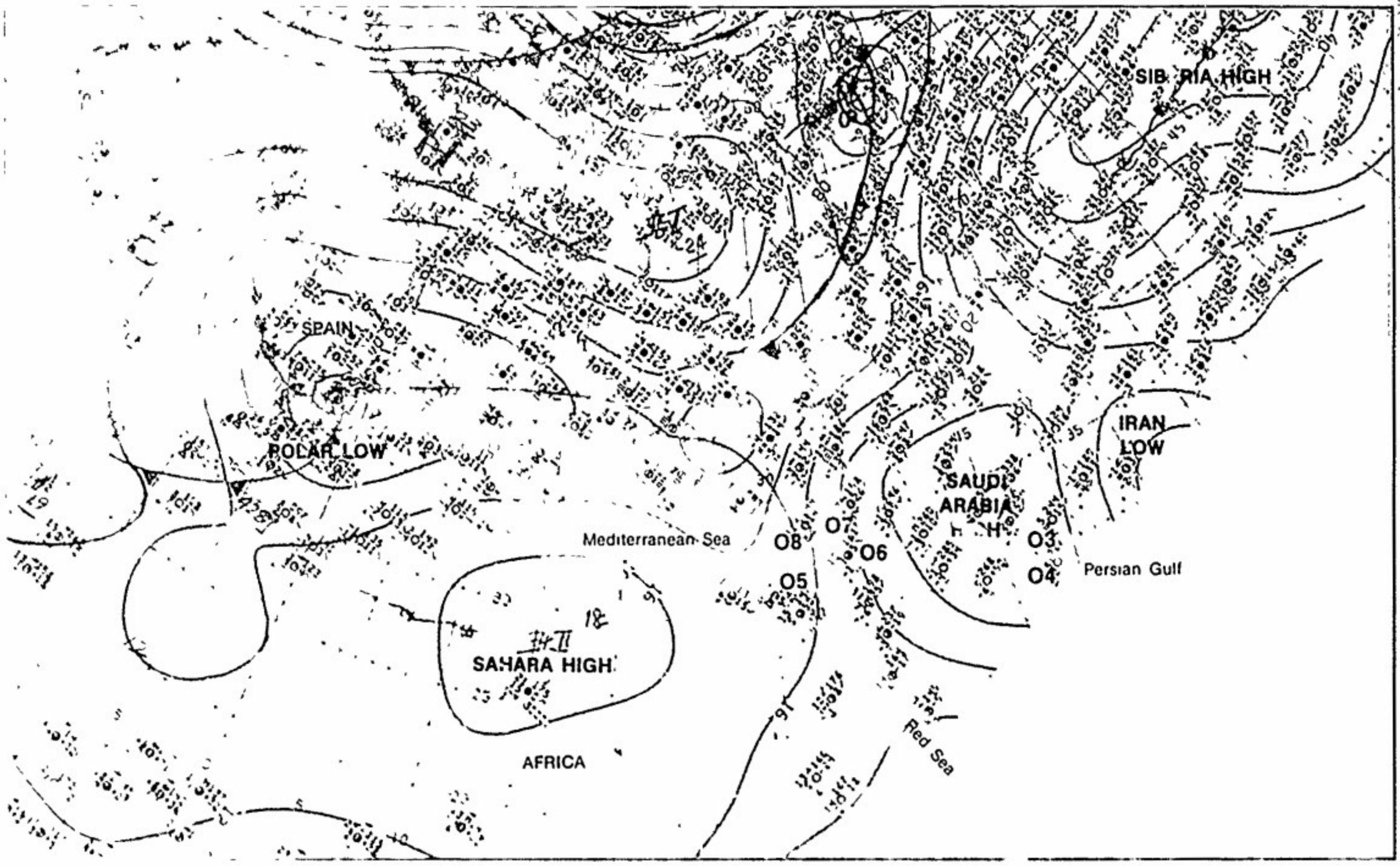


1C-3a. NMC Surface Analysis. 0600 GMT 17 January 1980.

surface

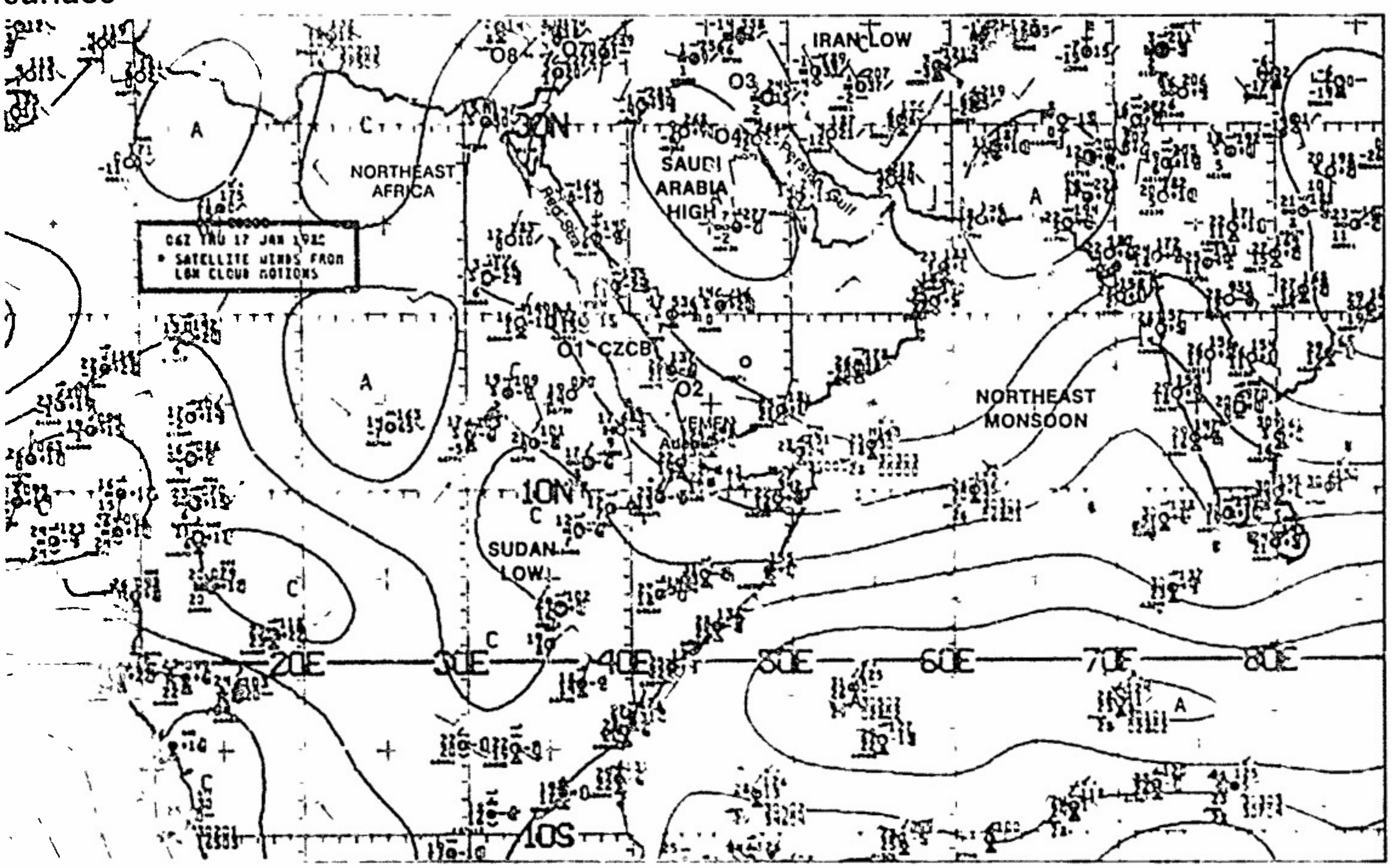


1C-3b NMC Tropical Surface Streamline Analysis 0600 GMT 17 January 1980

## 200 mb

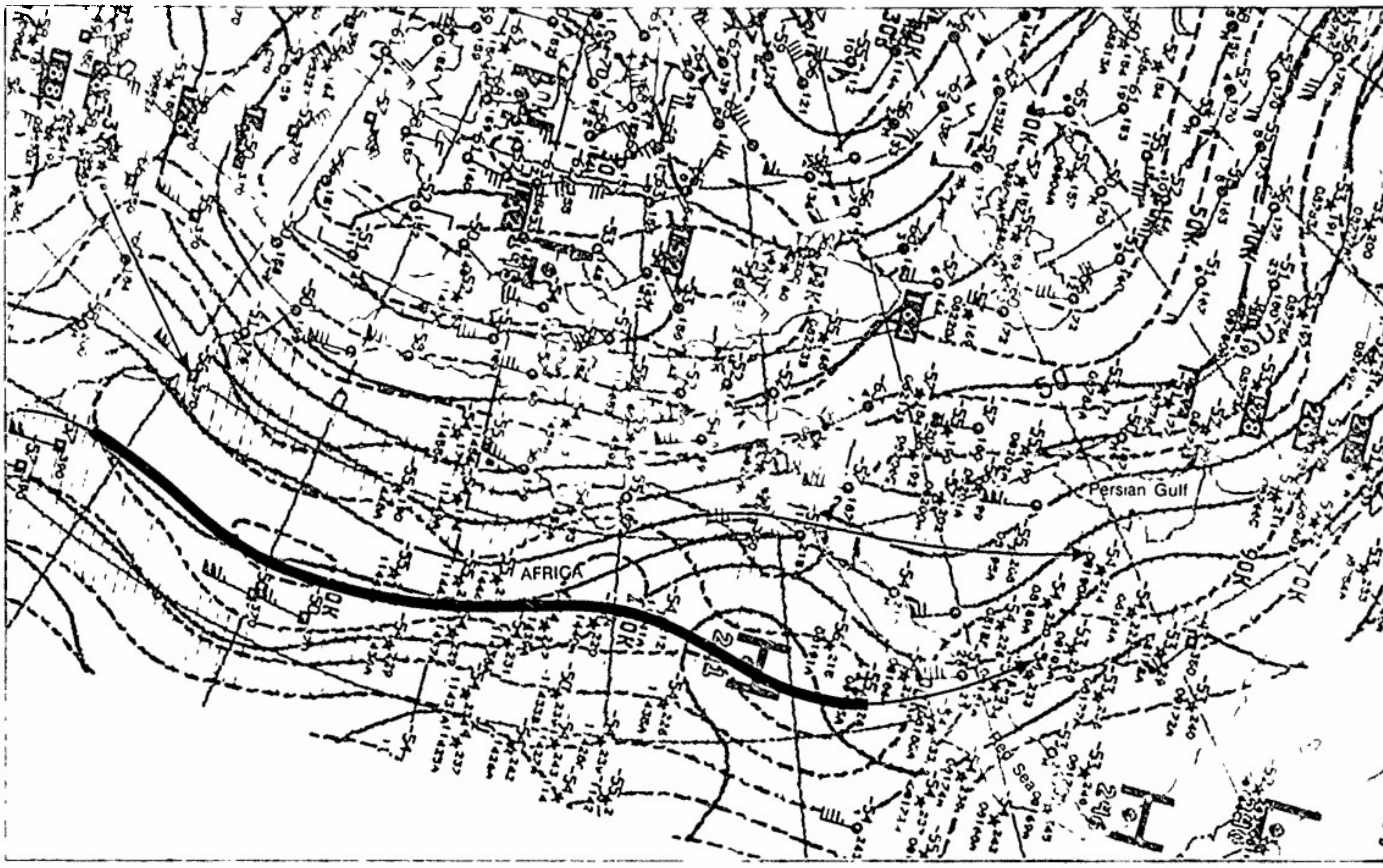


1C-4a NMC 200-mb Analysis, 1200 GMT 17 January 1980.

## 500 mb

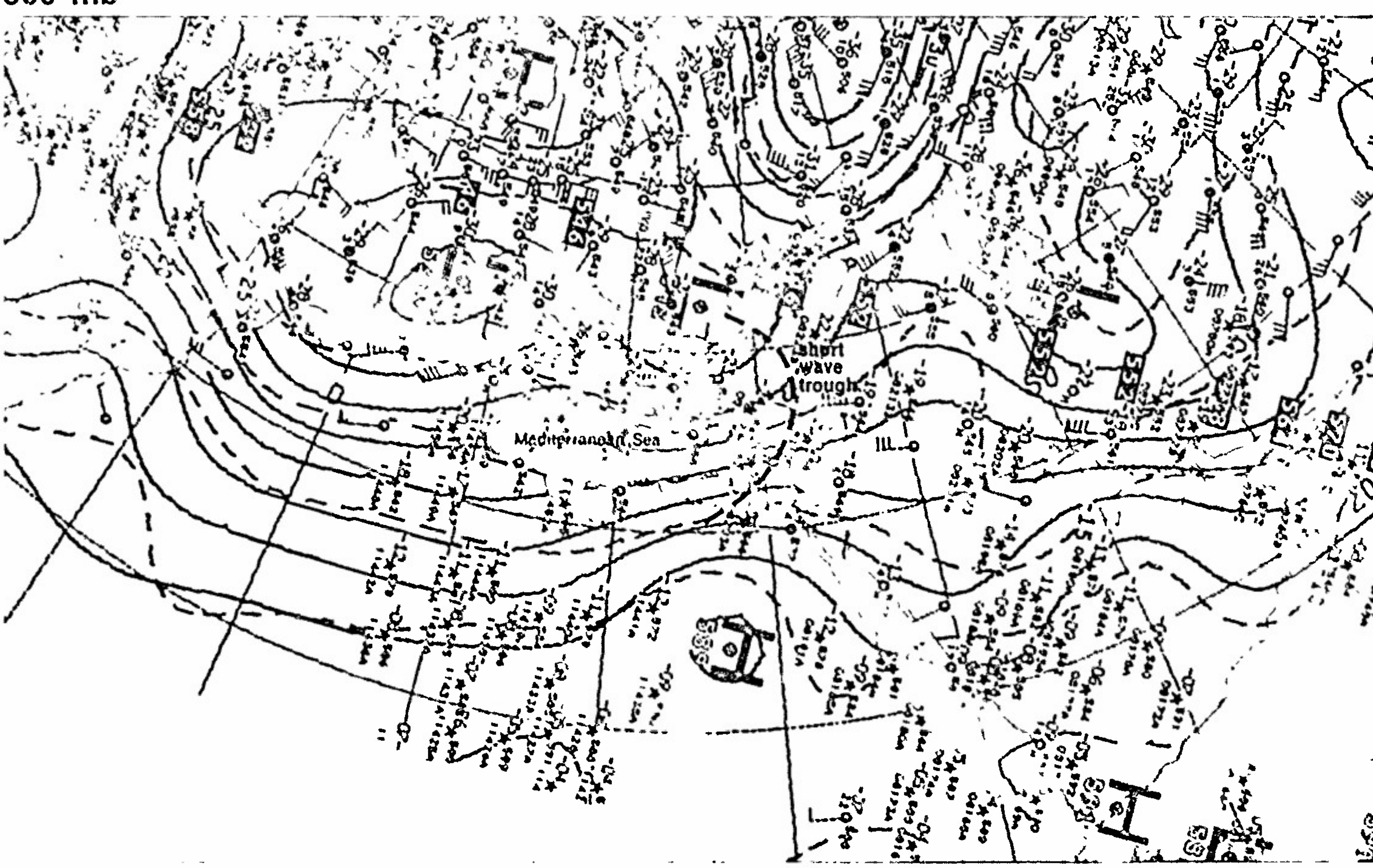


1C-4b NMC 500-mb Analysis 1200 GMT 17 January 1980

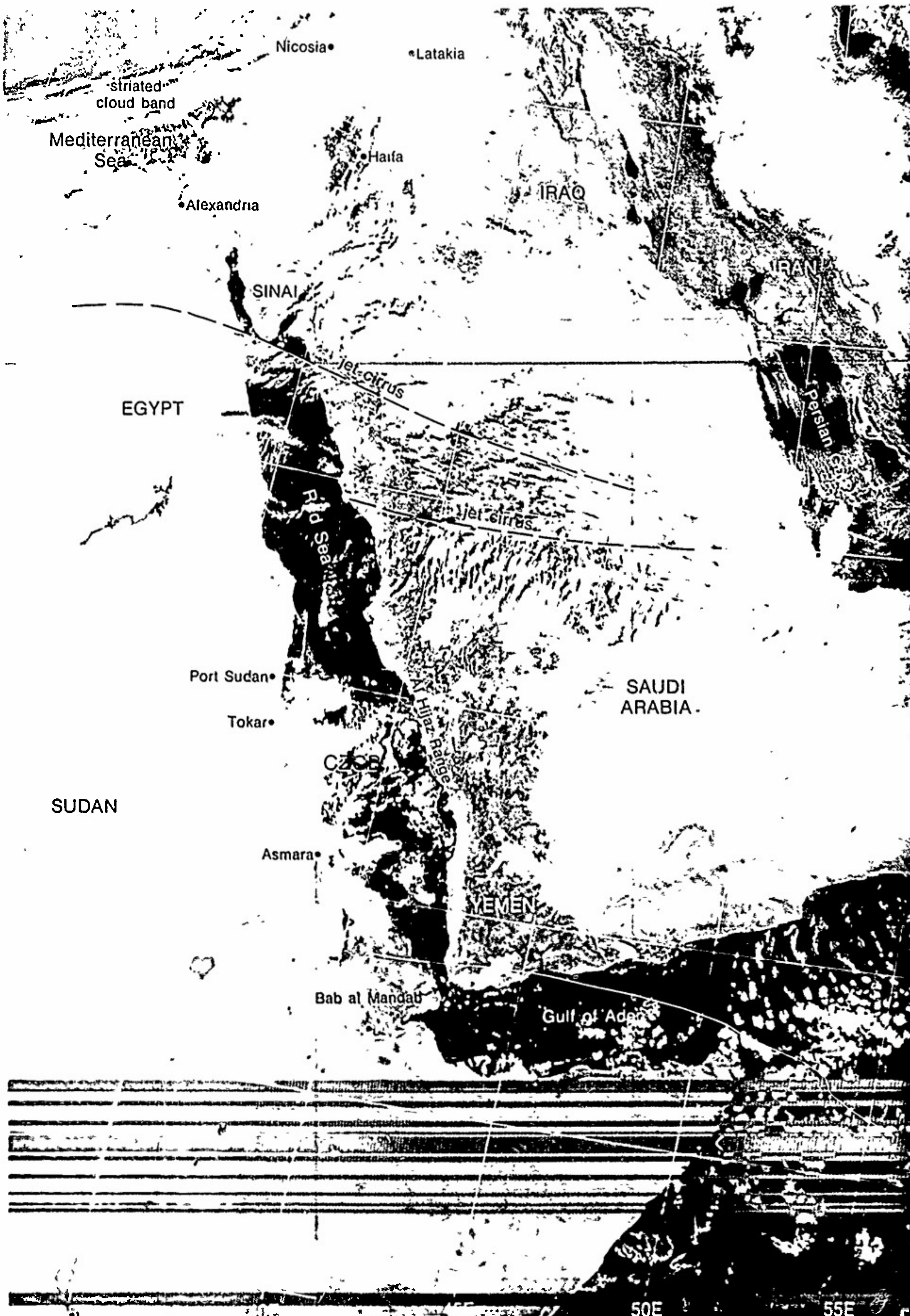


1C-5a 1-2. DMSP LF Log Enhancement 0524 GMT 17 January 1980 (Note this picture is a repeat of 1C-2a.)

18 January

The DMSP picture (1C-7a) on this day reveals that the CZCB has not moved from its location between Port Sudan and Asmara. As on the previous day (1C-2a), fair weather prevails over the Red Sea. The large-scale surface features (1C-7b and 7c) attending the CZCB are also identifiable: the Sahara high (which shows as a weak ridge of high pressure across North Africa), the Saudi Arabia high, the Sudan low, and the northeast monsoon flow over the Arabian Sea. The continued presence of cloud lines in the Bab al Mandab (1C-7a) shows that the northeast monsoon flow into the Gulf of Aden and the Red Sea has not been disrupted. Thus, there has been no major change in the surface circulation pattern over the southern Red Sea This is not the case, however, along the northern border of the Red Sea region.

The cloud cover (1C-7a) associated with the upper-level disturbance passing to the north of the Red Sea has become more widespread, and a line of enhanced convection has developed over northern Saudi Arabia At 500 mb (1C-6b), the short-wave trough (see 1C-4b) has sharpened significantly during the past 24 hours and accounts for the enhanced convection observed over northern Saudi Arabia. The deepening of the 500-mb trough is due to increased cold air advection upstream. Note also that the trough is in phase with the sharp high-latitude trough to the north (50°N, 50°E). In the satellite picture, the comma-shaped cloud vortex over the Caspian Sea is located at the base of the high-latitude trough. The presence of this cloud vortex indicates that a deep baroclinic zone extends from the polar trough to Saudi Arabia.

At 200 mb (1C-6a), the broad band of zonal subtropical westerlies continues to show a double wind maxima structure. Only faint jet stream cirrus is observed over the north-central Red Sea in the satellite picture on this day, in comparison to the double jet cirrus streak pattern 24 hours earlier.

The line of enhanced convection (1C-7a) over northern Saudi Arabia indicates that the baroclinic zone associated with the 500-mb short-wave trough has reached to surface levels. This increases the potential for surface frontogenesis in the region. Although the surface pressure analysis does not show frontogenesis, a distinct wind shift line S1-S2 is in evidence as shown on the surface analyses (1C-7b and 7d). Note that showers are reported along the wind shift line The Saudi Arabia high (1C-7c) has shifted to the southeast in response to the intrusion of the 500-mb trough to the north.

With the passage of the upper-level disturbance to the north of the CZCB, it is significant that the location of this band has not been disrupted. A pronounced deepening of the short-wave trough occurred; however, its influence remained well to the north of the CZCB region, as shown by the cloud patterns in the satellite pictures.

200 mb

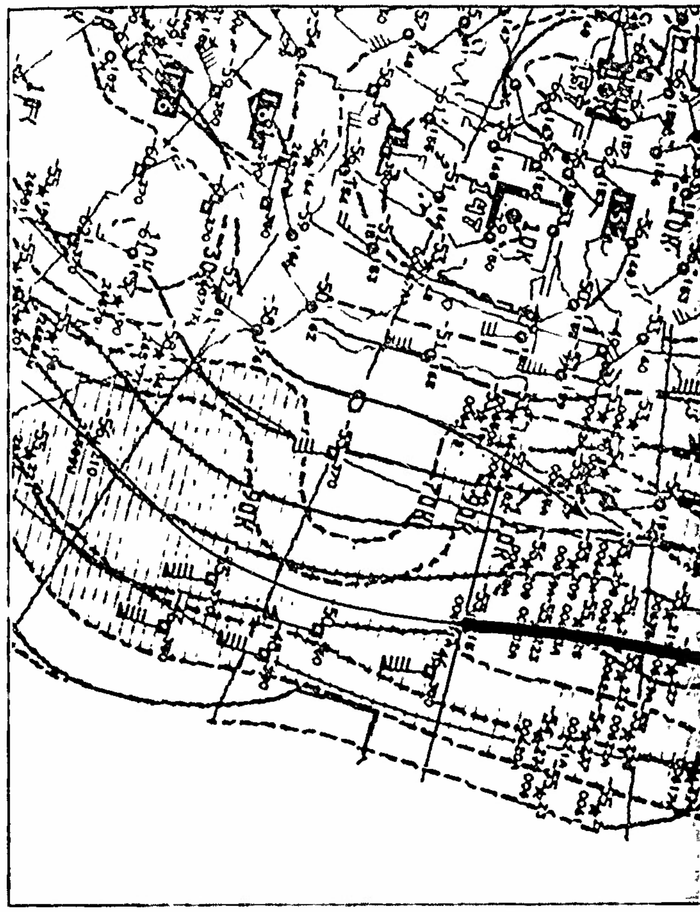

1C-6a. NMC 200-mb Analysis. 1200 GMT 18 January 1980

500 mb

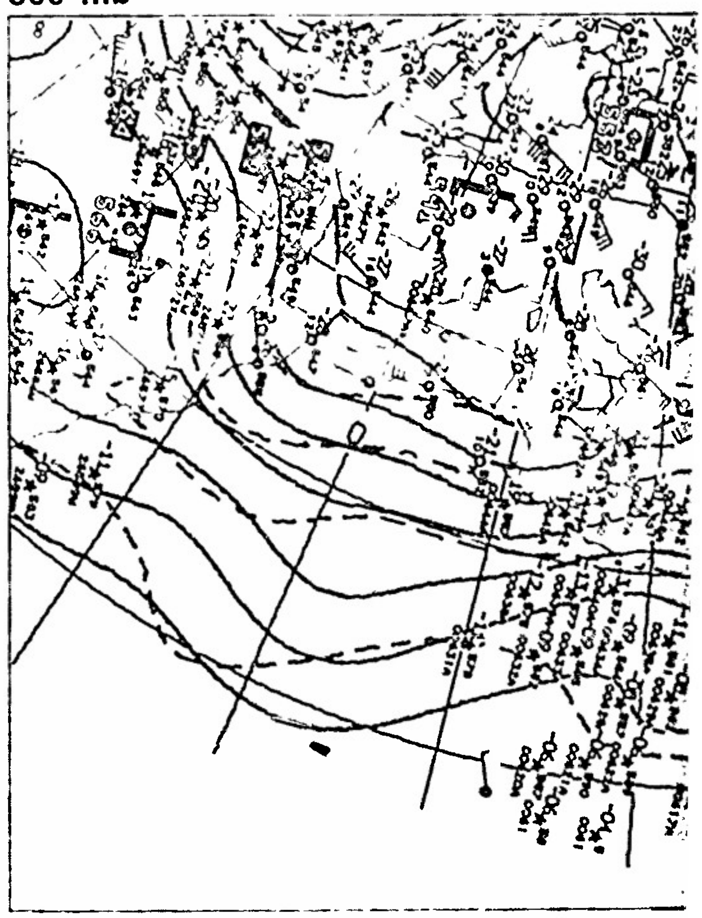

1C-6b. NMC 500-mb Analysis 1200 GMT 18 January 1980.

**200 mb**

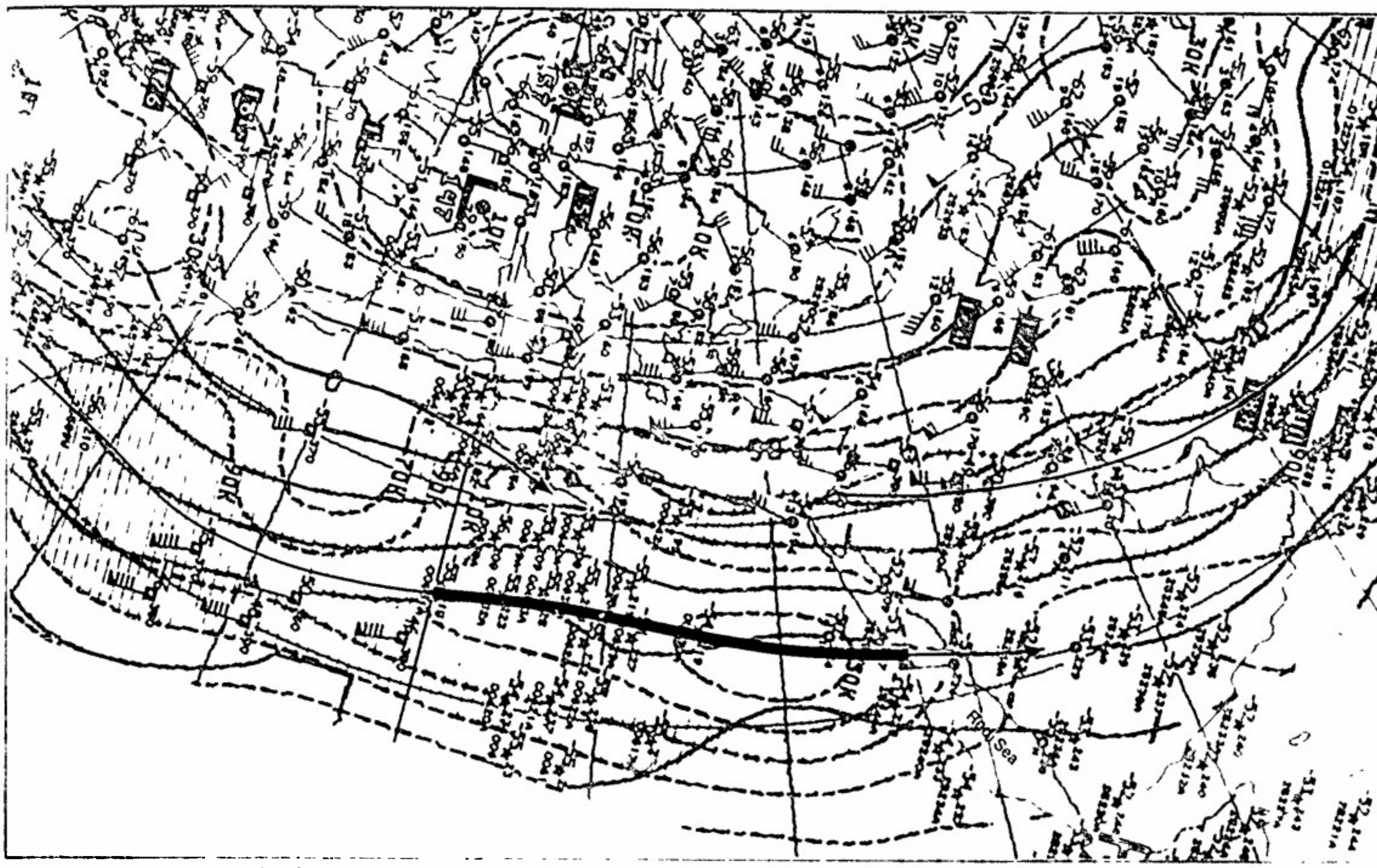


1C-6a. NMC 200-mb Analysis. 1200 GMT 18 January 1980.

**500 mb**

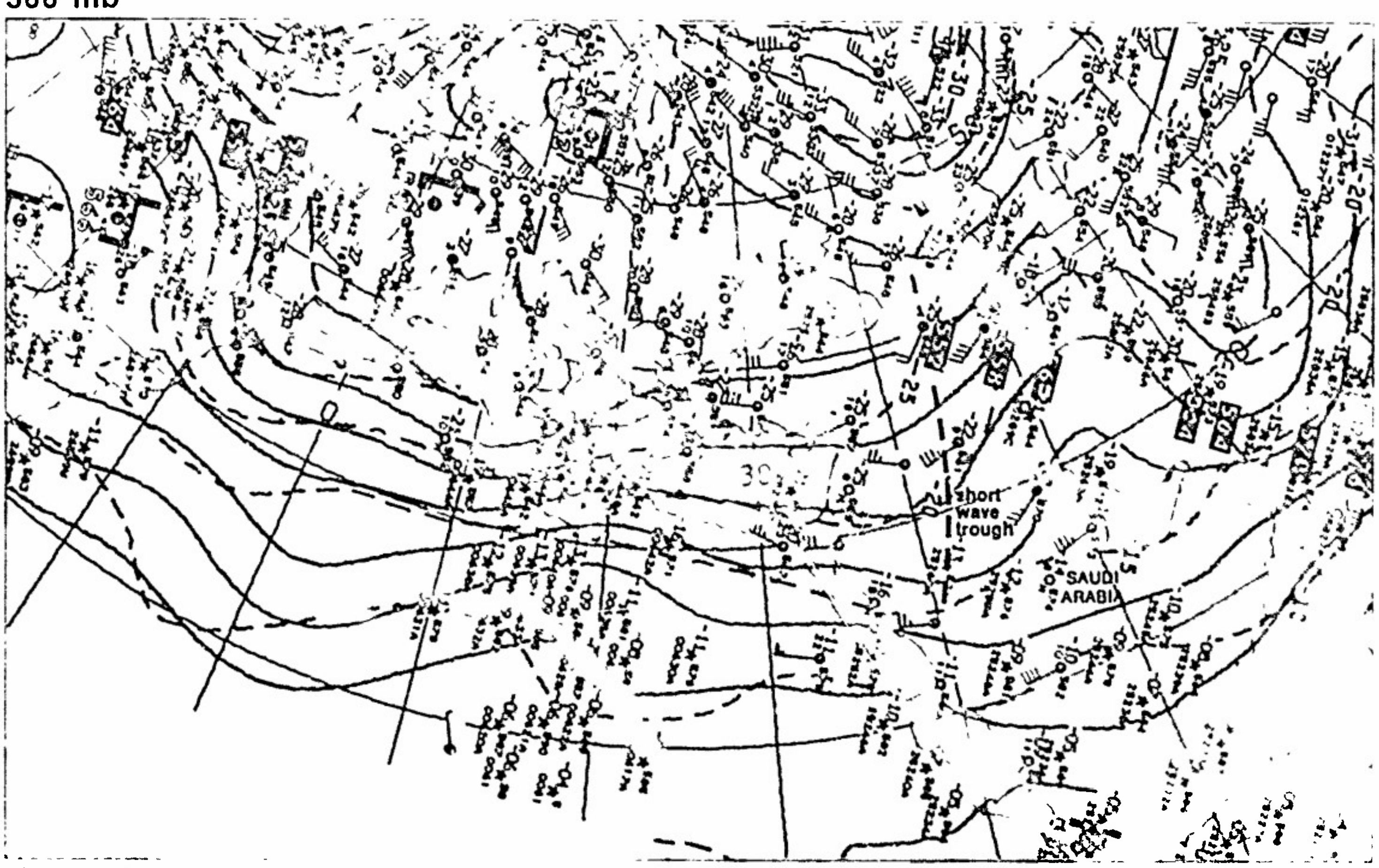


1C-6b NMC 500-mb Analysis 1200 GMT 18 January 1980

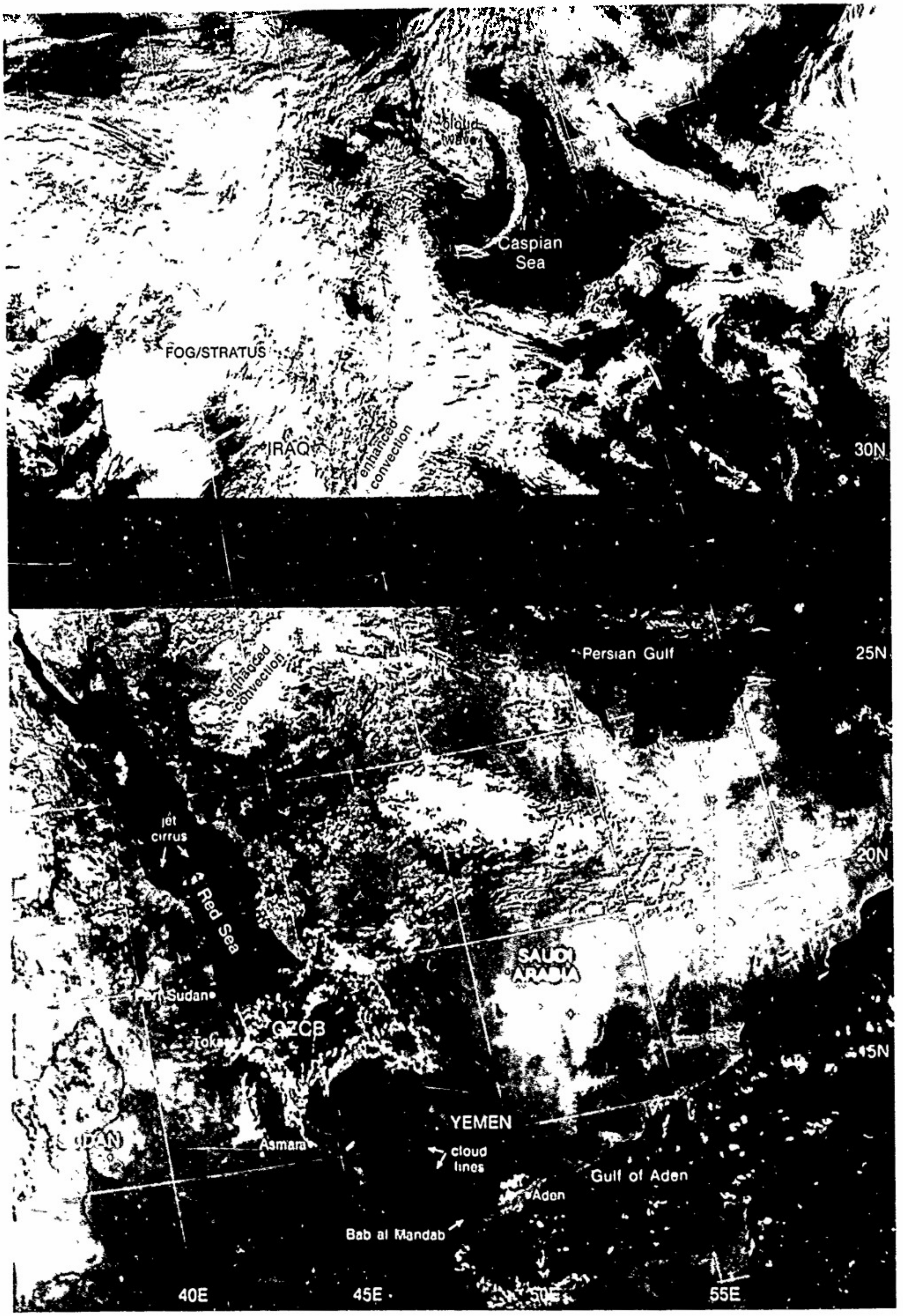


1C-7a 1-4 DMSP LF Low Enhancement 0631 GMT 18 January 1980


...ce

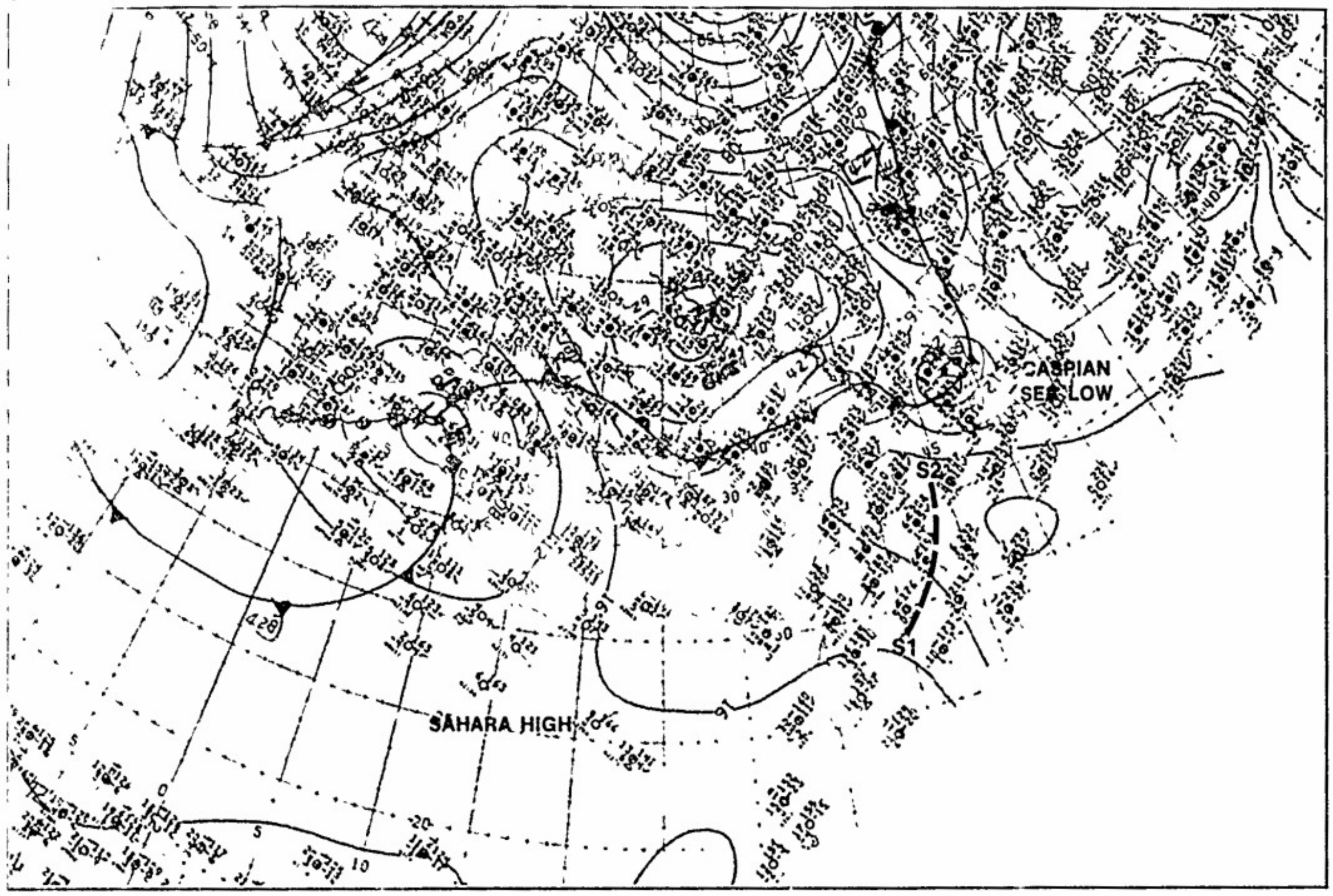


IC-7b. NMC Surface Analysis. 0600 GMT 18 January 1980.

surface

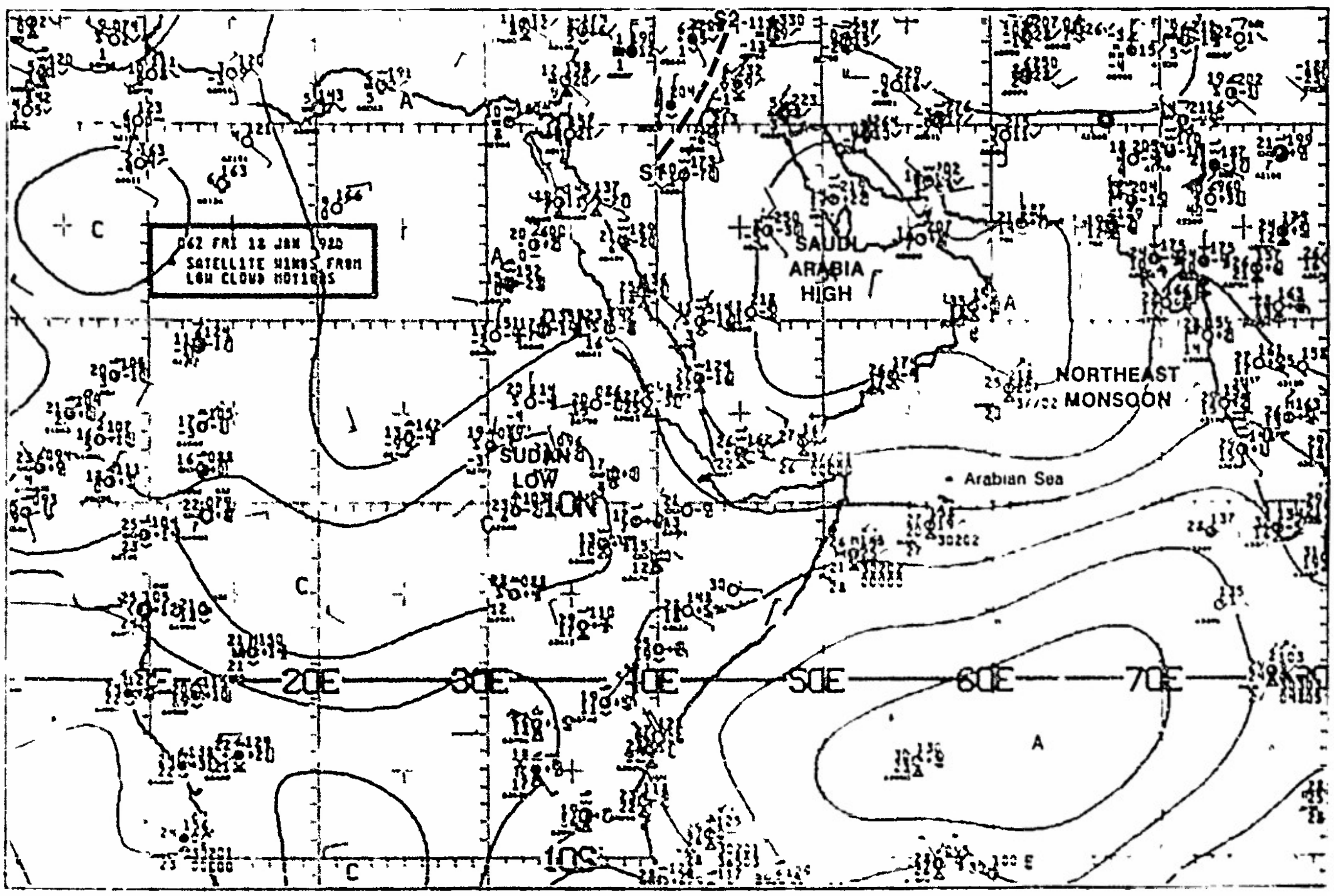


IC-7c. NMC Tropical Surface Streamline Analysis. 0600 GMT 18 January 1980.

# Case 2 Red Sea/Persian Gulf—Winter

## Red Sea Convergence Zone Cloud Band Displacement from Normal Winter Location

The Red Sea convergence zone cloud band (CZCB) is typically located near 18°–20° N during the winter. Under fair weather conditions, day-to-day variations in the position of the CZCB are small because the winds are generally light and variable along the Red Sea Convergence Zone (RSCZ). The displacement of the CZCB from this location indicates a change in the normal winter synoptic-scale circulation over the region. On occasion, a portion of the equatorial trough (Sudan low) will be observed over the northern Red Sea (1C-9a). This brings southerly winds around its eastern periphery which advance the RSCZ to the north of its normal position. A further evolution is for the Sudan low to move eastward, across the Red Sea to Saudi Arabia, in response to upper-level troughs or depressions crossing the eastern Mediterranean. Under such circumstances northwesterly winds appear over the northern Red Sea and the RSCZ recedes southward toward its normal winter location. When northwesterly flow is especially strong the RSCZ may be displaced southward to 13°–15° N for periods of several days.

**References**

Solot, Samuel B., 1950. General circulation over the Anglo-Egyptian Sudan and adjacent regions. *Bull. AMS* 31, p. 88.

NEPRF, 1980. Weather in the Indian Ocean to Latitude 30° S and Longitude 95° E including the Red Sea and Persian Gulf. Vol. 2, Part 1. NAVENVPREDRSCHFAC Technical Bulletin 80-02, Naval Environmental Prediction Research Facility, Monterey, Calif., 83 pp.

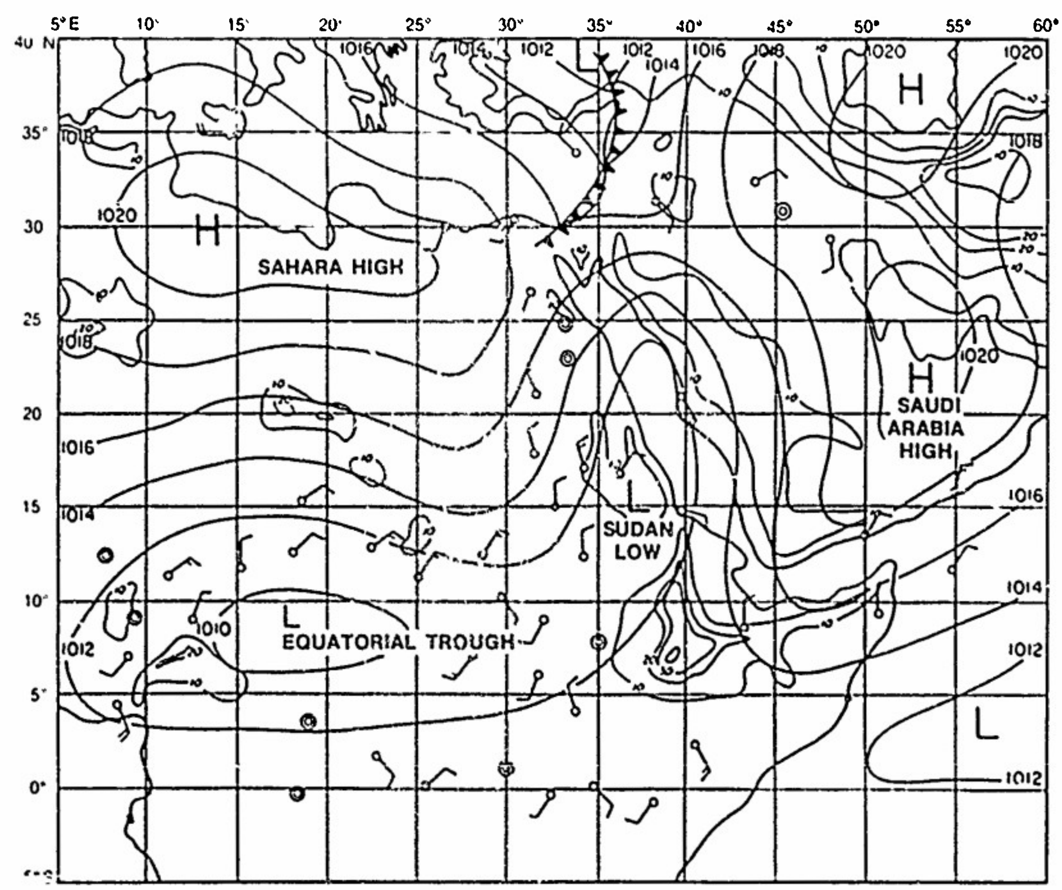


1C-9a Typical surface analysis showing extension of the equatorial trough to the north of the Red Sea (Solot 1950)

*Pronounced Northward Displacement of the CZCB by a Low Pressure Development in the Equatorial Trough (Sudan Low)*
*Red Sea*
*January 1980*

22 January

The DMSP picture (1C-10a) for 17 January 1980, from Case 1 (1C-2a), shows the Red Sea and adjacent land areas on a typical winter fair weather day. Except for the thin filaments of jet stream associated cirrus passing to the south of Sinai and across Saudi Arabia, the only major cloudiness over the Red Sea is the CZCB. The CZCB is at its normal winter position, near Port Sudan. Five days later, on 22 January, the DMSP picture (1C-11a) shows the CZCB near 25°N, almost 300 n mi north of its normal winter position. In addition, a band of cumuliform cloudiness, followed by dense stratus and fog, extends across the northern Arabian Peninsula which suggests the presence of a front.

The NMC surface analysis (1C-12a) confirms the presence of a weak baroclinic zone T1 over the northern Arabian Peninsula. Note that the baroclinic zone does not extend across the Red Sea, but curves abruptly northward. This abrupt change of direction is important to recognize because in a cursory examination of the satellite picture a likely misinterpretation would be to include the CZCB as part of the baroclinic zone cloud band. The baroclinic zone is the location of a dissipating frontal system which had moved into the area from the eastern Mediterranean. Surface reports O1, O2, and O3 of rain and fog with obscured skies reveal that the baroclinic zone is an operationally important weather producer.

Further evidence that the two cloud bands are not part of the same baroclinic zone is provided by the NMC surface streamline analysis (1C-12b). This analysis shows the typical winter anticyclones over the eastern Arabian Peninsula and northern Africa. However, the equatorial trough over central Africa extends much further north than normal and shows a closed cyclonic circulation L1 over northern Sudan. Southerly flow around the eastern periphery of this low and the turning of the northeast monsoon from the Gulf of Aden northward through the Bab al Mandab produce a band of southeasterlies eventually extending to the northern portion of the Red Sea (1C-13b). This surge in the southeasterlies displaces the CZCB far to the north of its normal winter location, as shown on the satellite picture (1C-13a).

At upper levels, the NMC 300-mb analysis (1C-14a) shows a deep polar low L2 extending to lower latitudes over the eastern Mediterranean. A strong polar jet stream is located south of the low, with an elongated 110-kt jet streak PJS1 extending from northeast Africa to the Persian Gulf. At 500 mb (1C-14b), there is a short-wave trough T2 advancing toward the Red Sea in the strong westerlies across northern Africa. The minor trough T1, at 850 mb over the northern Arabian Peninsula (1C-14c), is the location of the baroclinic zone observed on the surface analysis (1C-12a). Note the packing of isotherms behind the trough T1, which defines the location of the baroclinic zone.

The presence of the ridge aloft at 850 mb (1C-14c) over the surface location of the Sudan low L1 confirms the thermal-low structure of this system. However, the strong cold air advection associated with the trough T2 to the west, and the fact that the trough extends almost to the latitude of the Sudan low, suggest that intensification of the low L1 may occur as the short wave crosses to the north. The NMC surface streamline analysis 12 hours later (1C-13b), near the daytime surface wind speed maximum, shows stronger winds around the northeastern periphery of the Sudan low L1, suggesting that this low is the primary influence in maintaining the CZCB at its northern location. In addition, numerous reports of dust (weather symbol S) raised by the surface winds, indicate that the low is deepening.

At 300 mb (1C-15a), 12 hours later, the polar low L2 has moved slowly to the southeast, and the jet streak pattern to the south has consolidated into a short, strong (110 kt) jet streak PJS1 over the Red Sea. The 500-mb short-wave trough T2 (1C-15b) advanced across the Red Sea and is followed by a new short-wave trough T3. Note that the northern portion of T2 is located in the left front quadrant of the 300-mb jet streak PJS1 a favorable area for low-level cyclogenesis. These upper-air conditions have contributed to the formation of the closed low L3 at 850 mb (1C-15c). The Sudan low L1, at this time, is located just in advance of the 500-mb trough T2 and, as indicated on the surface analysis (1C-13b), shows definite signs of deepening.

A comparison of the FNOC 36-hr 500-mb prognosis (1C-17a) and the initial 500-mb analysis (1C-16a) shows that the strong polar westerlies (tight contour gradient) will be maintained across the northern Arabian Peninsula. The low L2 (1C-16a) is forecast to move to the eastern Mediterranean (1C-17a), and the short-wave trough T2 is replaced by the upstream trough T3, as it deepens and advances eastward. With the Sudan low L1 coming under the influence of increased southwesterly flow aloft, the stage is set for this low to advance across the Red Sea.

*continued on page 1C-18*

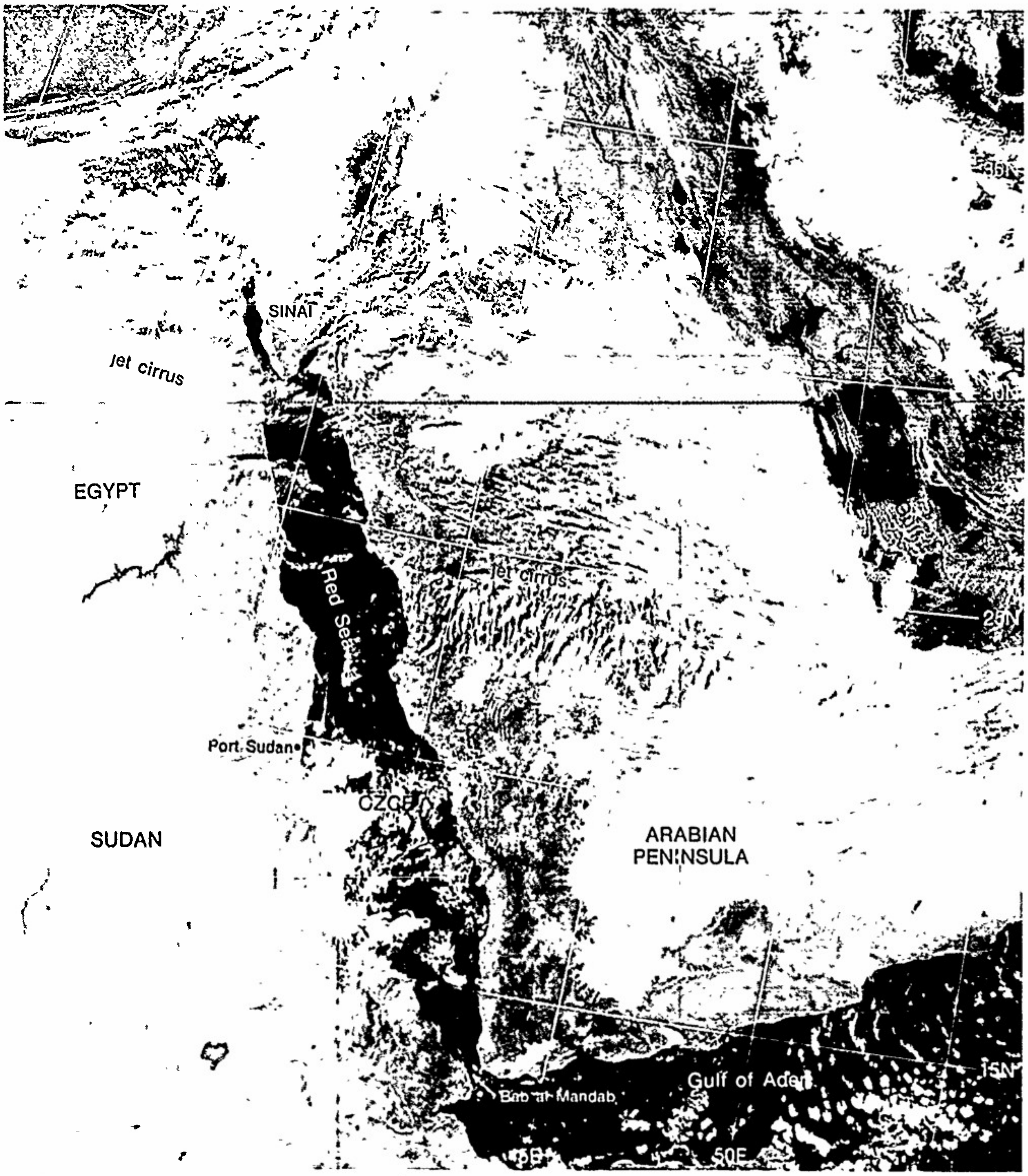


1C-10a. F-2 DMSP LF Log Enhancement. 0524 GMT 17 January 1980.

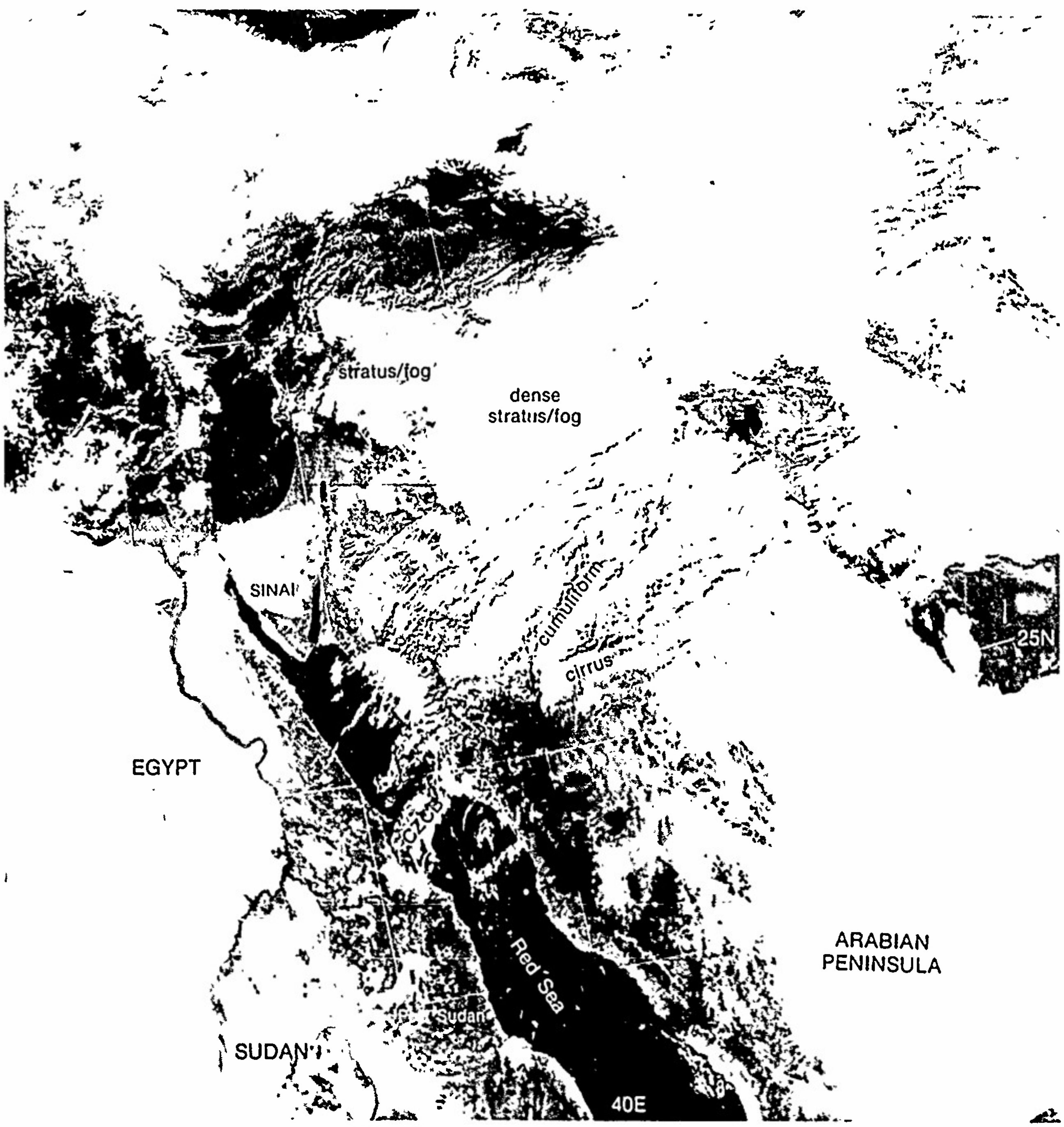


IC-11a. F-4. DMSP LF Log Enhancement. 0732 GMT 22 January 1980.

surface

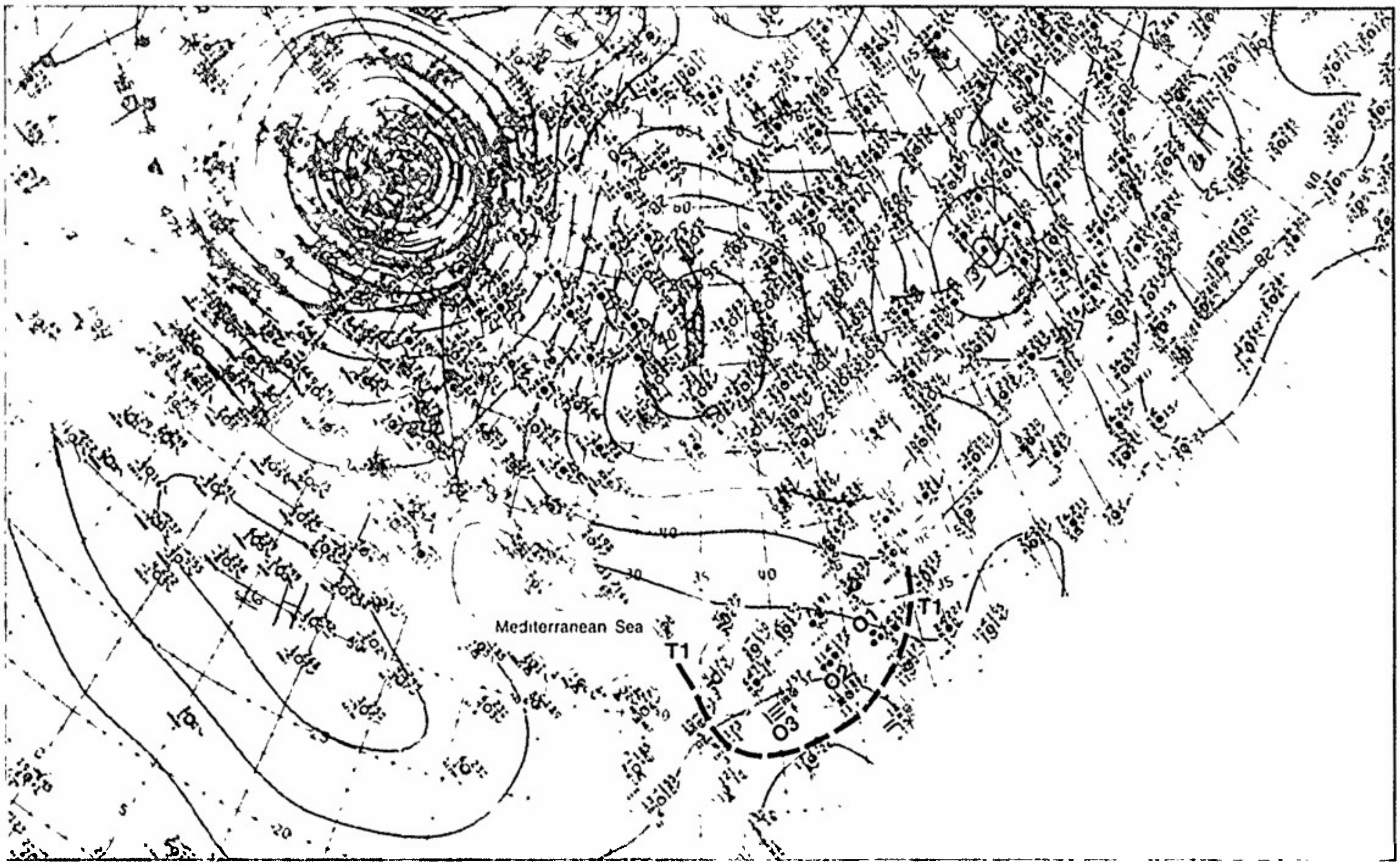


1C-12a. NMC Surface Analysis. 0600 GMT 22 January 1980

surface

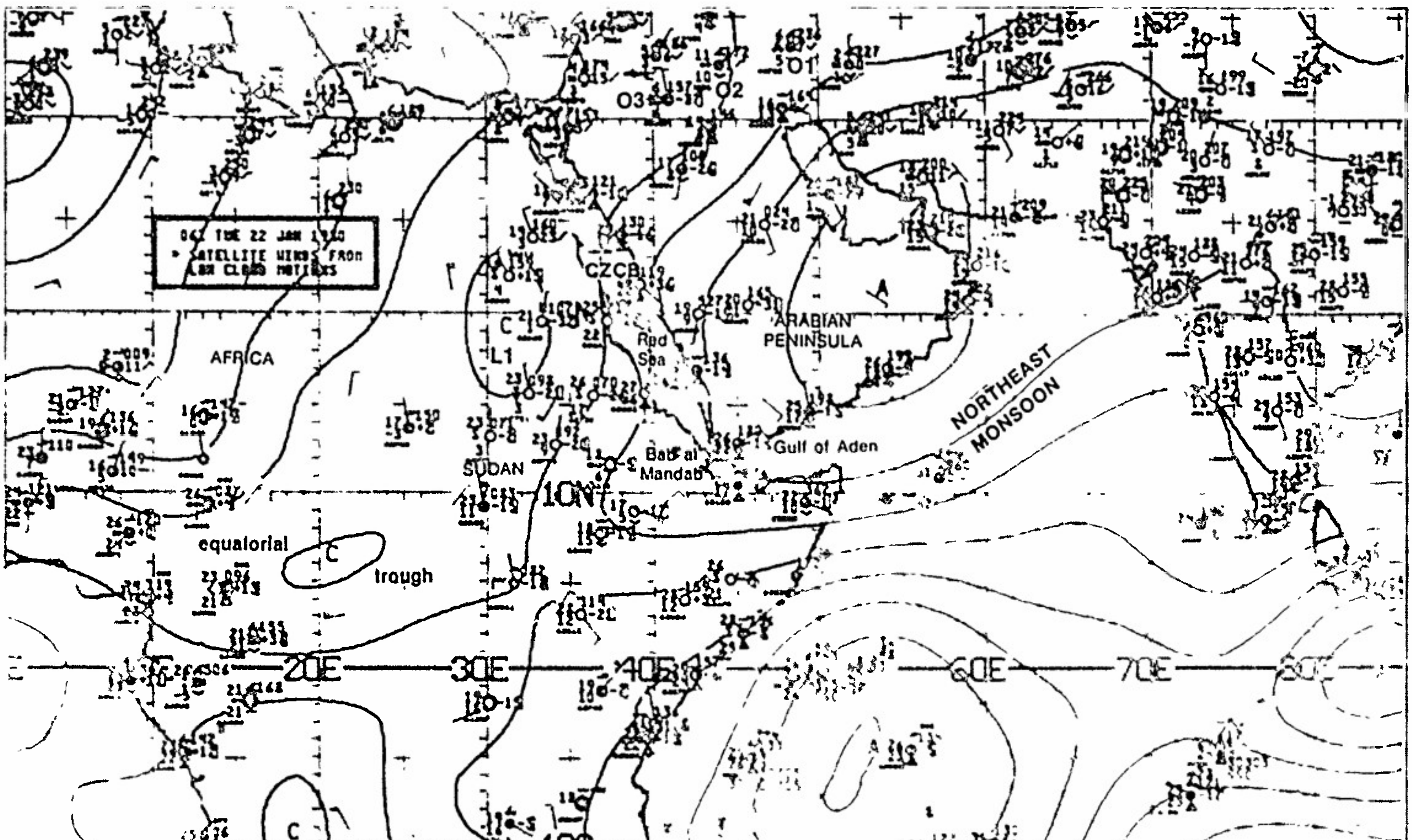


1C-12b. NMC Tropical Surface Streamline Analysis. 0600 GMT 22 January 1980.

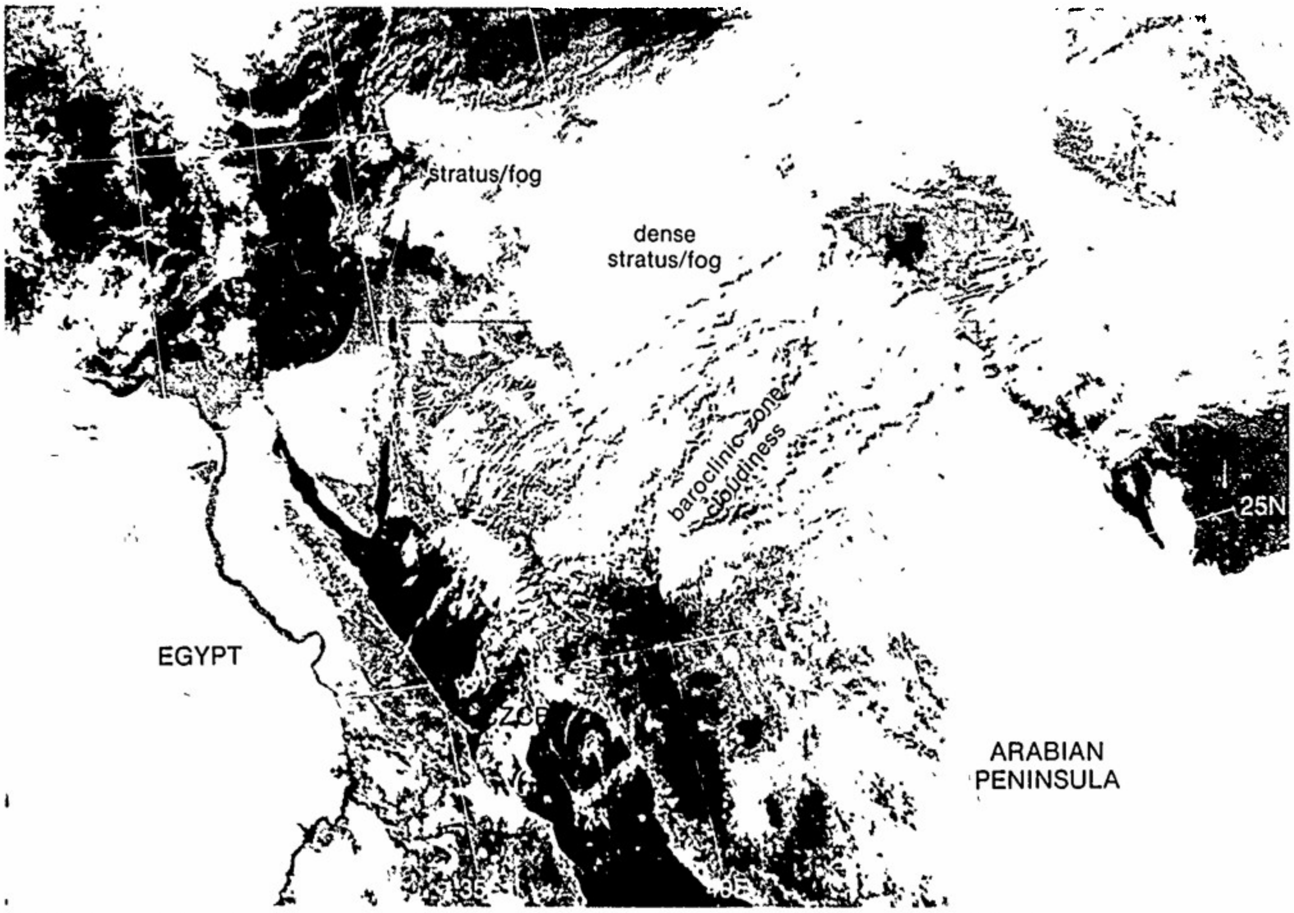


1C-13a F-4. DMSP LF Log Enhancement, 0732 GMT 22 January 1980 (Note this picture is a repeat of 1C-11a.)

surface

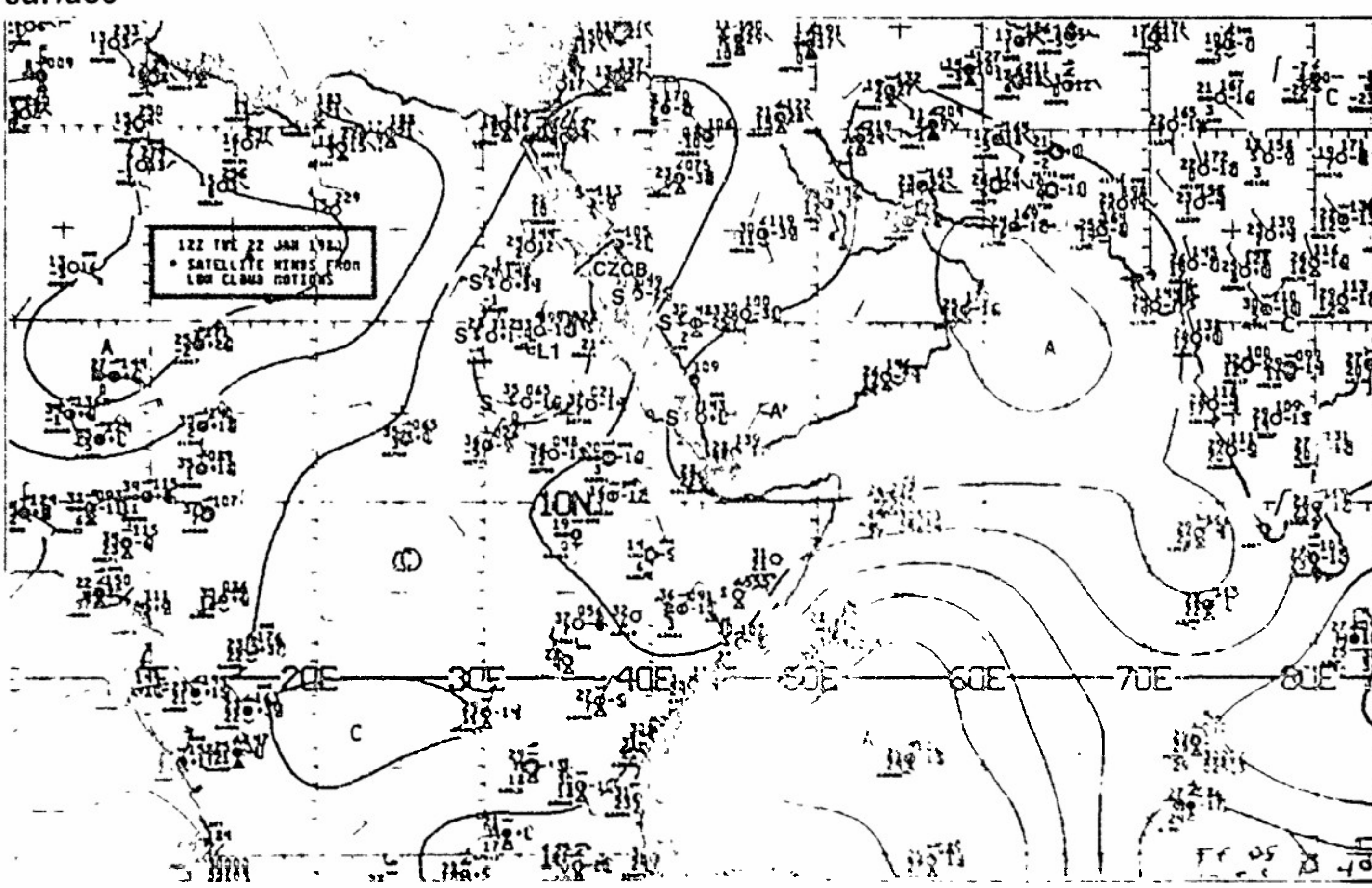


1C-13b NMC Tropical Surface Streamline Analysis 1200 GMT 22 January 1980

300 mb

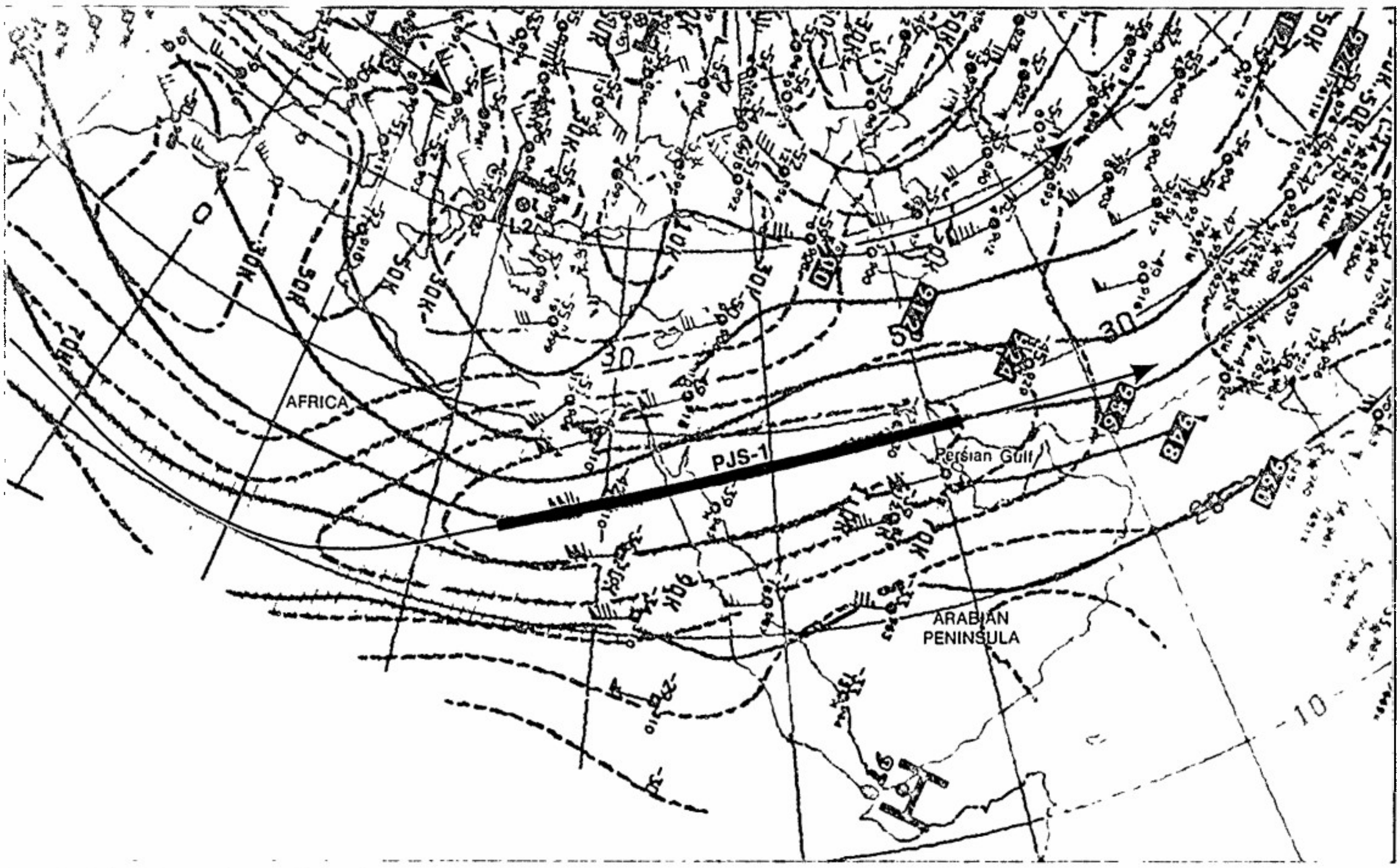


1C-14a. NMC 300-mb Analysis. 0000 GMT 22 January 1980.

500 mb

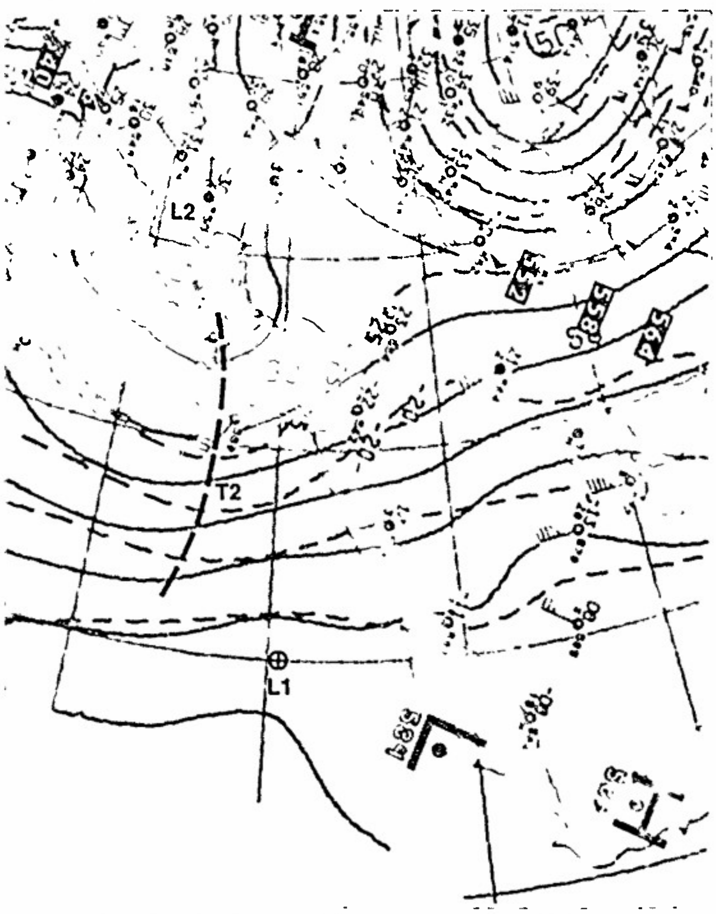


1C-14b. NMC 500-mb Analysis. 0000 GMT 22 January 1980

850 mb

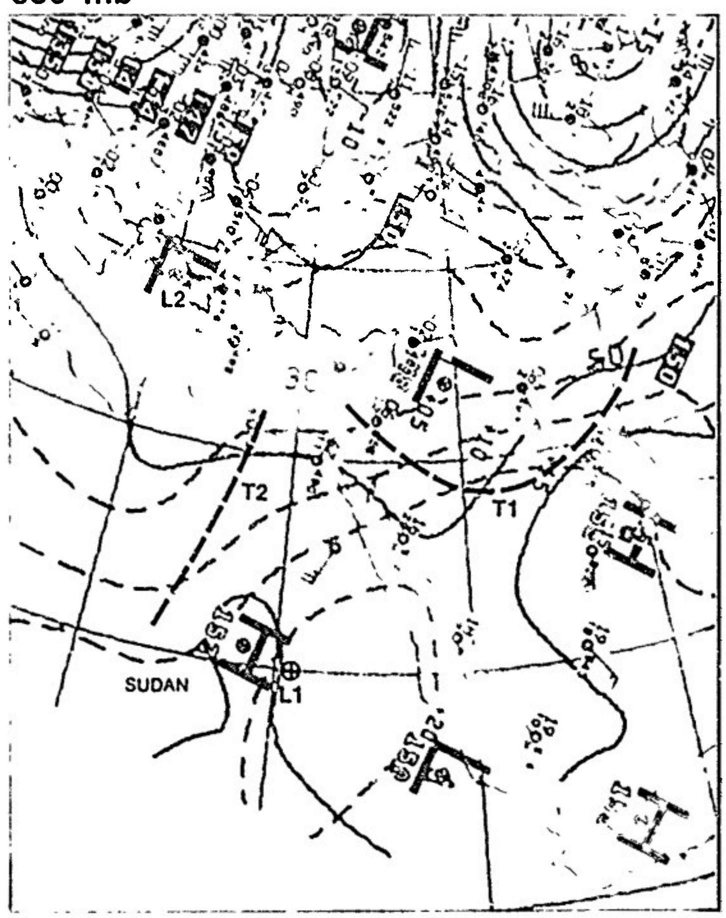


1C-14c. NMC 850-mb Analysis. 0000 GMT 22 January 1980.

## 300 mb

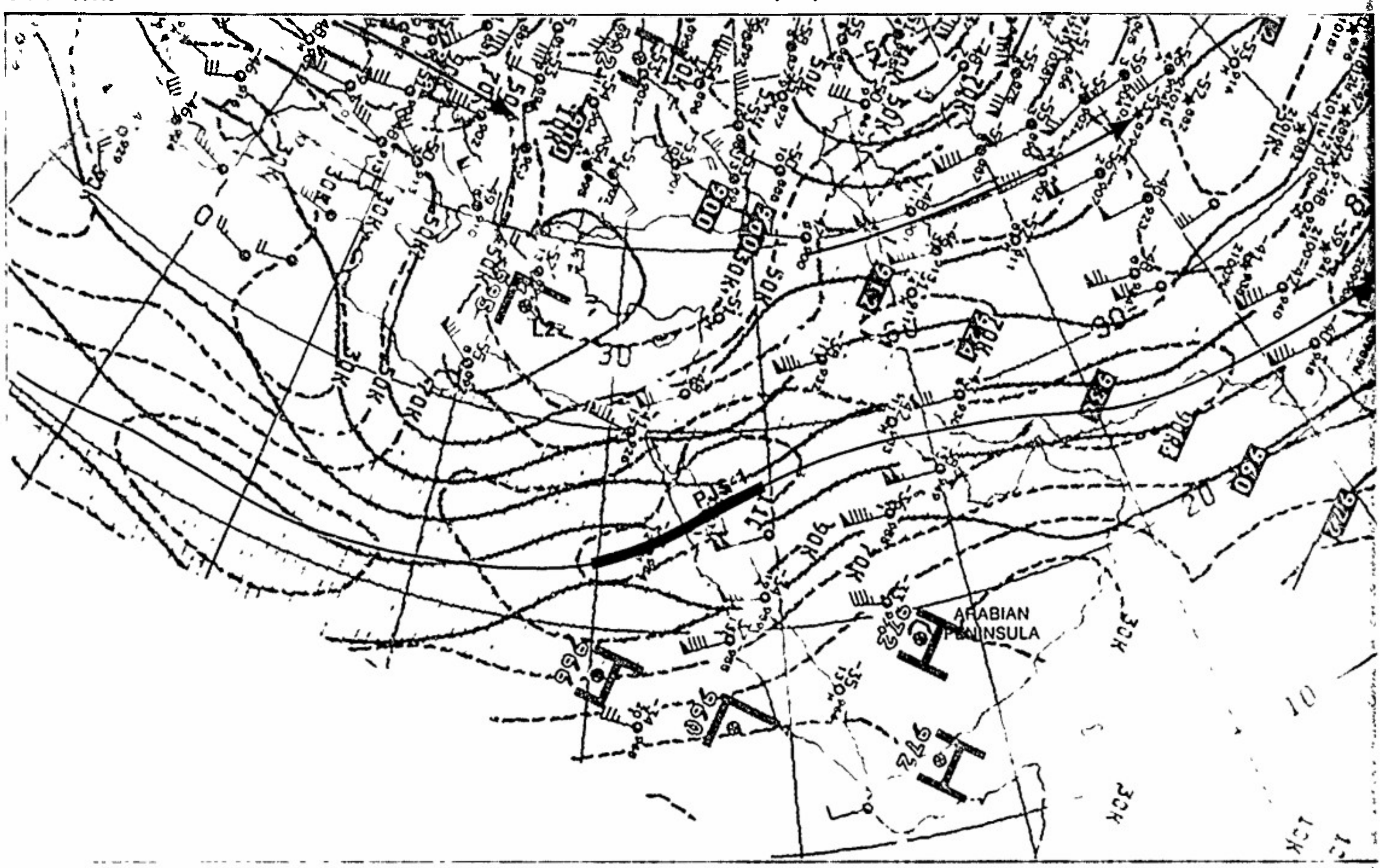


IC-15a. NMC 300-mb Analysis. 1200 GMT 22 January 1980.

## 500 mb

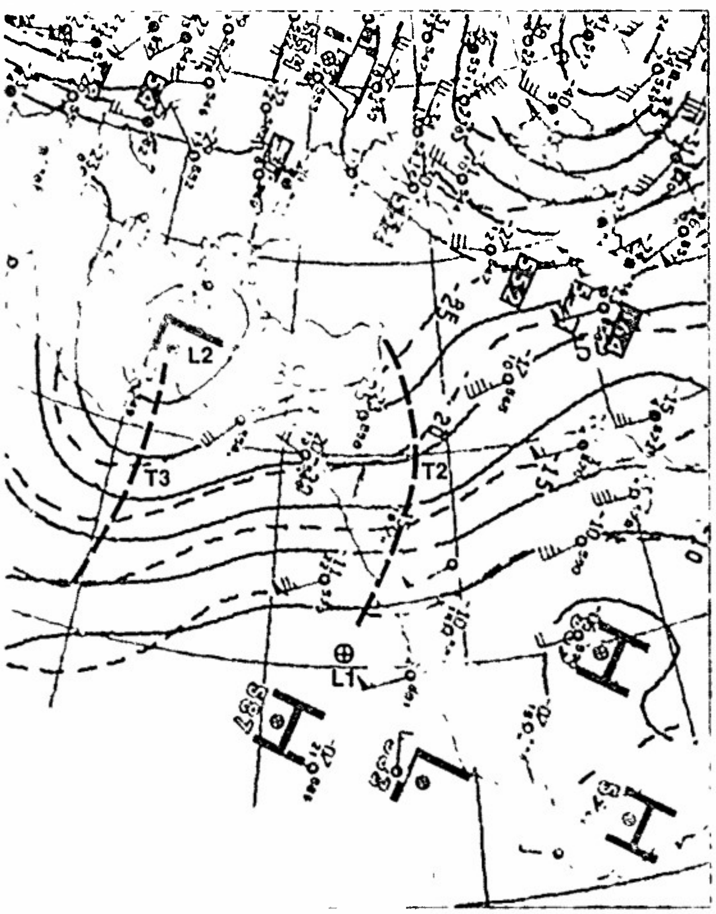


IC-15b NMC 500-mb Analysis 1200 GMT 22 January 1980.

## 850 mb

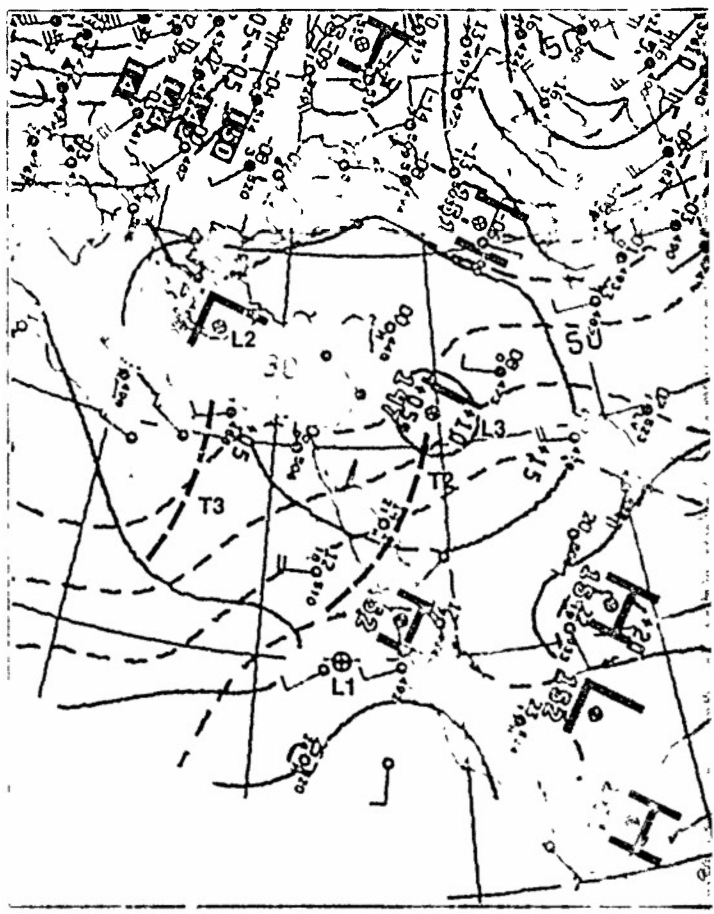


IC-15c. NMC 850-mb Analysis. 1200 GMT 22 January 1980.

500 mb

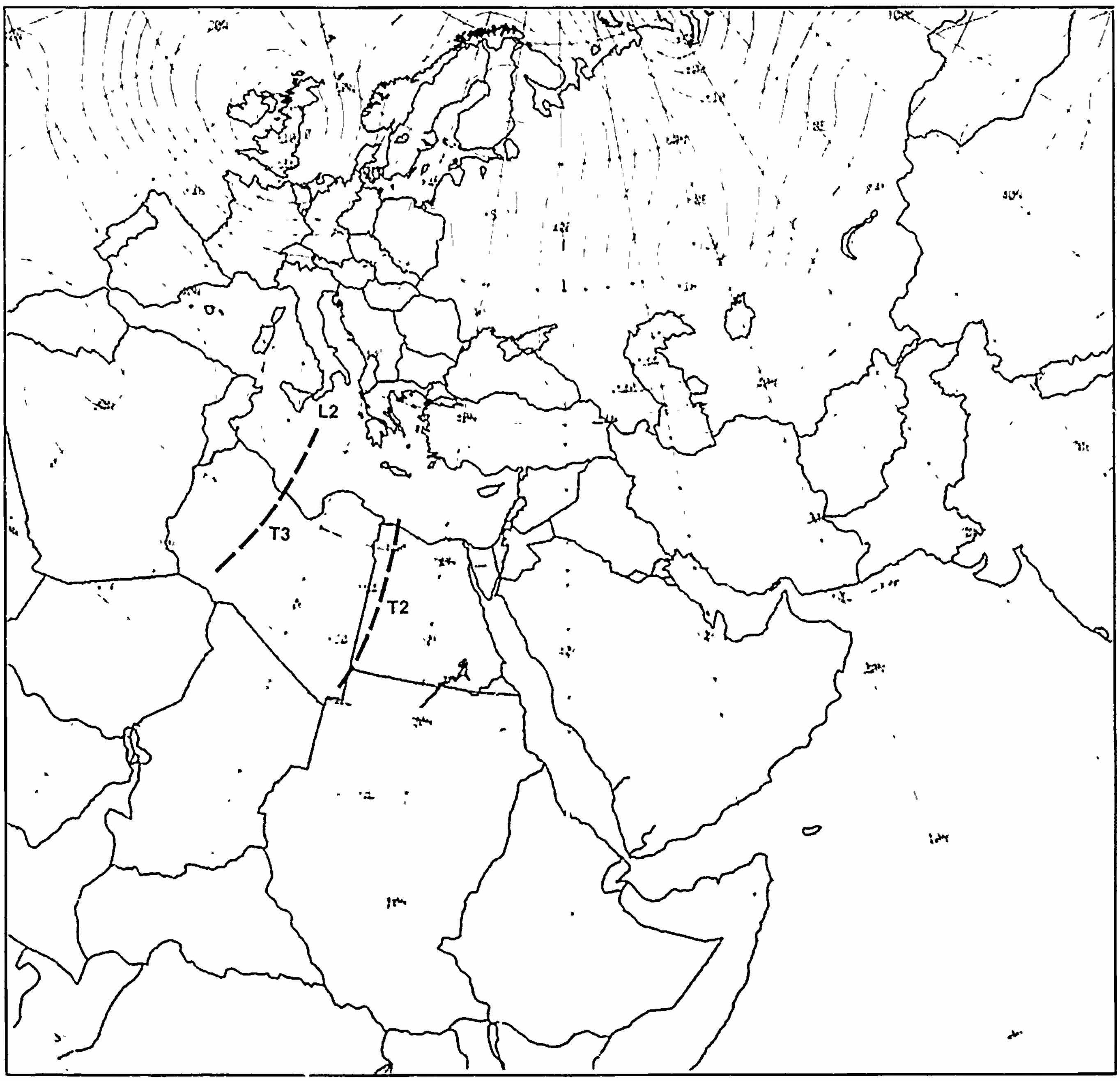


IC-16a. FNOC PE Initial 500-mb Analysis, 0000 GMT 22 January 1980.

500 mb

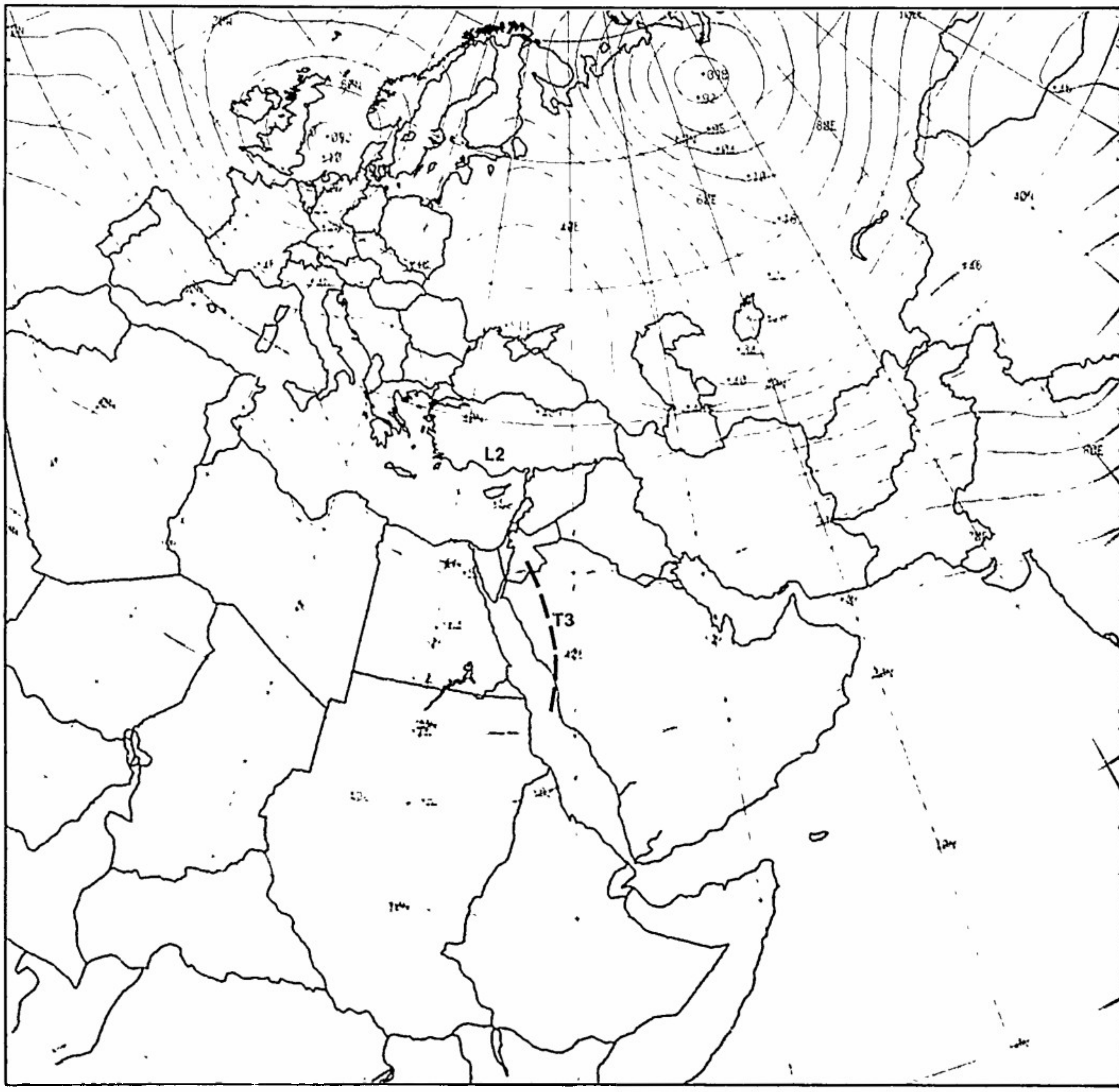


1C-17a FNOC PE 36-hr 500-mb Prognosis Valid 1200 GMT 23 January 1980.

**23 January**

On the early morning DMSP picture (1C-19a), the spiral cloud pattern L1 shows that the Sudan low has crossed the Red Sea and is located over central Saudi Arabia Note also that the CZCB has been displaced southward to a position just north of 20°N. This represents a movement of the CZCB of about 240 n mi in 24 hours (see 1C-11a). An examination of the NMC surface streamline analysis (1C-18a) reveals the reason for the pronounced displacement. (Note: the NMC surface streamline analysis for 0600 GMT was not available.) As the Sudan low L1 crossed the Red Sea, northwesterly flow developed over the northern Red Sea and, by 1200 GMT (1C-18b), strong northwesterlies (20 30 kt) are reported over the Red Sea down to 20°N. Twenty-four hours earlier (1C-13b), southeasterlies extended as far north as 26°N over the same area. The development of numerous convective cloud lines north of the CZCB (1C-19a) indicates the advection of colder air over the warmer sea surface and serves as an indicator of the northwesterly flow advancing southward over the Red Sea.

At 300 mb (1C-20a and 21a), the polar low L2 advances to the eastern Mediterranean, as forecast (1C-17a), and strong polar westerlies are located across the Arabian Peninsula. At 500 mb the short wave T2 (1C-20b) is replaced by the new trough T3 (1C-21b), as forecast. During this period the Sudan low L1 advances across the Red Sea (1C-18a and 18b) in response to the southwesterly flow aloft. With the persistence of the jet streak PJS1 over the Red Sea region, the northern part of the trough T3 is located in the front left quadrant of the jet streak at 300 mb (1C-21a), and deepening to lower levels is enhanced, as reflected by the persistence of the 850-mb low (1C-20c and 21c). As a result, northwesterlies develop over the northern Red Sea and, by 1200 GMT, they extend to 20°N.

*continued on page 1C-22*

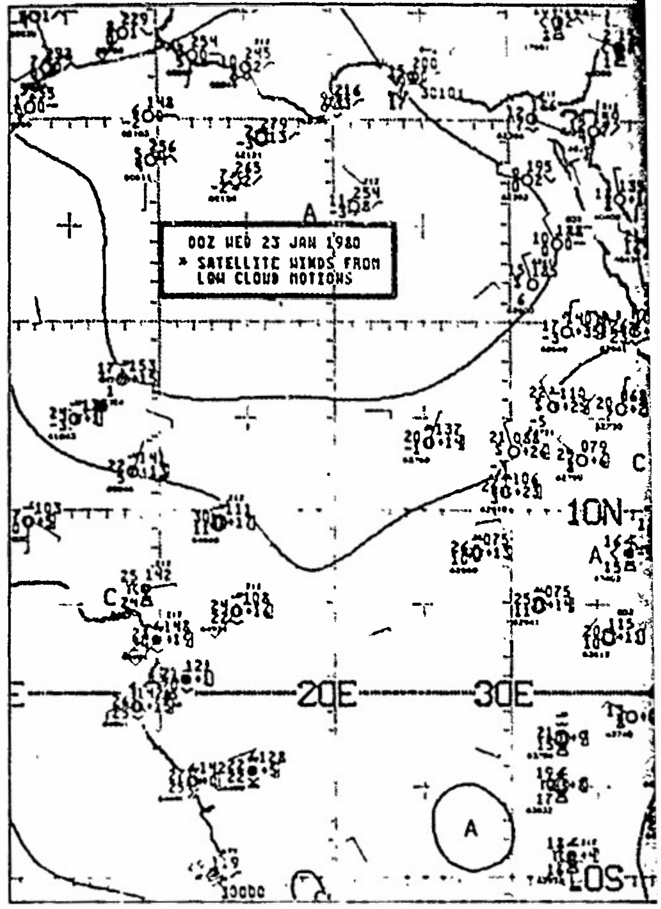


1C-18a NMC Tropical Surface Streamline Analysis, 0000 GMT 23 J

**surface**

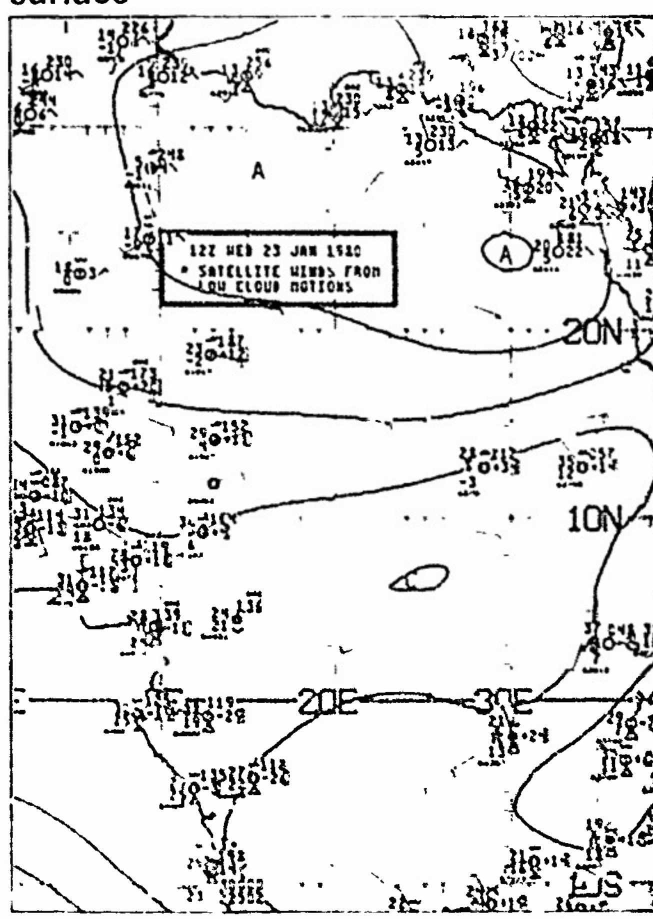


1C-18b NMC Tropical Surface Streamline Analysis 1200 GMT 23 Ja

surface

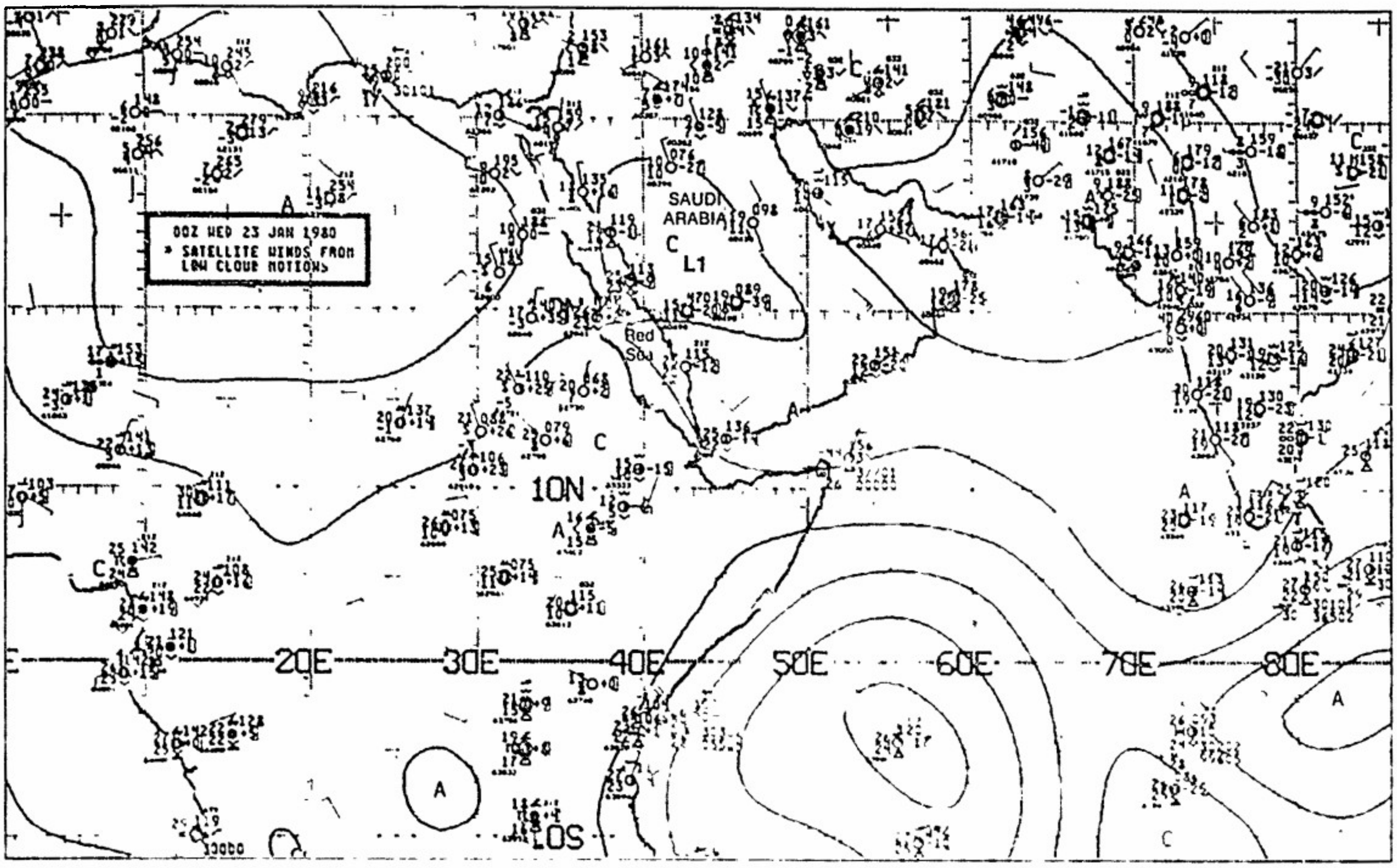


1C-18a. NMC Tropical Surface Streamline Analysis 0000 GMT 23 January 1980.

surface

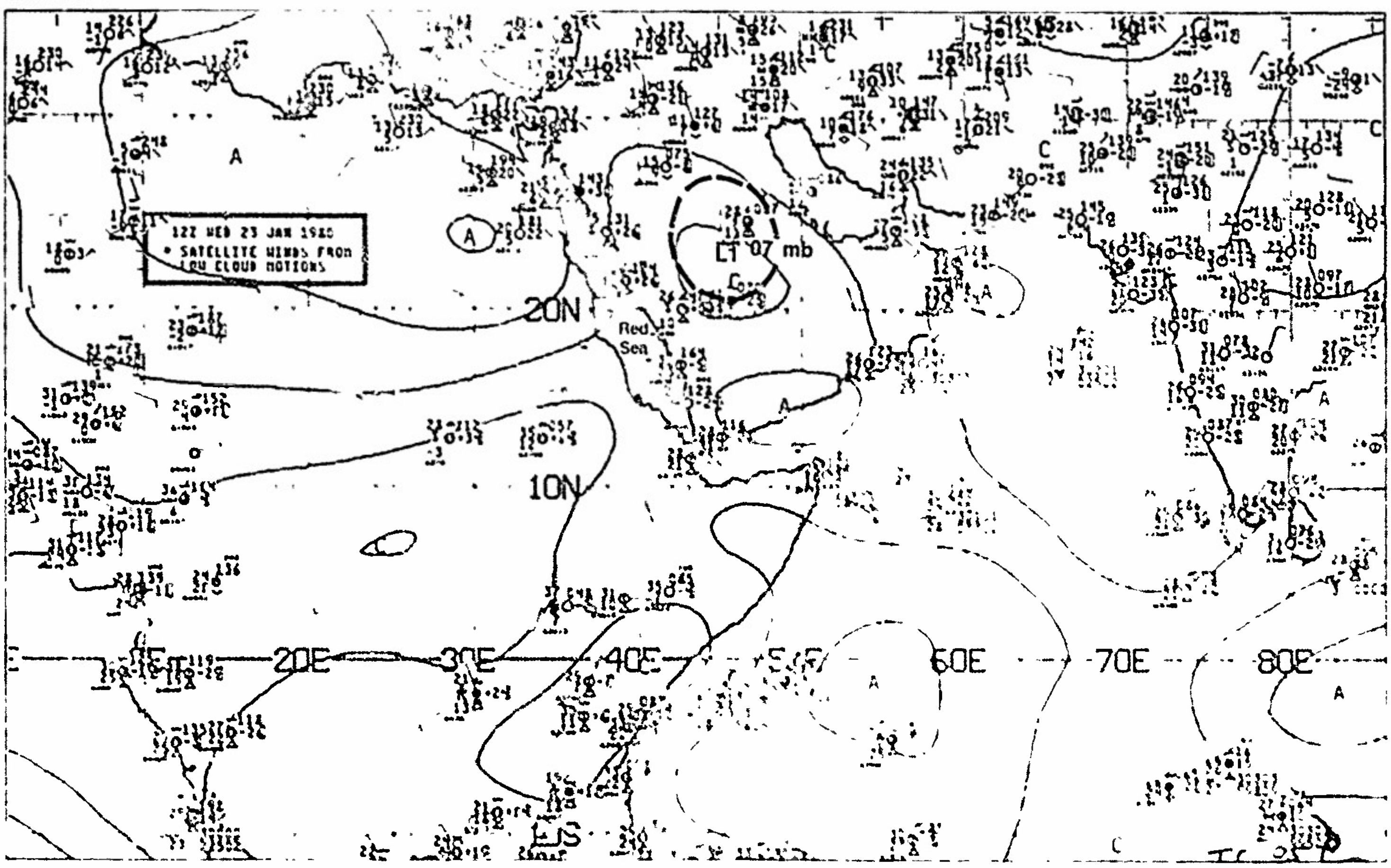


1C-18b NMC Tropical Surface Streamline Analysis 1200 GMT 23 January 1980

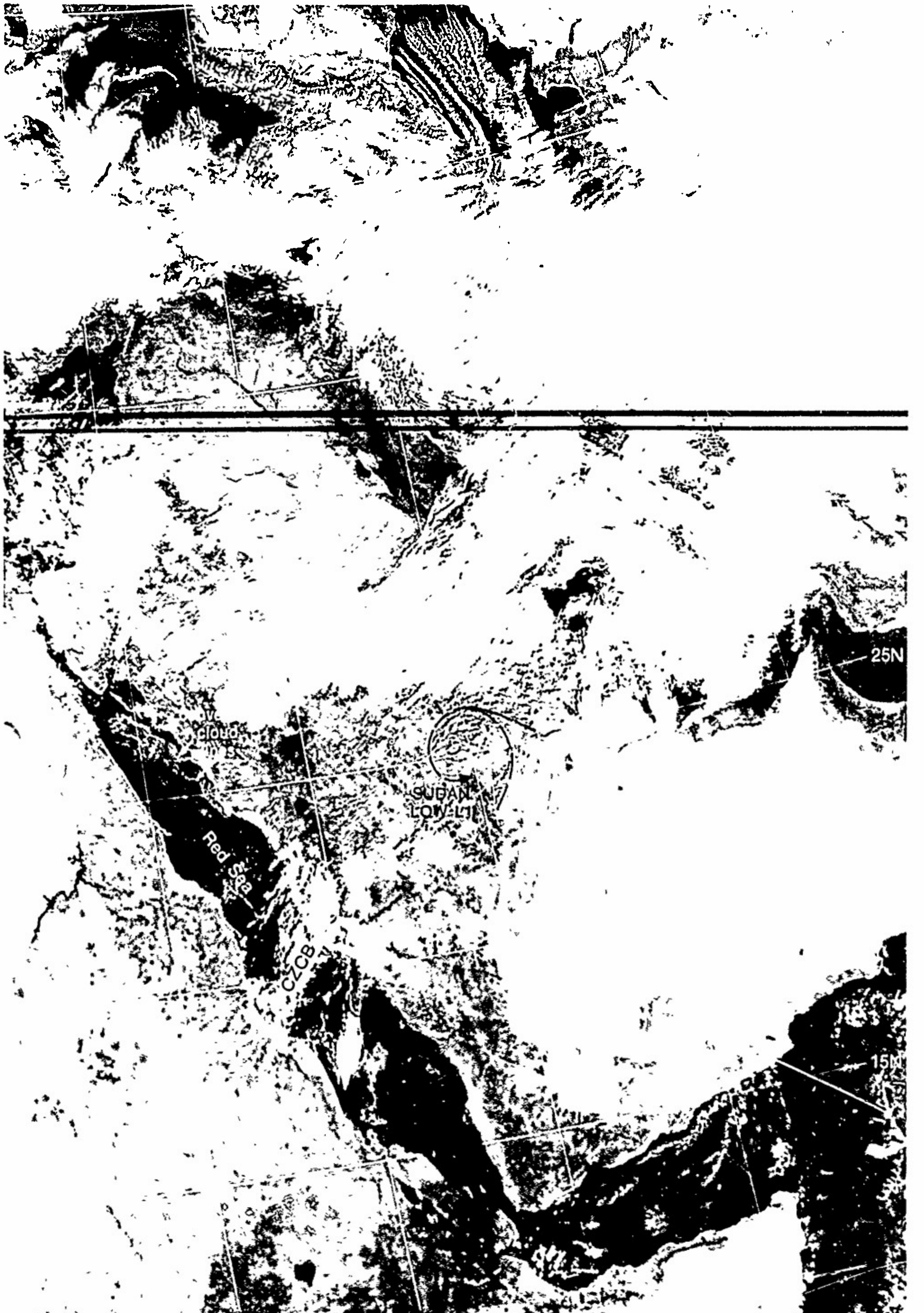


1C-19a F-4 DMSP LF Log Enhancement 0712 GMT 23 January 1980.

300 mb

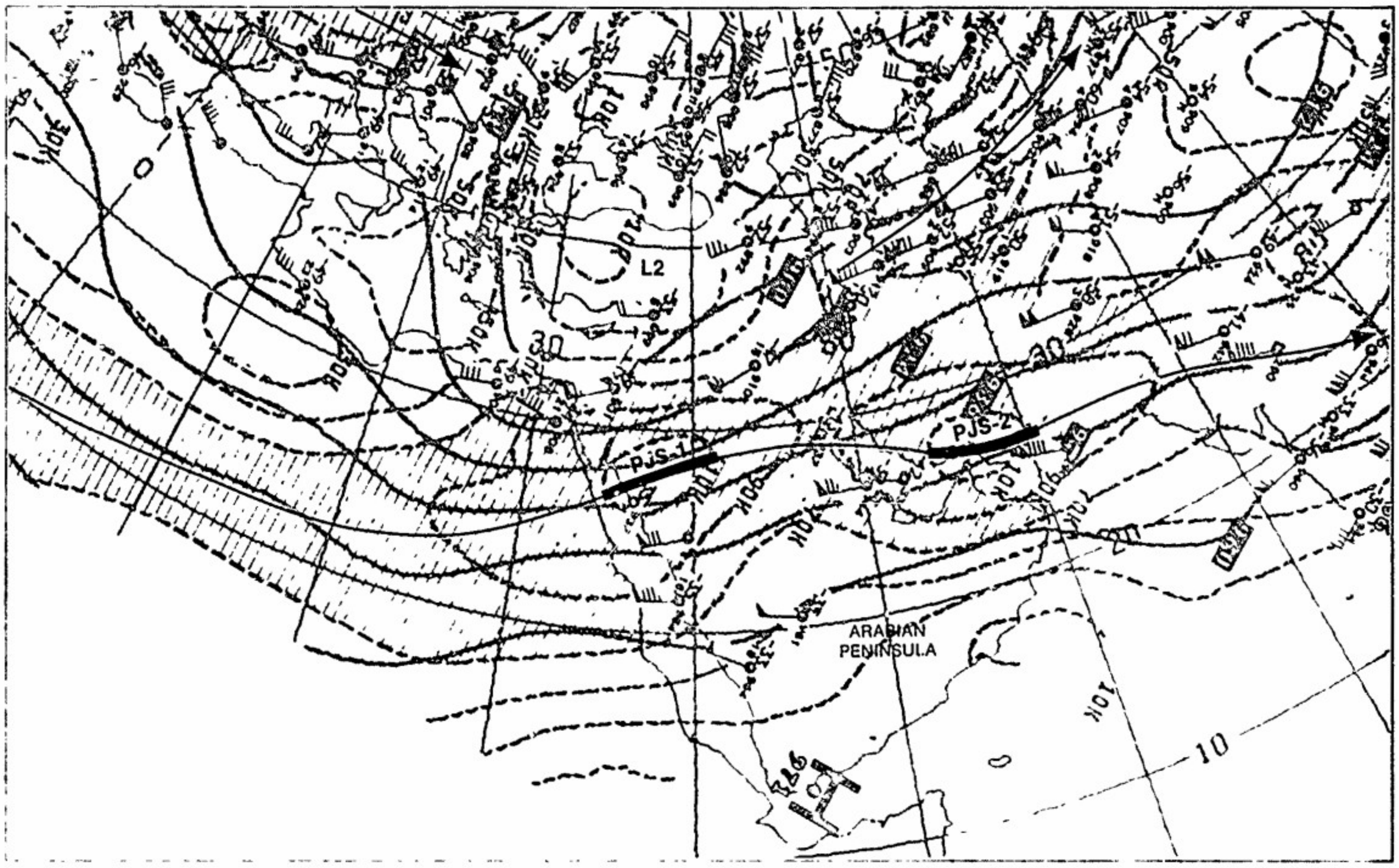


1C-20a. NMC 300-mb Analysis, 0000 GMT 23 January 1980

500 mb

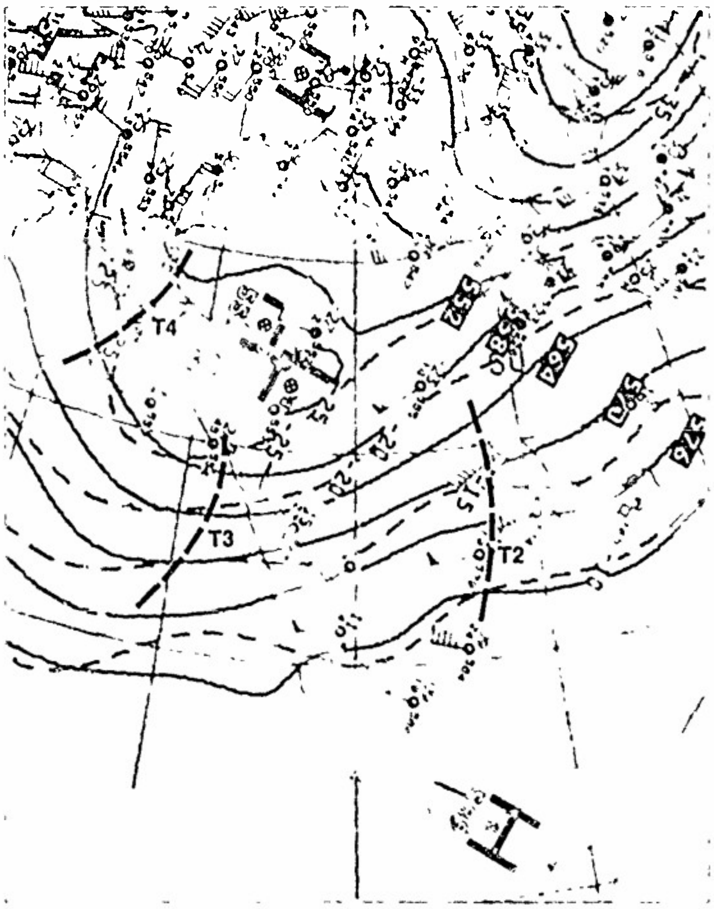


1C-20b. NMC 500-mb Analysis 0000 GMT 23 January 1980

850 mb

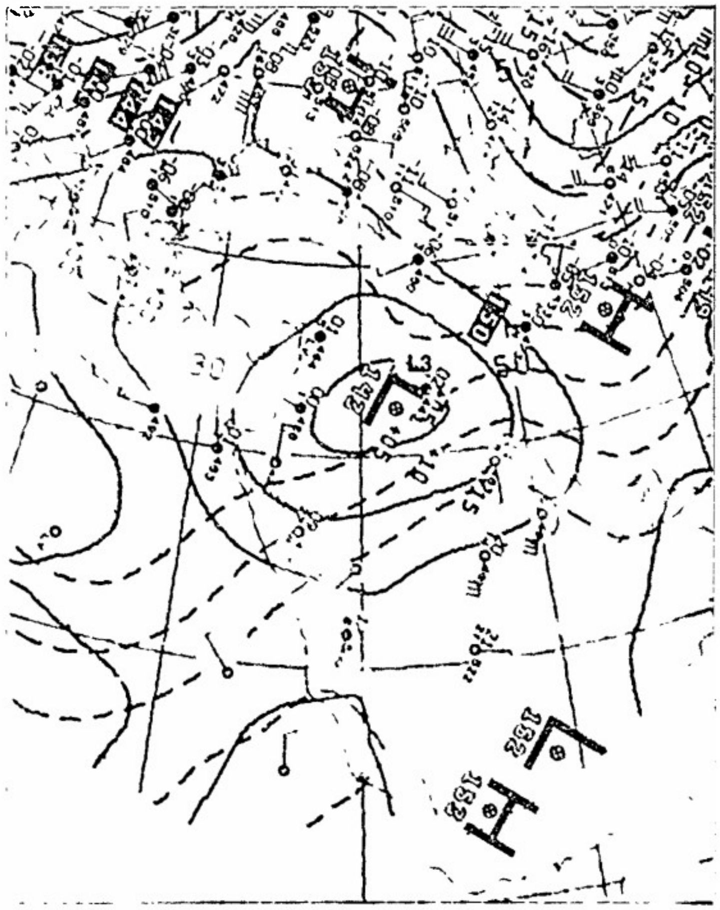


1C-20c. NMC 850-mb Analysis 0000 GMT 23 January 1980

300 mb

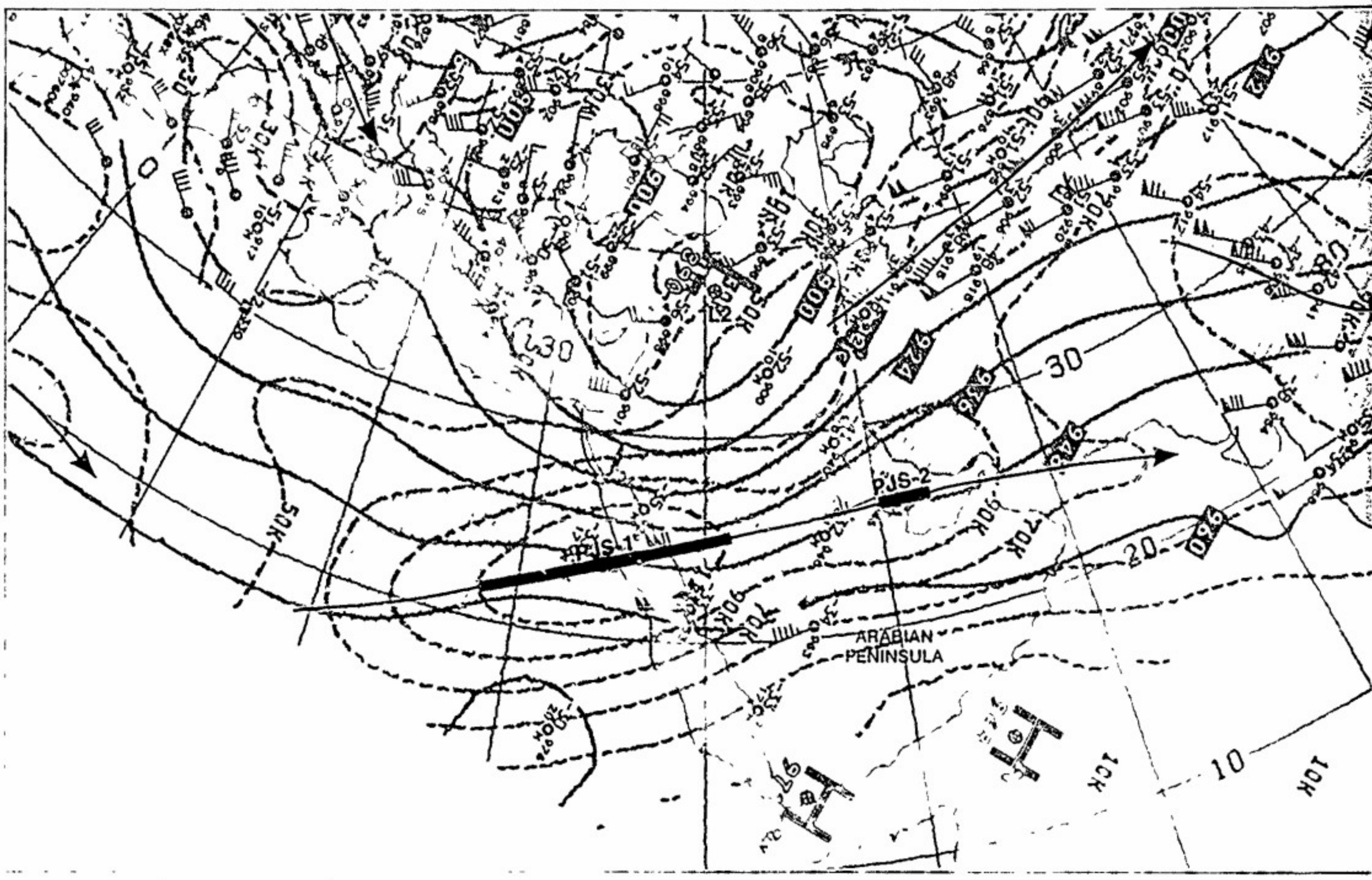


1C-21a. NMC 300-mb Analysis, 1200 GMT 23 January 1980.

500 mb

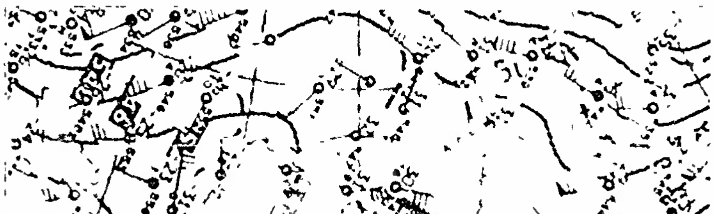


1C-21b. NMC 500-mb Analysis, 1200 GMT 23 January 1980.

850 mb

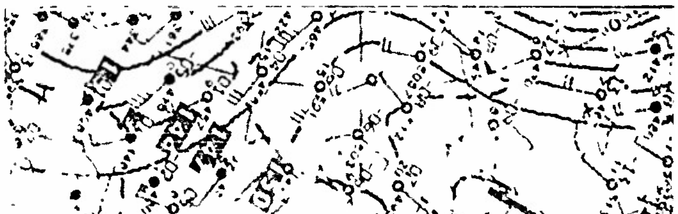


1C-21c. NMC 850-mb Analysis, 1200 GMT 23 January 1980.

## Summary

The movement of the Sudan low from Africa across the Red Sea to central Saudi Arabia, in response to the eastward progression of upper-level troughs extending to lower latitudes, has been shown to be associated with a sudden northward and then southward shift of the CZCB. The weather occurring with this movement was the result of a complex interaction of flow patterns extending from the surface to upper levels.

Through satellite analysis, a shift from the normal position of the CZCB provided the clue to an important change in weather affecting a large portion of the Middle East. The charts on page 1C-22 and satellite picture on page 1C-23 are useful in reviewing some of the significant features. Fog and stratus that had developed over the northern Arabian Peninsula as the moist Mediterranean air moved in behind the original baroclinic zone (1C-13a) was further enhanced on 23 January (1C-23a) by southerly flow around the eastern periphery of the Sudan low L1 as it advanced to central Saudi Arabia. From a larger perspective, the 850-mb flow (1C-22b and 22c) produced warm air advection over Iran which was overrunning cold arctic air, streaming southward from the surface anticyclone north of the Black Sea (1C-22a). This produced the widespread poor weather conditions with low ceilings and heavy snow over that region. Evidence of the intensity of the cold, cross-isobaric arctic flow can be seen in the closely-spaced convective cloud lines over the Caspian Sea (1C-23a). Moist air from the Persian Gulf and the Arabian Sea has also resulted in thunderstorm and shower reports (1C-22a) over the higher elevations of the Zagros Mountains bordering on Iran.

To the east, the 850-mb low (1C-22b and 22c) produced northerly winds which combined with the flow around the Sudan low (1C-18a and 18b) to produce strong northerlies in the Red Sea, driving the CZCB southward.

### surface

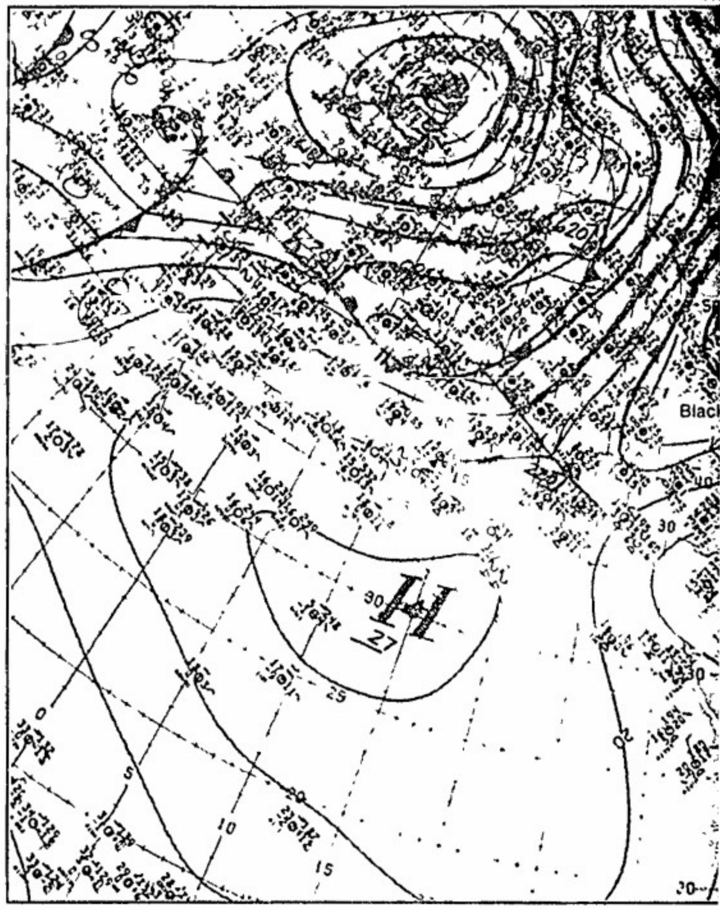


1C-22a. NMC Surface Analysis. 1200 GMT 23 January 1980.

### 850 mb

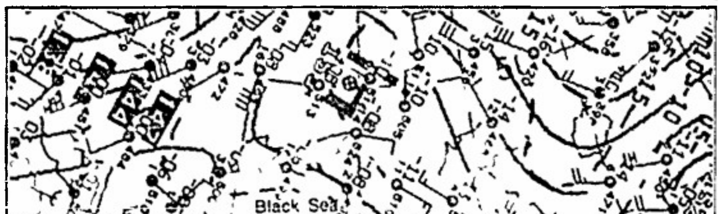


1C-22b. NMC 850-mb Analysis. 0000 GMT 23 January 1980.

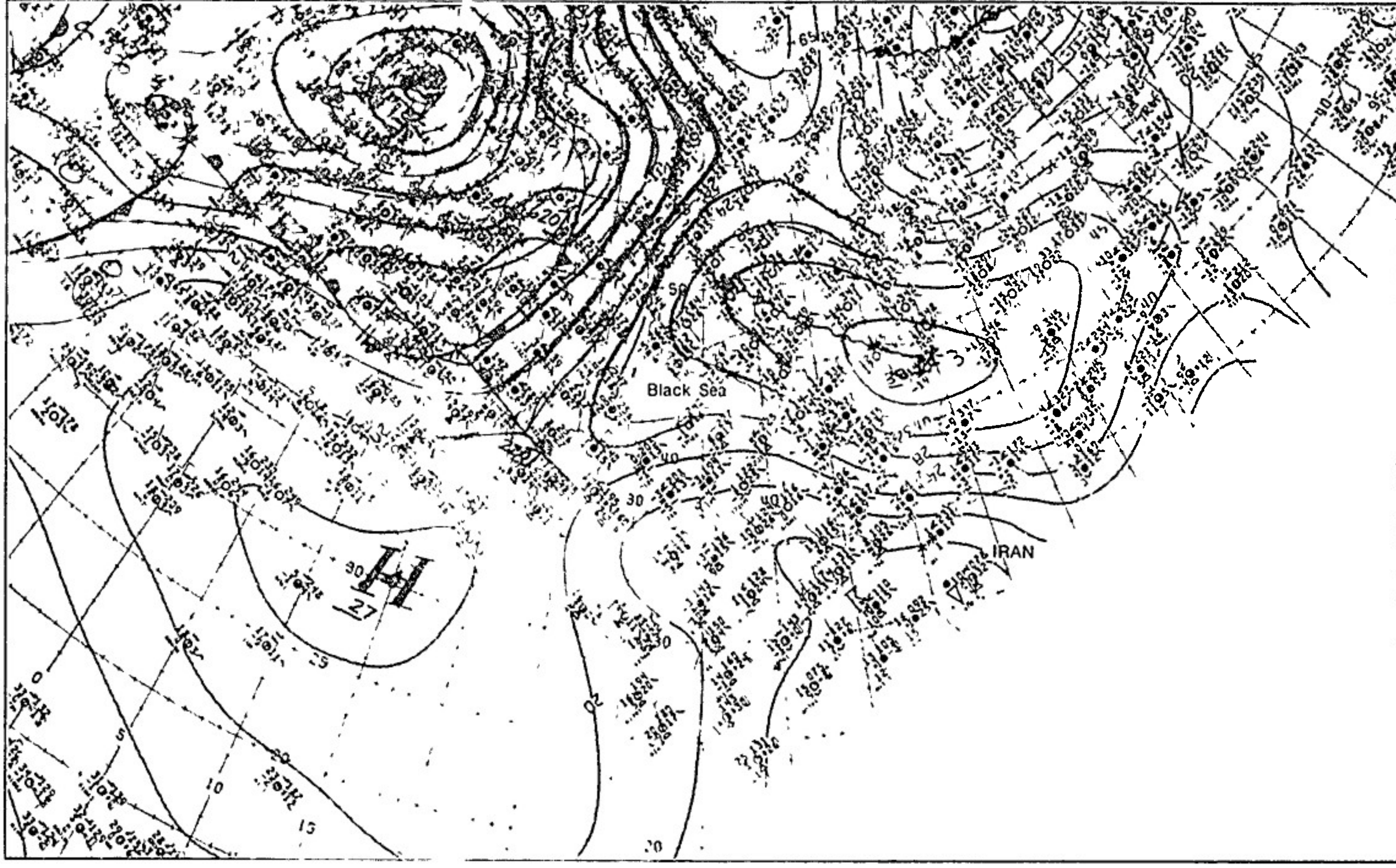


IC-22a. NMC Surface Analysis. 1200 GMT 23 January 1980.

850 mb

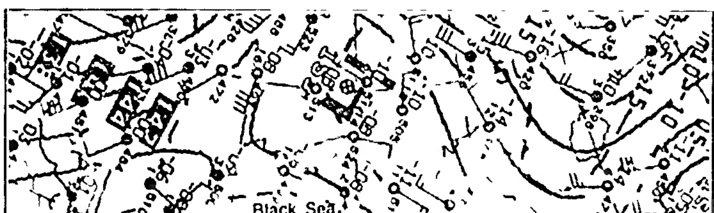


IC-22b. NMC 850-mb Analysis 0000 GMT 23 January 1980

850 mb

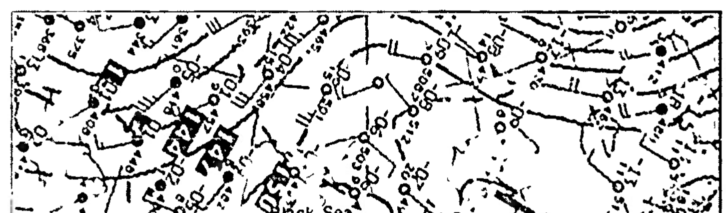


IC-22c. NMC 850-mb Analysis. 1200 GMT 23 January 1980.

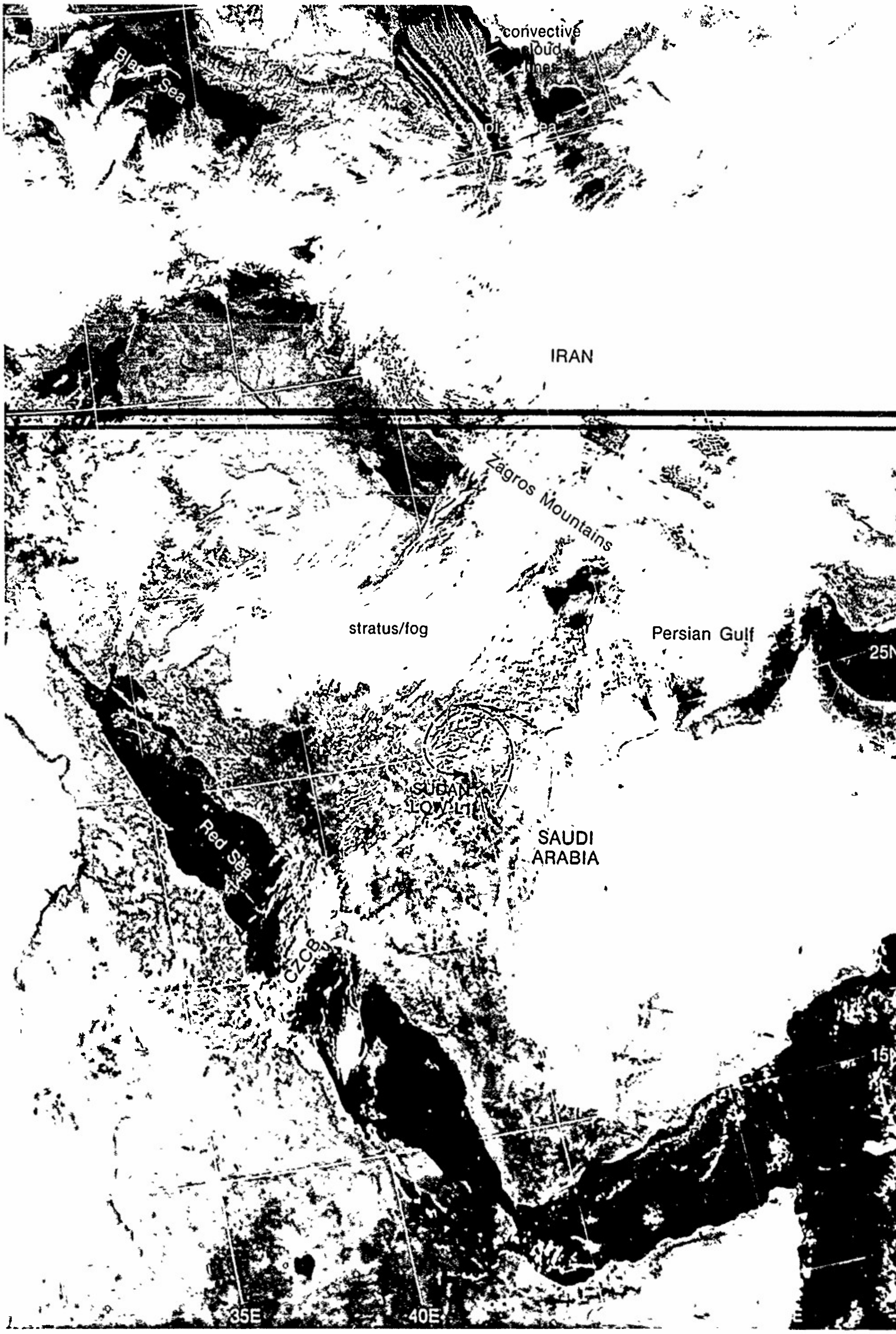


1C-23a 1-4 DMSP LI Fog Enhancement 0712 GMT 23 January 1980. (Note this picture is a repeat of 1C-19a.)

# Case 3 Red Sea/Persian Gulf—Winter

## Subtropical Jet Streams and Surface Anticyclones

The mean meridional circulation in the Northern Hemisphere during winter (1C-25a) shows two prominent jet stream systems: the polar-front jet stream and the subtropical jet stream. At mid latitudes, the polar jet stream is characterized by strong horizontal mixing at mid levels and weak subsidence at low levels. Since the subtropical jet stream is located over the descending branch of the Hadley cell, horizontal mixing at mid levels, as observed with the polar jet, is absent and the development of deep baroclinic zones below the subtropical jet are inhibited.

Subsidence in the descending branch of the Hadley cell accounts for the subtropical high-pressure belt along 30°N. The subtropical high-pressure belt is a persistent climatological feature at low latitudes. From a forecast point of view, however, it is important to recognize that high-pressure centers in the subtropical belt can undergo dissipation and new formation because of the dynamics associated with the subtropical jet stream flow (Reiter, 1963). These effects are most pronounced when deep polar troughs in the westerlies extend to low latitudes.

**References**
Reiter, E R , 1963 *Jet-Stream Meteorology* Chicago: University of Chicago Press, p. 235
Reiter, E R , 1975 Handbook for Forecasters in the Mediterranean. ENVPREDRSCH-FAC Technical Paper 5-75. Naval Environmental Prediction Research Facility, Monterey, Calif , p. III-3

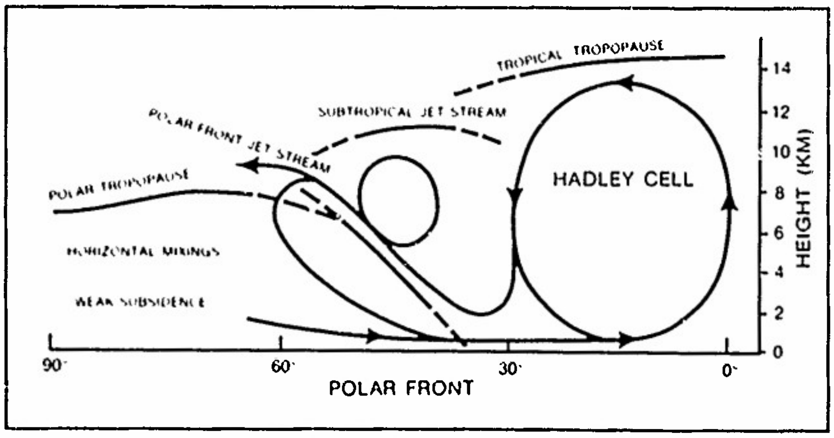


1C-25a Schematic diagram of the mean meridional circulation in the Northern Hemisphere during winter (Reiter, 1975)

18 December

The NMC surface streamline analysis for 0000 GMT (1C-26c) shows the typical winter anticyclone over the Arabian Peninsula The surface high is weak and the areal extent of the anticyclonic circulation is outlined by the pattern of the surface winds. Fair weather prevails over the Arabian Peninsula under the influence of this surface anticyclone.

Although the surface high over the Arabian Peninsula is weak, the height contour pattern at 700 mb (1C-26b) shows a distinct ridge aloft. This ridge is located ahead of a deep polar low L1, which extends to the 200-mb level (1C-26a) On the 200-mb analysis, note that the polar jet associated with the low L1 has apparently merged with the subtropical jet to the south. A single 110-kt jet streak PJS/SJS appears over the northern Arabian Peninsula where the two jets have merged Jet stream cirrus on the DMSP infrared picture (1C-27a), however, reveals the double structure of the merged jets. The polar jet cloudiness is striated in appearance with numerous small-scale transverse cloud bands. The subtropical jet cloudiness shows cirrus cloud streaks and filaments oriented perpendicular to a denser band of cirrus along the northern edge This is an excellent example of the appearance of subtropical jet stream cirrus in satellite imagery.

An examination of the location of the ridge at 700 mb over the Arabian Peninsula (1C-26b) with respect to the PJS/SJS at 200 mb (1C-26a) shows that the ridge is under the right-front quadrant of the 110-kt jet streak, which is an area of upper-level convergence and lower-level divergence. As a result, subsidence associated with the low-level divergence under the merged polar subtropical jet acts to enhance the ridging observed at 700 mb; however, the subsidence is not pronounced because only a weak anticyclonic circulation is observed at the surface (1C-26c).

By 1200 GMT, the 110-kt jet streak PJS/SJS at 200 mb (1C-28a) has advanced eastward over the Persian Gulf, and the central and southern Arabian Peninsula is no longer under the influence of the right-front quadrant of this jet streak The consequences of this change aloft are the sharp reduction in the amplitude of the 700-mb ridge (1C-28b) over the southern Arabian Peninsula and a corresponding weakening of the surface anticyclone (1C-28c). The enhancement of the low-level ridge and its subsequent weakening is in accordance with Reiter's comments (see page 1C-25) on the change in intensity of surface anticyclones because of changes in the dynamics associated with the subtropical jet stream.

On the satellite picture (1C-29a), the cirrus over the central Arabian Peninsula has increased in response to a new 110-kt polar jet streak crossing the Red Sea at 200 mb (1C-28a). The dense cirrus shield observed on the satellite picture is typical of polar jet cirrus. Intermittent light rain at O1 (1C-28c) indicates that baroclinic instability and deep convection extend to low levels beneath the jet

19 December

On the NMC 200-mb analysis at 0000 GMT (1C-30a), a broad, merged jet stream system extends from northeast Africa to India. Prominent 130-kt jet streaks PJS/SJS are located over the Arabian Peninsula and northwest India. The deep polar low L1 has become stationary over the eastern Mediterranean. The NMC surface streamline analysis (1C-30c) shows a very weak anticyclonic circulation and a flat high-pressure gradient over the eastern and southern Arabian Peninsula—the center of the surface high over this area is located to the northeast over Afghanistan. This indicates that there is no localized area of subsidence extending through a deep layer of the atmosphere over the southern Arabian Peninsula to enhance surface high pressure, as occurred on the previous day (1C-26b and 26c). There is a ridge at 700 mb (1C-30b) over the southern Arabian Peninsula; however, it is a reflection of the general anticyclonic pattern which extends to 200 mb in advance of the upper low L1.

Fair weather prevails over the southern Arabian Peninsula, which is under the influence of the general anticyclonic flow aloft. On the satellite picture (1C-31a), the isolated cirrus band located over central Saudi Arabia is anvil cirrus. The general southwest-northeast orientation of the cirrus streaks is in response to the 200-mb (1C-30a) SJS (J1-J1) which extends from Africa, across the Red Sea, to central Saudi Arabia. Note also the development of the low-level convergence zone cloud band (CZCB) over the central Red Sea (see Case 1).

Important Conclusions

1. High-pressure centers in the subtropical belt undergo changes in intensity because of the dynamics associated with jet streaks in the upper atmosphere.

2. The changes in intensity of surface high-pressure centers are most pronounced when the subtropical jet is associated with deep polar troughs in the westerlies extending to low latitudes.

3. On satellite imagery, cirrus cloudiness provides details on jet streak structure in areas of polar subtropical jet stream surface anticyclone teleconnections.

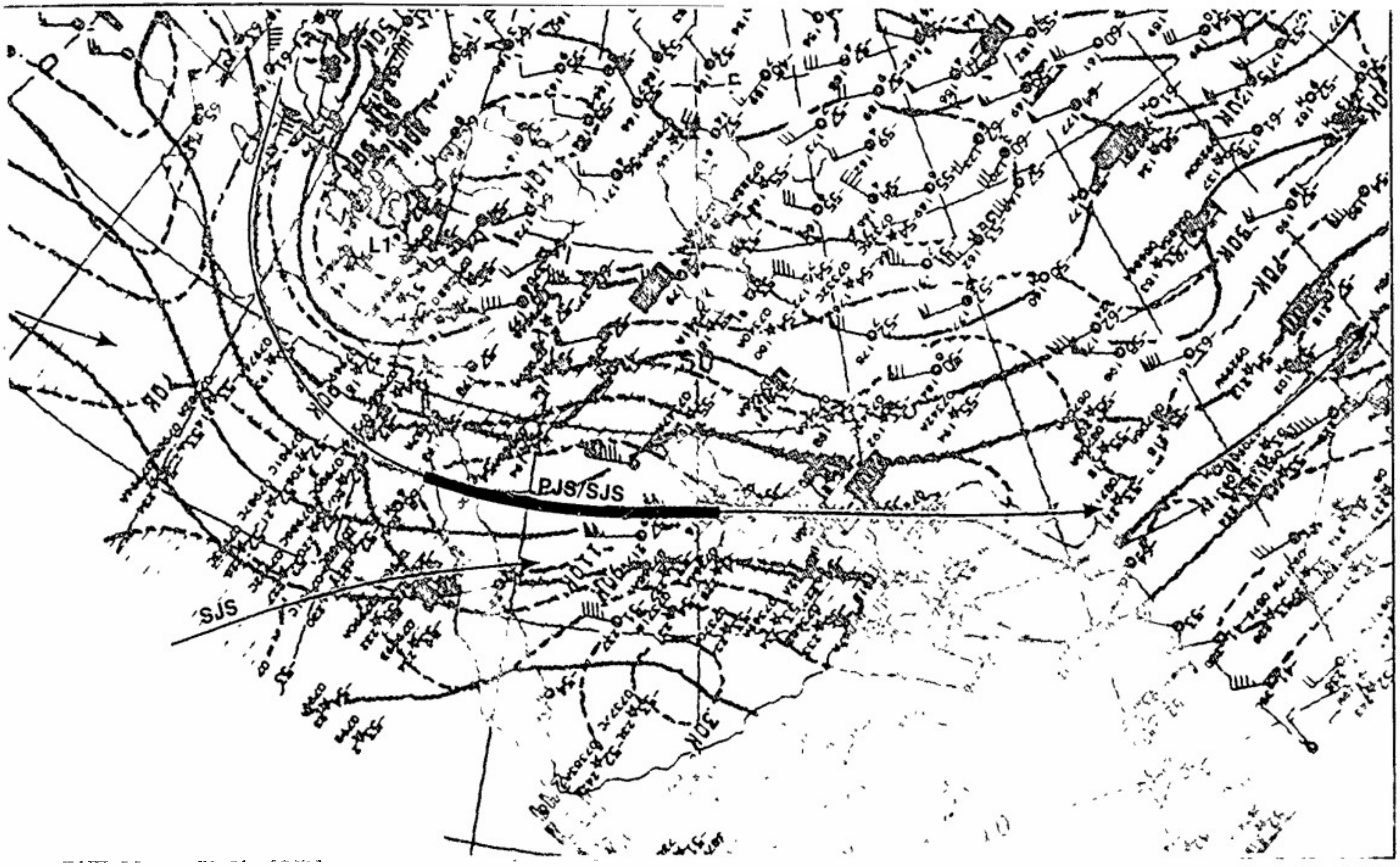


1C-26a. NMC 200-mb Analysis. 0000 GMT 18 December 1979.

**700 mb**


1C-26b. NMC 700-mb Analysis. 0000 GMT 18 December 1979.

**surface**

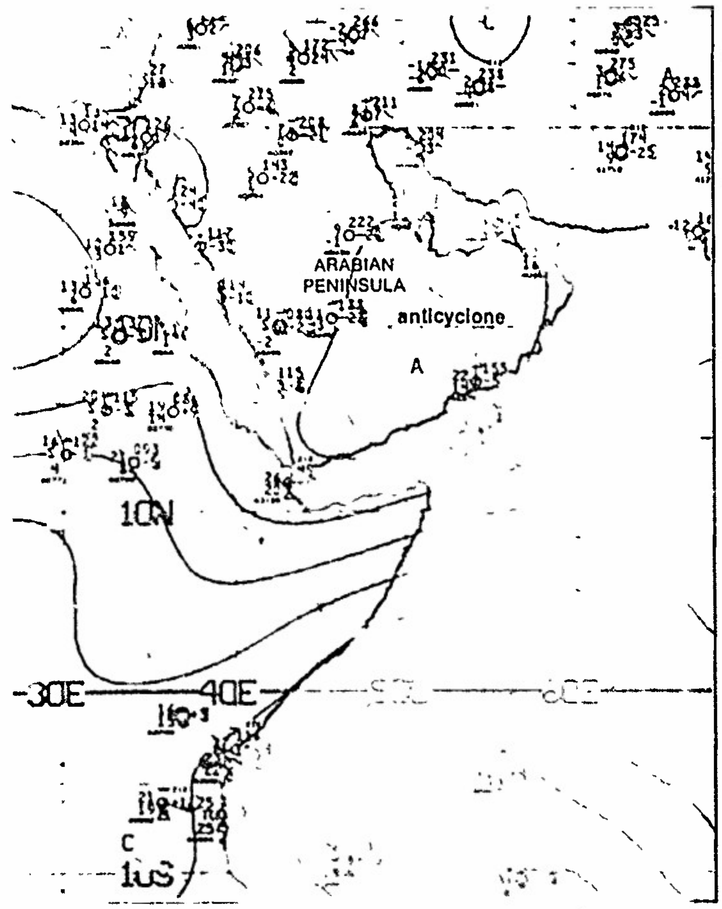


1C-26c. NMC Tropical Surface Streamline Analysis 0000 GMT 18 December 1979

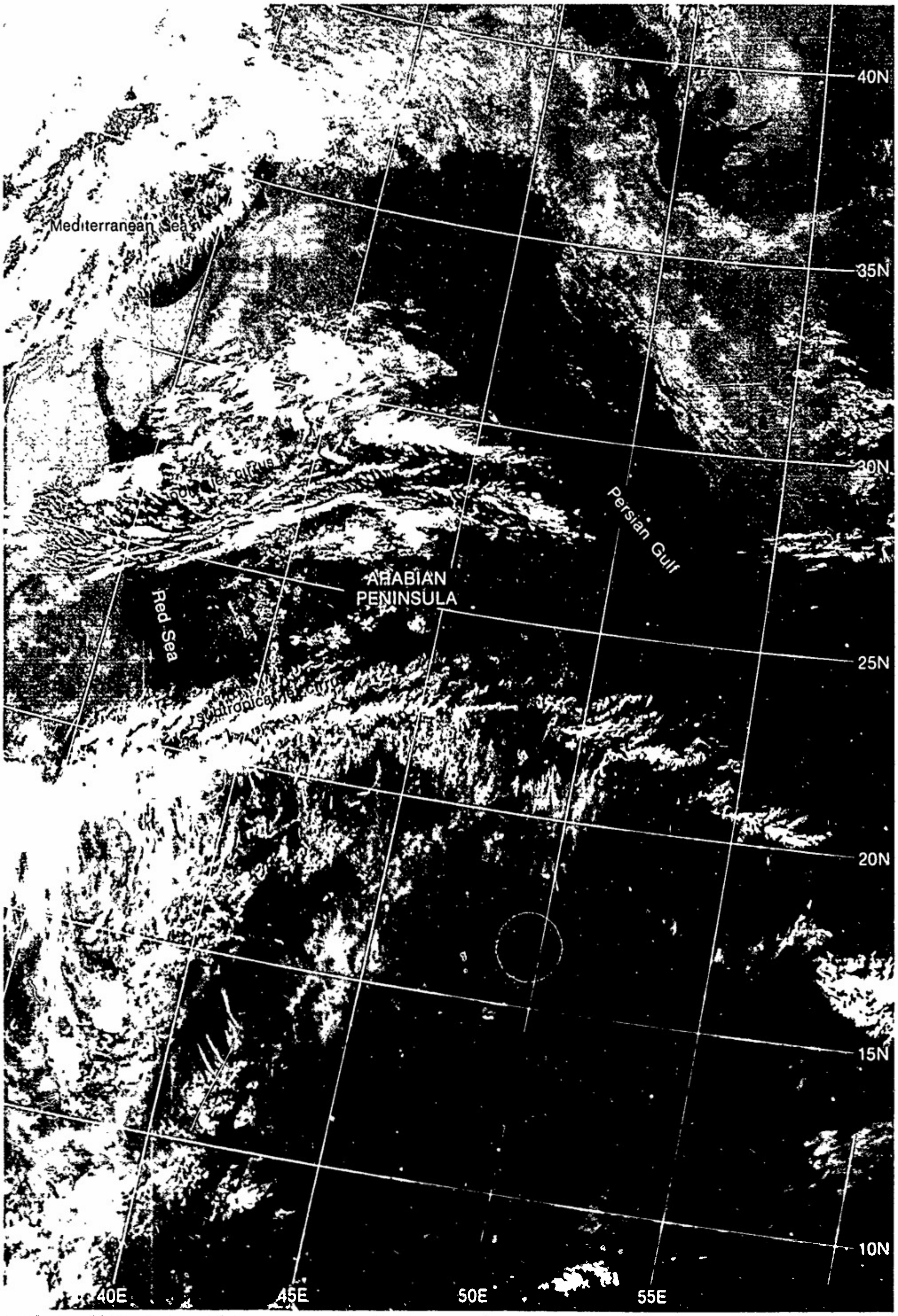


IC-27a F-4 DMSP TF Normal Enhancement 1745 GMT 17 December 1979

## 200 mb

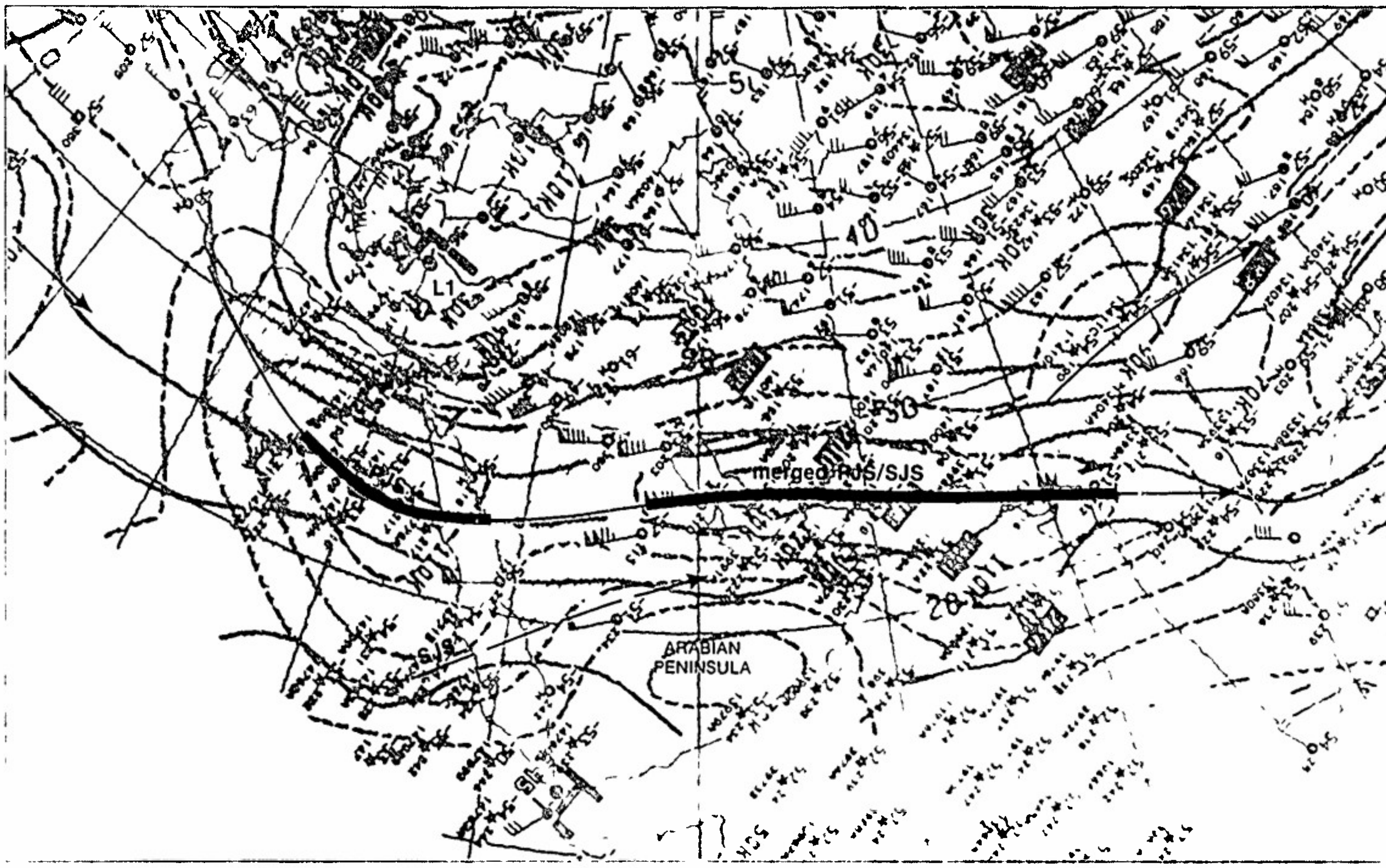


1C-28a. NMC 200-mb Analysis. 1200 GMT 18 December 1979.

## 700 mb

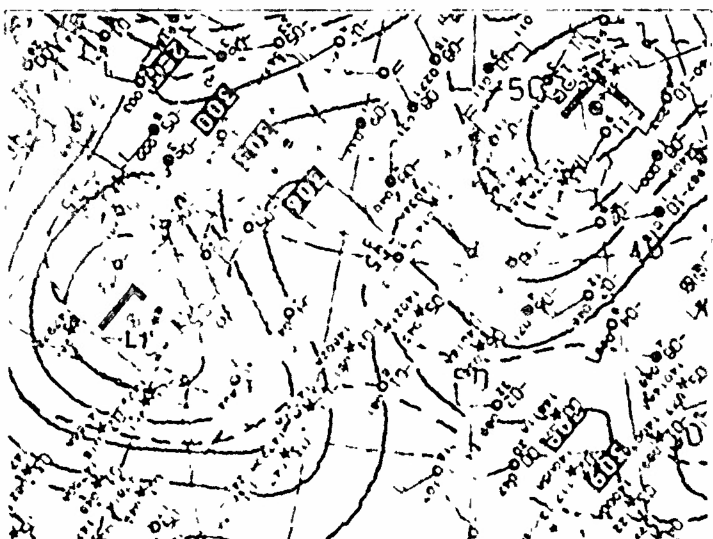


1C-28b. NMC 700-mb Analysis. 1200 GMT 18 December 1979.

## surface

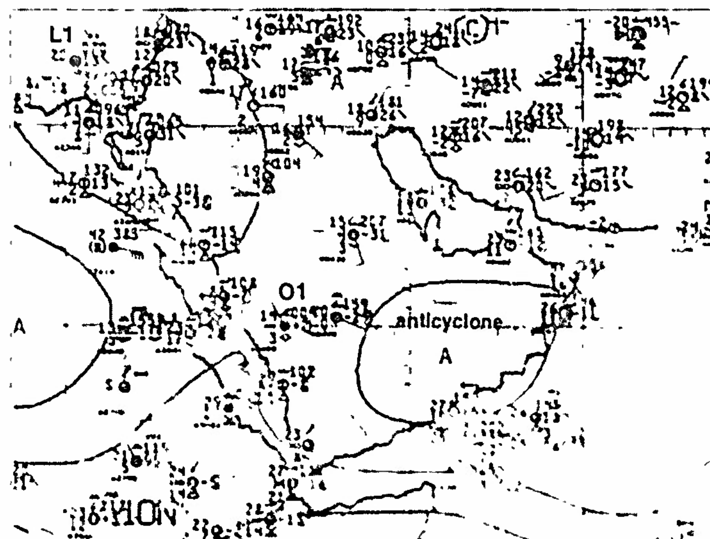


1C-28c. NMC Tropical Surface Streamline Analysis. 1200 GMT 18 December 1979

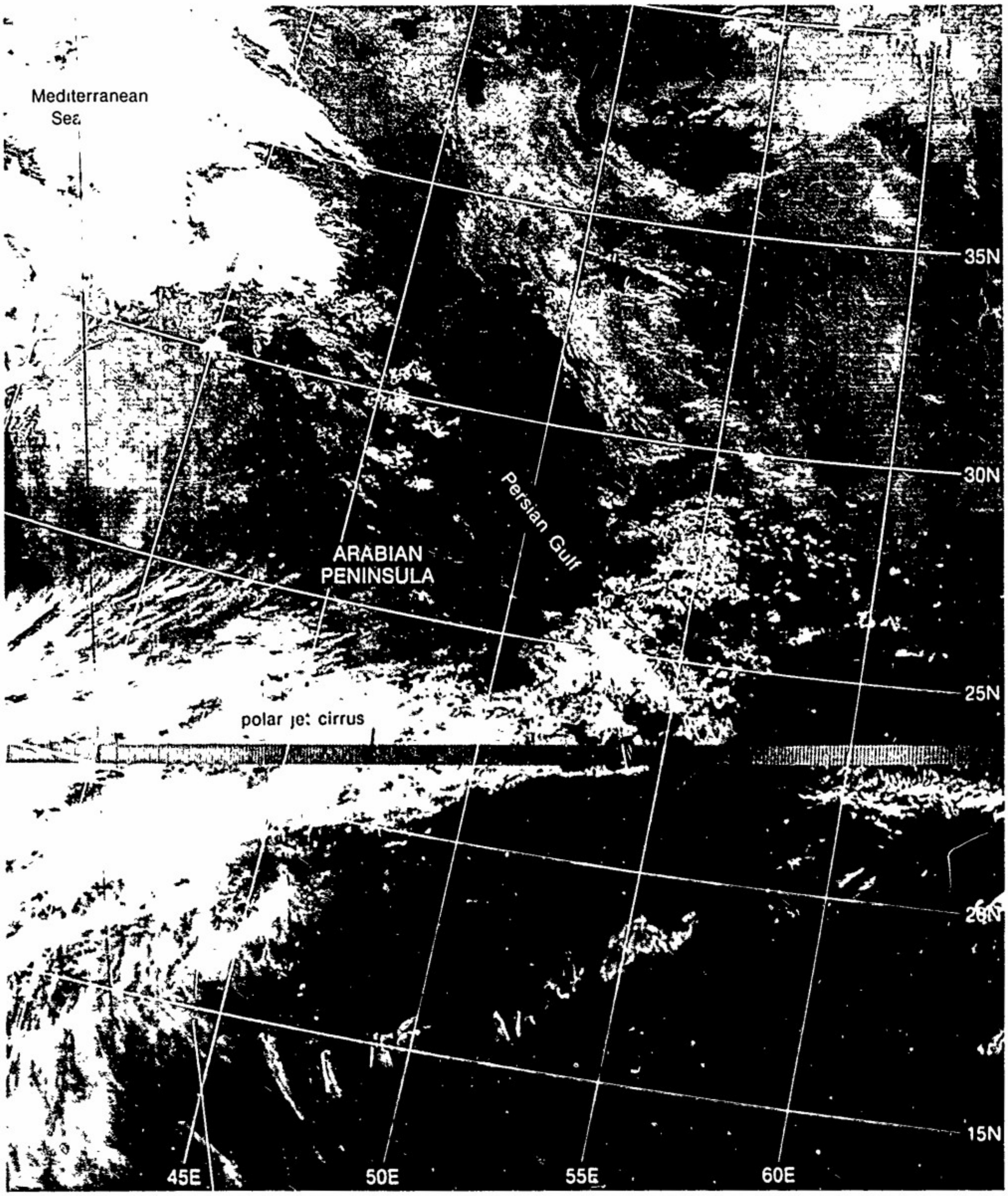


1C-29a F-4. DMSP TF Normal Enhancement. 1725 GMT 18 December 1979

**200 mb**

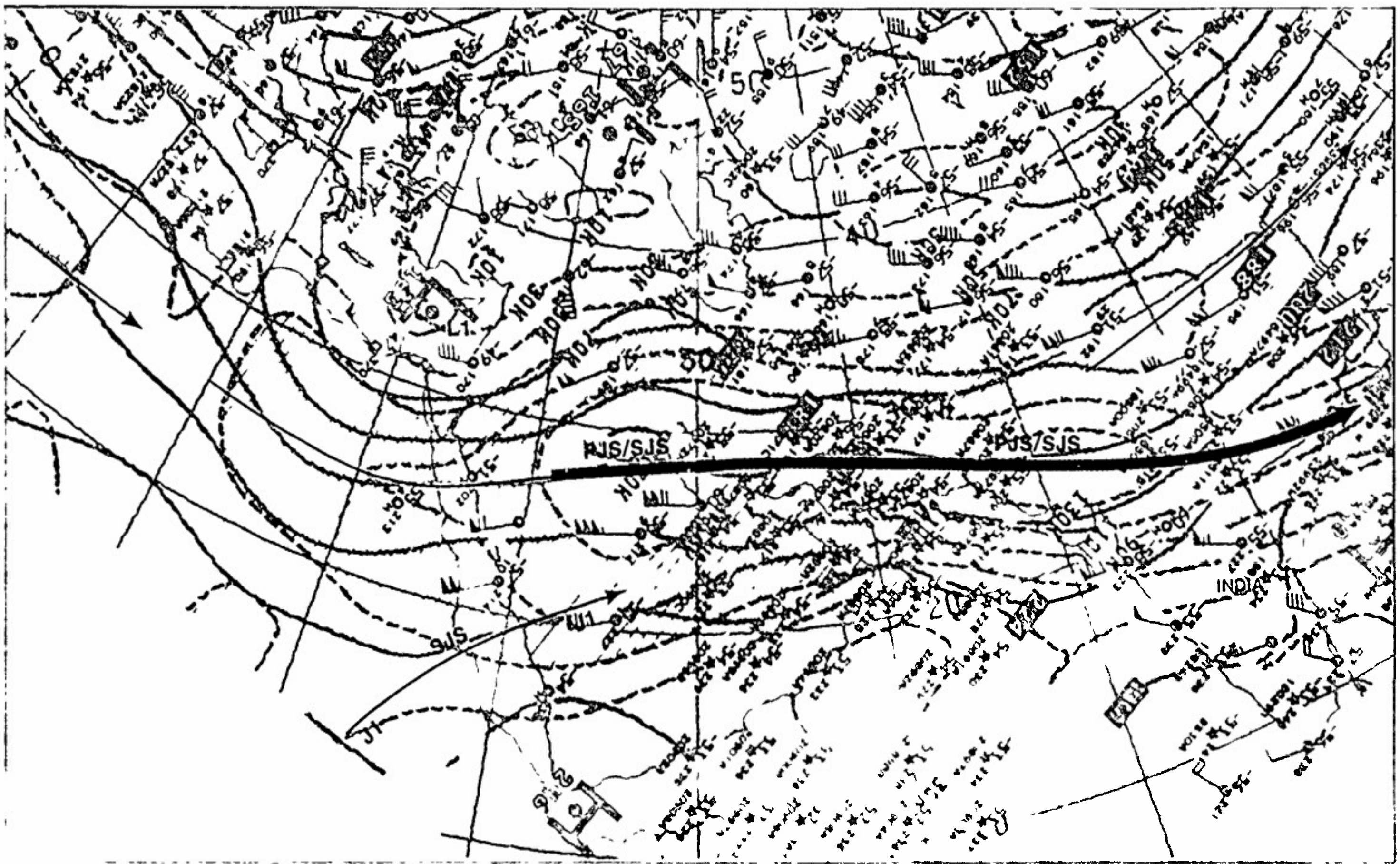


1C-30a. NMC 200-mb Analysis. 0000 GMT 19 December 1979.

**700 mb**

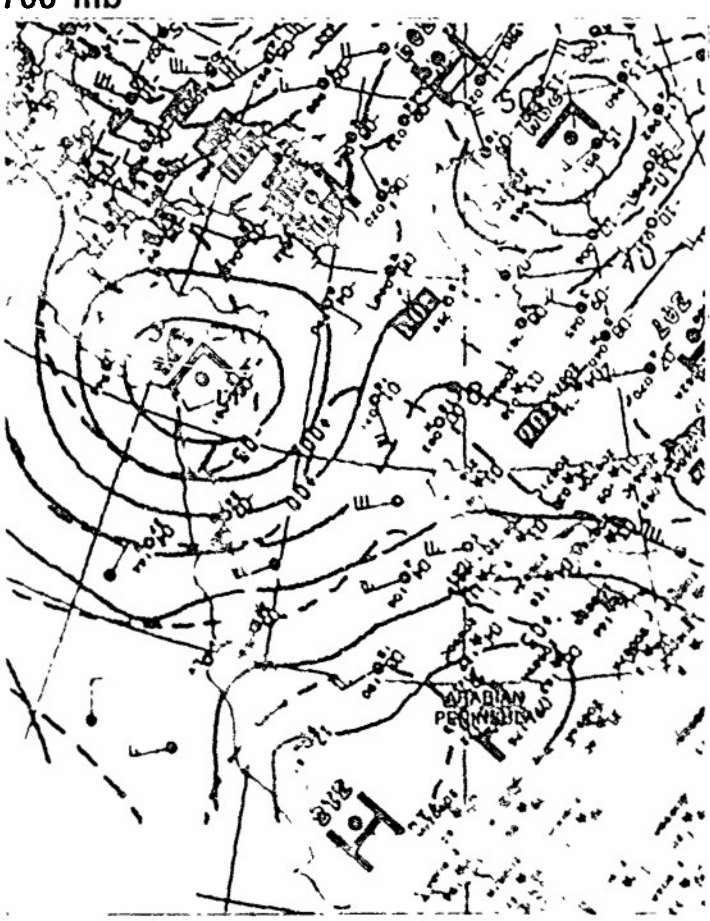

1C-30b. NMC 700-mb Analysis. 0000 GMT 19 December 1979

**surface**

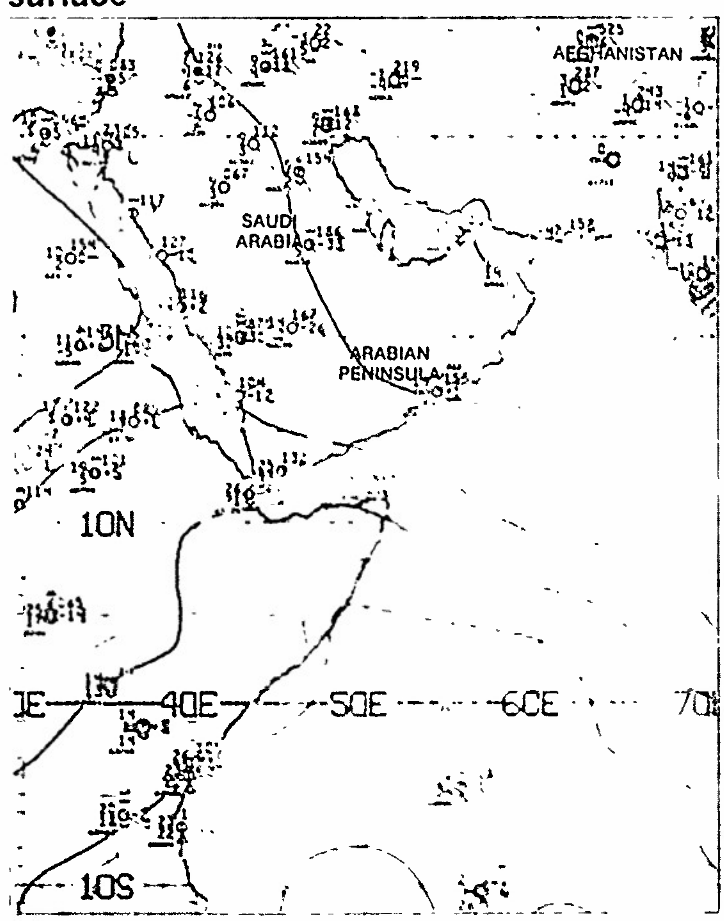


1C-30c. NMC Tropical Surface Streamline Analysis. 0000 GMT 19 December 1979

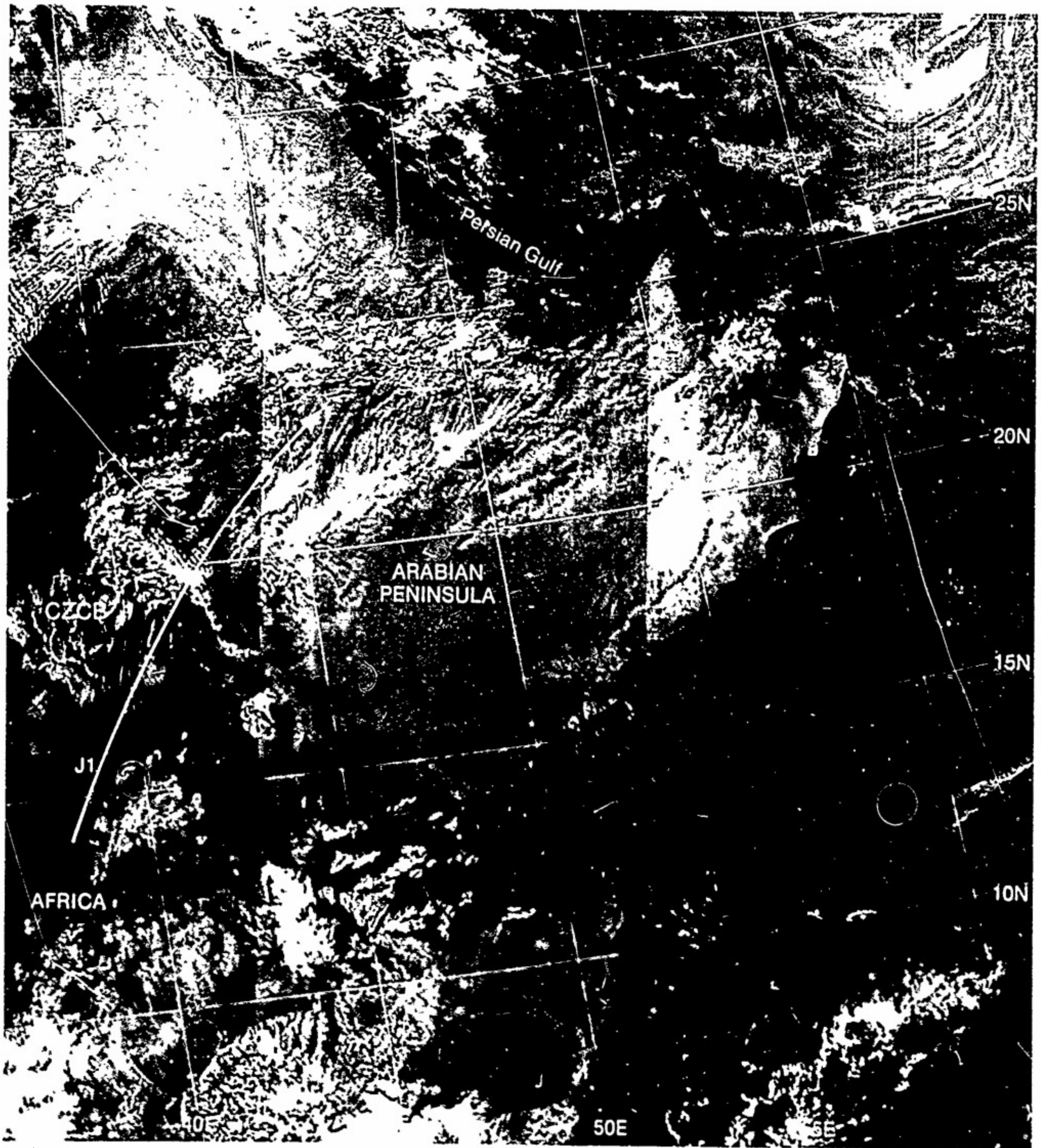


1C-31a F-4 DMSP LF Normal Enhancement 0607 GMT 19 December 1979

# Case 4 Red Sea/Persian Gulf—Winter

## *Winter Storms over the Arabian Peninsula*

During the cooler season, depressions which affect the Arabian Peninsula enter the region from the Mediterranean. Most of these depressions tend to fill and weaken as they progress inland and, in general, they follow an easterly track. Fronts associated with the disturbances may show sharp changes of wind direction and have heavy squalls, but as a rule there is very little or no rain. Downdrafts from thunderstorms along squall lines often generate vigorous dust storms at the surface.

The following case study covers part of the same period, 18-19 December 1979, as the previous case (Case 3). In the previous case, the emphasis was on the changes in intensity of the surface anticyclone over the southern Arabian Peninsula in response to dynamics of the subtropical jet stream flow. This case examines a winter storm development in a Mediterranean depression that moves inland over the northern Arabian Peninsula. Rapid intensification of the depression occurs following the movement of a jet streak around the base of the upper-level trough in which the depression is located. Of particular interest is the development of a squall line in response to the dynamics of a merged polar jet and subtropical jet in advance of the trough aloft.

Since the supporting baroclinic zone with the subtropical jet stream exists only in the upper troposphere beneath the jet core, the wind field at middle levels is only barely affected and the potential for instability and growth of deep convection is inhibited. However, a polar jet stream with its characteristic deep tropospheric baroclinic zone in close proximity to the northern border of a subtropical jet can provide the mechanism for convection to develop through a deep vertical layer. Convection is sharply inhibited south of the subtropical jet core beginning in the region where wind speeds decrease abruptly.

**17 December**

The NMC 200-mb analysis for 1200 GMT (1C-34a) shows an upper-level trough L1 in the westerlies extending to low latitudes, and a strong subtropical jet stream to the south with a jet streak maximum over the Red Sea and one further east over the Persian Gulf. An examination of the DMSP infrared picture (1C-35a), acquired about 6 hours after chart time, shows typical anticyclonically curved subtropical jet stream cirrus over the south-central Arabian Peninsula. In addition, the presence of the striated band of cirrus over the north-central Arabian Peninsula is characteristic of the polar jet stream. The proximity of these cirrus bands indicates that the polar westerlies from the Mediterranean have merged with the subtropical flow over the central Arabian Peninsula. This accounts for the analyzed single PJS/SJS1 wind maximum over the Red Sea. Upstream of the trough L1 at 200 mb (1C-34a), a 90-kt polar jet streak PJS2 in the westerlies is digging southward toward the subtropical jet. At 300 mb (1C-34b), this wind maximum increases to 150 kt.

At lower levels over the eastern Mediterranean, there is a closed low L1 at 850 mb (1C-36a) and at the surface (1C-36b). Although the surface low is not particularly deep (1008 mb), the satellite picture (1C-37a) shows a squall line, exhibiting the characteristic line of globular convection clouds, in progress ahead of the surface cold front. This indicates strong convective instability aloft in the flow in advance of the upper-level low which is strongly diffluent in the mid through upper troposphere (1C-34a, 34b, and 36a). In the satellite picture, the decrease in cloud cover inland reveals that the surface warm front (1C-36b) is weak and dissipating. Note also the southerly winds on the surface streamline analysis (1C-36c) over the southern Red Sea and the advection of warm, moist air at 850 mb (1C-36a) northward along the western periphery of the high over the Arabian Peninsula. This is a primary source of moisture for convective developments over the central Arabian Peninsula.

**18 December**

On the early morning DMSP visible picture (1C-39a), the absence of organized cloudiness over western Iraq, which showed baroclinic zone clouds 12 hours earlier (1C-37a), indicates that the surface low L1 over the eastern Mediterranean has not intensified. This is confirmed by the 0600 GMT surface analysis (1C-38d) which shows that the surface low L1 has remained weak (1008 mb) and advanced slowly eastward during the preceding 12 hours. On the satellite picture, the overcast area south of the Caspian Sea is upslope fog and stratus along the Elburz Mountains produced by the southerly flow around the eastern periphery of the surface low L1. The most significant weather change in the region has occurred over the central Arabian Peninsula, where local areas of deep convection have been initiated and cumulonimbus have developed.

The convective instability is occurring in the region under the merged polar westerlies and subtropical jet stream at 200 mb (1C-38a), where the moist, warm air has advanced over the Arabian Peninsula at 850 mb (1C-38c). Note that the location of the jet stream core, as superimposed on the satellite picture (1C-39a), is not the dividing line between the convectively unstable region to the north and the mostly clear region over the southern Arabian Peninsula, as might be expected. The separation is more precisely defined by the axis of maximum anticyclonic vorticity, that is, where the jet-force winds at 200 mb decrease in speed to the south of the jet core most rapidly. This occurs near 20 N, or about 5 degrees south of the jet core, and is roughly where the change from deep convection to mostly clear occurs on the satellite picture. At 300 mb (1C-38b), the polar jet streak PJS2 continues to move southward in the westerlies that have merged with the subtropical jet over the Arabian Peninsula.

On the late afternoon DMSP infrared picture (1C-41a), jet-associated cirrus covers the central Arabian Peninsula from the Red Sea to the Persian Gulf. This jet cirrus has developed in the newly formed 110-kt jet streak PJS/SJS2 at 200 mb (1C-40a). The new jet streak developed as the polar jet streak PJS2 in the westerlies advanced around the base of the 200-mb low L1 and merged with the subtropical jet over the central Arabian Peninsula. The merger is more clearly evident from a comparison of the isotach analysis over the Red Sea at 300 mb (1C-40b) and the corresponding isotach analysis (1C-38b) 12 hours earlier. Note that the jet streak PJS/SJS1 has moved eastward beyond the Persian Gulf.

On the satellite picture (1C-41a), cirrus debris from convective activity below the jet extends across the Persian Gulf. Intermittent light rain from convective buildups beneath the jet cirrus was observed at 1200 GMT (not shown). However, the surface report O1 on the 1800 GMT surface streamline analysis (1C-40d) shows dust in suspension. In all probability the dust was raised by mesoscale convective activity in the region.

The cumulonimbus buildups and precipitation observed along the eastern Mediterranean coast (1C-40d) indicate that the surface low L1 is intensifying as it moves eastward. The bright, dense overcast (baroclinic zone cloudiness) over the eastern Mediterranean and northwest Iraq (1C-41a) is associated with the convective developments along the coast and the short-wave trough T1 which has developed along the southeastern periphery of the 850-mb low L1 (1C-40c).

*continued on page 1C-42*

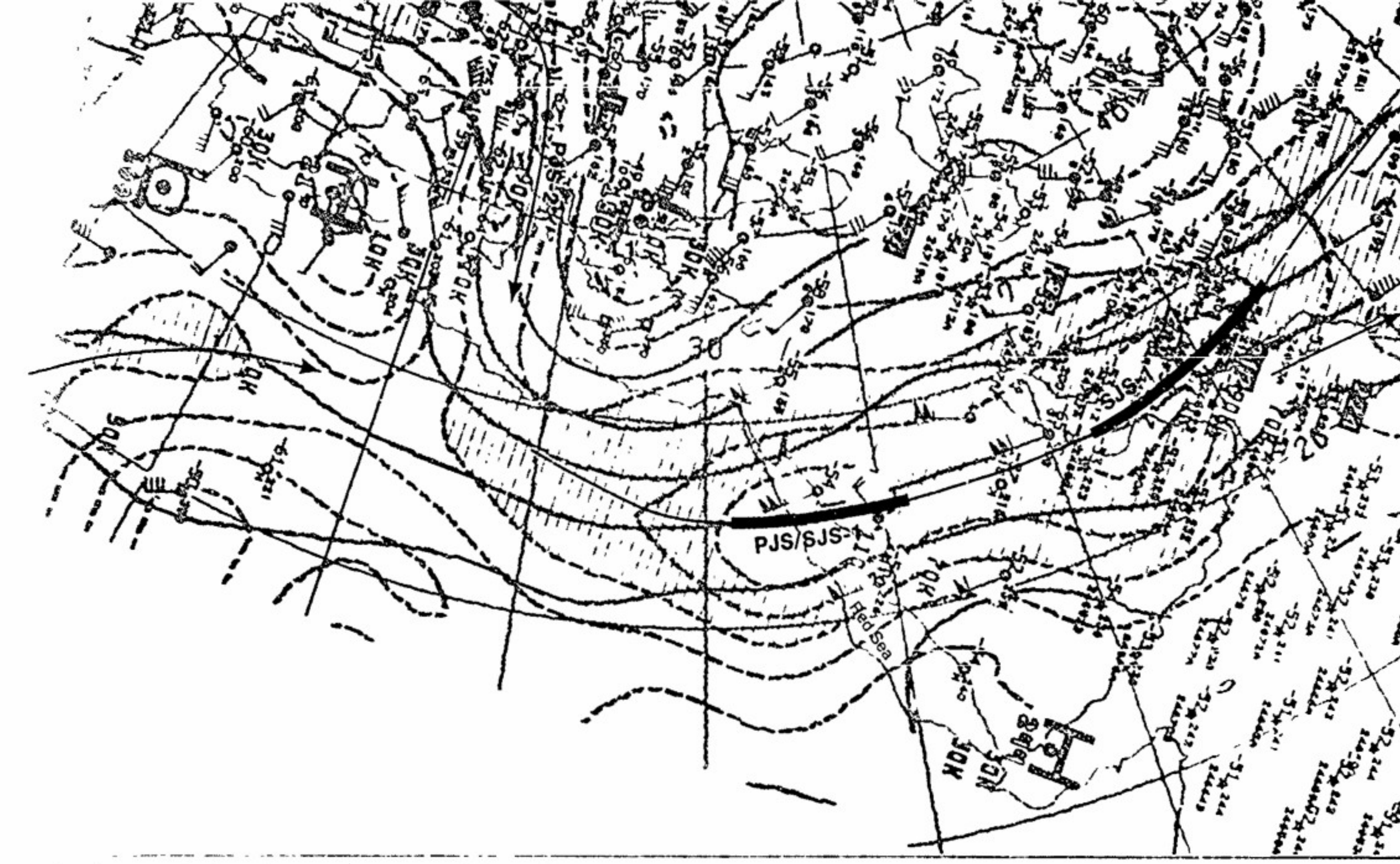


1C-34a NMC 200-mb Analysis. 1200 GMT 17 December 1979.

300 mb

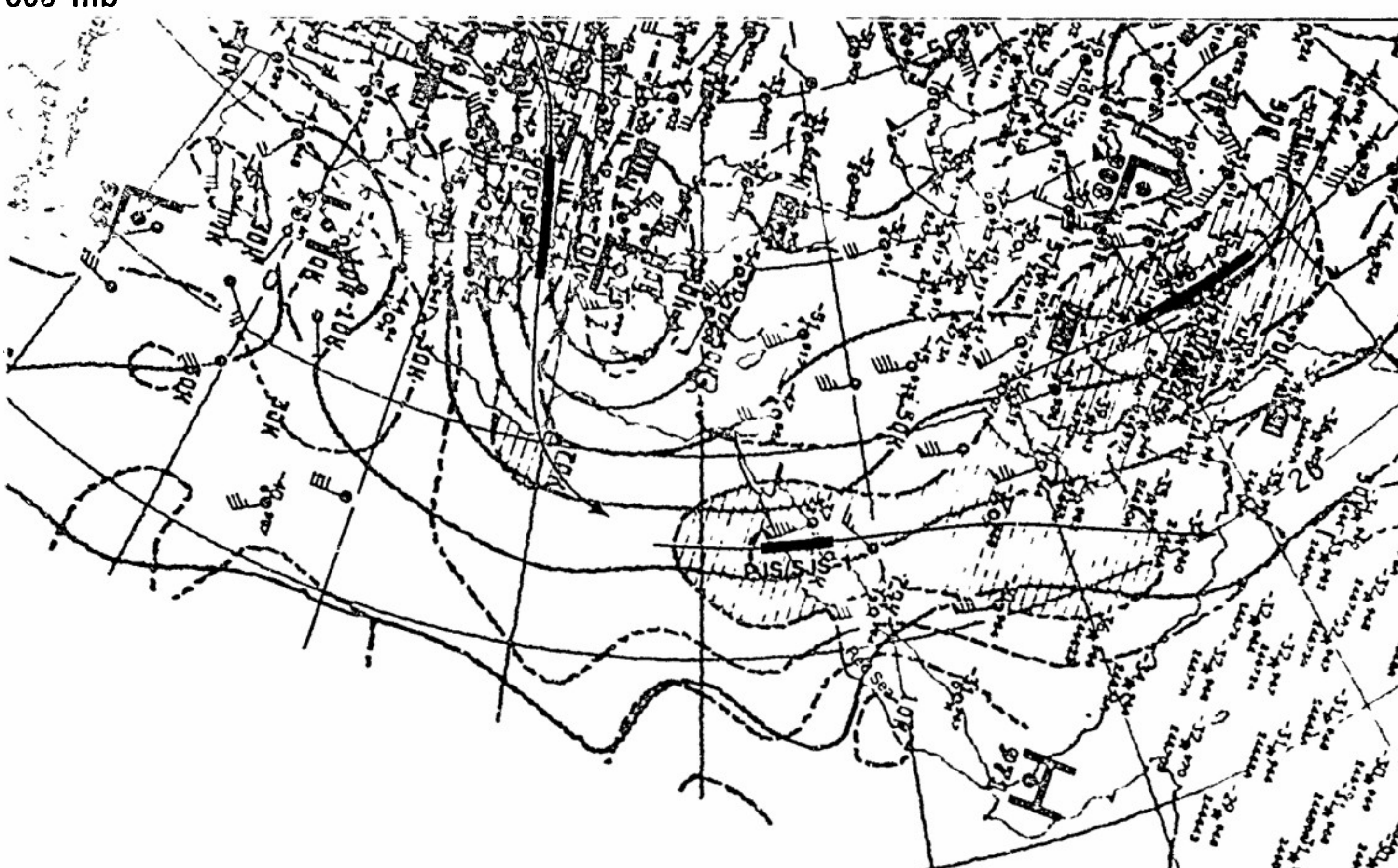


1C-34b NMC 300-mb Analysis 1200 GMT 17 December 1979

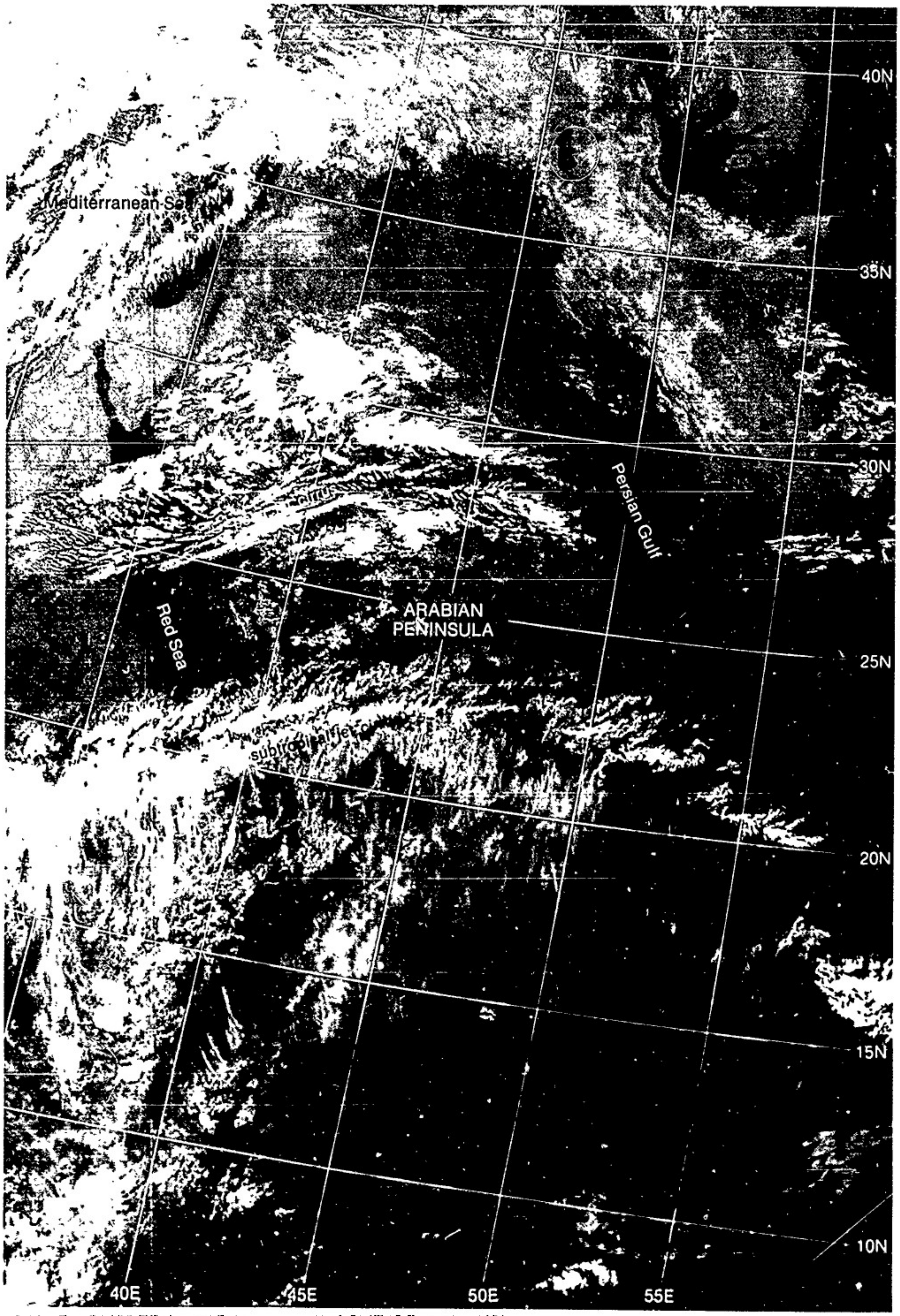


1C-35a. F-4. DMSP TF Normal Enhancement. 1745 GMT 17 December 1979

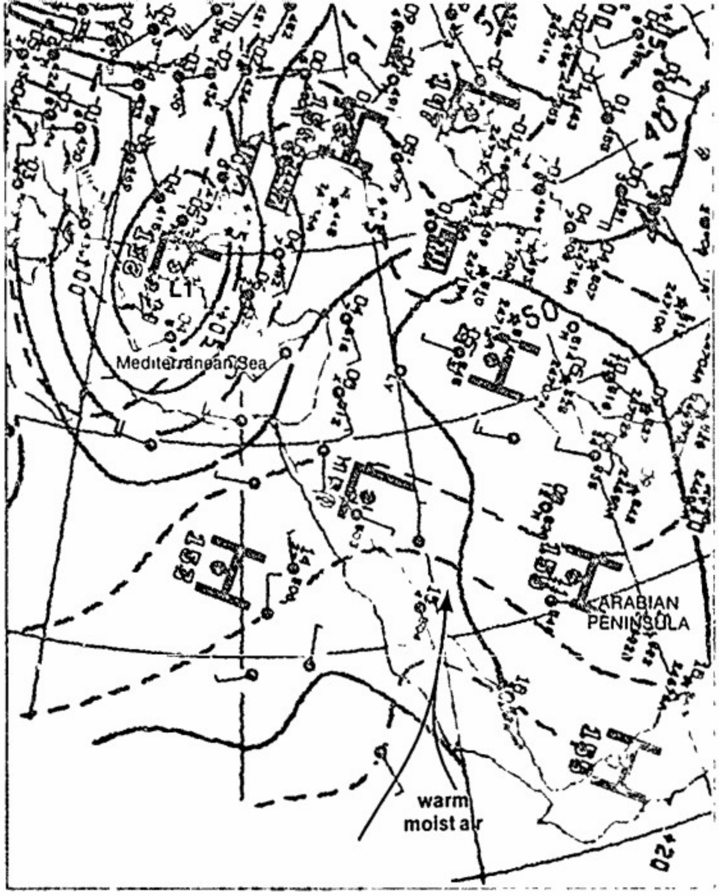


1C-36a. NMC 850-mb Analysis. 1200 GMT 17 December 1979

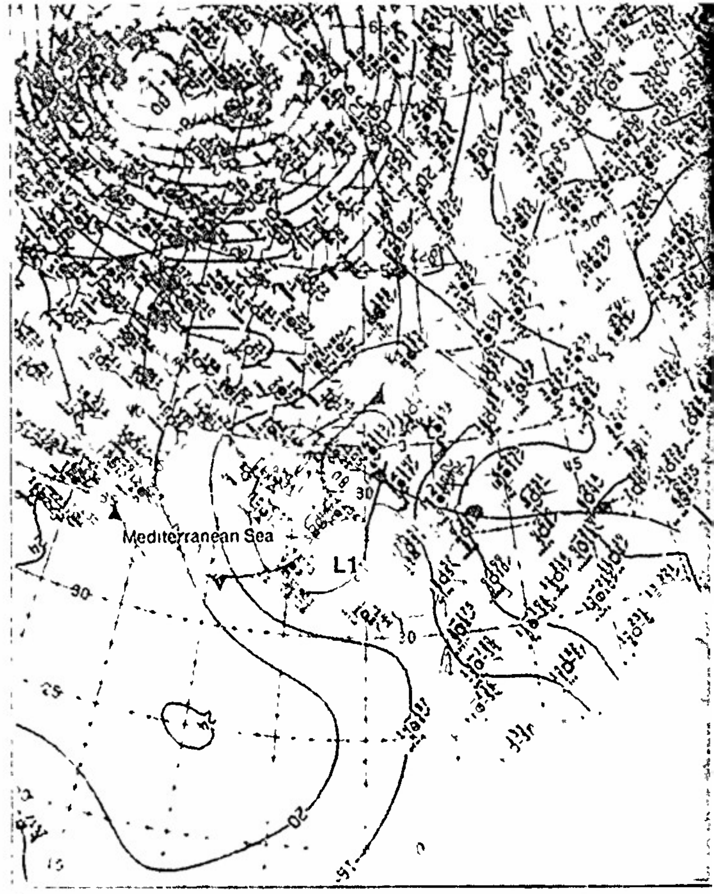


1C-36b. NMC Surface Analysis. 1800 GMT 17 December 1979.

**surface**

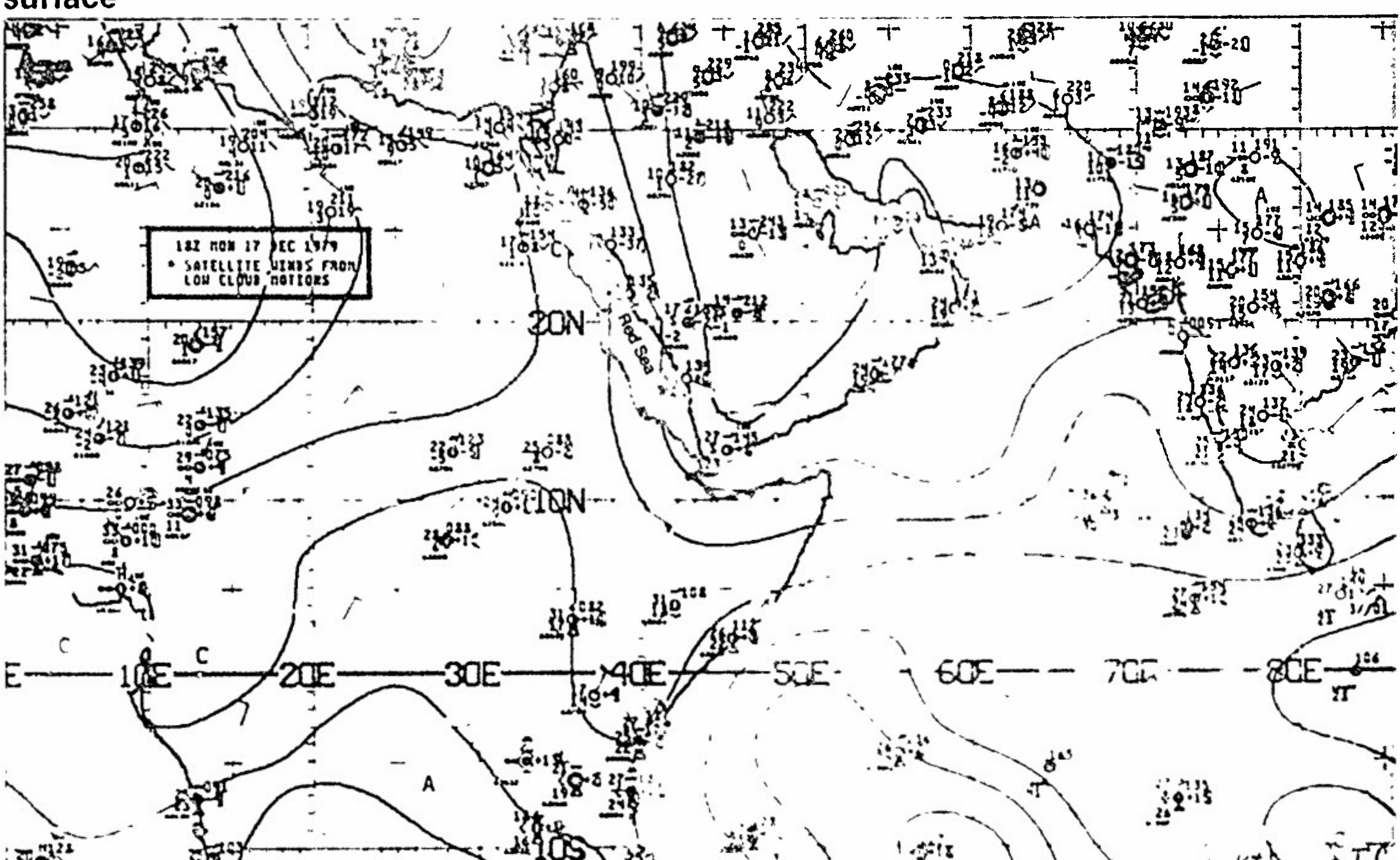


1C-36c. NMC Tropical Surface Streamline Analysis 1800 GMT 17 December 1979

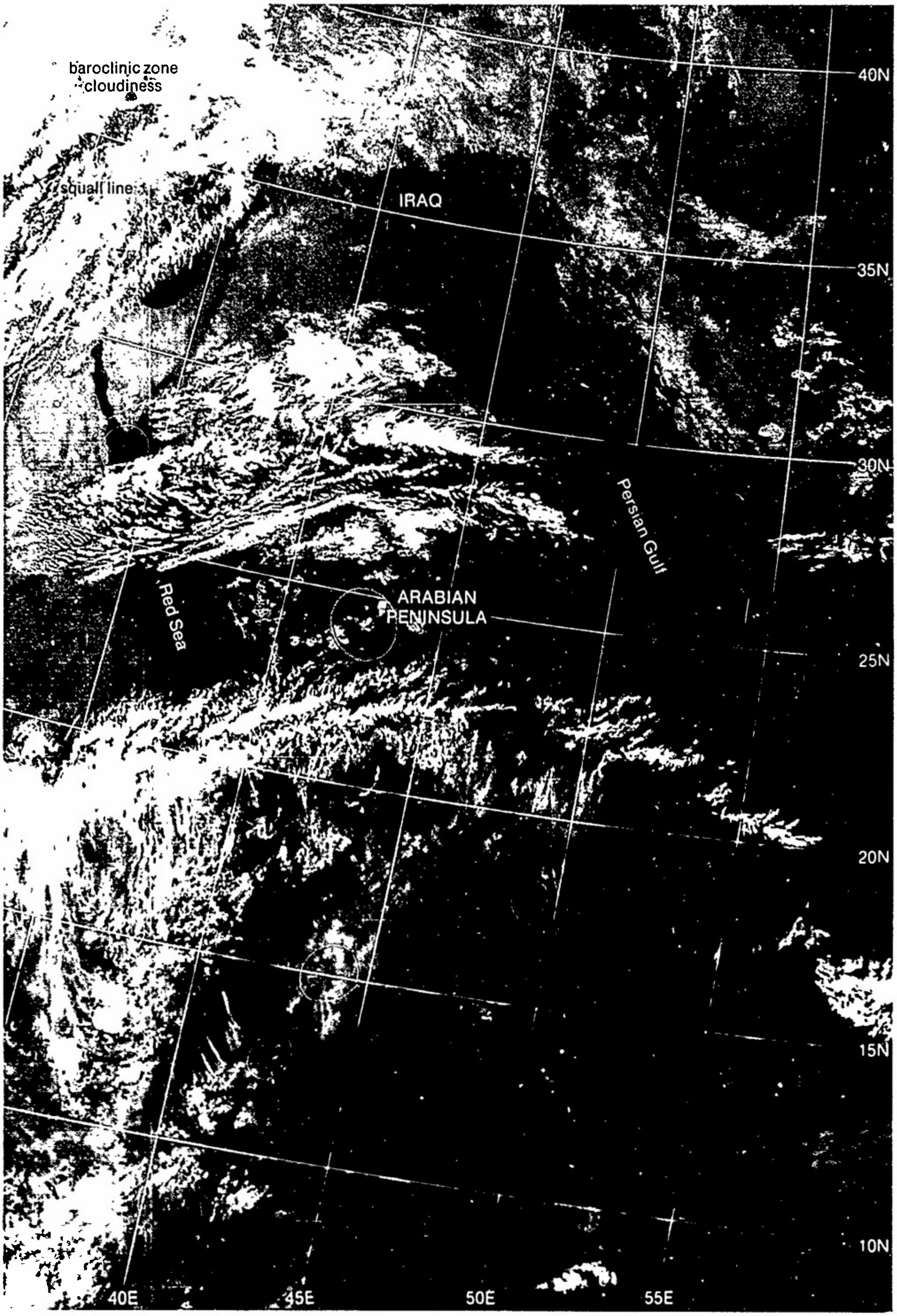


1C-37a. F-4. DMSP TF Normal Enhancement, 1745 GMT 17 December 1979. (Note this picture is a repeat of 1C-35a.)

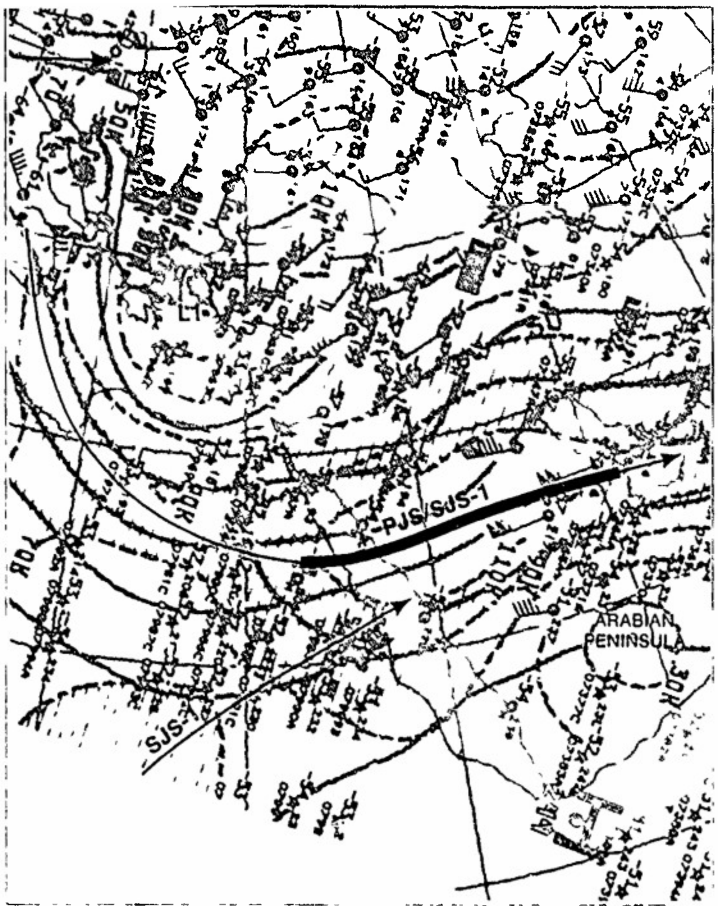


IC-38a NMC 200-mb Analysis, 0000 GMT 18 December 1979.

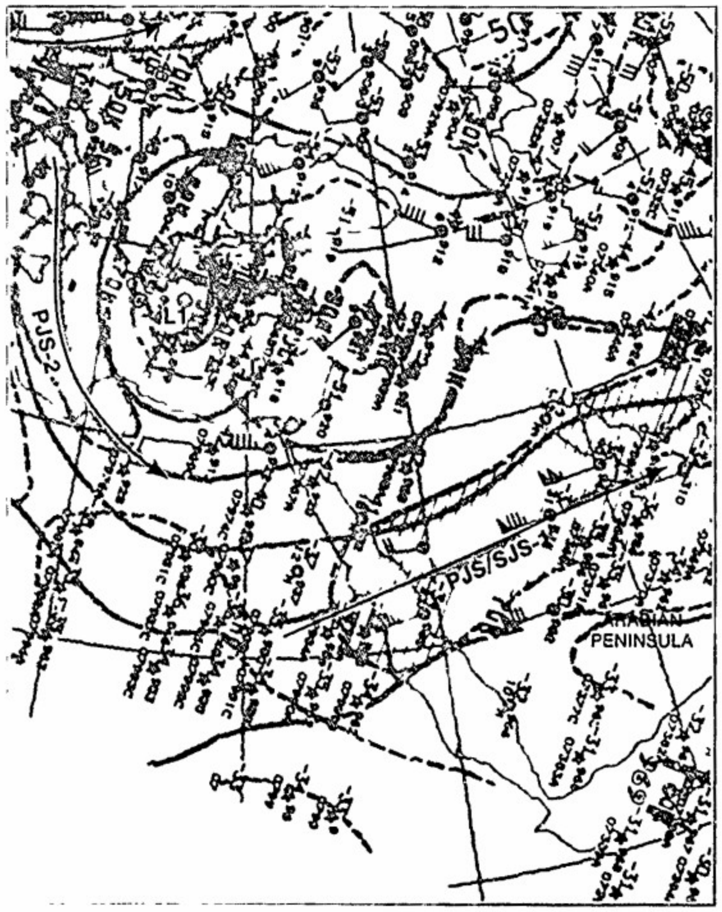


IC-38b. NMC 300-mb Analysis, 0000 GMT 18 December 1979.

850 mb

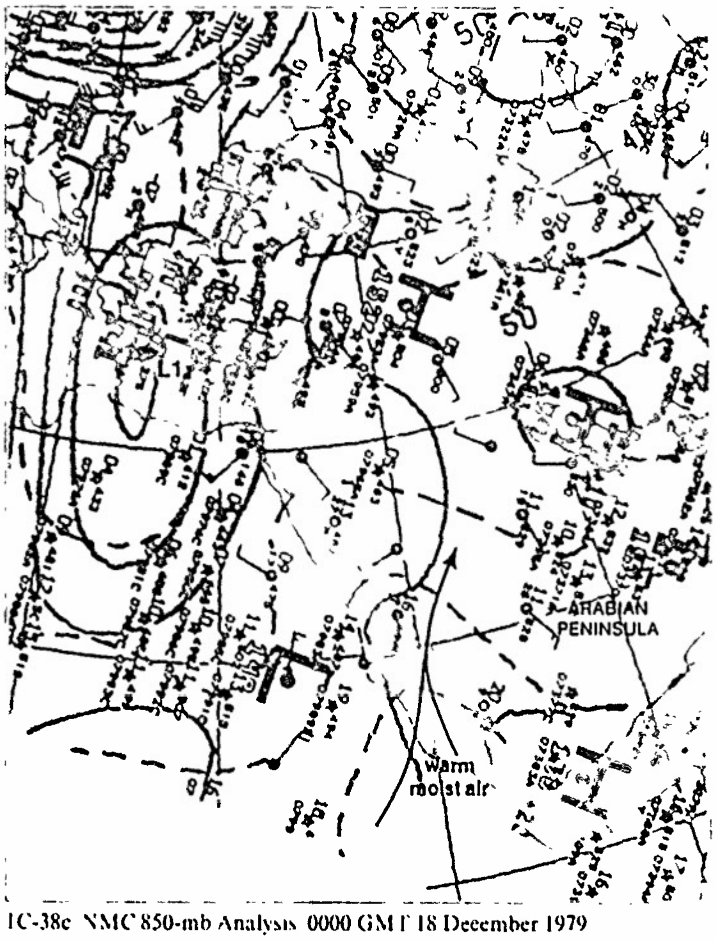


IC-38c NMC 850-mb Analysis 0000 GMT 18 December 1979

surface

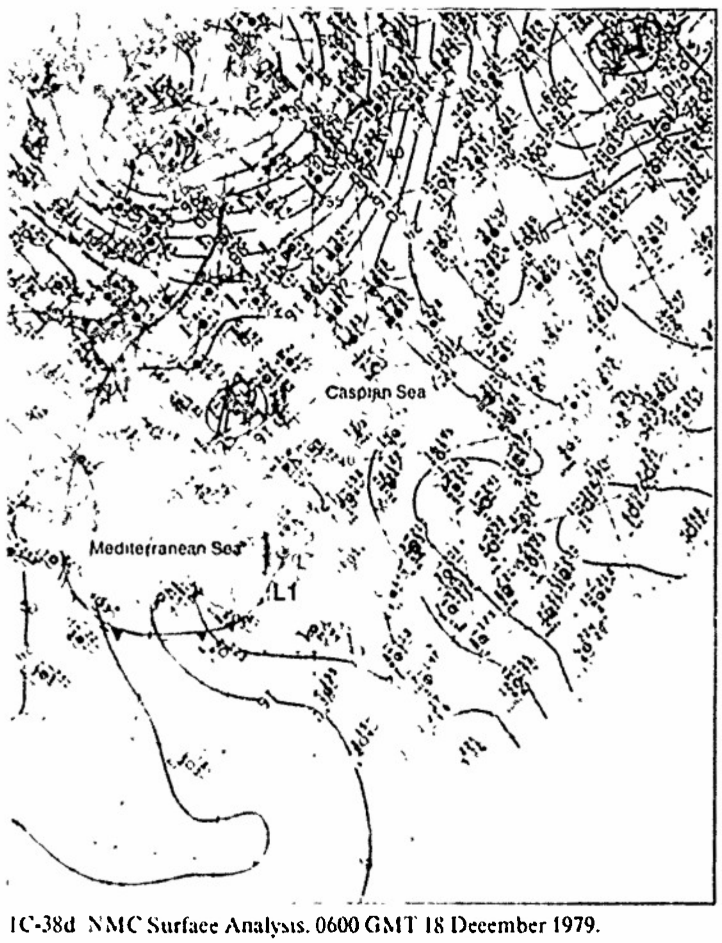


IC-38d NMC Surface Analysis, 0600 GMT 18 December 1979.

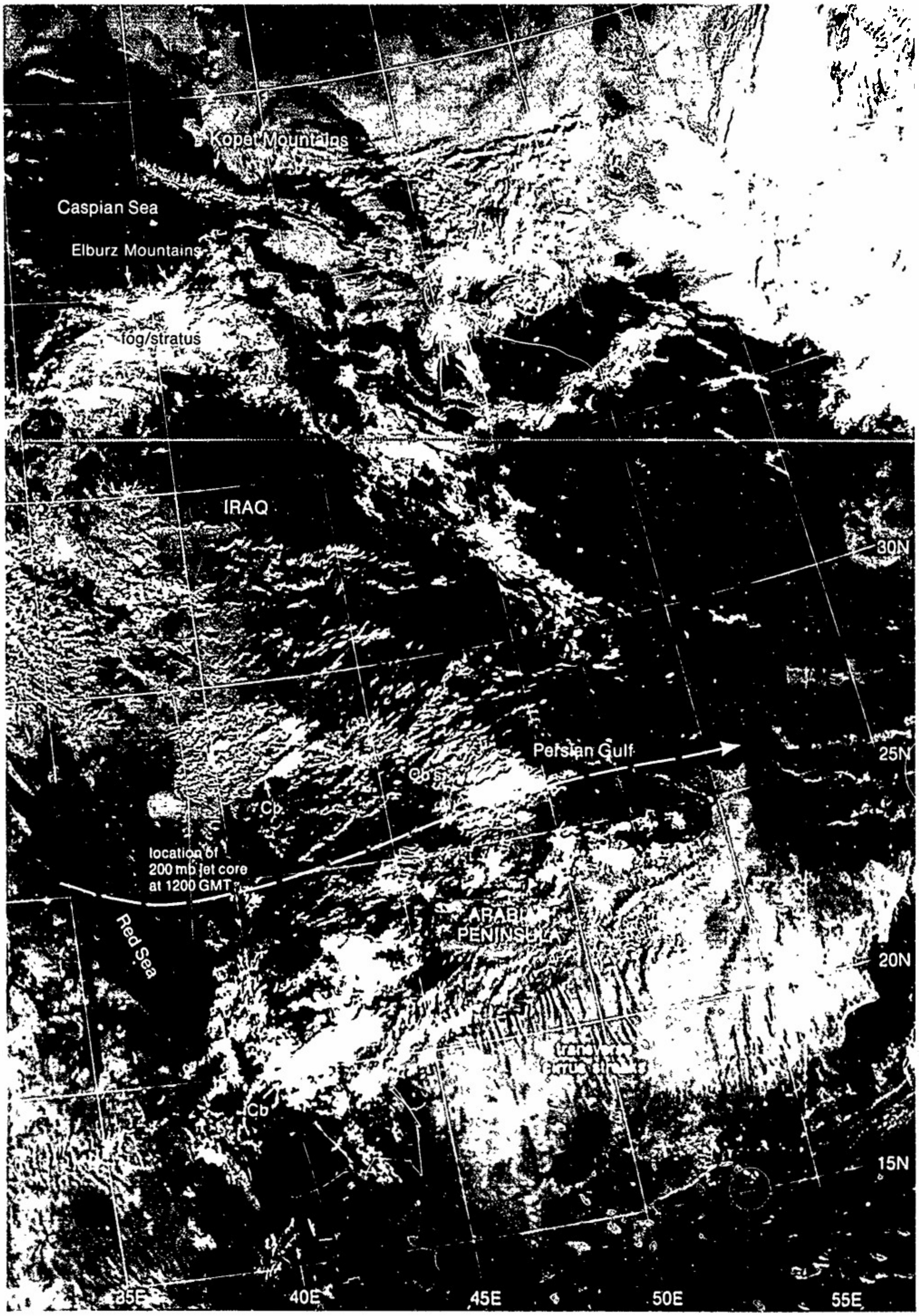


1C-39a. F-4. DMSP LF Normal Enhancement. 0626 GMT 18 December 1979.

## 200 mb


1C-40a NMC 200-mb Analysis 1200 GMT 18 December 1979

## 300 mb

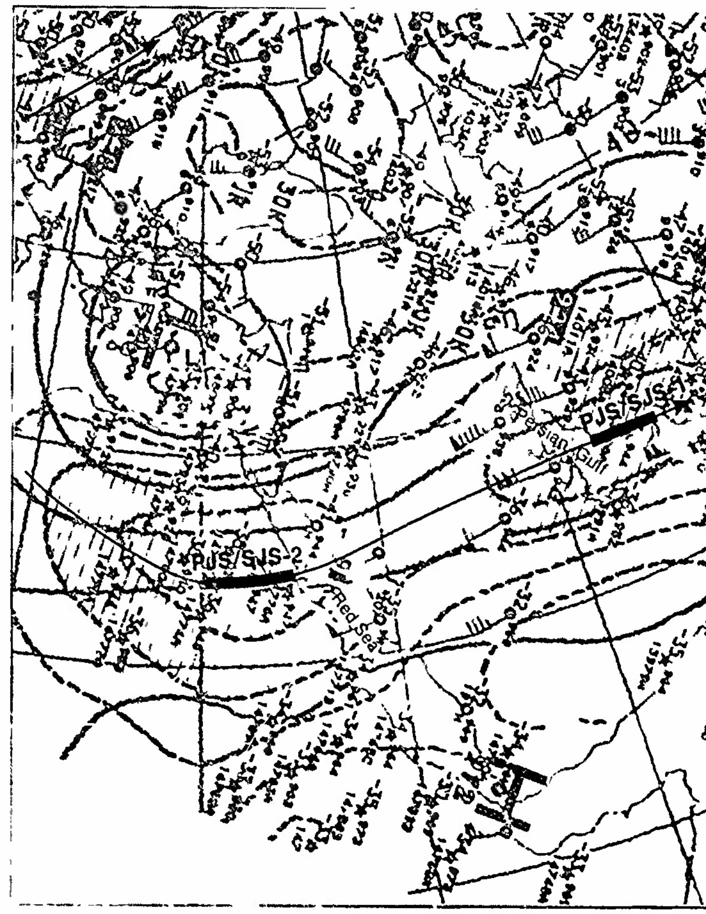


1C-40b NMC 300-mb Analysis 1200 GMT 18 December 1979.

## 850 mb

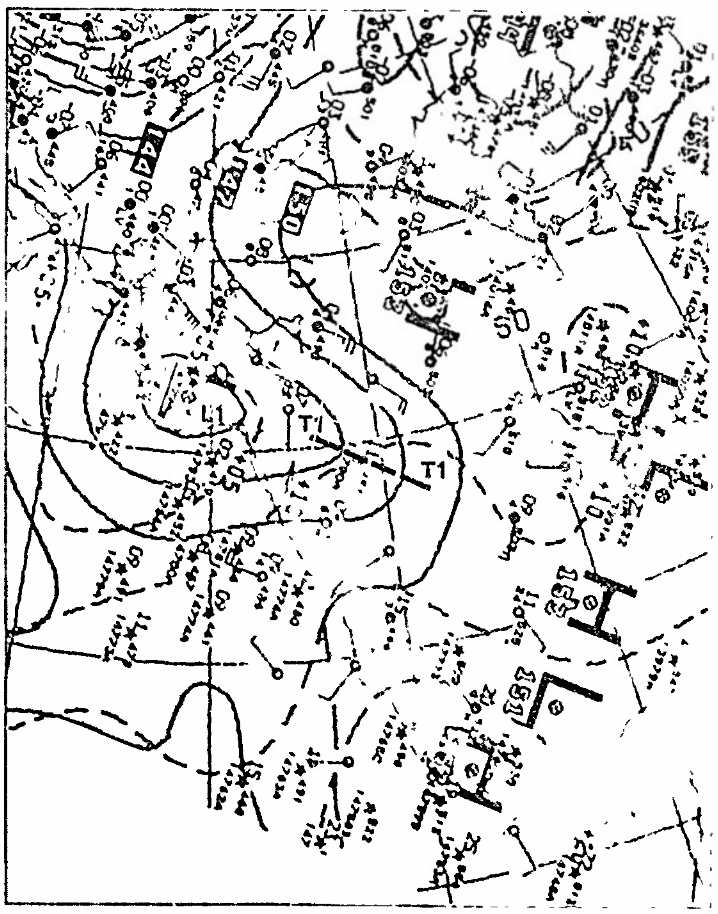


1C-40c NMC 850-mb Analysis 1200 GMT 18 December 1979

## surface

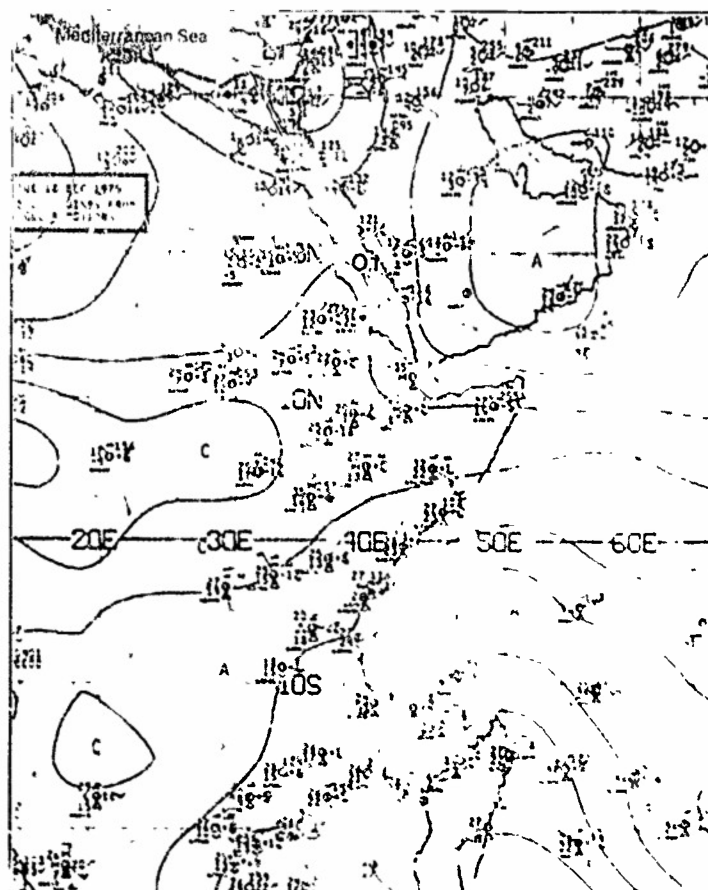


1C-40d. NMC Tropical Surface Streamline Analysis, 1800 GMT 18 December 1979.

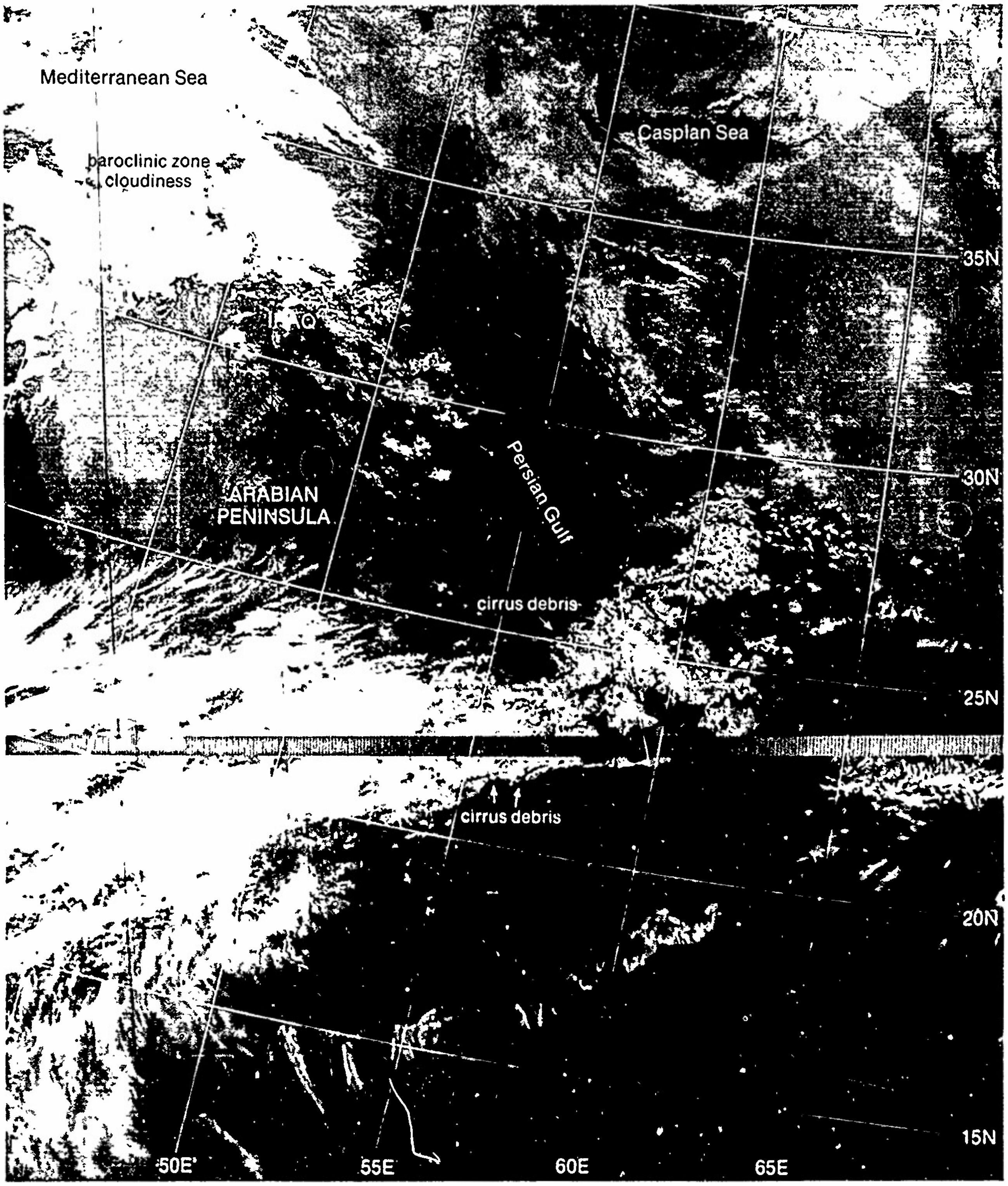


1C-41a. F-4 DMSP TF Normal Enhancement 1725 GMT 18 December 1979.

## 19 December

The surface streamline analysis at 0600 GMT (1C-42d) shows that the low L1 over the eastern Mediterranean has moved inland, and southerly flow extends from the southern Red Sea to the northern Persian Gulf ahead of the surface low. At 200 mb (1C-42a), the wind speed maximum PJS/SJS2 has advanced eastward, and cyclonically-curved southwesterly flow has developed ahead of the low L1 over Iraq. Pronounced cyclonic flow is also occurring in this area at 300 mb (1C-42b). The most pronounced cyclonic flow, however, occurs over southern Iraq at 700 mb (1C-42c). As the surface low L1 advances inland, it is in a favorable location (southwesterly cyclonic flow aloft) for further development. The reports of showers and rain along the northern portion of the surface low L1 (1C-42d) indicate that development may already be occurring.

The strong southwesterly flow ahead of the upper-level low L1 at 700 mb (1C-42c) has resulted in an increase in the amplitude of the ridging over the southern Arabian Peninsula. On the DMSP visible picture (1C-43a), early morning convective activity is observed over central Arabia; however, it is suppressed compared to the early morning convective activity observed on the DMSP picture 24 hours before (1C-39a). The reduced convective activity is due to the increased ridging and anticyclonic flow aloft over the region.

By late afternoon, a major change in the weather has occurred over the Arabian Peninsula. The DMSP infrared picture (1C-45a) shows that a large, winter storm spiral cloud vortex has developed over Iraq, and deep convection (Cb's) is occurring along a sharp baroclinic zone which extends to the southwest over the Arabian Peninsula. The 200-mb analysis for 1200 GMT (1C-44a) shows that the low L1 has become a mobile trough; however, closed centers are observed at 300 mb (1C-44b) and 700 mb (1C-45b) which indicate an intense disturbance at mid-tropospheric levels.

The reason for the rapid development can be inferred from the change in the arrangement of the merged jet streaks PJS/SJS2. A separate polar jet streak PJS2 is observed at 300 mb (1C-44b), and the subtropical jet streak SJS2 at 200 mb (1C-44a) has advanced eastward relative to the jet streak PJS2. A close examination of the arrangement of these two jet streaks shows that the right rear quadrant of the jet streak SJS2 is superimposed over the left front quadrant of the jet streak PJS2. It is well known that the right rear quadrants and the left front quadrants of jet streaks are cyclogenetic areas. Therefore, the superposition of the cyclogenetic area of the SJS2 at 200 mb over the cyclogenetic area of the PJS2 at 300 mb accounts for the rapid development of the disturbance over northwest Iraq which was located in this favorable cyclogenetic region.

The absence of a deep closed low L1 on the surface analysis (1C-45c), which would be expected with the pronounced spiral cloud vortex on the satellite picture, reveals that the storm is primarily a mid- to upper-tropospheric disturbance. There is a well-defined wind shift line S1 at the surface across central Arabia associated with the baroclinic zone aloft, as indicated on the surface contour analysis (1C-45c) and the surface streamline analysis (1C-45d), however, there are no corresponding sharp surface temperature gradients which would indicate a polar front-type surface frontal zone development. Surface reports show that the most pronounced temperature changes occur around the northern periphery of the surface low L1, where the disturbance borders on the colder air masses to the north. In addition, the sharp, ragged rear edge of the cloudiness over central Arabia, on the satellite picture (1C-45a), is more characteristic of the appearance of squall line development in a baroclinic zone aloft than of a surface cold front.

### Important Conclusions

1. Polar jet streaks in the westerlies (300 mb) need to be monitored as they progress in the flow around major troughs in which short-wave disturbances are located, because they can trigger the rapid development of short-wave disturbances into significant weather producing storms.

2. Convection through a deep layer is not normally associated with the subtropical jet when it is well to the south of the polar jet; however, a merger of the two jet systems can produce ideal conditions for deep convection.

3. When deep convection is observed south of the core of the subtropical jet stream, convection will be sharply inhibited equatorward of the axis of maximum anticyclonic vorticity associated with the jet. This axis is located in the region where the jet-force winds decrease most rapidly to the south of the jet core.

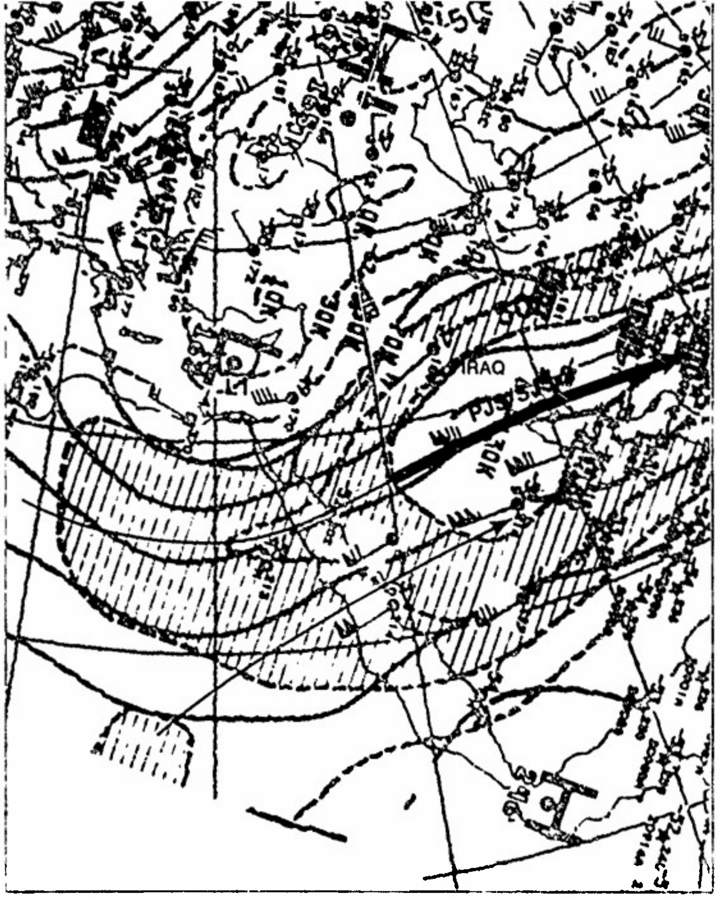


1C-42a. NMC 200-mb Analysis. 0000 GMT 19 December 1979.

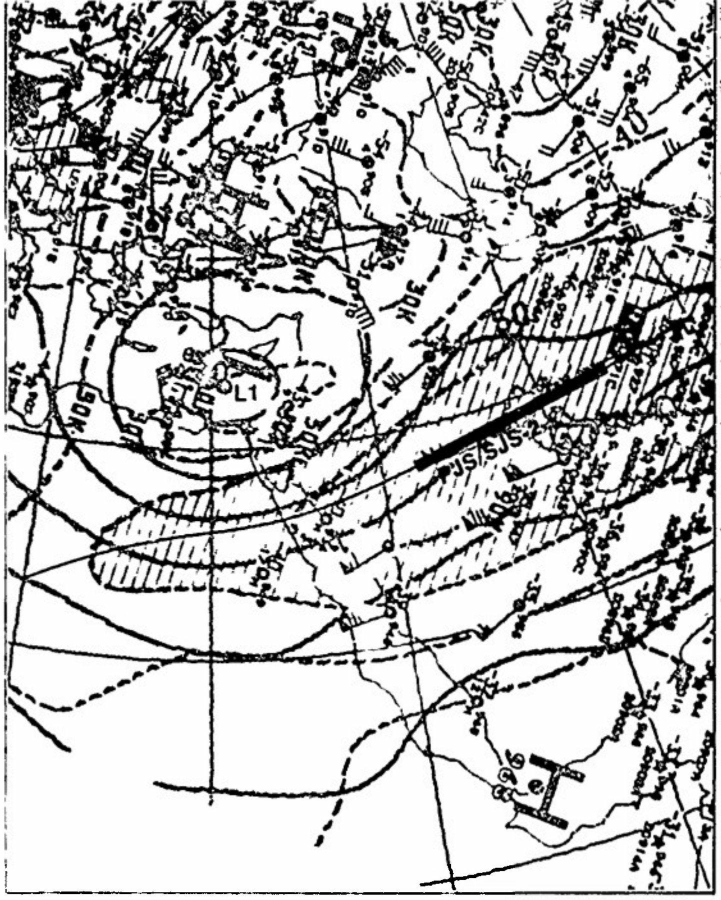


1C-42b NMC 300-mb Analysis. 0000 GMT 19 December 1979.

**700 mb**


1C-42c NMC 700-mb Analysis 0000 GMT 19 December 1979

**surface**

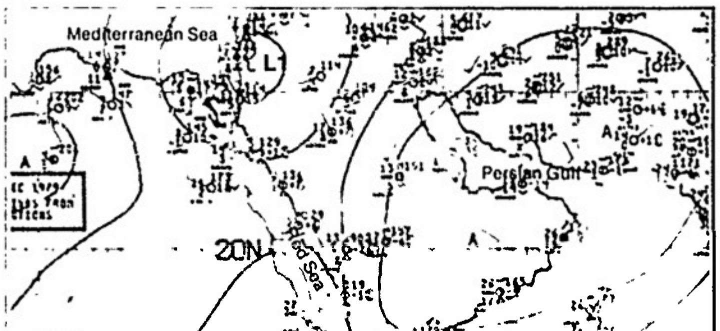


1C-42d. NMC Tropical Surface Streamline Analysis. 0600 GMT 19 December 1979.

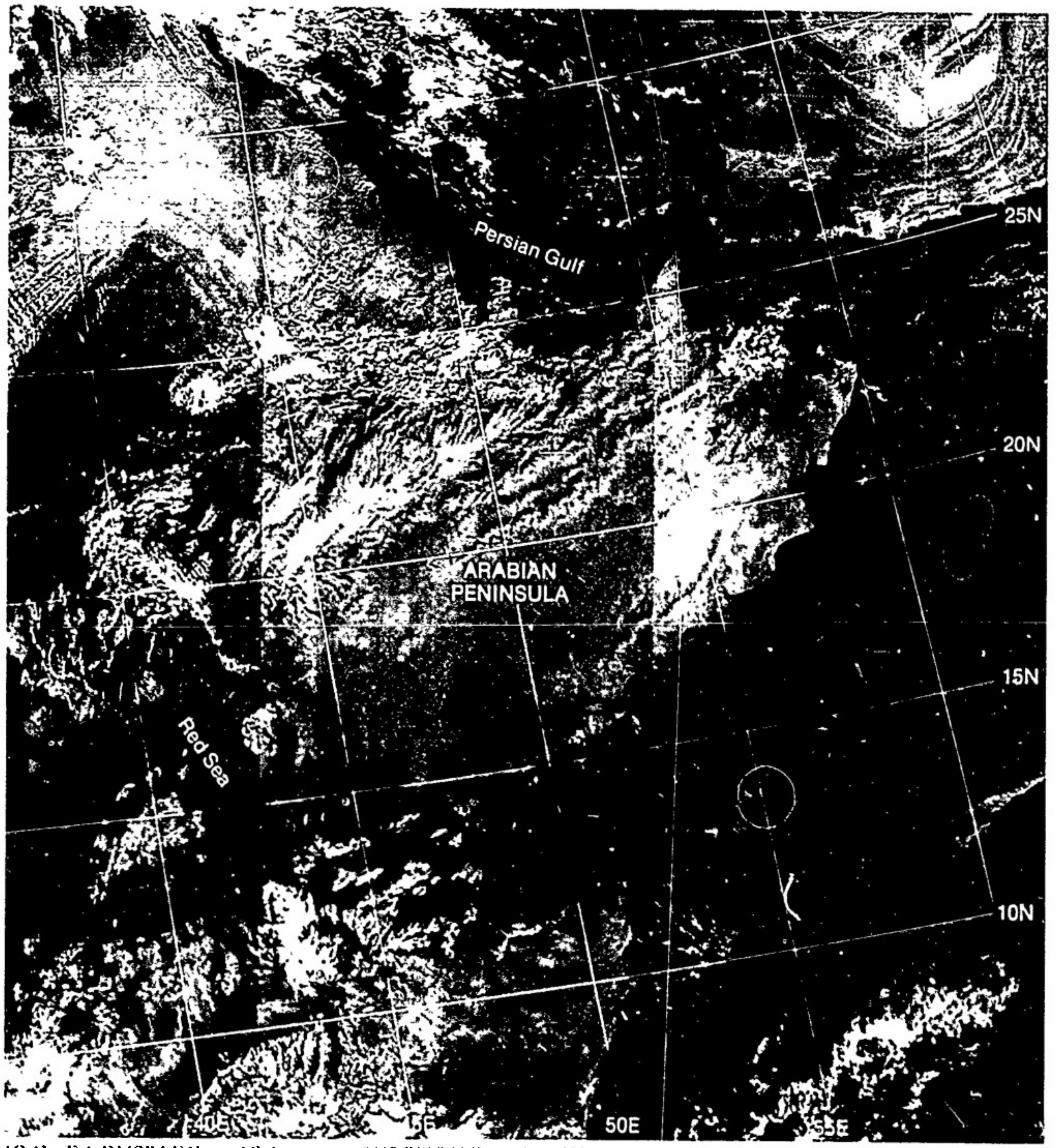


1C-43a F-4. DMSP LF Normal Enhancement 0607 GMT 19 December 1979.

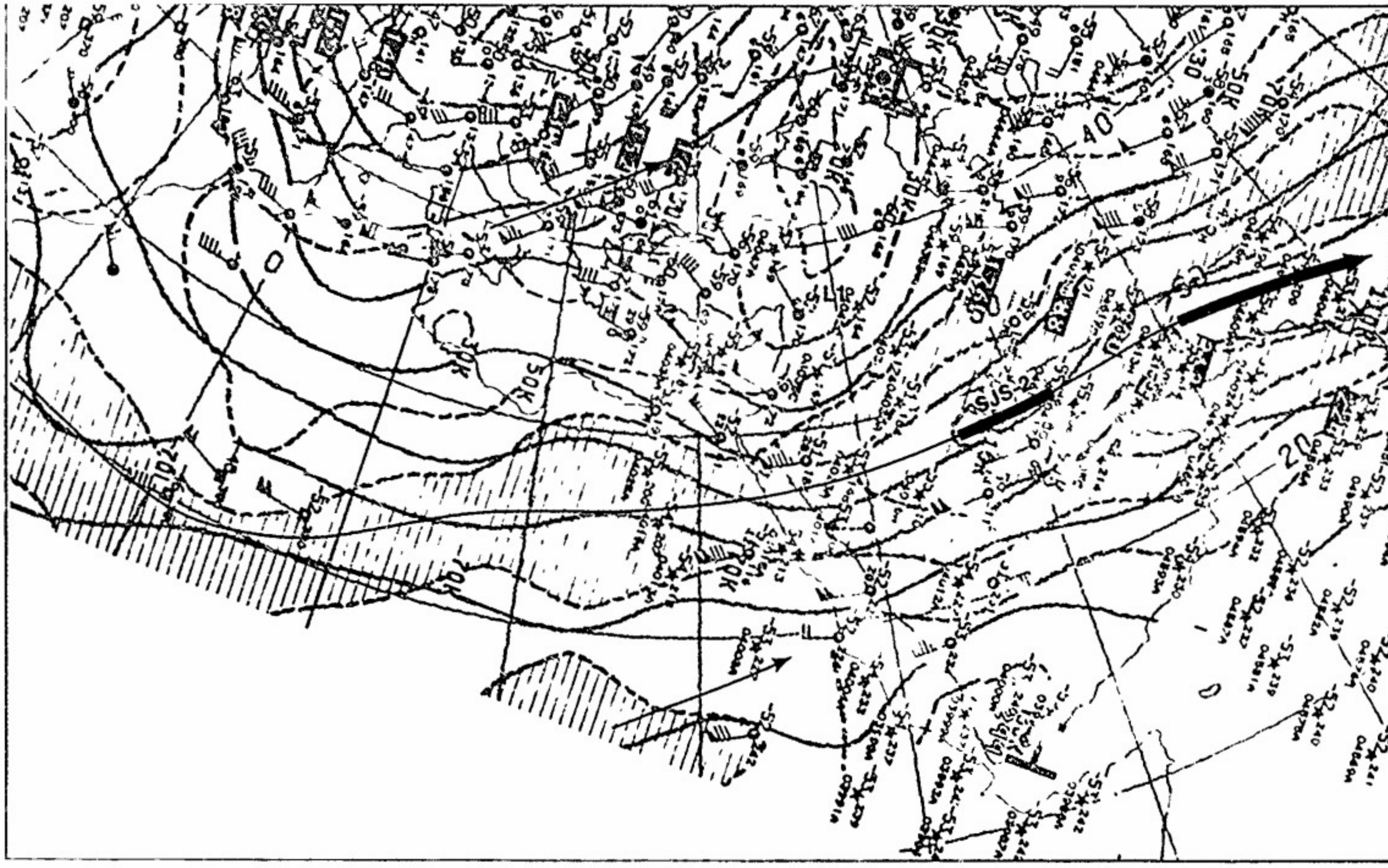

1C-44a. NMC 200-mb Analysis. 1200 GMT 19 December 1979.

**300 mb**

1C-44b. NMC 300-mb Analysis. 1200 GMT 19 December 1979

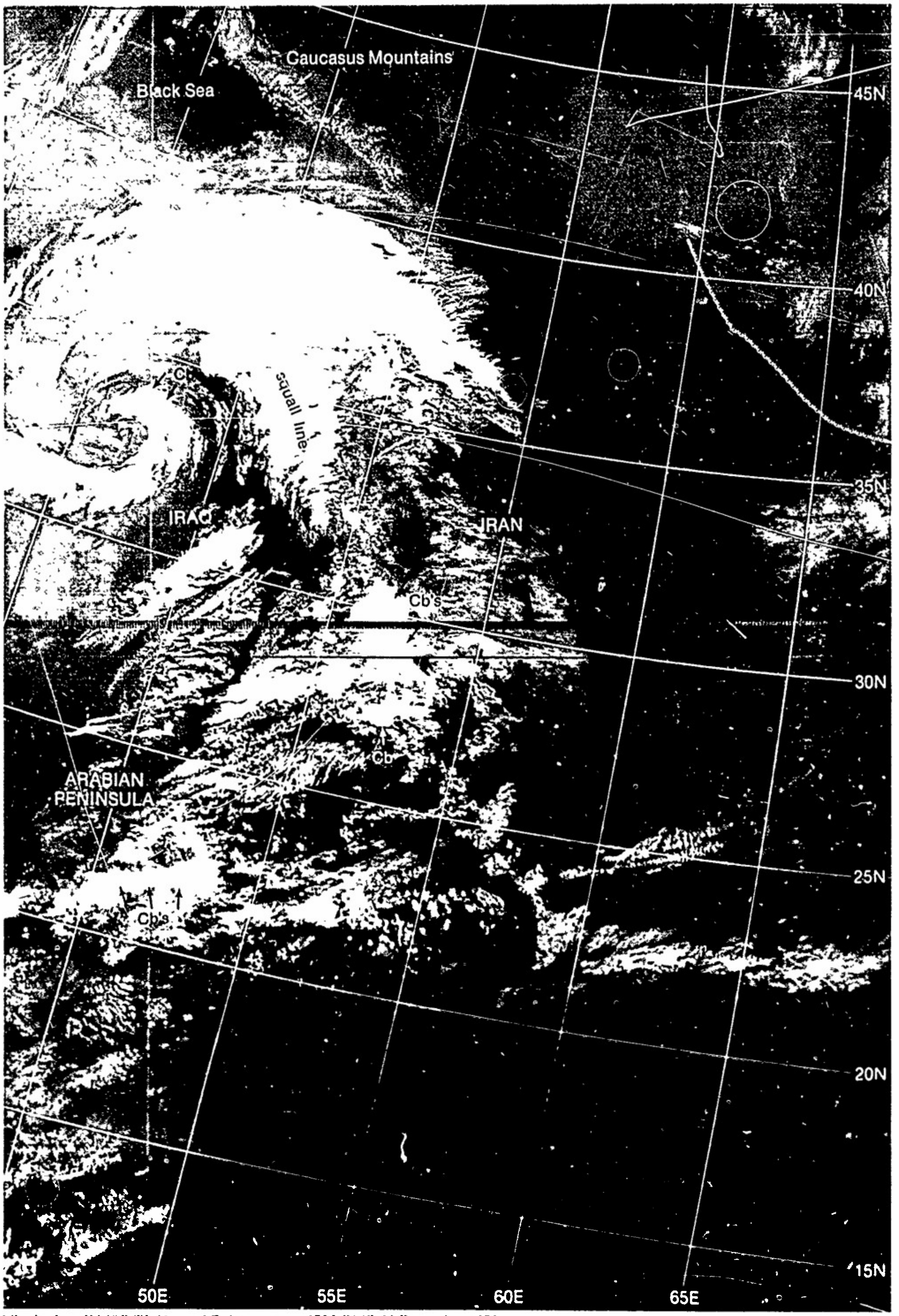


1C-45a F-4 DMSP TF Normal Enhancement 1725 GMT 19 December 1979


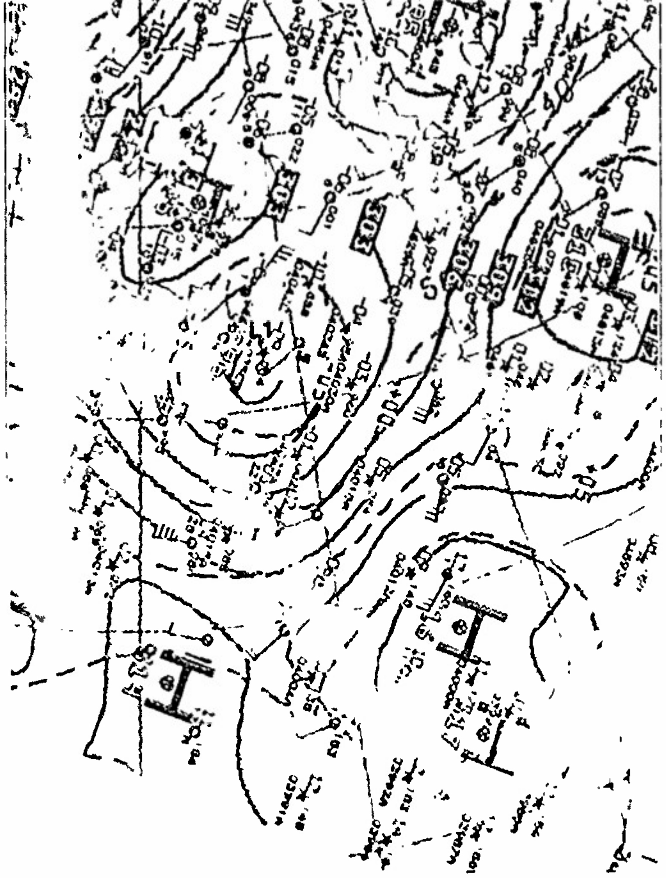

IC-45b NMC 700-mb Analysis 1200 GMT 19 December 1979

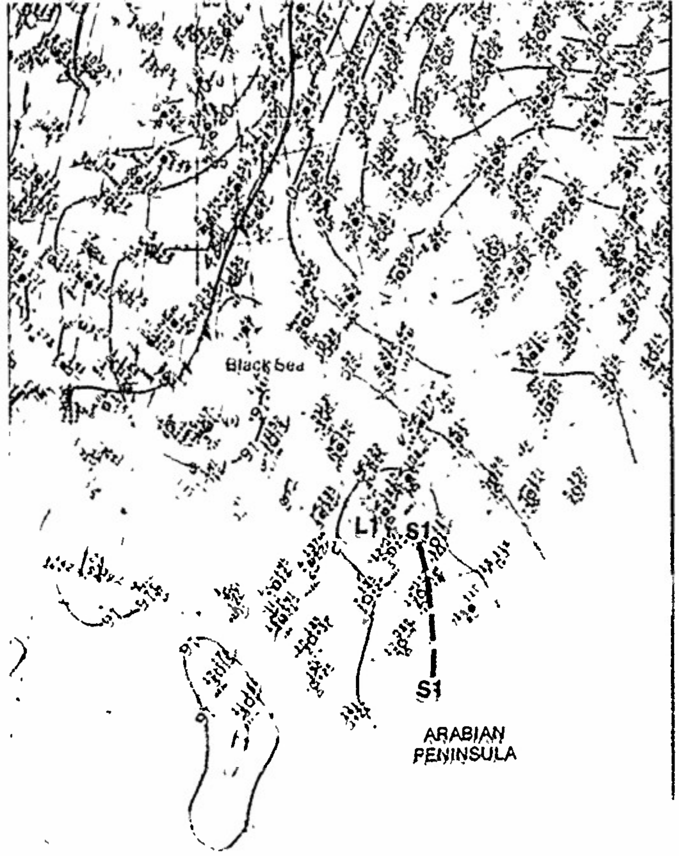


IC-45c NMC Surface Analysis 1800 GMT 19 December 1979

surface

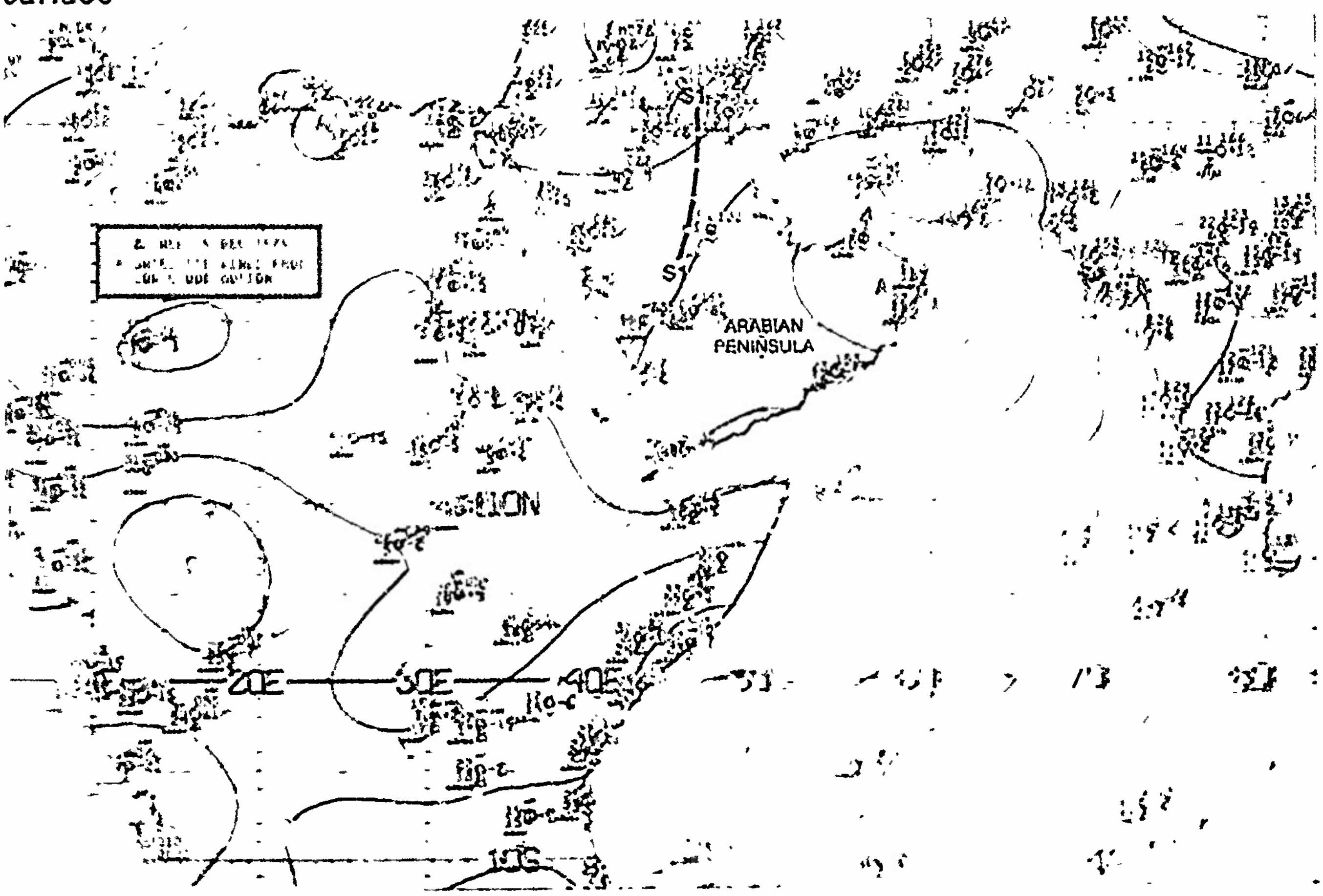


IC-45d NMC Tropical Surface Streamline Analysis 1800 GMT 19 December 1979

This section is
under development
and will be forwarded
for inclusion in this volume.

# Case 1 Red Sea/Persian Gulf—Summer

## *Development of Convection in Southwest Monsoon Flow over the Southern Arabian Peninsula*

As the sun advances into the Northern Hemisphere in summer, a major change occurs in the surface pressure pattern over the Red Sea/Persian Gulf region. The winter anticyclone over the Arabian Peninsula is replaced at lower levels by a thermal low (1E-1a). This thermal low is capped by an anticyclonic circulation aloft which effectively inhibits the development of deep convection. The Saharan anticyclone over northern Africa (1E-1a) shifts eastward and its long axis is oriented north-south over the eastern Sahara. As a result of the northerly circulation between the Saharan anticyclone and the Arabian thermal low, hot, dry northerly winds penetrate to the Gulf of Aden during the summer months.

By late June, the southwest monsoon is established over the Arabian Sea. As the southwest monsoon advances northward over East Africa, the intertropical convergence zone (ITCZ) moves into the Northern Hemisphere (1E-1b). North of the surface ITCZ there is the northerly current composed of hot, dry air between the Saharan anticyclone and the Arabian thermal low. South of the ITCZ, the southwest monsoon brings warm, moist air across Somalia and the Arabian Sea. Generally the southwesterlies across Somalia do not contain much moisture because most of it is lost in the long meridional trajectory over the uplands of East Africa and further south. In addition, the flow over the Kenya-Somalia area is strongly diffluent so that low-level subsidence prevails. On occasion, however, moist air is advected across the southern Arabian Peninsula land mass, and heavy showers are experienced.


**Reference**

Solot, Samuel B., 1950 General circulation over the Anglo-Egyptian Sudan and adjacent regions *Bull AMS*, 31, pp 91


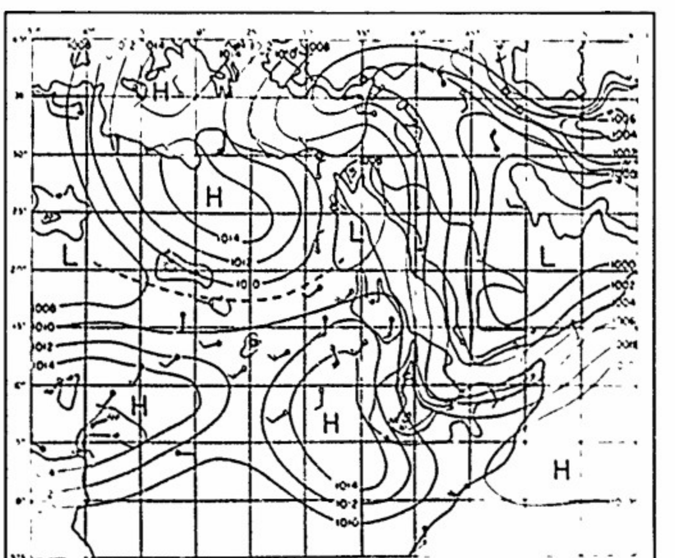


1E-1a Typical summer Surface Analysis 0600 GMT 26 July 1943 (Solot, 1950)

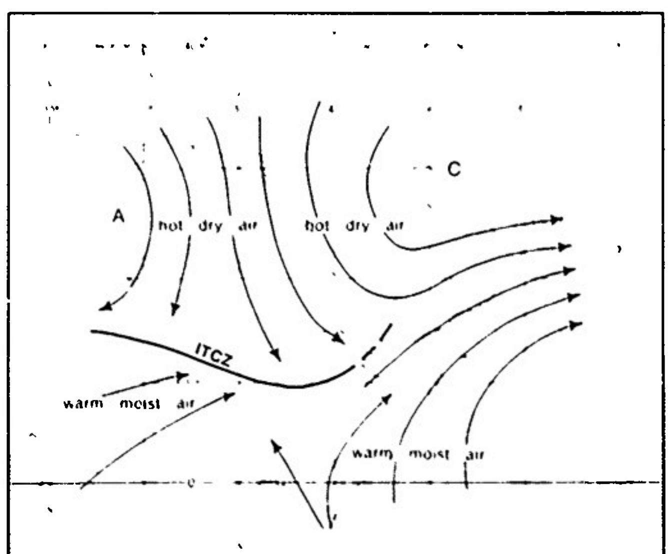


1E-1b Typical summer air mass movement over Red Sea/Persian Gulf

**29 June**

The DMSP visible picture at 0809 GMT (1E-2a) shows the typical cloud-free summer view of the Arabian Peninsula and adjacent areas, and provides an unusually clear display of the major rivers and desert regions. In Egypt, the Nile River stands out prominently against the adjacent land, from the Nile Delta on the Mediterranean to the Sudan. Similarly, the Tigris and Euphrates Rivers in Iraq are readily identified in the imagery. Where the rivers stand out in marked contrast to the land areas, the desert regions, such as the Libyan Desert, the Syrian Desert, the plateau region of the An Nafud, and the Empty Quarter Desert, are displayed as uniform light tone areas. Finally, the land areas to the west and east of the Red Sea show irregular patterns of light and dark tones, which reveal the large variations in soil, rock formation, and vegetation of the region, in the visible mode.

The NMC surface streamline analysis for 1200 GMT (1E-3b) shows a well-developed thermal low over the Persian Gulf and northeasterly flow across the Arabian Peninsula to the southern Red Sea. The limitation of the thermal low to the lower troposphere with an overlying anticyclone over the Arabian Peninsula is illustrated by comparing the distribution of the pressure centers at upper levels with respect to the surface heat low and trough positions. At 850 mb (1E-3a) a trough T1 extends over the Persian Gulf to northern India, and a weak anticyclone is located over the Arabian Peninsula. At 700 mb (1E-3d) the anticyclone over the Arabian Peninsula is more intense and the trough T1 is weaker. At 500 mb (1E-3c) the region from the Red Sea to western India is dominated by the anticyclonic circulation aloft.

This summer large-scale circulation pattern aloft and at the surface is generally unchanging. The extreme surface heating typical of the land areas adjacent to the Red Sea during the summer is revealed by the temperature reports (1E-3b), which range from 33°–39° C (91°–102° F). Strong local effects, such as dust storms, tend to be the dominant phenomenon observed in the vicinity of the Red Sea. Note the numerous reports of suspended dust and haze to the west of the Red Sea.

Suspended dust occurs regularly over the southern Red Sea. In the satellite picture (1E-2a), suspended dust (light gray shades) is observed south of 20°N. On the western coastline, a plume of dust extends from the Tokar gap over the Red Sea. This break in the terrain along the western shore is where dust generated inland can move freely over the Red Sea. Typically, the suspended dust moving out over the Red Sea through the Tokar gap is dust raised by convective activity to the west over the northern Sudan and advected eastward by the prevailing flow. Observations of suspended dust ( S ) raised by convective activity over the Sudan are indicated by surface reports (1E-3b). There are also surface reports of suspended dust to the north and west of the Persian Gulf. The satellite picture shows several long, narrow, northwest to southeast oriented dust plumes just north of the Persian ( . . and an accumulation of dust over the central Pe. Gulf. This dust is not raised by convective activity is the result of strong prevailing northwester (shamal) over the area.

As a result of the northerly circulation between the Saharan anticyclone and the Arabian thermal lo., hot, dry, northerly winds penetrate to the Gulf of Aden during the summer months (see schematic 1E-1b). On occasion, however, the southwest monsoon flow extends northward across the Gulf of Aden and the southern Arabian Peninsula. This brings warm, moist air with thunderstorms and showers to the southern Arabian Peninsula region. The southwest monsoon flow rarely penetrates more than several hundred kilometers (150–250 n mi) inland.

On the satellite picture (1E-2a), cumulus clouds are observed over the Yemen Highlands and along portions of the elevated topography of northern Oman. Patches of early morning fog and stratus are also located off the coasts of Yemen and Oman. These are signs of an incursion of moist southwest monsoon air over the southern Arabian Peninsula. The satellite picture also shows an extensive area of convective clouds from the Sudan, across Ethiopia, to the Somalia coast, which is additional evidence of the advance of moist southwest monsoon air over East Africa.

Although the surface streamline analysis (1E-3b) does not show direct airflow from East Africa across the Gulf of Aden to the southern Arabian Peninsula, such a flow pattern did exist during the preceding 24 hours (not shown). A close examination of surface reports along the southern Arabian Peninsula, which are about 4 hours after the picture time, reveal that cumulonimbus and showers have developed over the Yemen Highlands. The strong, gusty winds produced by these mesoscale convective systems are responsible for numerous dust storms and the advection of dust over the Gulf of Aden during the summer.

Important Conclusions

1. Over the Arabian Peninsula the anticyclone of winter is replaced in summer at lower levels by a thermal low. Above the thermal low an anticyclonic circulation continues to persist.

2. Strong local effects, such as dust storms, tend to be the dominant phenomenon observed.

3. Convective clouds and showers over the Yemen Highlands and elevated terrain of Oman are indicators of an incursion of moist southwest monsoon air over the southern Arabian Peninsula. This flow is strictly a low-level phenomenon (850 mb and below).

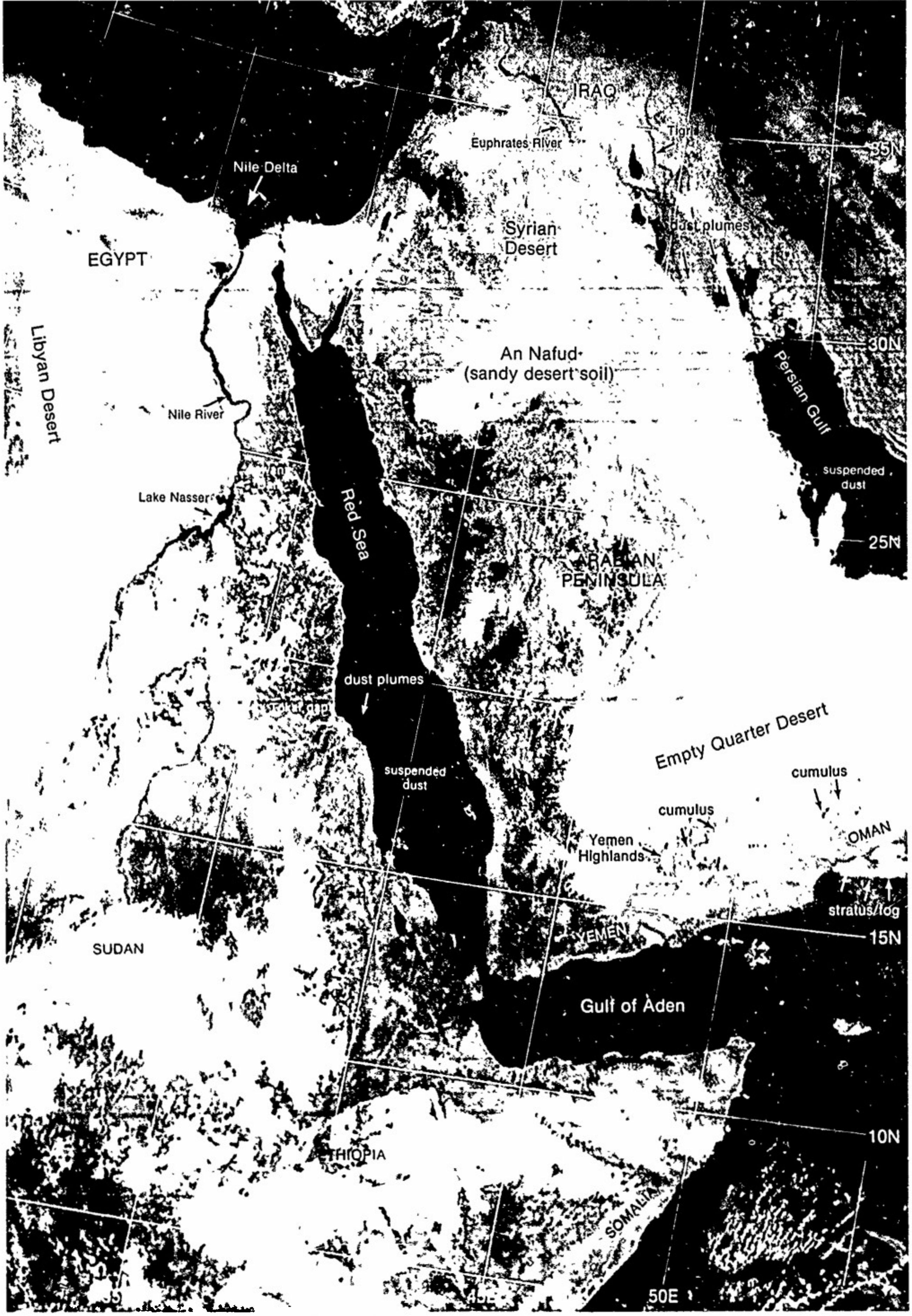


1E-2a F-1 DMSP LS Low Enhancement 0809 GMT 29 June 1979

850 mb

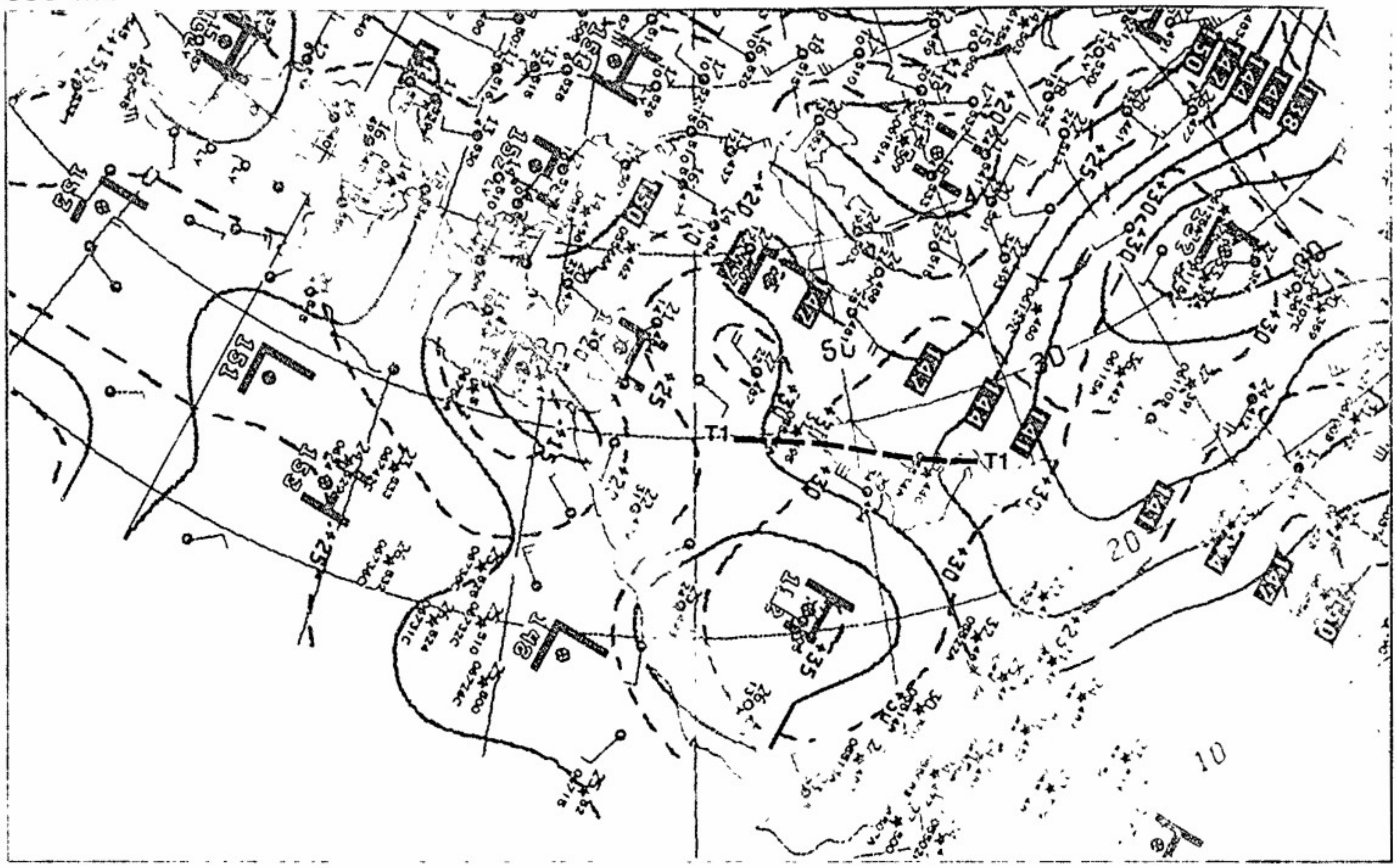

1E-3a. NMC 850-mb Analysis 1200 GMT 29 June 1979

surface

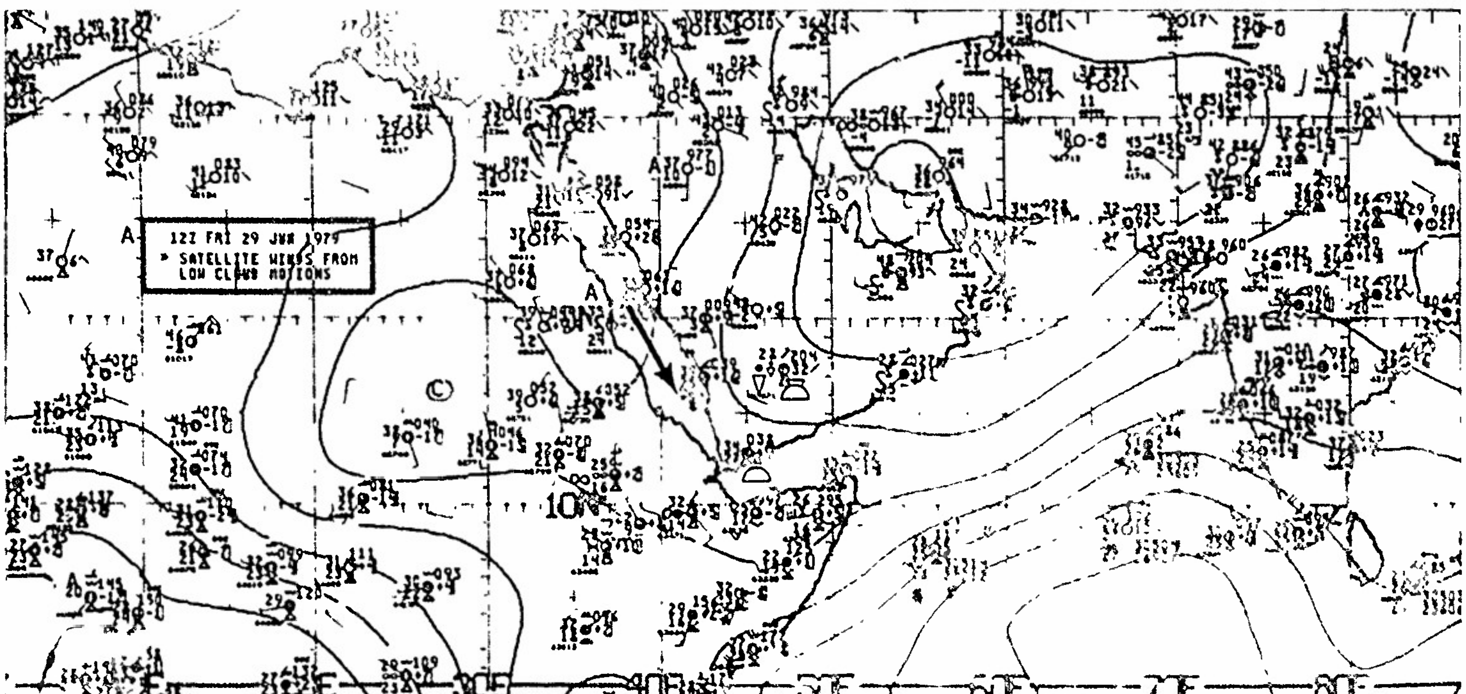


1F-3b. NMC Tropical Surface Streamline Analysis 1200 GMT 29 June 1979

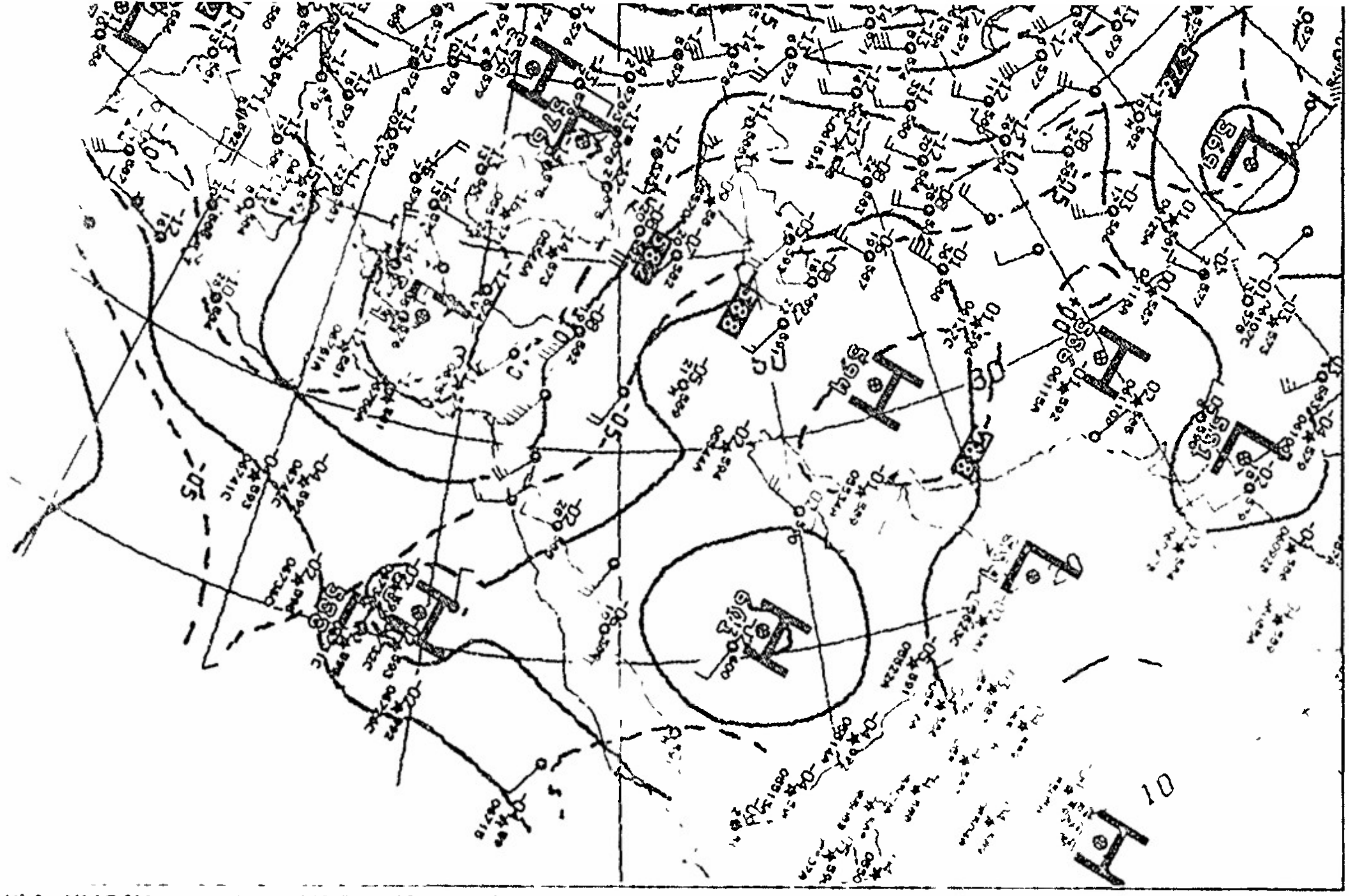

1E-3c NMC 500-mb Analysis 1200 GMT 29 June 1979.

## 700 mb

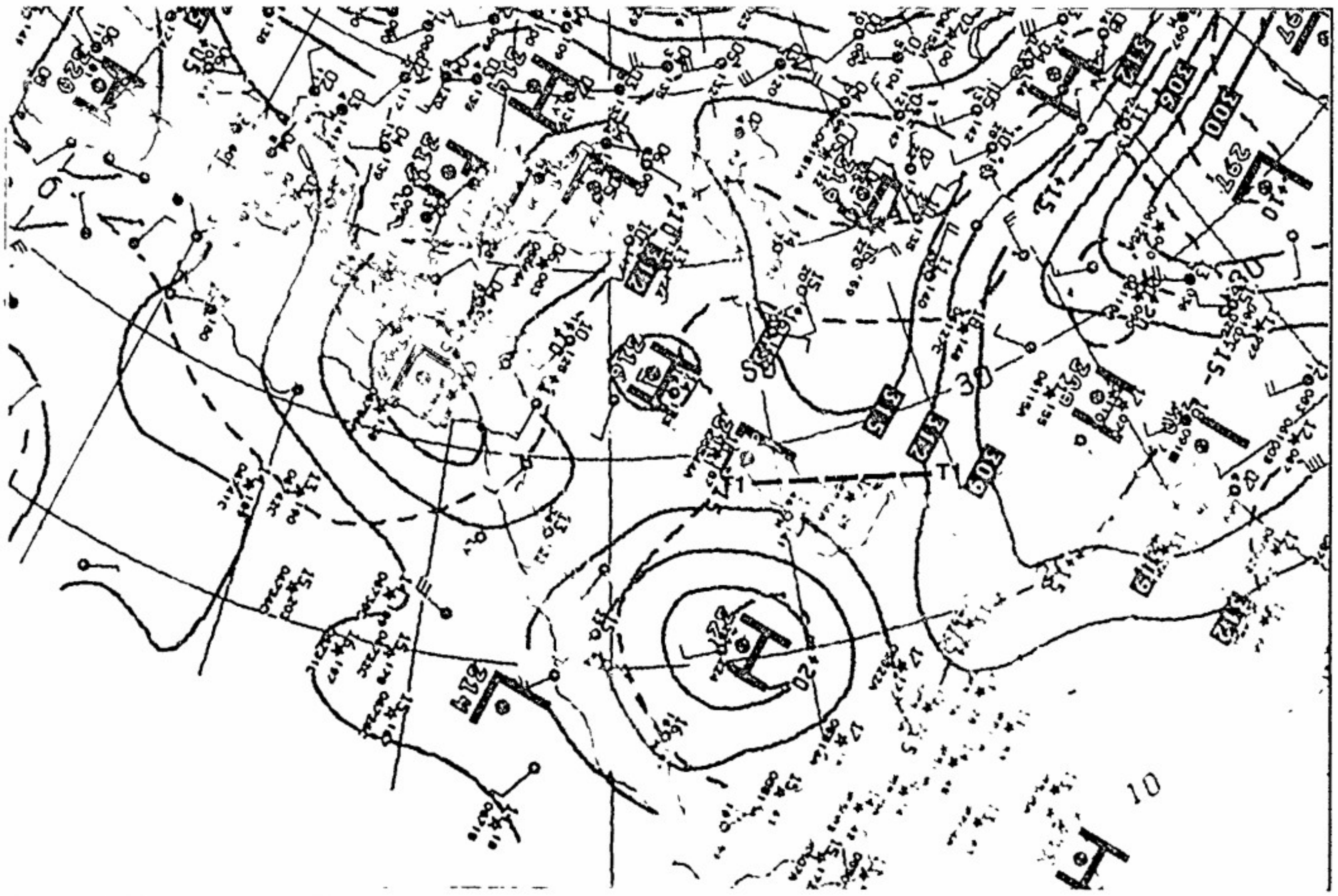

1E-3d NMC 700-mb Analysis 1200 GMT 29 June 1979

# Case 2 Red Sea/Persian Gulf—Summer

## Red Sea Region Duststorms

The Haboob, a regional term which originated in the Sudan of East Africa, is a duststorm produced by convective (thunderstorm) activity. Downbursts and gust fronts from these storms generate dust plumes that have a distinct leading edge and appear as a wall of dust. Haboobs are primarily a summer phenomenon, with a maximum in June, and they occur most frequently in late afternoon. The average wind speed accompanying Haboobs is 25–50 kt. Dust may be carried upwards to form a cloud of dust often extending from the ground to 15,000 ft or higher.

Under certain large-scale thunderstorm-generating weather patterns over the Sudan, such as a tropical disturbance, dust raised by complexes of convective activity associated with the disturbance may evolve into a widespread duststorm. This occurs when a deep polar trough in the westerlies passes to the north of the tropical disturbance, and the raised dust is picked up in the southwesterly flow ahead of the trough. The raised dust forms a huge cloud of dust which is then advected over the Red Sea. As a result, visibilities can be severely reduced over a large area of the Red Sea.

**12 June**

The NMC 300-mb analysis at 1200 GMT (1E-6a) shows a polar trough **T1** extending over the eastern Mediterranean to Africa. The mid-latitude westerlies along the base of the trough **T1**, just north of the Red Sea, appear to have merged with the subtropical jet stream SJS extending across the northern Arabian Peninsula. At 500 mb (1E-6b), the base of the trough **T1** is farther advanced over the eastern Mediterranean than at 300 mb, and northwesterly flow is directed over northeast Africa and across the northern Red Sea.

The surface streamline analysis (1E-7c) shows reports of suspended dust, under clear sky conditions, in the northerly flow over Egypt and northern Sudan. This is where the upper-level trough **T1** at 850 mb (1E-7b) has moved across the northern Red Sea in advance of the trough **T1** at 500 mb (1E-6b), bringing northerly upper-level flow over the region. Northerly winds of 20–30 kt, behind the trough **T1** at 850 mb, are superimposed over northerly flow at the surface and are sufficient, under unstable daytime (1500 LST) conditions, to result in the turbulent transfer of momentum from aloft to raise dust, as indicated by the surface reports. The report of suspended dust to the southwest of Khartoum is probably associated with convective activity (note the report of a thunderstorm in progress at Kadugli, station 62810).

A METEOSAT infrared picture at 1155 GMT (1E-7a) shows that skies are generally cloud-free over northeast Africa. Subtle changes in tonality (gray shades) can be detected, however, over the desert areas. Water vapor absorption is unlikely to be a factor in producing such gray shade changes under dry desert conditions. The changes over the area are due to dust in the atmosphere which radiates as a black body at the temperature of the air in which it is located. Since dust can be lifted to high altitudes, its presence will be indicated in satellite infrared data as a lighter shade of gray (cooler temperature). For this reason, satellite infrared data should be viewed as a primary tool for duststorm detection.

On the satellite picture (1E-7a) light gray shades, indicating dust in the atmosphere, should be apparent over Egypt and the northern Sudan which is the region of the numerous surface reports of dust (1E-7c). The dust is not heavy and is probably only at low levels so that it is too faint to be recorded in the imagery. There is a tropical disturbance located south of Khartoum showing large clusters of convective activity. At this time there is no indication of dust (areas of light gray shades) spreading outward from the storm. In the tropical disturbance over western Africa, however, the irregular shaped, light tone area along the northern border is dust in suspension raised to high elevations. This is the characteristic appearance of suspended dust associated with a Haboob in progress at the surface. The large geographical extent of the Haboob indicates that it is being generated by a complex of thunderstorms, rather than by an isolated storm.

**13 June**

A casual examination of the late morning 0759 GMT (1059 LST) DMSP visible picture (1E-8a), reveals no apparent obscurations of geograp[illegible] features due to dust over the central Sudan. How[illegible] suspended dust, or a duststorm in progress in its e[illegible] stages, can be identified in visible satellite image[illegible] general, only by comparison with imagery [illegible] shows a cloud-free view of the same geographical [illegible] A comparison of the DMSP picture (1E-8a) wi[illegible] previous cloud-free DMSP picture (1E-9a) over the same area reveals that a section of the Nile River north of Khartoum is obscured from view. The cause for the change is a duststorm in progress, or suspended dust from a previous duststorm in the region. Note that the light gray shade band over the Gulf of Aden is not suspended dust but is sunglint, which is to be expected in this area for a late morning (1059 LST) descending DMSP pass.

An enlargement of the METEOSAT infrared picture (1E-11a), acquired a few hours after the DMSP picture, shows the characteristic irregular-shaped, light-tone area which identifies dust generated by thunderstorm activity. Although the surface reports (1E-10c) do not show thunderstorm activity in the vicinity of Khartoum, the satellite picture clearly shows convective clusters identifiable with thunderstorms in the area. This is, therefore, a classic example of a Haboob in progress at the surface. The distinct, light-tone area extending outward from the northeast boundary of the tropical disturbance precisely overlays the region of the Nile River obscured in the morning DMSP visible picture (1E-8a) The same region of the Nile is also obscured in the corresponding METEOSAT picture (1E-11b).

The suspended dust area (light gray shade) in the infrared picture (1E-11a) is elongated in a southwest to northeast direction, suggesting that winds in the dust layer are southerly or southwesterly. Verification of the duststorm and southerly flow is obtained from a time sequence of surface reports (1E-11c), which show a duststorm in progress at Atbara at the time of the METEOSAT picture. Reports from two additional stations provide evidence of a trough line or low-pressure center just to the north of the duststorm The surface streamline analysis (1E-10c) shows the trough **T2** and reports of dust in the vicinity of Khartoum The trough **T2** is clearly revealed at the 500-mb level (1E-10a) and the 850-mb level (1E-10b), with Khartoum reporting a 30-kt southwesterly wind

The FNOC 500-mb analysis (1E-12a) shows that the northern Sudan is under the influence of southwesterly winds ahead of the trough **T2**. This is favorable for advecting the dust over the Red Sea that has been raised by the thunderstorm complexes south of Khartoum. There is also a new trough **T3** which has developed upstream of the trough **T2**.

The FNOC 36-hour 500-mb prognosis (1E-13a), valid at 1200 GMT on 14 June, shows that the trough **T2** dissipates, and the new trough **T3** advances to a position over the eastern Mediterranean. This will continue to provide favorable conditions for the advection of dust at this level from Sudan into the Red Sea region. *continued on page 1E-14*

phical
wever,
earlier
ery, in
which
l area.
with a
er the
north
for the
d dust
hat the
is not
pected
ending

frared
DMSP
haped,
ed by
eports
in the
clearly
with
classic
e. The
in the
bance
ccured
). The
n the

in the
vest to
e dust
ion of
rom a
show
of the
tional
r low-
n. The
rough
toum.
00-mb
, with
l.

at the
sterly
le for
been
th of
h has

-13a).
rough
to a
will
r the
e Red
IE-14

00 mb

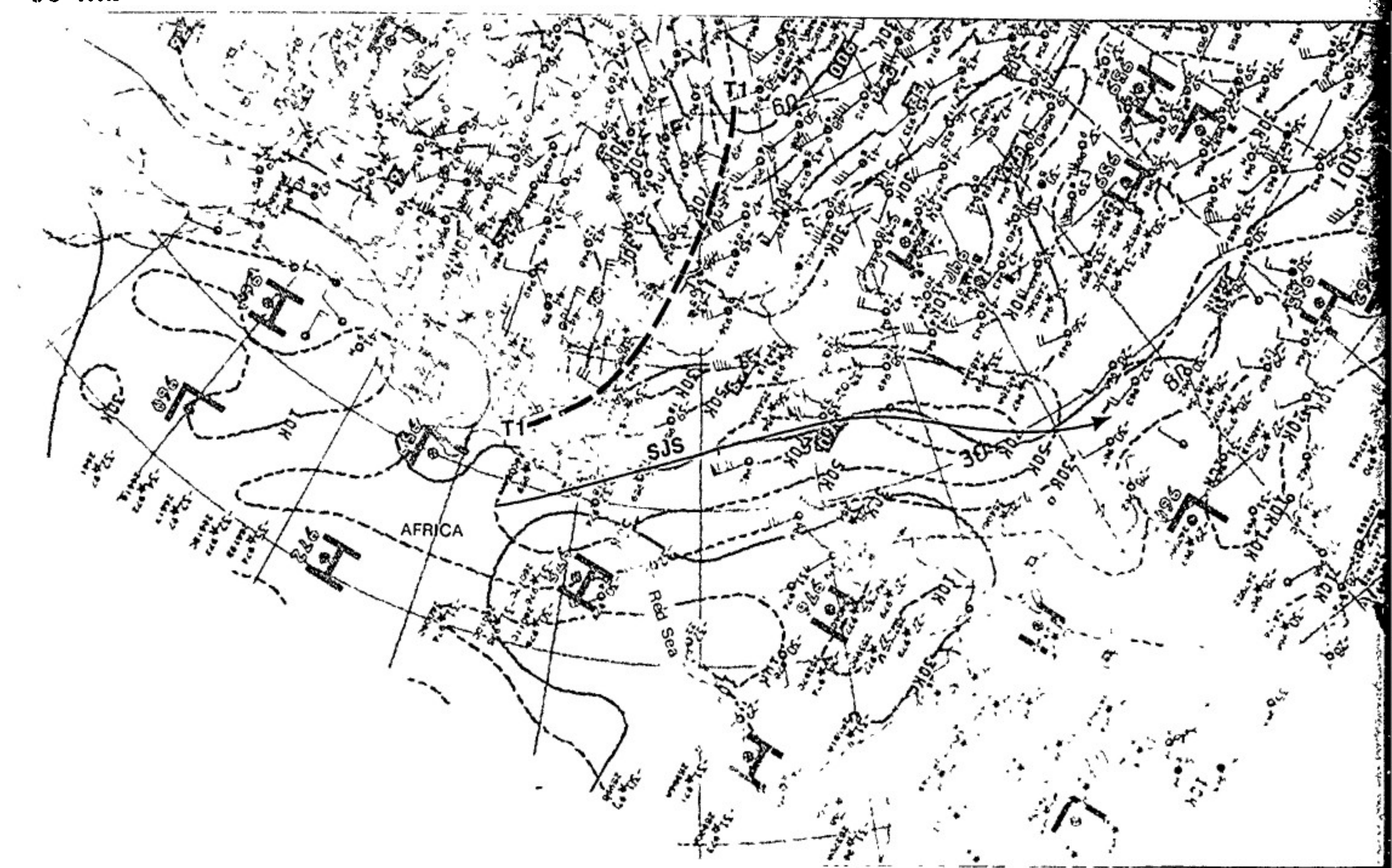


IE-6a NMC 300-mb Analysis 1200 GMT 12 June 1979

500 mb


IE-6b NMC 500-mb Analysis 1200 GMT 12 June 1979


IE-7a METEOSAT Enlarged View Infrared Picture 1155 GMT 12 June 1979

850 mb


IE-7b NMC 850-mb Analysis 1200 GMT 12 June 1979

surface

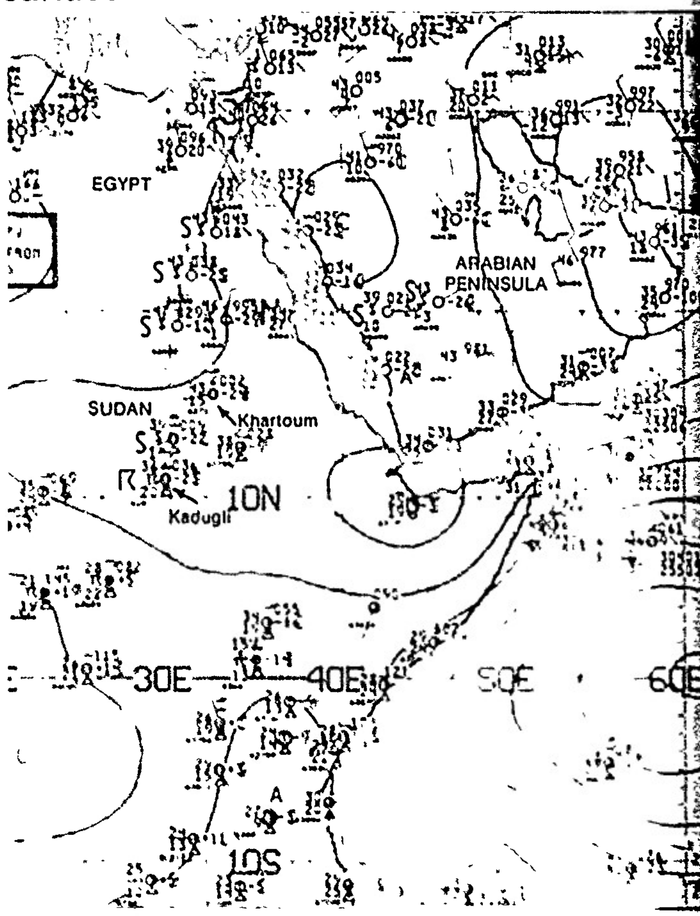


IE-7c NMC Tropical Surface Streamline Analysis 1200 GMT 12 June 1979.

IE-8a E-E DMSP LS Low Enhancement 0759 GMT 13 June 1979

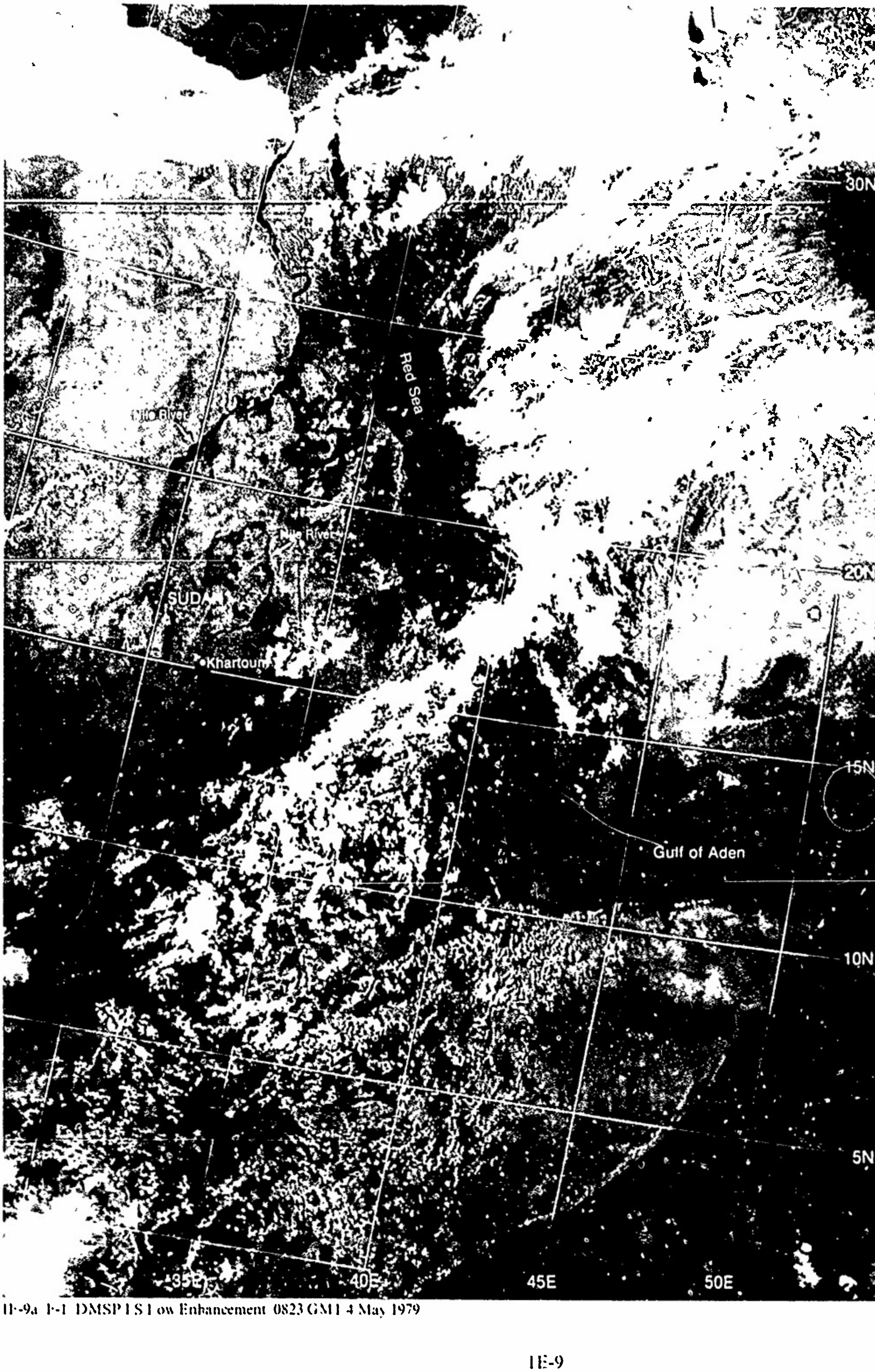


1E-9a F-1 DMSP LS Low Enhancement 0823 GMT 4 May 1979

500 mb

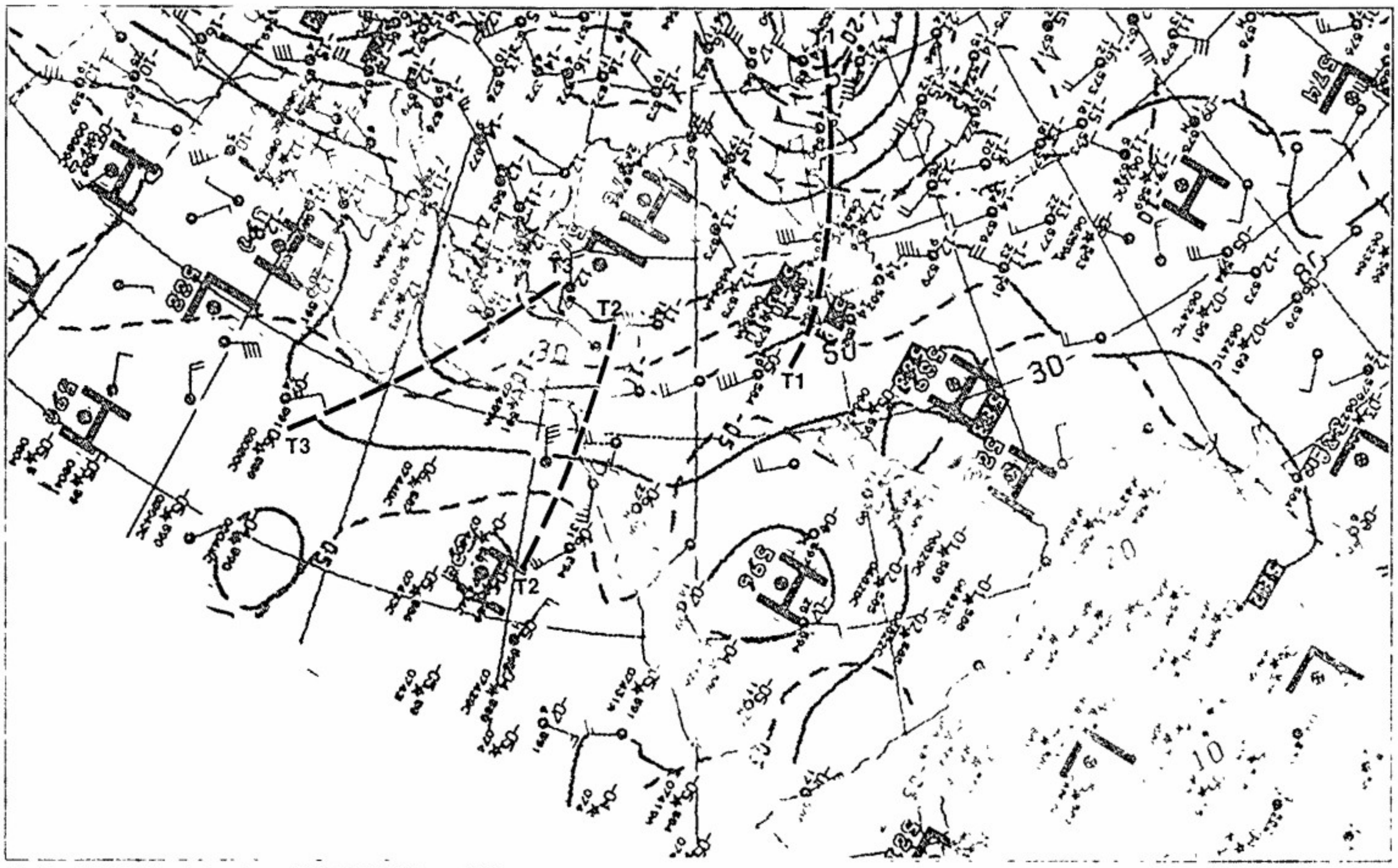


IE-10a NMC 500-mb Analysis. 1200 GMT 13 June 1979

850 mb

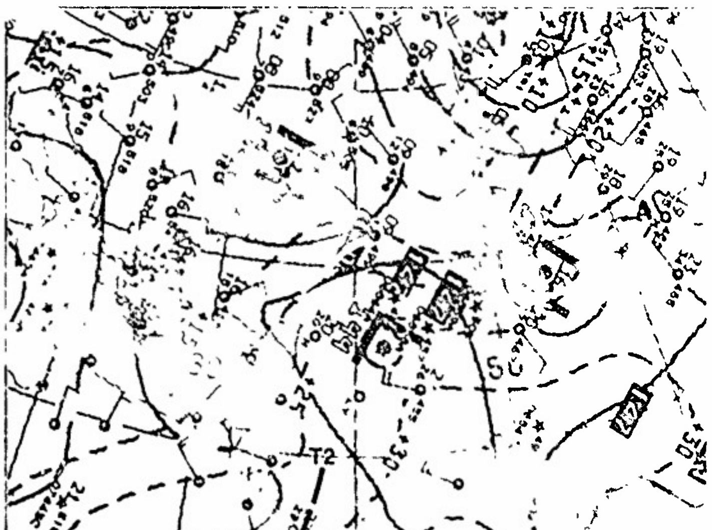


II [illegible] lysis 1200 GMT 13 June 1979

surface

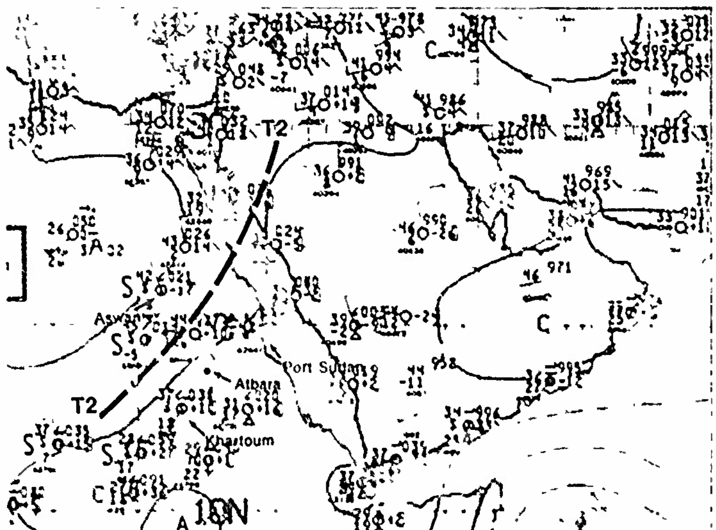


II-10c NMC Tropical Surface Streamline Analysis 1200 GMT 13 June 1979

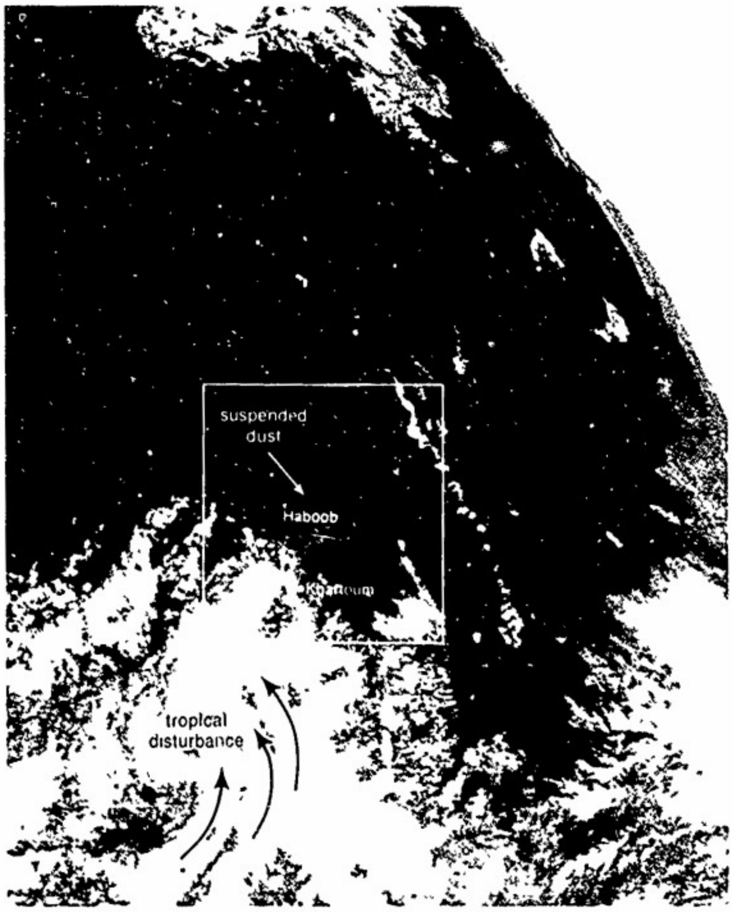


1E-11a METEOSAT Enlarged View Infrared Picture 1155 GMT 13 June 1979


1E-11b METEOSAT Enlarged View Visible Picture 1155 GMT 13 June 1979

| STATION | 62414 (Aswan) 24 0N 32 8E | | | 62641 (Port Sudan) 19 6N 37 2E | | | 62680 (Atbara) 17 7N 34 0E | | |
|---|---|---|---|---|---|---|---|---|---|
| DATE TIME | ww | SLP | dd/ff | ww | SLP | dd/ff | ww | SLP | dd/ff |
| 13/00 | | 1005 4 | 35/07 | | | | | | |
| 13/06 | | 1005 6 | 02/06 | | | | | | |
| 13/12 | | 1002 6 | 35/10 | | 1002 9 | 09/11 | 31 | 1001 6 | 22/11 |
| 13/18 | | 1003 4 | 10/06 | | | | 6 | 1002 3 | 20/16 |
| 14/00 | | 1005 8 | 36/08 | 6 | 1004 4 | miss | 31 | 1008 4 | 17/14 |
| 14/06 | | 1008 4 | 02/12 | 6 | 1006 7 | miss | 6 | 1008 8 | 18/08 |
| 14/12 | | 1006 2 | 34/06 | | 1004 3 | 08/17 | 6 | 1006 3 | 20/10 |

Surface observations for stations 62414, 62641, and 62680 located in the vicinity of the 13-14 June 1979 Haboob originating over the Sudan

Surface wind (dd/ff)

Sea level pressure (SLP)

Present weather (ww)

6 Widespread dust in suspension in the air, not raised by wind, at time of observation

31 Slight or moderate duststorm or sandstorm no appreciable change during past hour

1E-11c Table of Surface Weather Reports.

Inset of the Haboob.
Infrared Picture
1155 GMT 13 June 1979

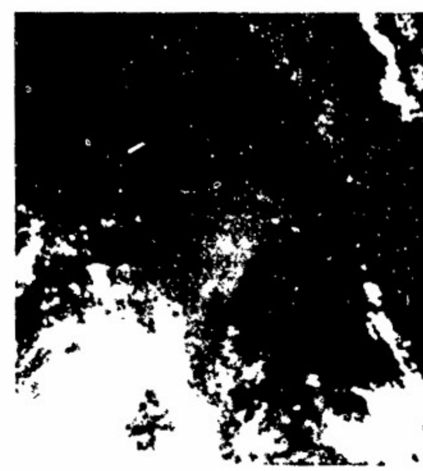

Inset of the Haboob
Visible Picture
1155 GMT 13 June 1979.

500 mb

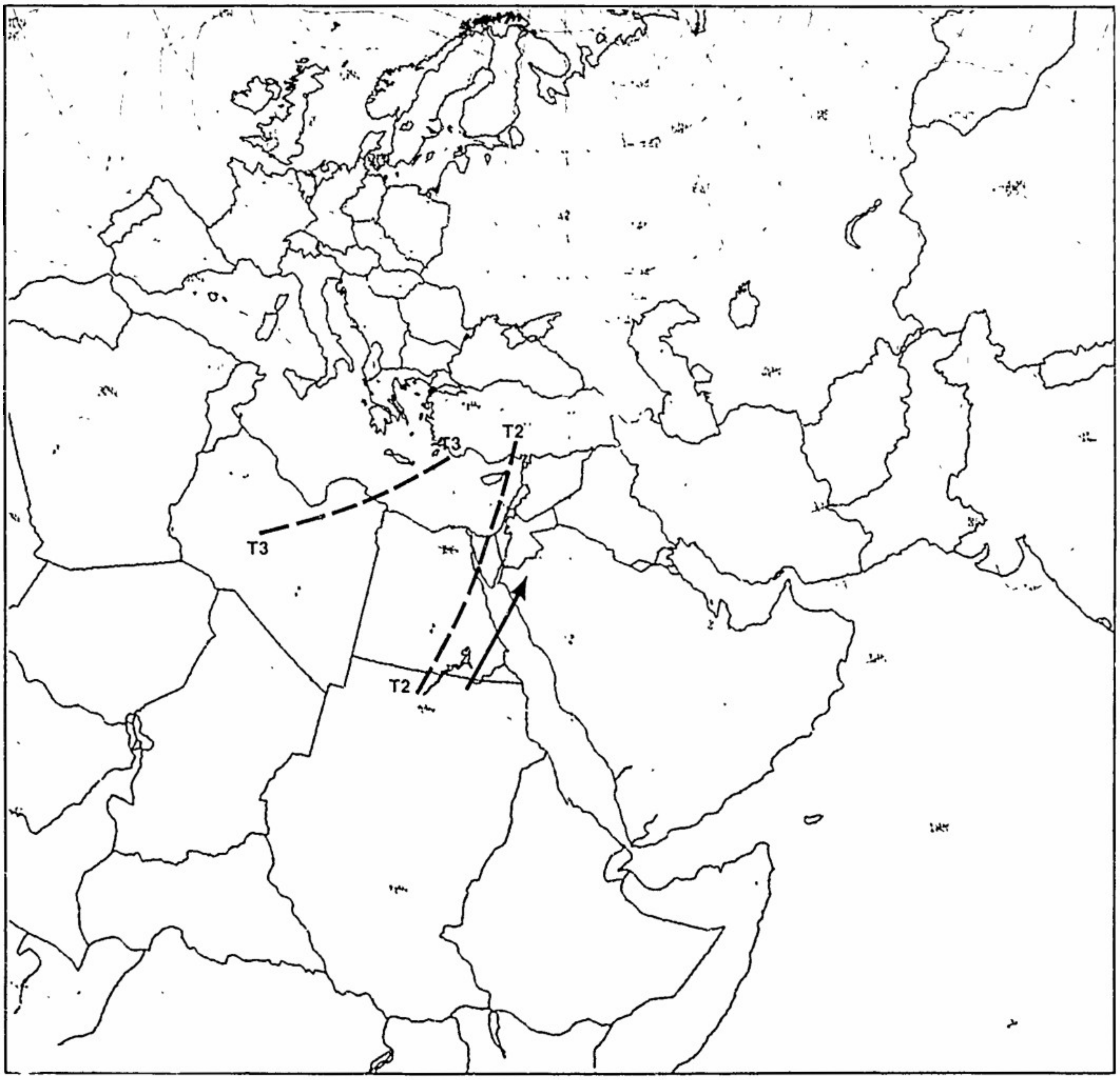


1E-12a FNOC PE Initial 500-mb Analysis 0000 GMT 13 June 1979

**500 mb**

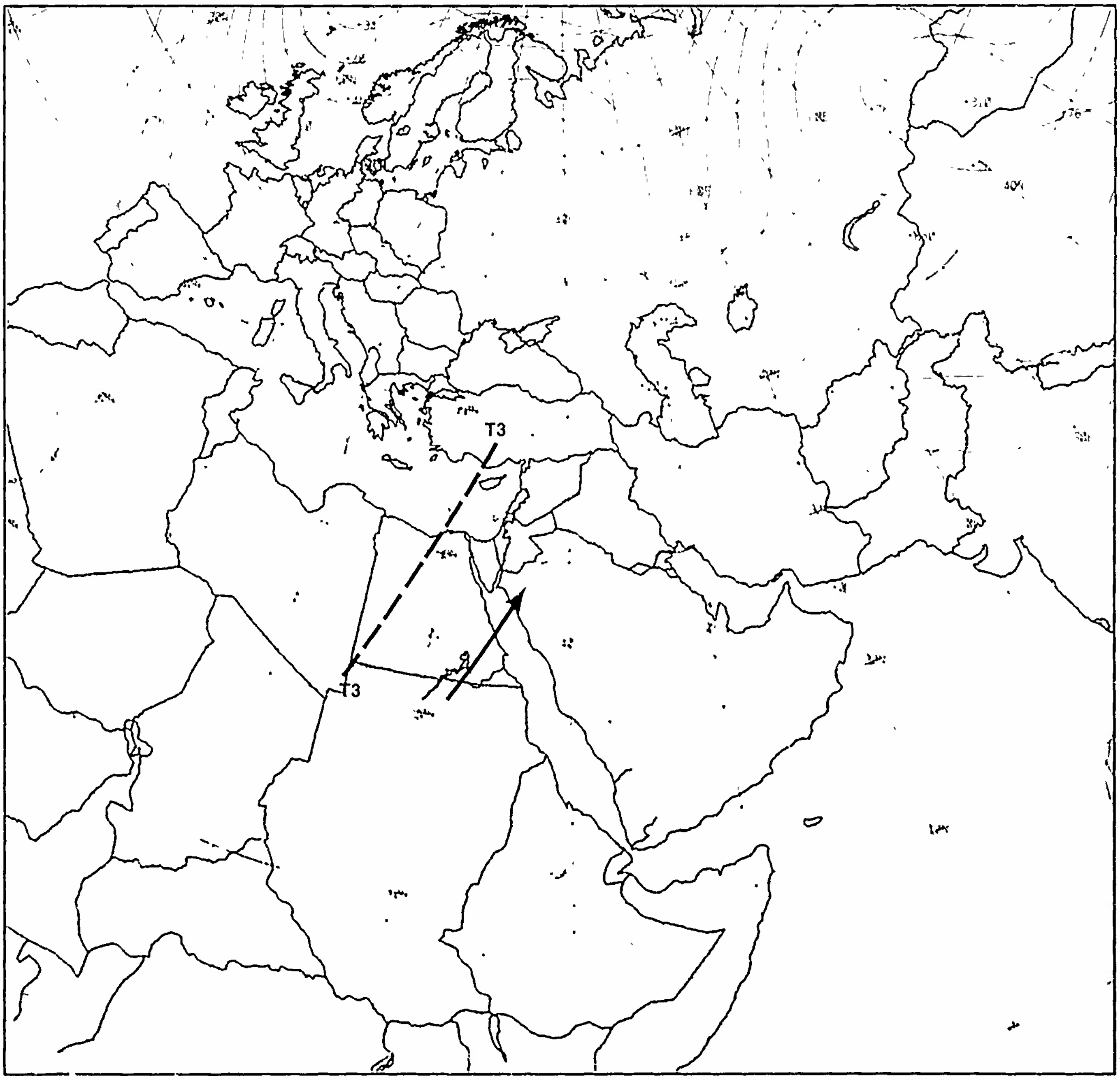


IE-13a FNOC PE 36-hr 500-mb Prognosis Valid 1200 GMT 14 June 1979

The DMSP visible picture at 0559 GMT (1E-15a) provides an excellent view of the suspended dust which has been advected over the Red Sea from the Sudan. The light gray shade area in the simultaneous DMSP infrared picture (1E-15b) precisely outlines the duststorm area as a region of moderately cold temperature, indicating that the dust extends vertically to mid-tropospheric altitudes.

The 500-mb analysis for 1200 GMT (1E-14a) shows a generally good correspondence of the circulation features as indicated by the FNOC 36-hour 500-mb prognosis (1E-13a). Note the anticyclonic turning of winds around the high, bringing southerly flow over Khartoum at the 500-mb level. However, evidence on the 850-mb analysis for 0000 (1E-14b) and 1200 GMT (1E-14c) reveal a complexity not captured at the 500-mb level. These latter analyses show that the original trough T2, associated with the duststorm development, has merged with the low pressure belt over southern Saudi Arabia, and that a new trough T3 has moved to a position over the northern portion of the Red Sea. This places the dust source area, near Khartoum, under flow having a more northerly component instead of a southwest to west component so that continued advection of dust into the central and southern portion of the Red Sea at low levels would not occur.

The surface streamline analysis at 1200 GMT (1E-16b) reveals an intensified low-pressure area near the southern portion of the Red Sea, and widely scattered thunderstorms, with little evidence of any strong westerly component to bring additional dust over the Red Sea. Verification of the decrease in dust over the Red Sea is revealed in METEOSAT visible (1E-16a) and infrared (1E-17a) pictures. These pictures show a thin veil of suspended dust, as terrain features again are revealed in greater clarity over the Khartoum region and along the Nile River. By 1200 GMT on the following day (15 June), the METEOSAT visible picture (1E-17b) shows only a faint veil of dust in suspension over the southern portion of the Red Sea, with no evidence of renewed dust-generating thunderstorm complexes over the Sudan region.

Important Conclusions

1. Heavy convective activity, such as that associated with tropical disturbances over the Sudan, can generate Haboobs which lift large quantities of dust over extensive areas and to high altitudes.

2. Earliest detection of duststorms over land can be obtained by comparing visible imagery with previously cloud-free dust-free imagery over the same region.

3. Infrared imagery clearly reveals dust plumes as soon as the dust is raised to an altitude where it radiates at a temperature colder than the surrounding land surface.

4. During the summer monsoon, the southwesterly flow ahead of mobile polar troughs advancing across the eastern Mediterranean can pick up the dust from duststorms originating over the Sudan. The raised dust forms a huge cloud of dust which may be advected over the Red Sea, resulting in widespread reduced visibilities.

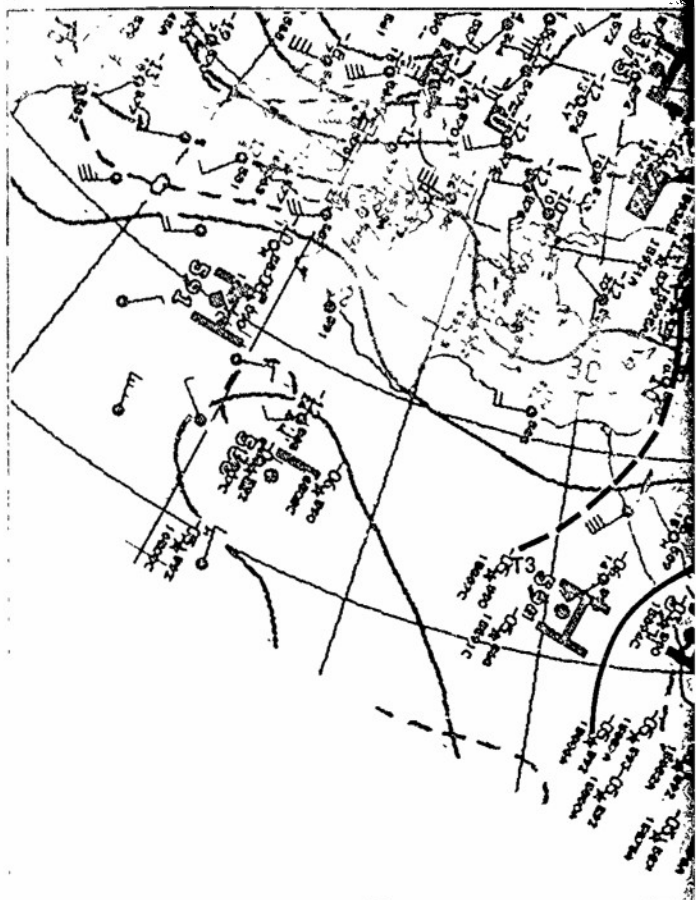


1E-14a NMC 500-mb Analysis 1200 GMT 14 June 1979

850 mb

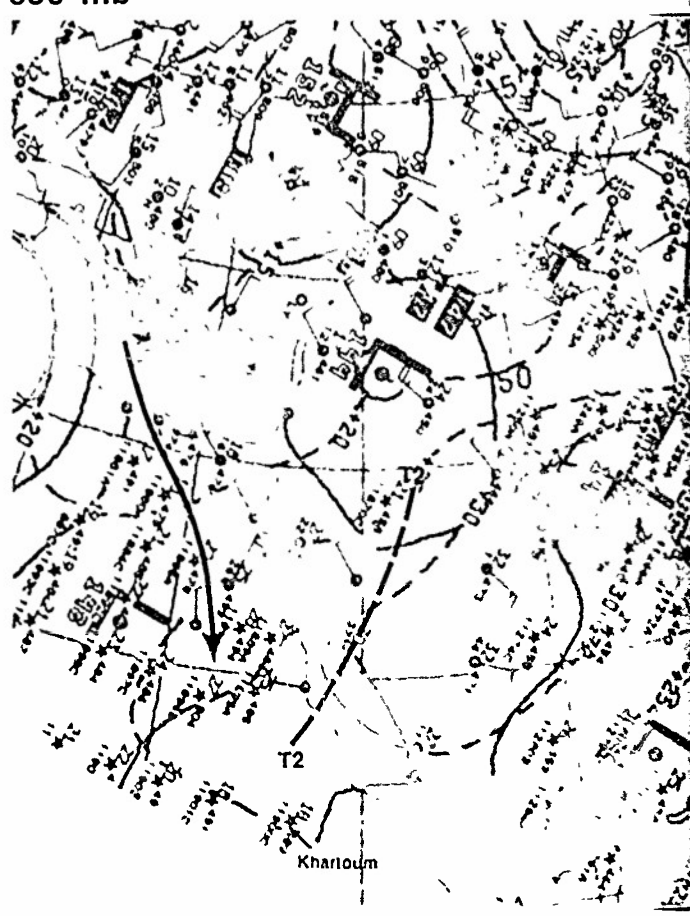


1E-14b NMC 850-mb Analysis 0000 GMT 14 June 1979

500 mb

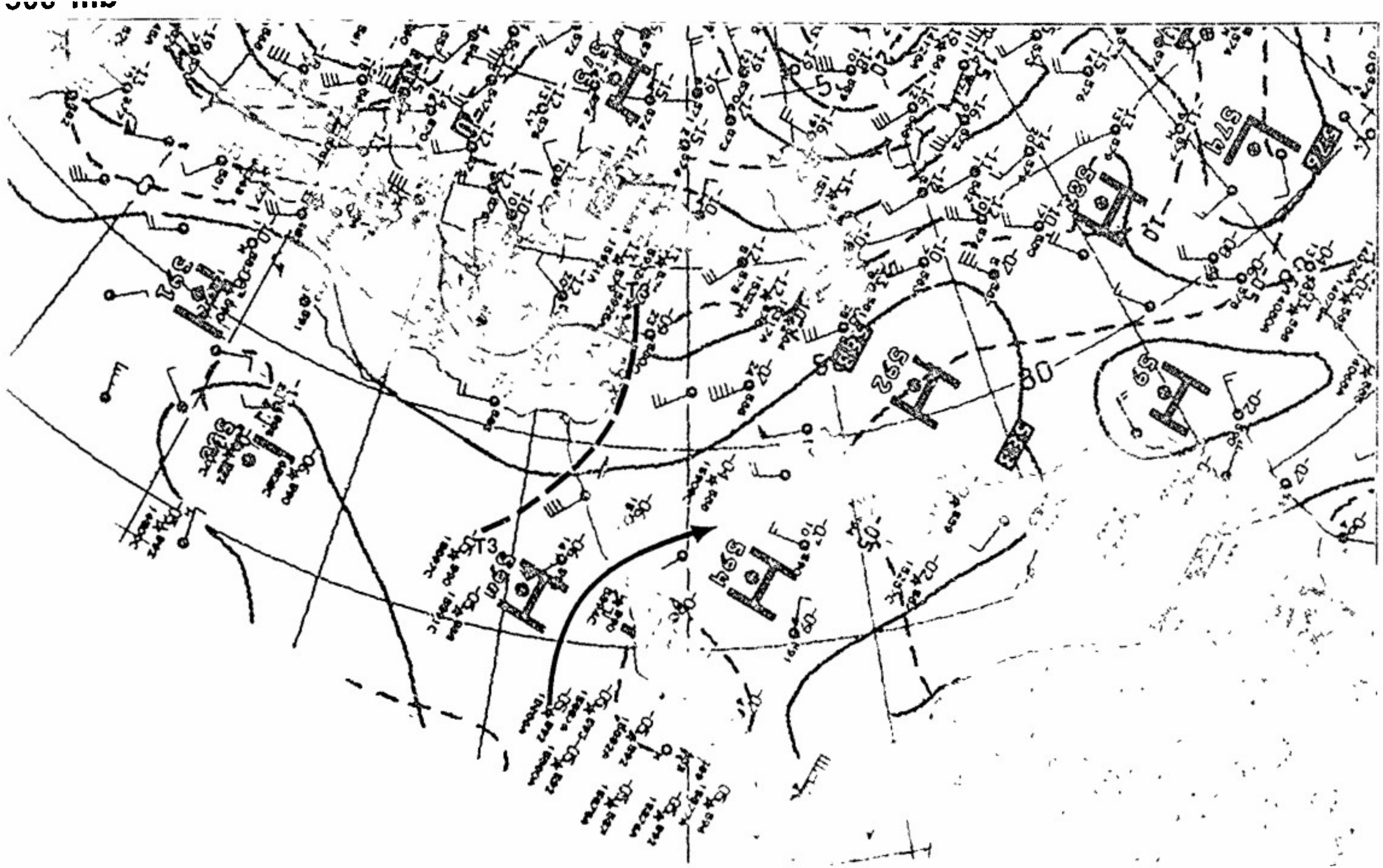


1F-14a NMC 500-mb Analysis 1200 GMT 14 June 1979

850 mb

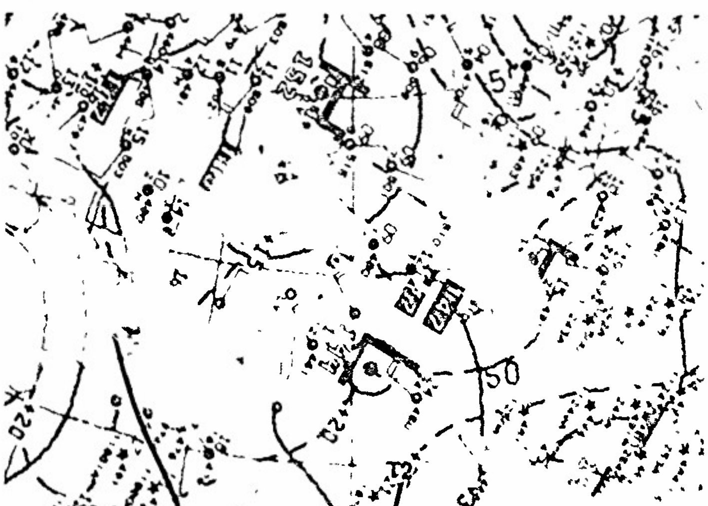


1F-14b NMC 850-mb Analysis 0000 GMT 14 June 1979

850 mb


1F-14c NMC 850-mb Analysis 1200 GMT 14 June 1979


1F-15a F-1 DMSP LS Low Enhancement 0559 GMT 14 June 1979


1E-15b F-1 DMSP 1S 1-Expand Enhancement 0559 GMT 14 June 1979

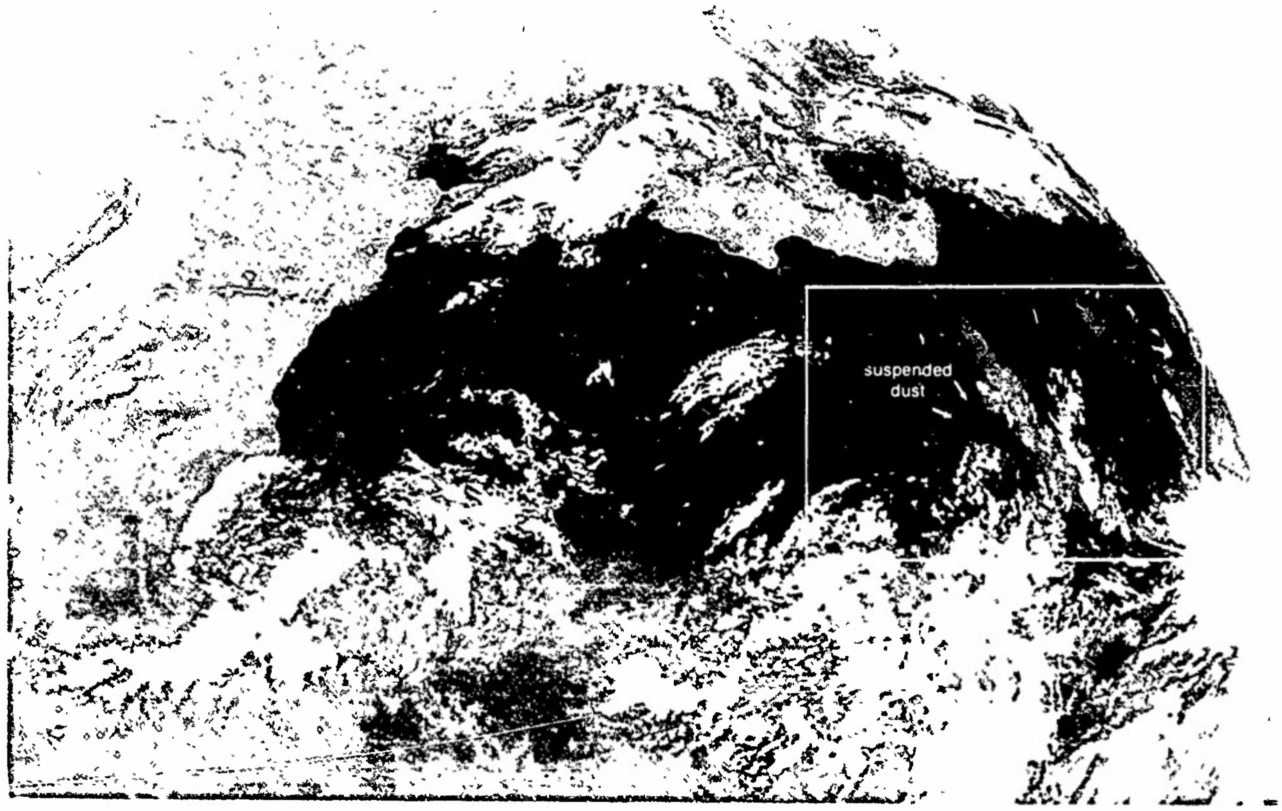


IE-17a METEOSAT Enlarged View Infrared Picture 1155 GMT 14 June 1979

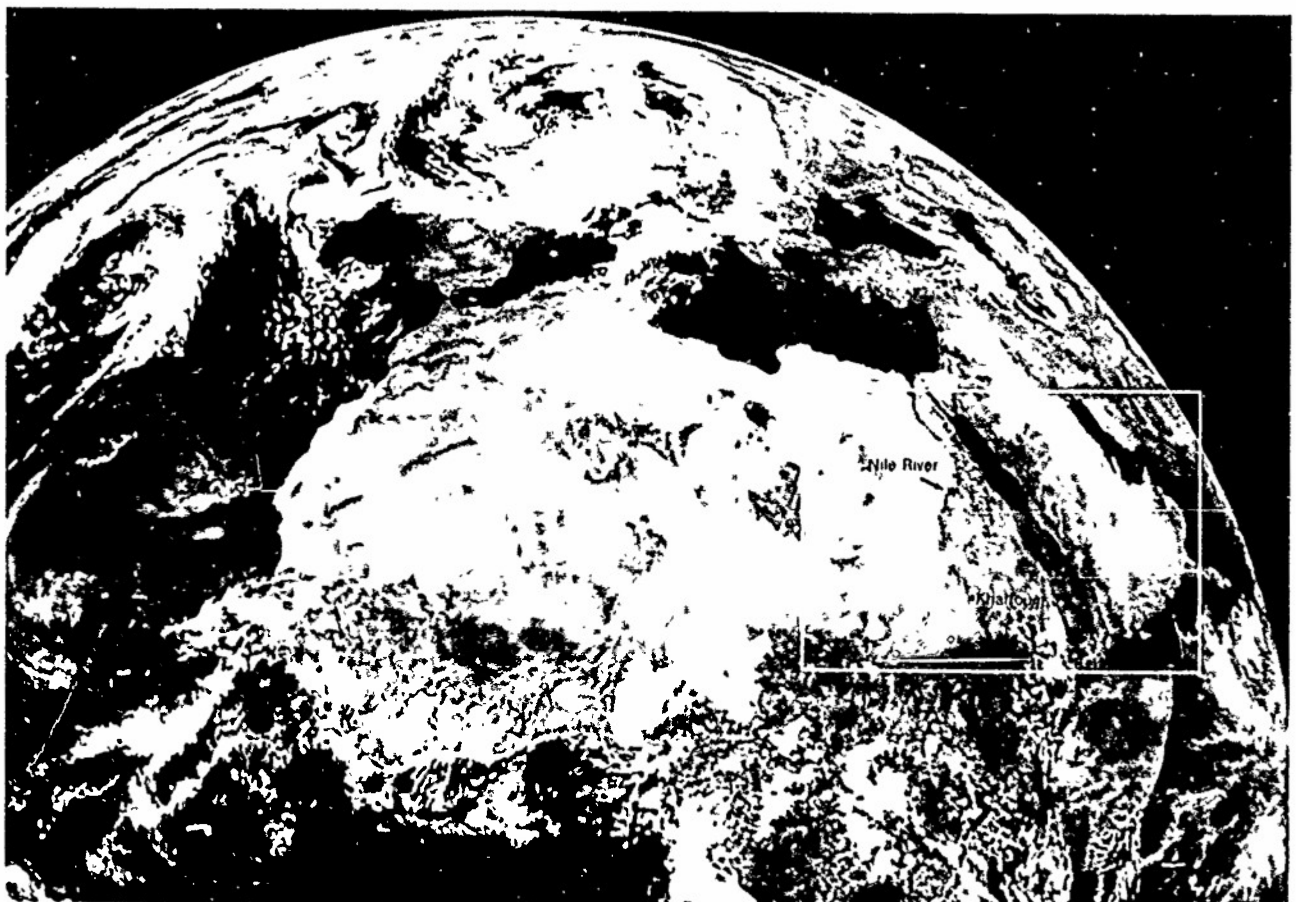


IF-17b METEOSAT Enlarged View Visible Picture 1155 GMT 15 June 1979

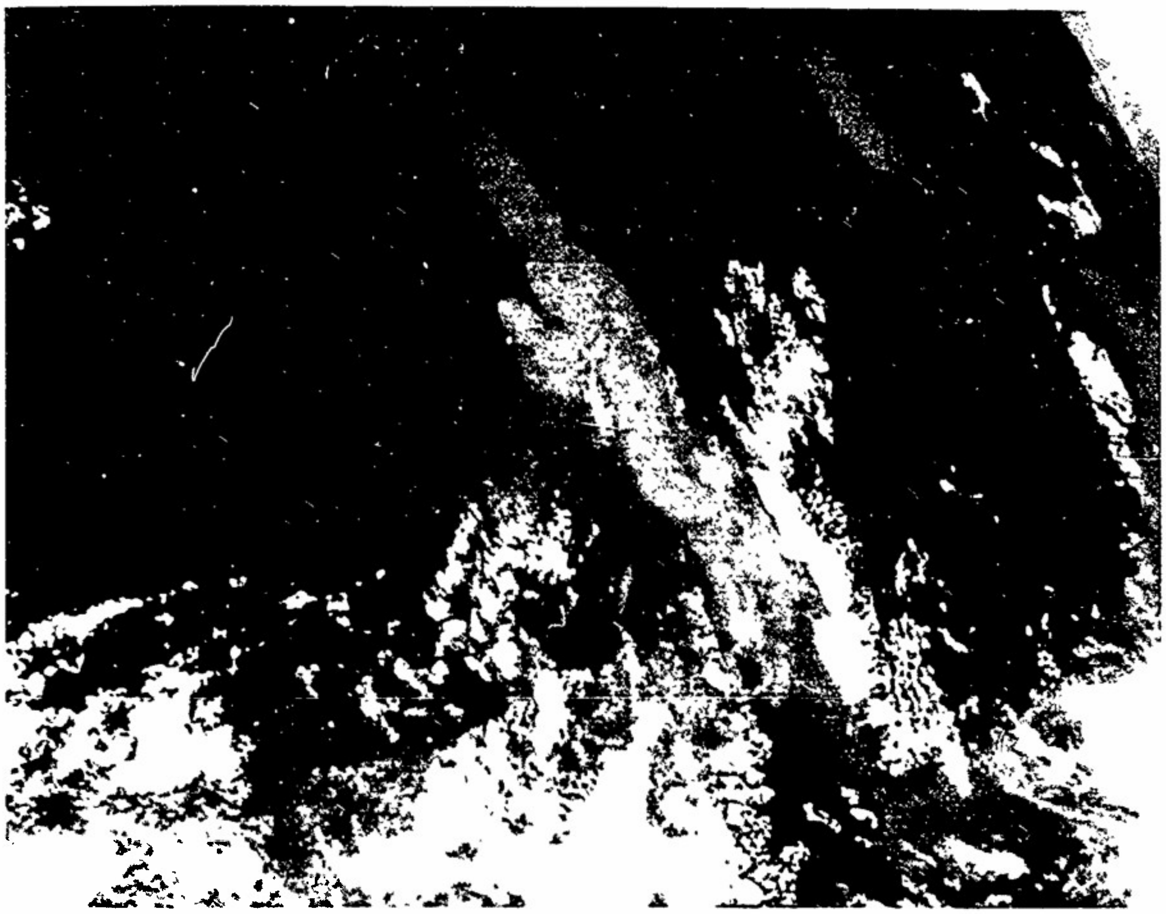

Inset of Suspended Dust Region Infrared Picture 1155 GMT 14 June 1979.

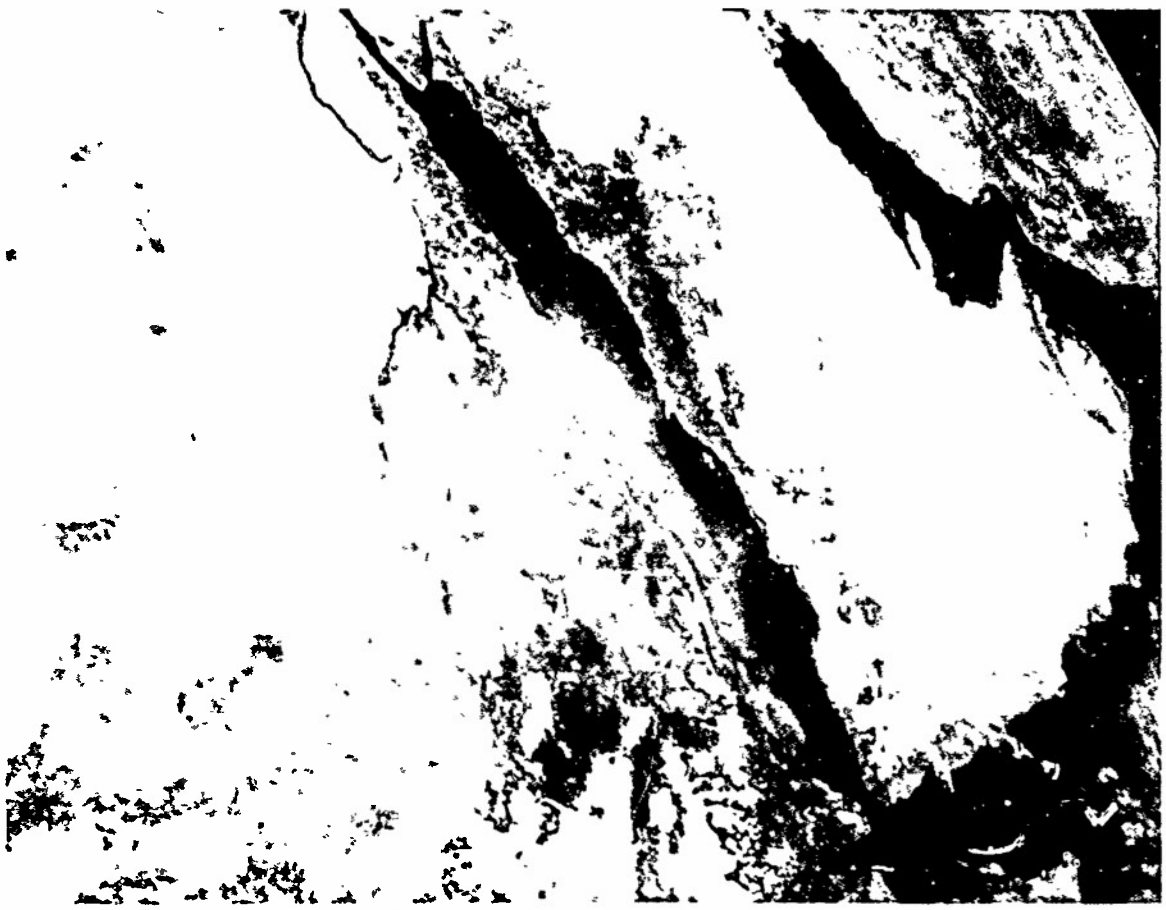

Inset of Suspended Dust Region Visible Picture 1155 GMT 15 June 1979

## Case 3 Red Sea/Persian Gulf—Summer

### *Persian Gulf Duststorms*

During the summer monsoon, the surface thermal low over Iran/Iraq/Afghanistan brings persistent northerly or northwesterly flow over the Arabian Peninsula/Persian Gulf region. Moderate to strong (15-25 kt) northwesterly winds develop over the Persian Gulf and are so persistent that the phenomenon has been identified as the "Forty-Day Shamal," which lasts from early June to mid July. Short duration (2-3 days) Shamal conditions, with attendant high winds, severe duststorms, and unusually high sea state on the Persian Gulf, occur when strong northerly, upper-level winds are superimposed on the lower-level northwesterly winds over the Persian Gulf area. The short-duration Shamals are laden with dust from the desert which reduces visibility, but they are rarely accompanied by thunderstorms or squalls.

**21 June**

By late June, the Shamal (persistent northerly flow over the Persian Gulf) is well established. The surface streamline analysis (1E-20b) confirms the presence of the Shamal—20-kt northwest winds are reported over the Persian Gulf at Bahrain (O1) and northwesterlies (speed illegible) at Basra, Iraq (O2), which also reports suspended dust. The low-level northerly flow over the northern Persian Gulf has developed from a merger of easterly flow around the northern periphery of the thermal low centered over the southeastern Arabian Peninsula and westerly flow around the anticyclonic cell over the north-central Arabian Peninsula.

At 500 mb (1E-20a), general high pressure, typical of upper-level summer conditions over the Red Sea/Persian Gulf region, extends from Africa, across the Arabian Peninsula, to Iran. Over northern Europe, the large-scale circulation shows a well-developed "Omega" type blocking high with a cutoff low L1 to the south. The presence of an omega block over northern Europe is a precursor condition for the development of intense, short-duration (2 3 day) duststorms over the Persian Gulf region. In the omega blocking pattern, the polar jet upstream of the block shows two branches—one branch moving northward over the block and the other branch advancing under the block across the Mediterranean. At 500 mb, the 60-kt westerly wind at Nicosia, Cyprus, just south of the cutoff low L1, identifies the southerly branch of the split flow, and general westerly flow is observed to the east across the eastern Mediterranean coastline.

The METEOSAT visible picture at 1155 GMT (1E-21a) shows a cloud-free view of the Arabian Peninsula and the adjacent Red Sea and Persian Gulf region. The corresponding infrared picture (1E-21b) shows no distinct light gray shade areas (colder temperatures) over the Arabian Peninsula that can be identified as active duststorms in the visible picture. In the visible picture, however, a well-defined narrow dust plume is observed across the northern Persian Gulf coastline a confirmation of the Shamal. The light gray shades over the southern Persian Gulf indicate an accumulation of suspended dust over the area. On the surface streamline analysis (1E-20b), suspended dust is reported at O2, which is in the general location of the dust plume on the satellite picture Although suspended dust is reported at Amman Jordan (O3), it cannot be identified in the visible imagery, but is apparent as a slightly cooler temperature response in the infrared imagery (1E-21b). Note how clearly the Dead Sea, just to the south of Amman, stands out on the visible satellite picture.

**22 June**

The METEOSAT visible picture at 1155 GMT (1E-23c) reveals a faint, light gray shade plume P1 in the Syrian Desert, just to the east of Lebanon, which suggests the presence of raised dust The simultaneous infrared picture (1E-23d) shows two distinct, light gray shade plumes P1 and P2, and a number of minor plumes, in the same geographical area. The light gray shade plumes P1 and P2 have the characteristic features (cold temperatures) associated with suspended dust, as observed on infrared imagery, which confirms the presence of dust on the visible picture. The dust plumes indicate that low-level winds have increased over the region.

On the surface streamline analysis (1E-23b) O3 shows a wind of 20 kt and suspended dust. Suspended dust and a surface wind of 15 kt is reported over the central Syrian Desert at Rutbah, Iraq (O4). Further east, suspended dust is also reported at O2, on the Persian Gulf. On the visible satellite picture (1E-23c), a dust plume (Shamal) is observed across the northern Persian Gulf coastline, just south of Basra, as on the previous day (1E-21a). Suspended dust is also reported at Hail (O5) and Riyadh (O6), Saudi Arabia, where winds have increased in speed about 10 kt from the previous day (1E-20b).

At upper levels, the southern branch of the split polar westerlies, associated with the omega block over northern Europe, dominates the flow pattern over the eastern Mediterranean. At 200 mb (1E-22a), the subtropical jet has merged with the polar westerlies along the base of the cutoff low L1, resulting in the 90-kt isotach maximum over the eastern Mediterranean coastline. At 500 mb (1E-22b), there are 40 50-kt westerly winds crossing the eastern Mediterranean coastline ahead of the cutoff low L1, and at 850 mb (1E-23a), westerly winds of 25-35 kt are also observed in the same region. The juxtaposition of westerlies from 200 mb to 850 mb across the eastern Mediterranean coastline produces strong, turbulent winds at low levels, which are generating the dust plumes P1 and P2 observed on the visible and infrared satellite pictures (1E-23c and 23d).

The westerlies crossing the eastern Mediterranean coastline at 500 mb (1E-22b) and 850 mb (1E-23a) are also influenced by the anticyclone centered over the northern Red Sea. The westerlies are turned anticyclonically around the high cell and are funnelled to the south over the southern Arabian Peninsula (500 mb) and to the east into the Persian Gulf region (500 mb and 850 mb). At 850 mb, the northerly winds approaching the Persian Gulf are enhanced by their location between the anticyclone over the northern Red Sea and the split trough T1 to the north of the Persian Gulf. The alignment of northerly upper-level winds approaching the Persian Gulf region signal the potential for the development of an intense Shamal over the Persian Gulf.

**23 June**

A most important development on this day is the increase in northwesterly wind speeds at 850 mb (1E-24b) from the eastern Mediterranean, across the Syrian Desert, to the Persian Gulf region (note the 50-kt wind at Basra, Iraq). This is primarily due to the increased height-contour gradient between the anticyclone over the northern Red Sea and the split trough T1 to the north of the Persian Gulf The

*23 June continued on page 1E-24*

d with
nagery,
visible
l winds

b), O3
pended
ver the
Further
on the
-23c), a
orthern
on the
ported
where
om the

e split
k over
ver the
a), the
sterlies
in the
editer-
re are
astern
ow L1.
5 kt are
tion of
eastern
rbulent
e dust
nfrared

ranean
3a) are
ver the
urned
nnelled
ninsula
region
winds
y their
orthern
of the
r-level
nal the
hamal

is the
0 mb
ss the
te the
to the
n the
e split
. The
*1E-24*

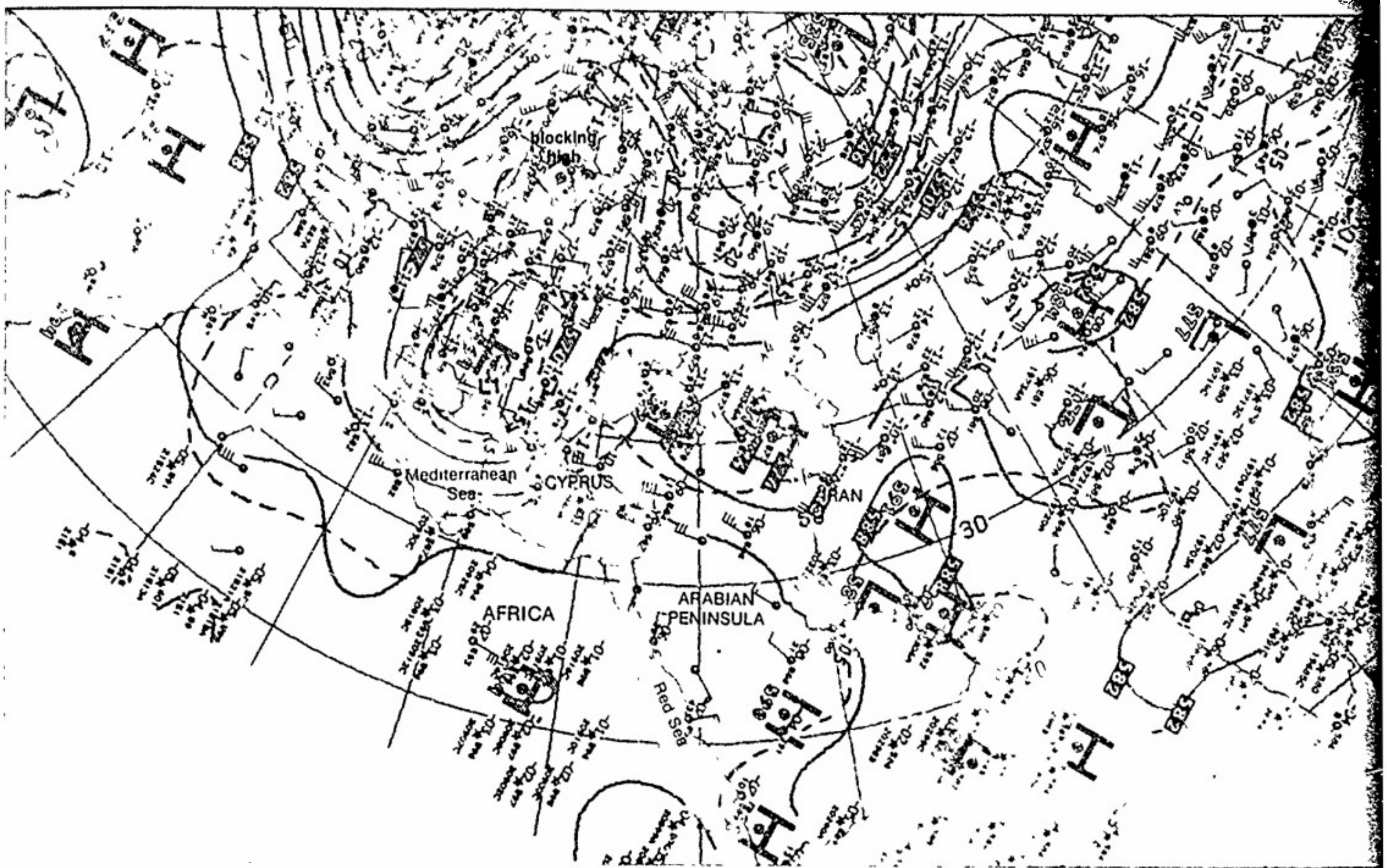


1E-20a NMC 500-mb Analysis 1200 GMT 21 June 1979

surface

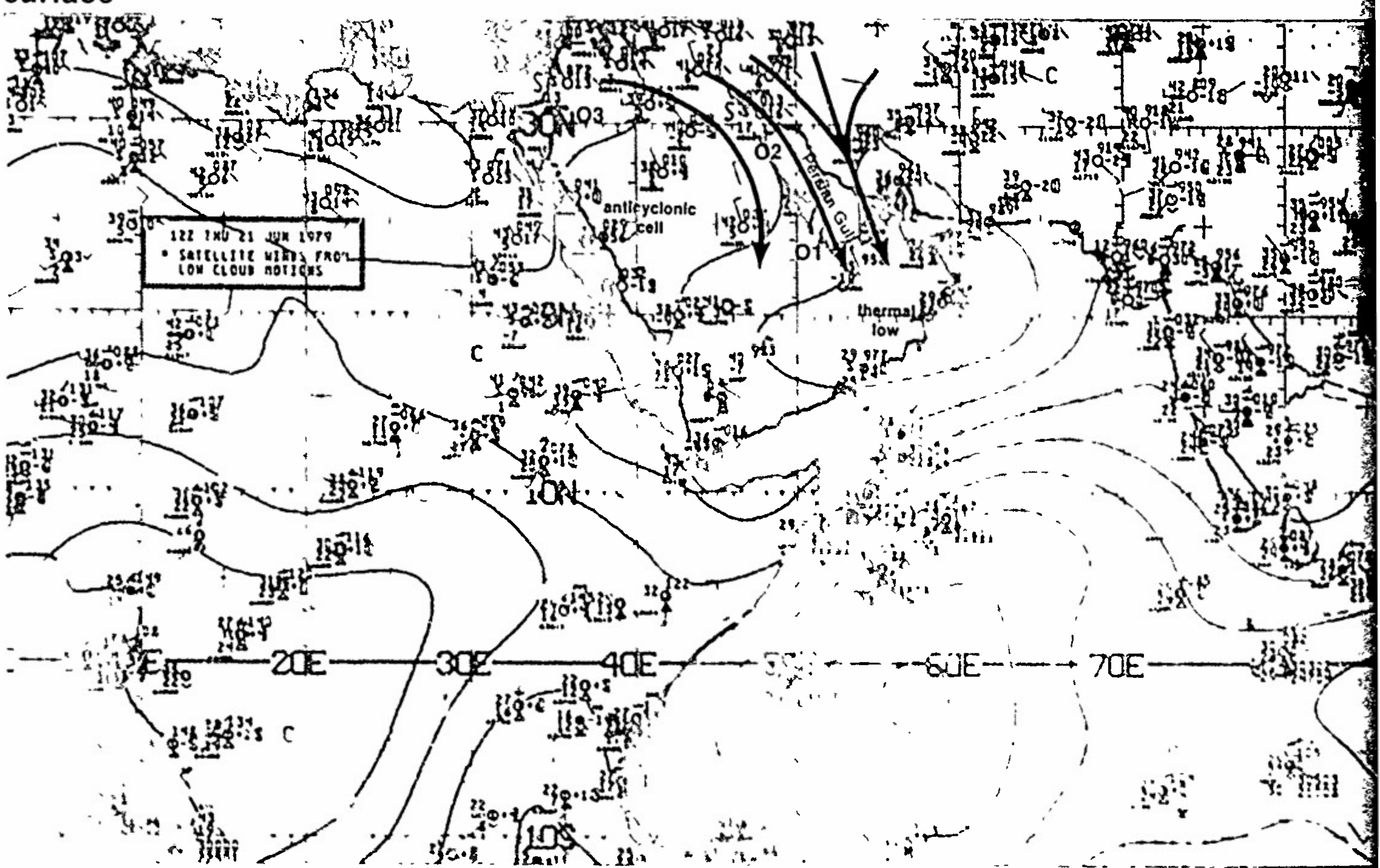


1E-20b NMC Tropical Surface Streamline Analysis 1200 GMT 21 June 1979

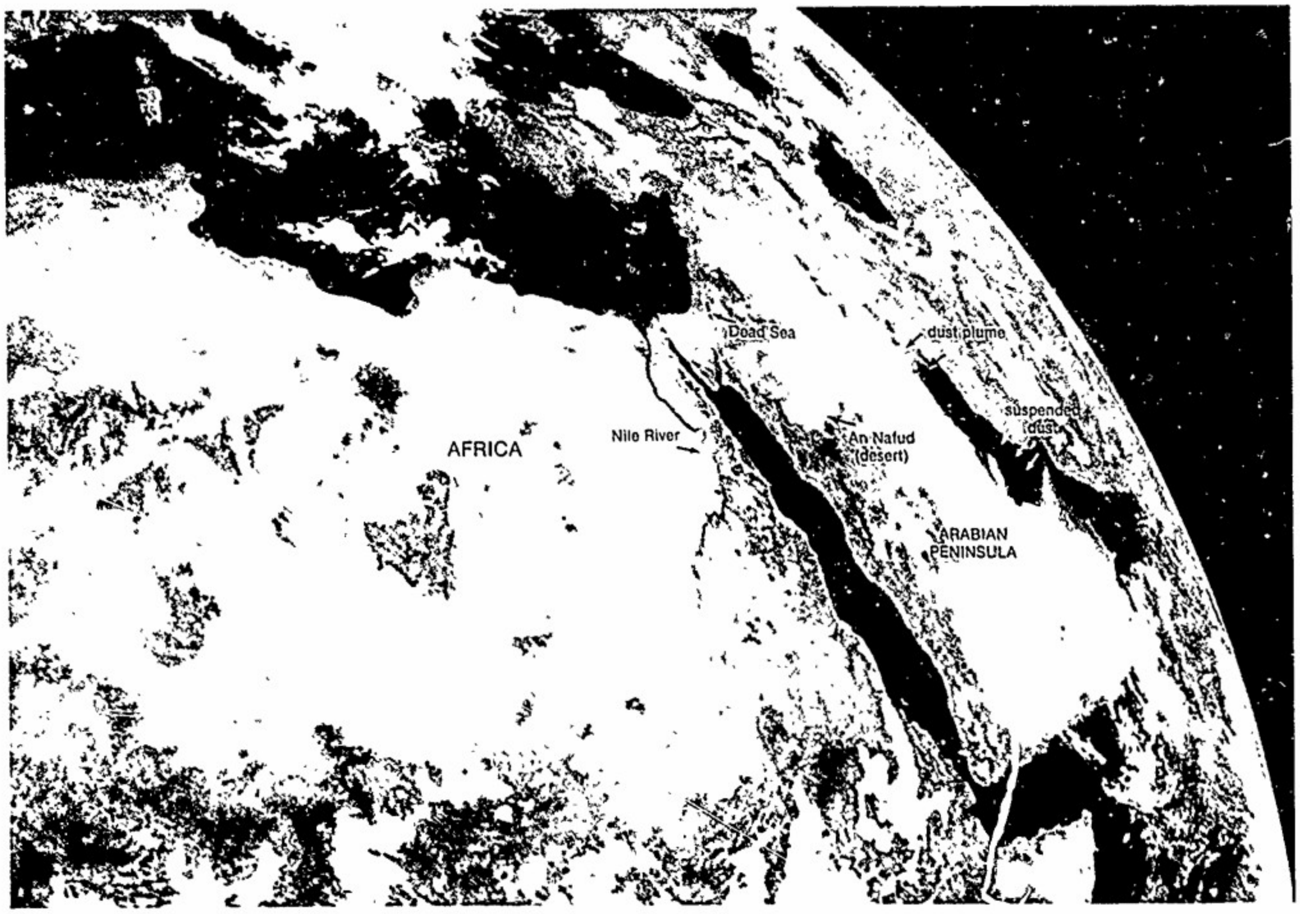


1E-21a. METEOSAT. Enlarged View Visible Picture 1155 GMT 21 June 1979.

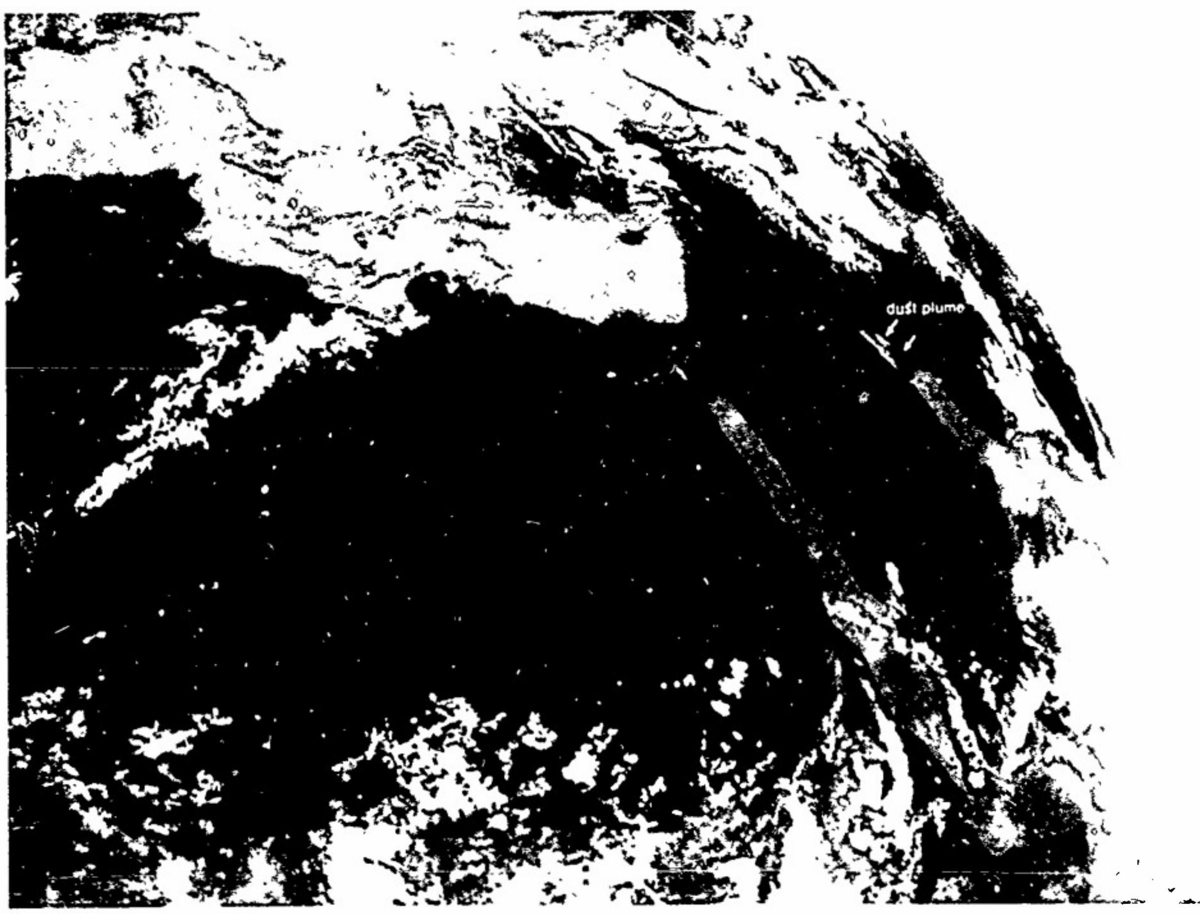


1E-21b METEOSAT Enlarged View Infrared Picture 1155 GMT 21 June 1979

## 200 mb

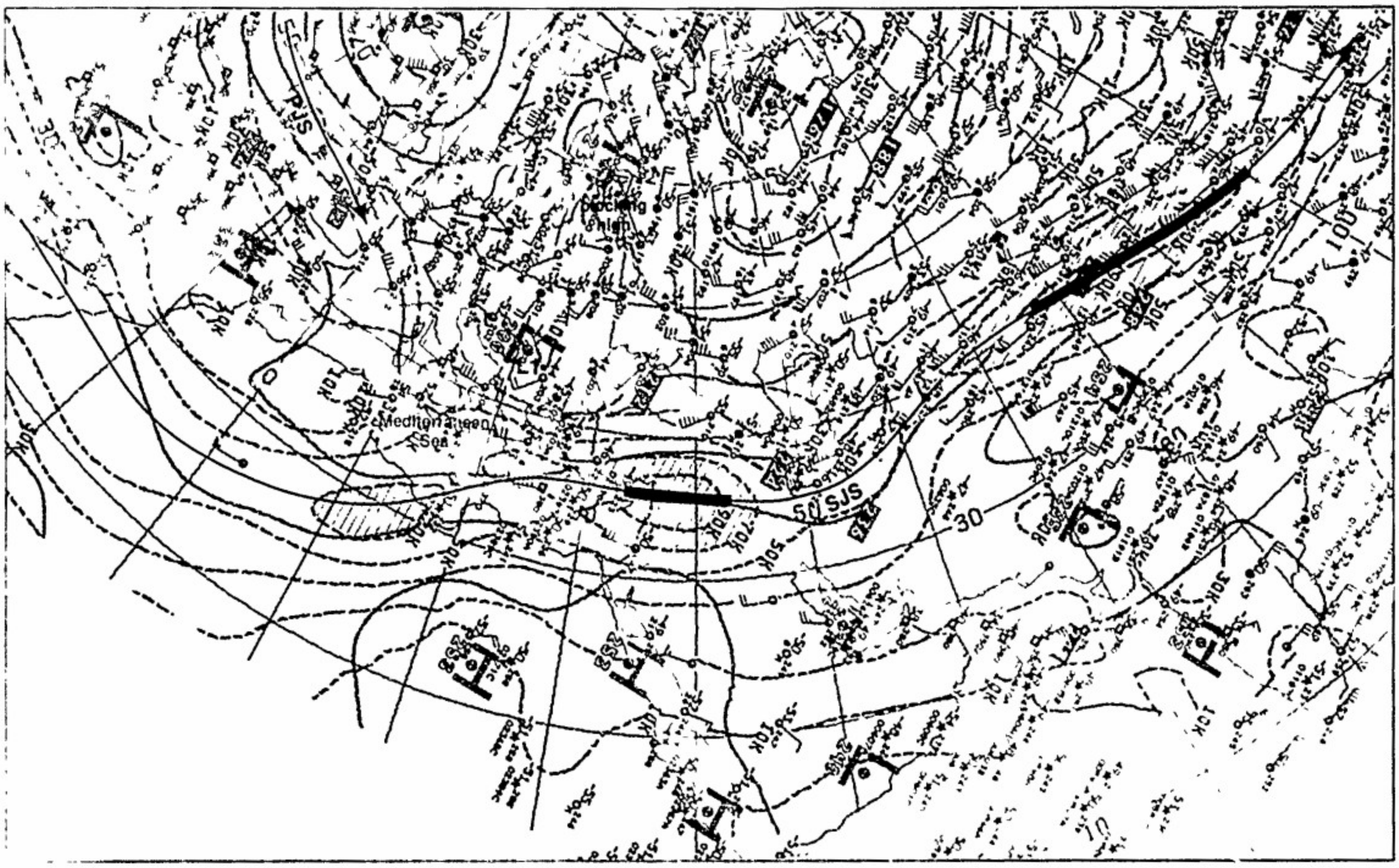


IE-22a. NMC 200-mb Analysis. 1200 GMT 22 June 1979.

## 500 mb

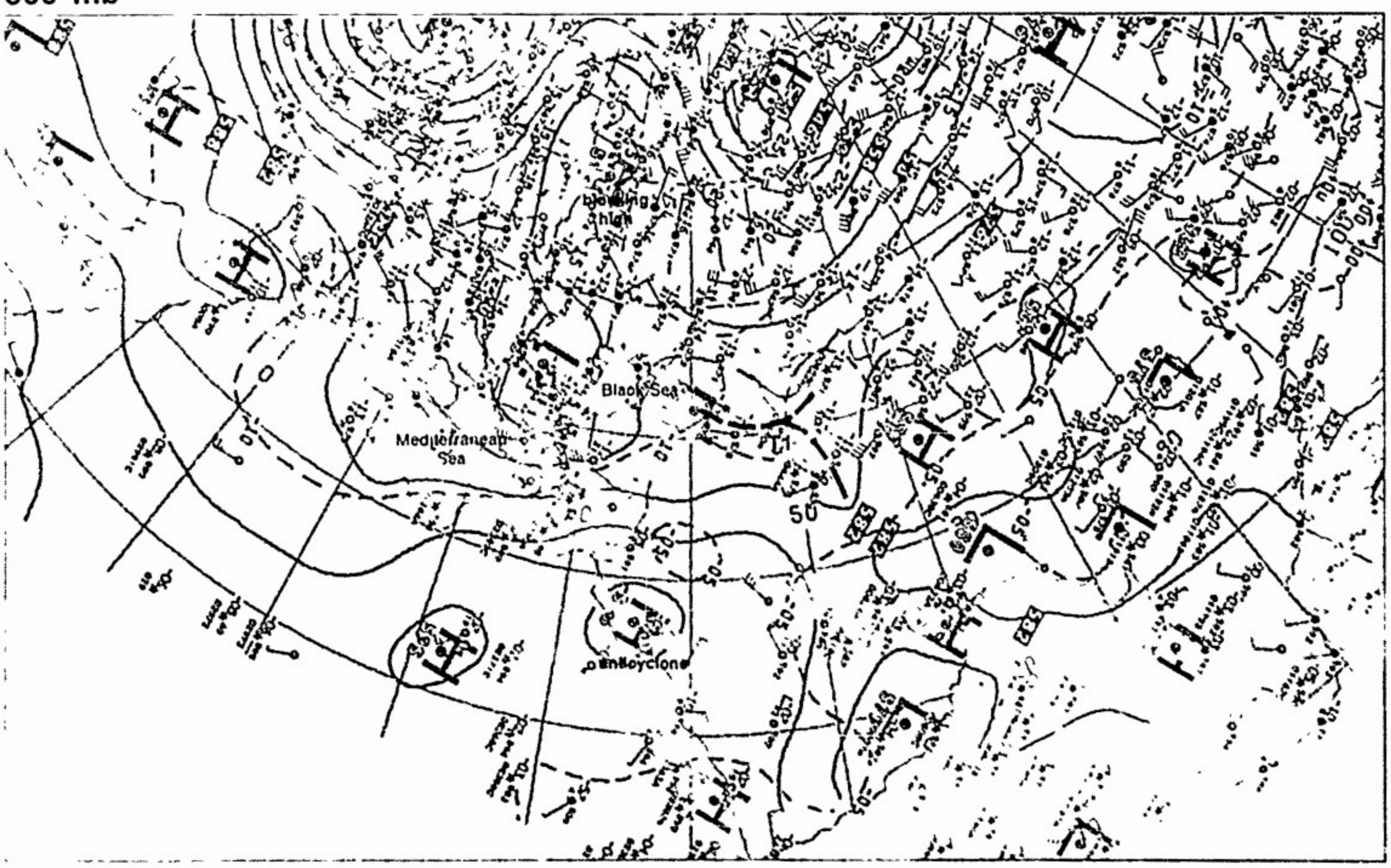


IE-22b NMC 500-mb Analysis 1200 GMT 22 June 1979

850 mb

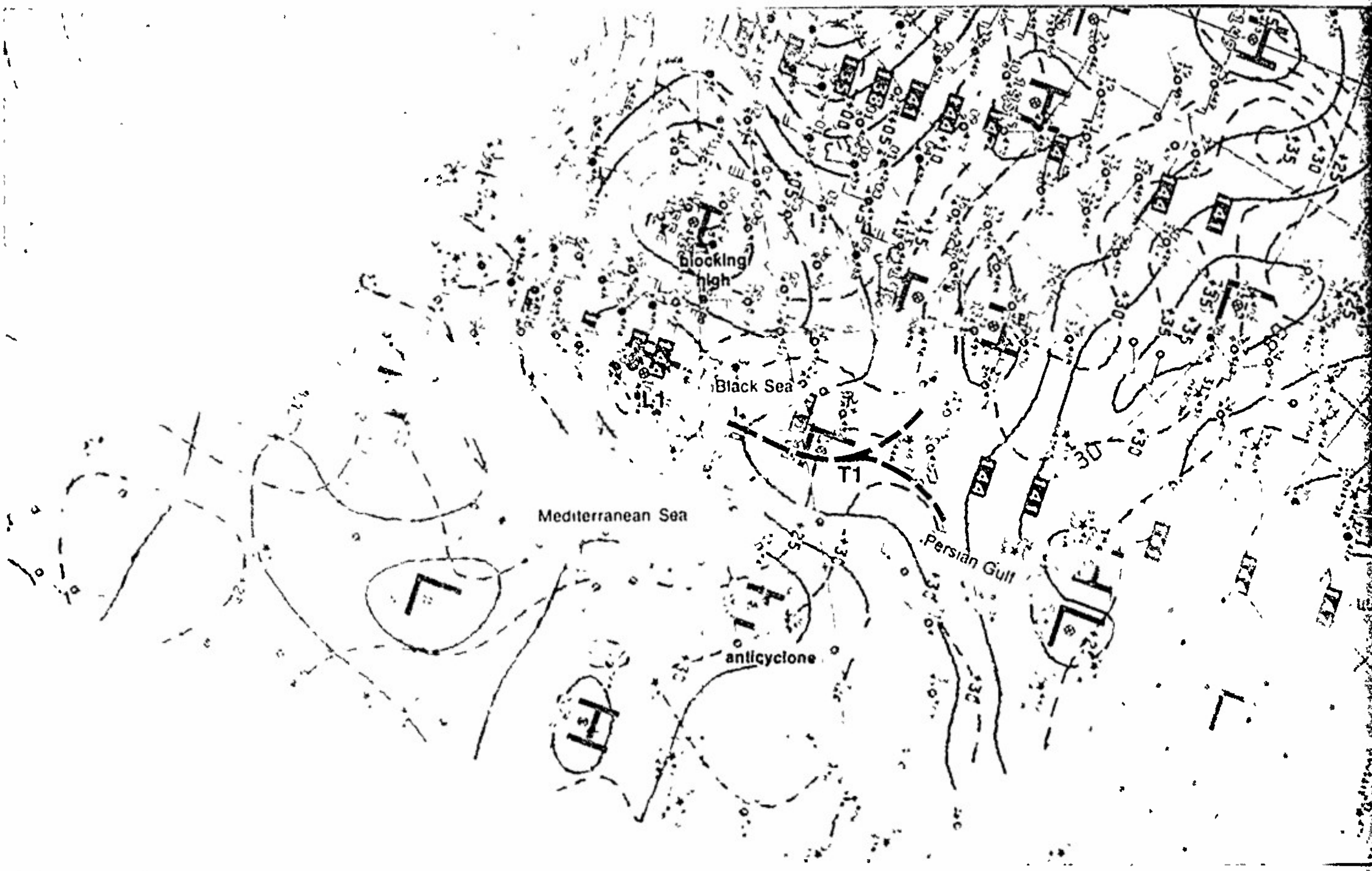


IE-23a. NMC 850-mb Analysis 1200 GMT 22 June 1979

surface

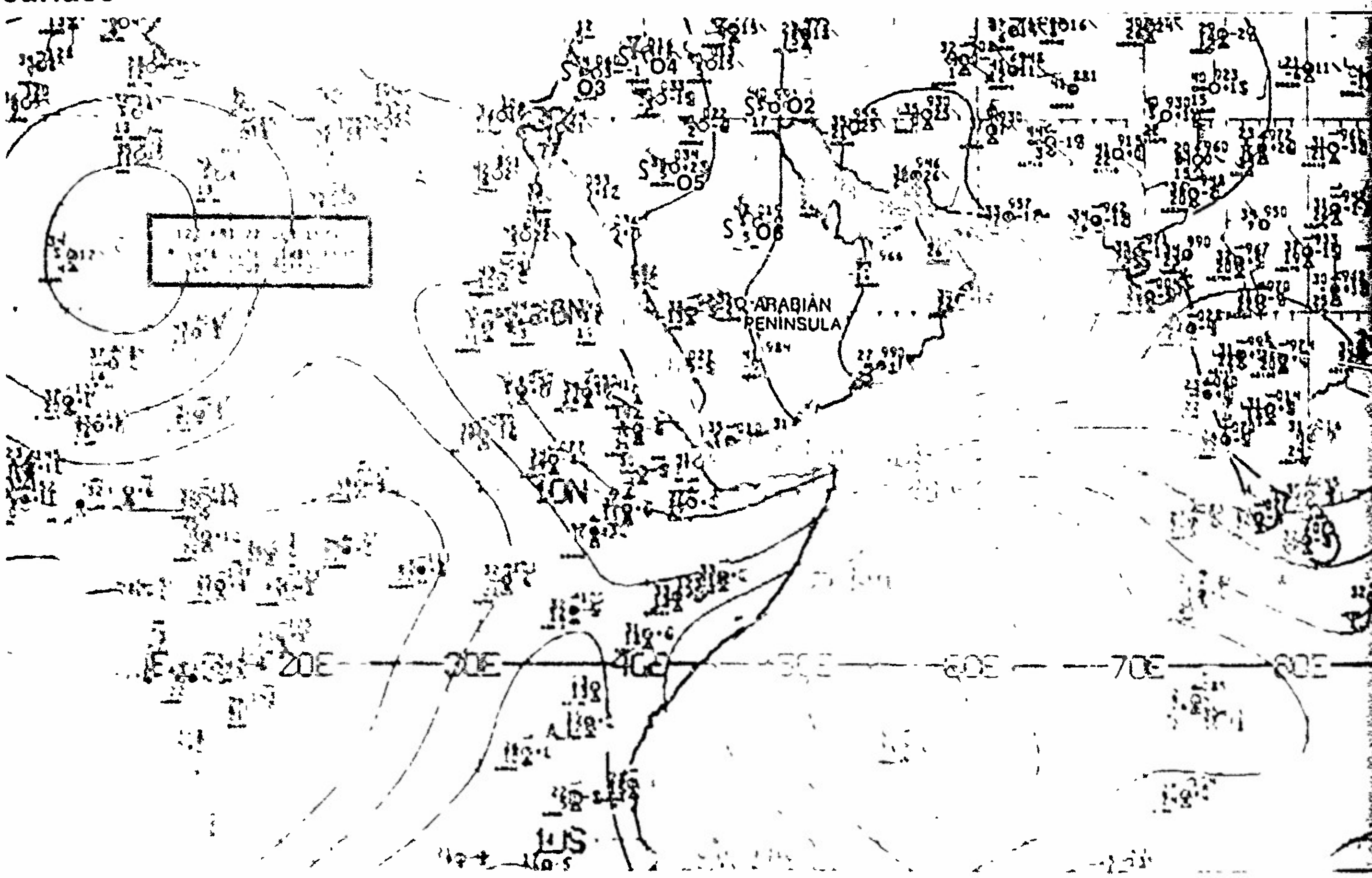


IE-23b. NMC Tropical Surface Streamline Analysis 1200 GMT 22 June 1979

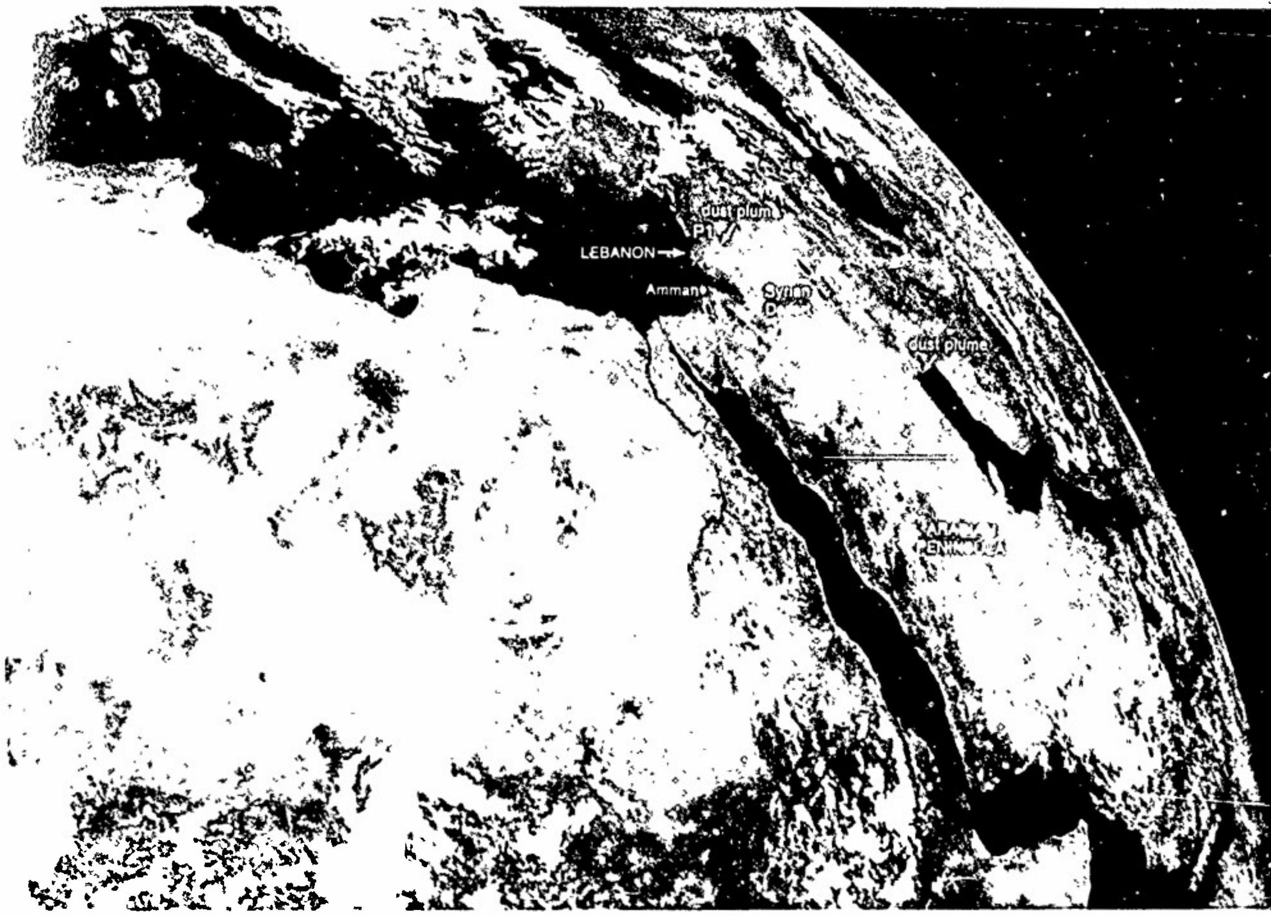


1F-23c METEOSAT. Enlarged View. Visible Picture 1155 GMT 22 June 1979

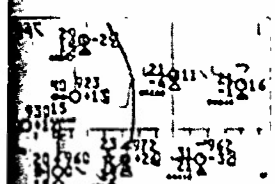


1F-23d METEOSAT Enlarged View Infrared Picture 1155 GMT 22 June 1979.

Duststorm over the Persian Gulf

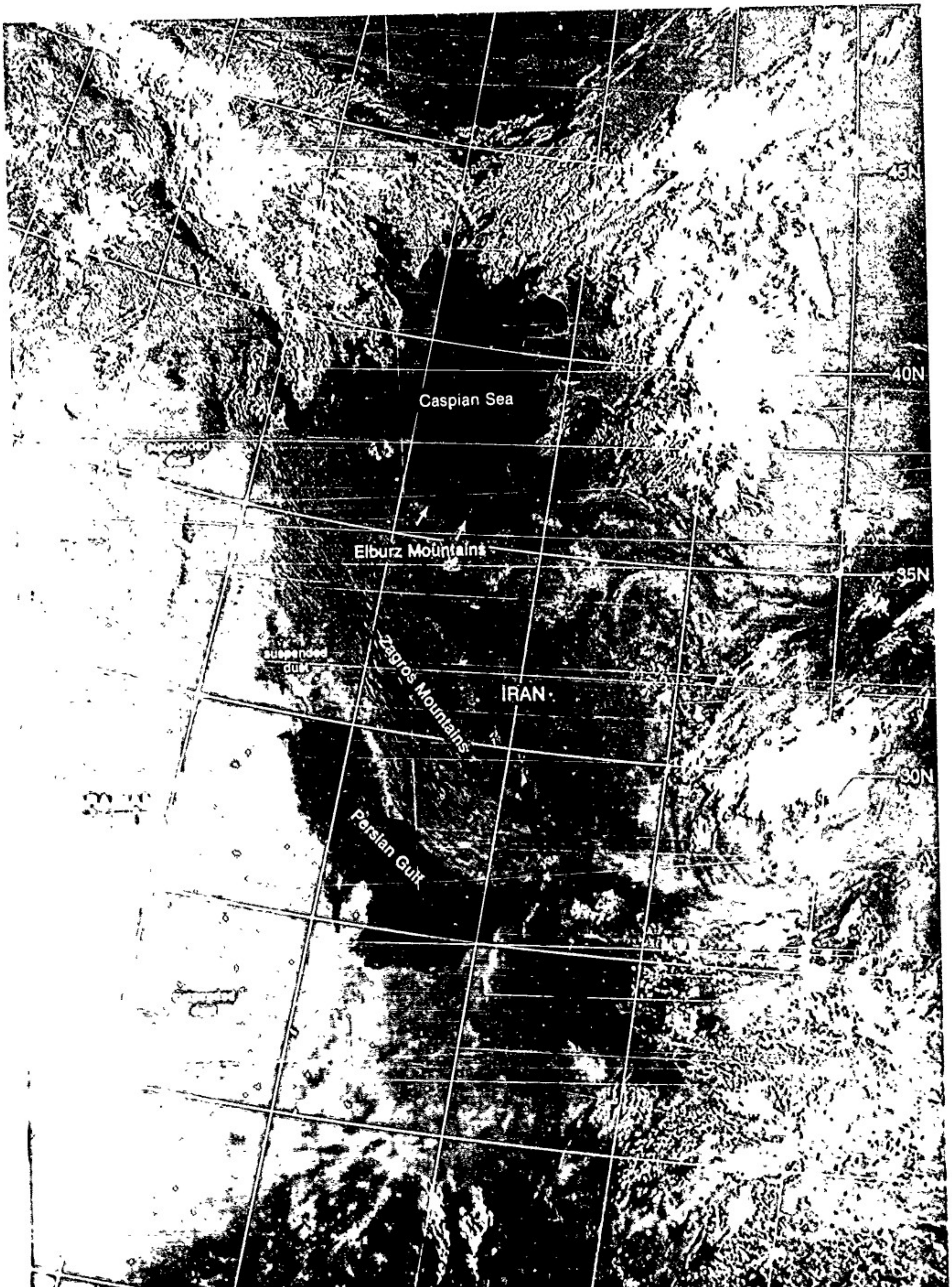


1E-25a. F-3. DMSP LF Low Enhancement 0231 GMT 23 June 1979

The FNOC 500-mb analysis for 0000 GMT (1E-26a), which is comparable to the NMC 500-mb analysis, shows the blocking high over northern Europe, the cutoff low **L1**, and the trough **T2** over northeast Africa. Note how clearly this analysis depicts the anticyclonic turning of the winds over the northern Red Sea which is producing northwesterly flow across the Persian Gulf region.

The FNOC 36-hr 500-mb prognosis (1E-27a), based on the initial 500-mb analysis (1E-26a), indicates that the blocking high will be maintained over northern Europe, the southern branch of the westerlies will persist across the eastern Mediterranean, and the anticyclone over the northern Red Sea will dominate the circulation over the Arabian Peninsula. With the persistence of the northwesterly flow over the Syrian Desert, increased amounts of raised dust can be expected to be transported to the south over the Arabian Peninsula and to the east over the Persian Gulf (duststorm already in progress at **O7**; see 1E-24c).

*23 June continued on page 1E-28*

**500 mb**

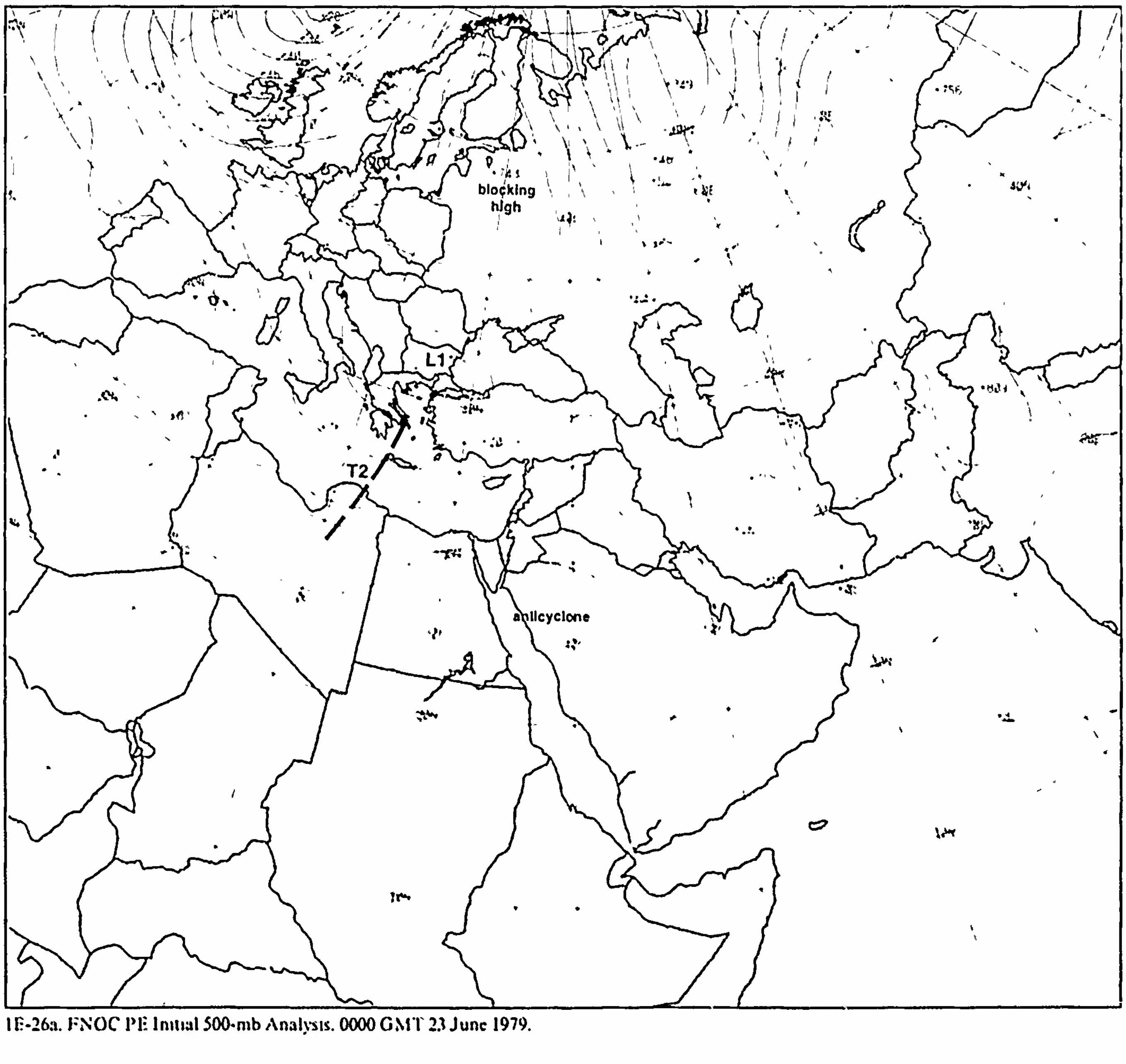


1E-26a. FNOC PE Initial 500-mb Analysis. 0000 GMT 23 June 1979.

500 mb

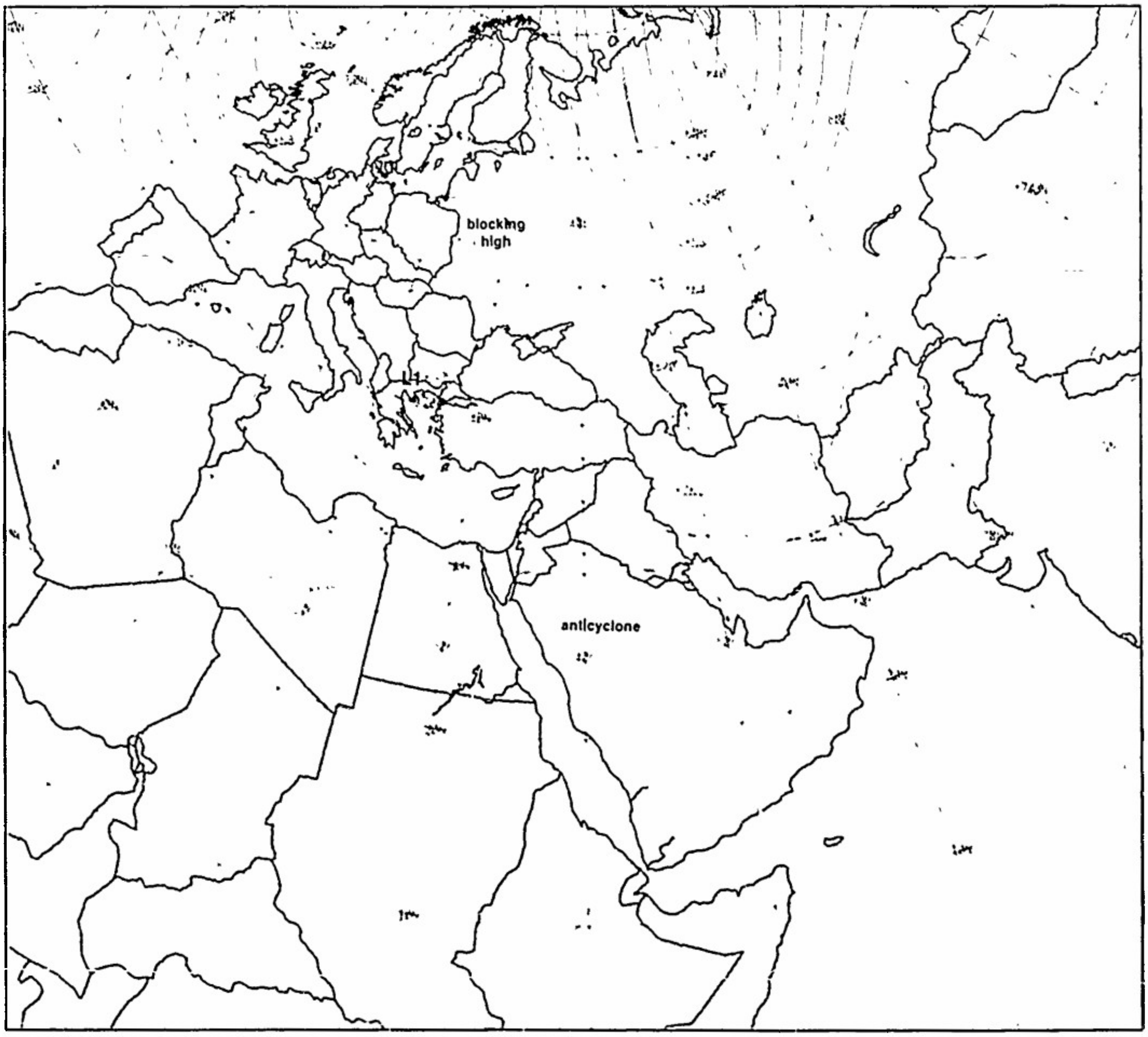


1E-27a. FNOC PE 36-hr 500-mb Prognosis. Valid 1200 GMT 24 June 1979.

At 200 mb (1E-28a), the wind speeds in the merged polar westerlies and subtropical jet over the eastern Mediterranean have increased to over 100 kt. A similar increase in wind speeds (85 kt) is observed at Beirut, Lebanon, at 500 mb (1E-28b). At 850 mb (1E-29a), strong (30 35 kt) winds extend from the eastern Mediterranean coastline to the central Persian Gulf. On the surface streamline analysis (1E-29b), reports of duststorms and suspended dust extend from the eastern Mediterranean to the central Persian Gulf—confirming that the dust suspended in strong upper-level winds has reached to the surface. Where skies were mostly clear in this region on the previous day (1E-24c), they are now obscured by dust.

At Toraybeel, Iraq (O9), in the Syrian Desert, a duststorm is in progress, wind is northwest at 35 kt. Further to the east, O2 is showing a northwest wind and a duststorm in progress. Suspended dust is reported over the Persian Gulf at O1 and at Dubai, United Arab Emirates (O10). The duststorm at O2 is reflecting the downward transport of the strong winds aloft and suggests that an intense Shamal is occurring over the Persian Gulf at this time. These intense Shamals are of short duration and can be expected to last for only about 3 days. Over the central Arabian Peninsula, a duststorm is reported at O6, and suspended dust is reported as far south as Salalah, Oman (O11).

The dust plumes over the Syrian Desert, first observed on the previous day (1E-23c) are very distinct on the METEOSAT visible imagery on this date (1E-29c). A careful comparison of the two views shows gray shade changes that suggest dust, first generated over the Syrian Desert, has now reached over the northern Persian Gulf and entered into the south-central Arabian Peninsula. Infrared imagery (1E-29d) fully confirms this situation. Note that temperatures are very cold over the Syrian Desert source region, and temperatures and dust amounts suggest no additional major source regions until the east-central Arabian Peninsula, where temperatures again appear colder and larger amounts of dust appear to be generated.

The DMSP visible picture at 0211 GMT (1E-30a) shows almost total obscuration of the Persian Gulf region by dust. A DMSP visible picture several hours later (1E-31a) shows that the dust covers the entire southern Arabian Peninsula and extends across the Red Sea into the Sudan.

An interesting phenomenon, that of gravity waves on the top of the dust layer, appears on the 0211 GMT picture (1E-32a), with a focal point near 30°N, 47.5°E. Basra, Iraq, located just to the northeast of the source of the gravity waves, reported $\frac{5}{16}$ mi visibility, with a duststorm in progress, at 0600 GMT (not shown), about 4 hours prior to the DMSP picture. The fact that the gravity waves have a focal point is very interesting since the terrain in the area is very flat and well removed from the mountains, so it is unlikely that the gravity waves are terrain induced.

The gravity wave generation point, however, is very near the center of a major oil field. The DMSP nighttime visible picture (1E-33a), obtained at a much later date, shows city lights and oil fires over the Persian Gulf region. A careful compariso[illegible]is picture and the DMSP visible picture (1E-[illegible])[illegible]ws that the Az Zubair oil fields are precisely a[illegible]al point of the gravity waves. The implicatio[illegible]e bouyant effect of hot air rising from the b[illegible] of natural gas over the oil field has induced gravity [illegible]es on the dust sweeping over the area. Gravity wave production implies that the heaviest concentration of dust is capped by an inversion. Such a concentration would likely occur at a lower, rather than higher, level. Unfortunately, probably due to the duststorm conditions, RAOB data were not available in the immediate area of the gravity waves. They were available further to the north, however, with Damascus, Syria, showing a very strong low-level inversion, with a top at about 2,500 ft MSL (station elevation 2,000 ft). Smaller dust particles undoubtedly extended well above this altitude.

The gravity waves in the DMSP picture (1E-32a) spread outward toward the southwest quadrant and in no other direction. This suggests a low-level wind from the northeast. A streamline superimposed on the 850-mb analysis (1E-32b) reveals northwesterly winds changing to northeasterly near the oil field area, which verifies the above hypothesis. The anticyclonic turning of the flow over the northern Arabian Peninsula additionally supports the concept of a stable layer (subsidence inversion) above the duststorm.

*continued on page 1E-34*

200 mb

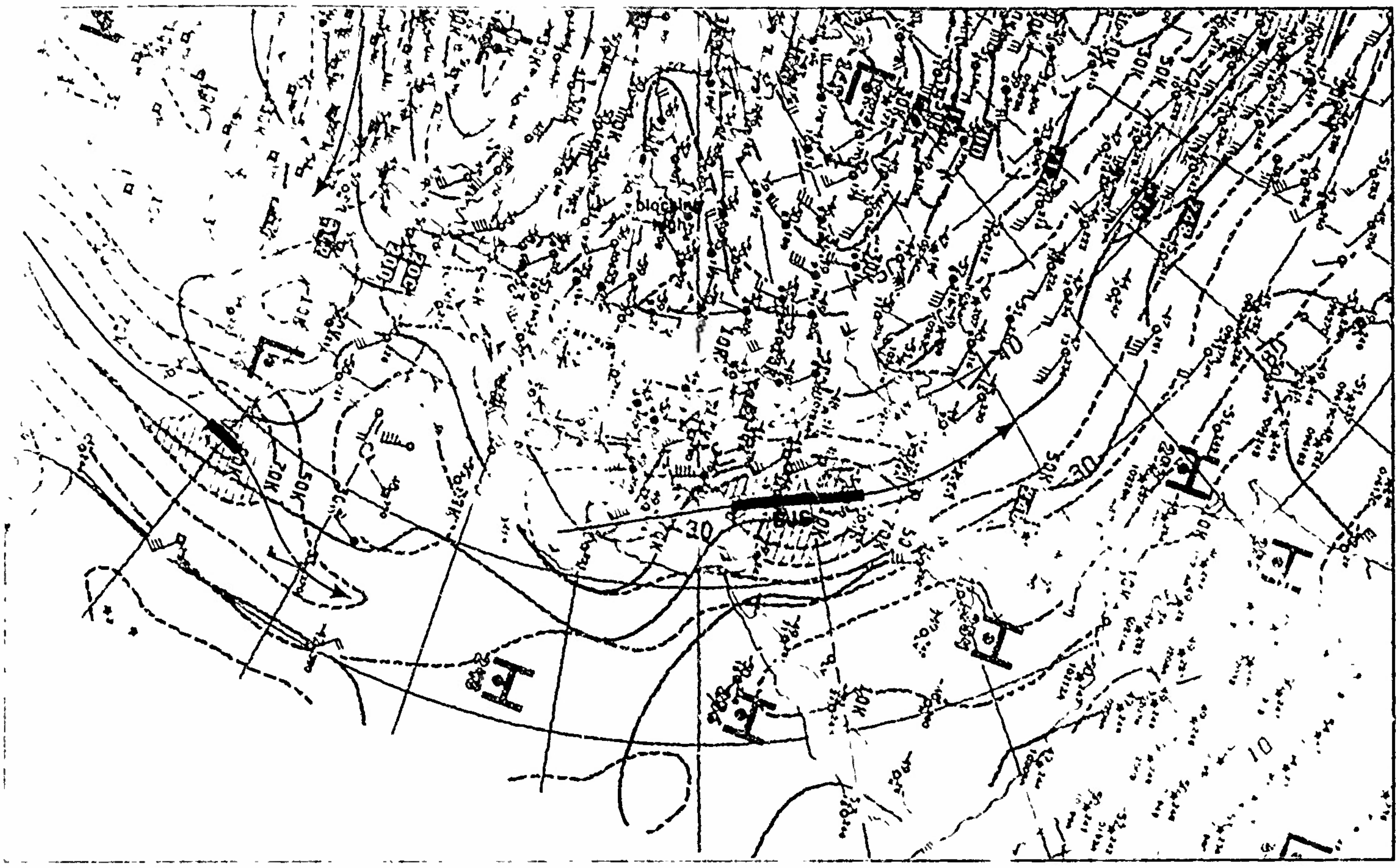


IE-28a NMC 200-mb Analysis 1200 GMT 23 June 1979

500 mb

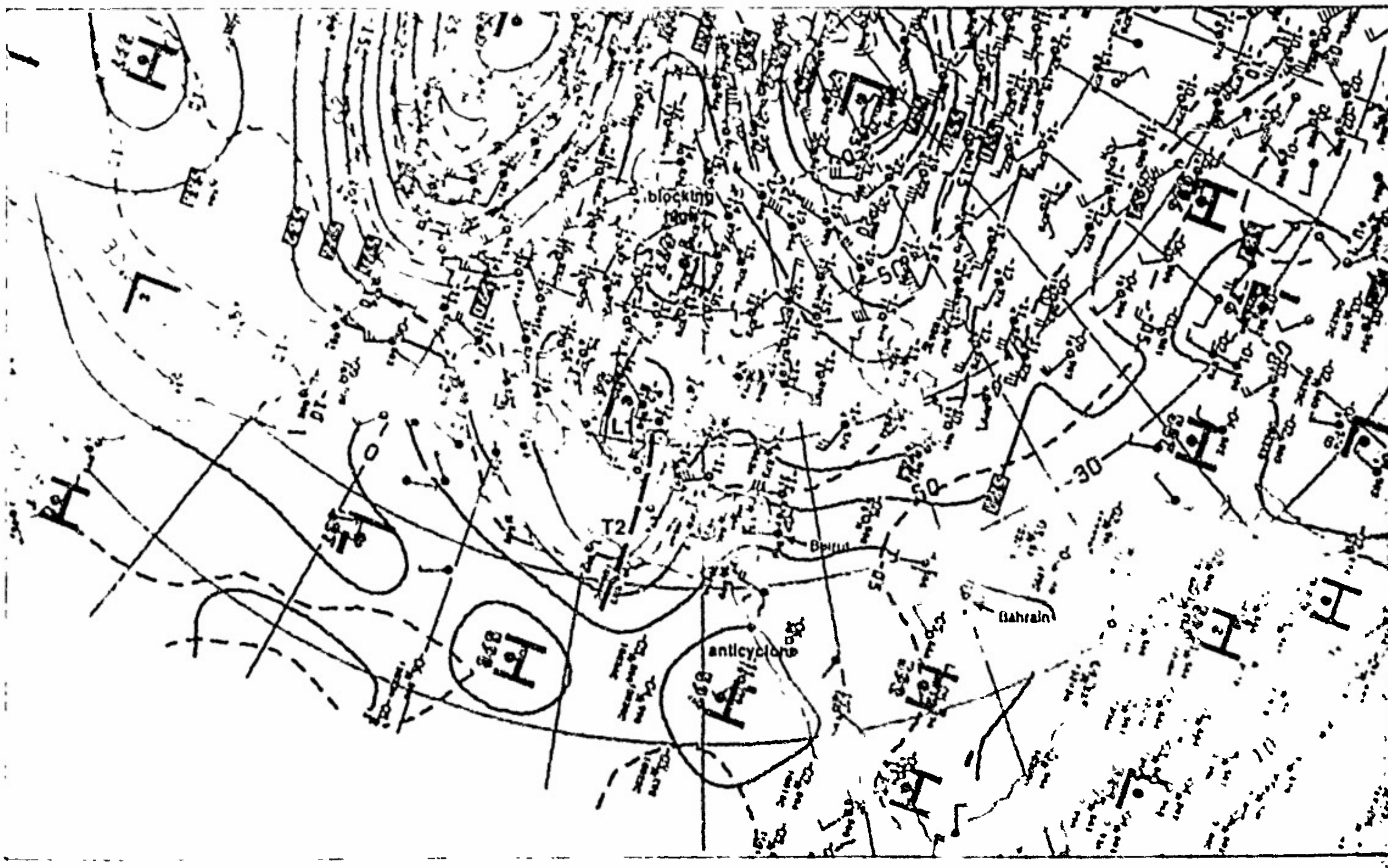


IE-28b NMC 500-mb Analysis 1200 GMT 23 June 1979

850 mb

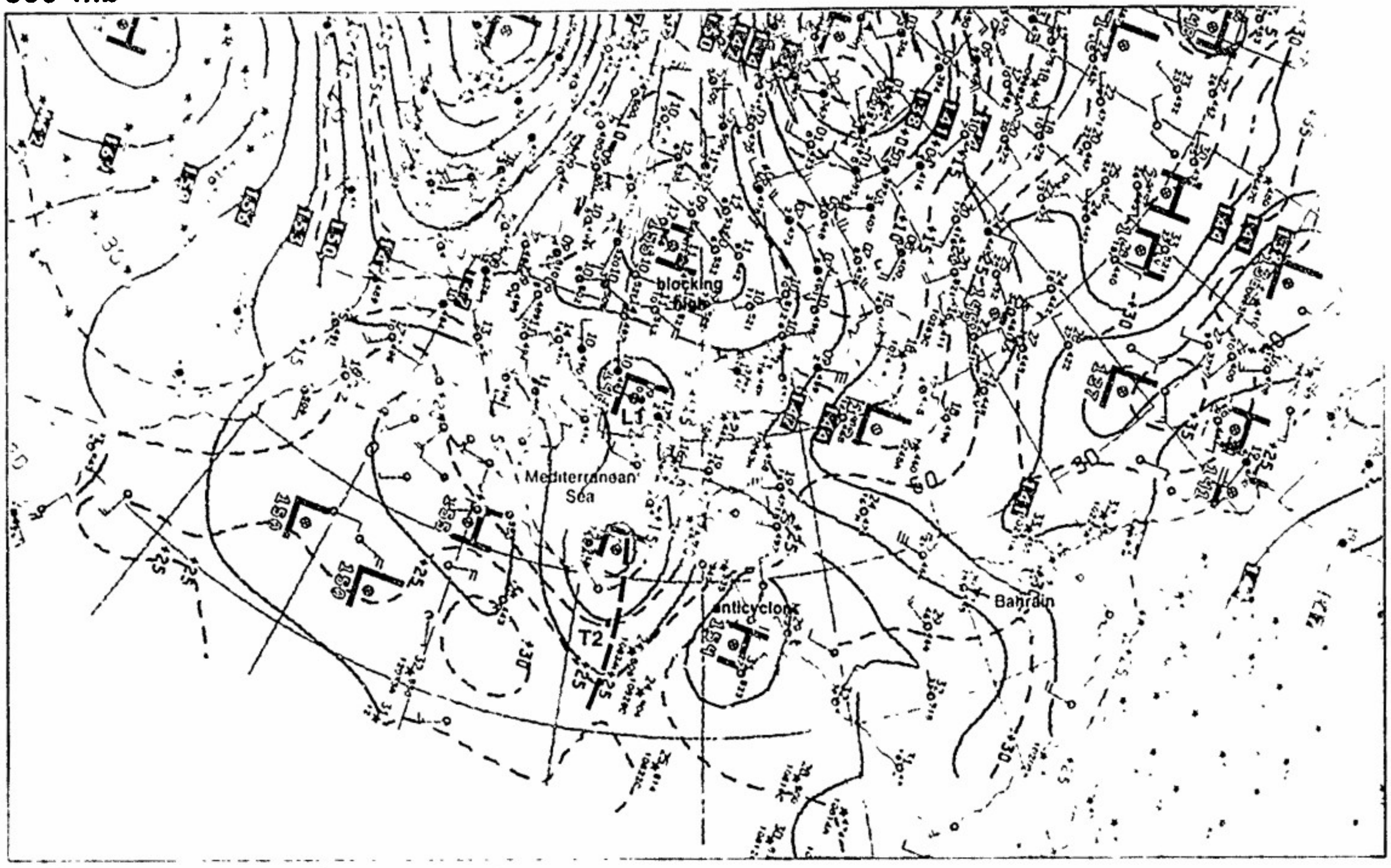


1E-29a. NMC 850-mb Analysis. 1200 GMT 23 June 1979.

surface

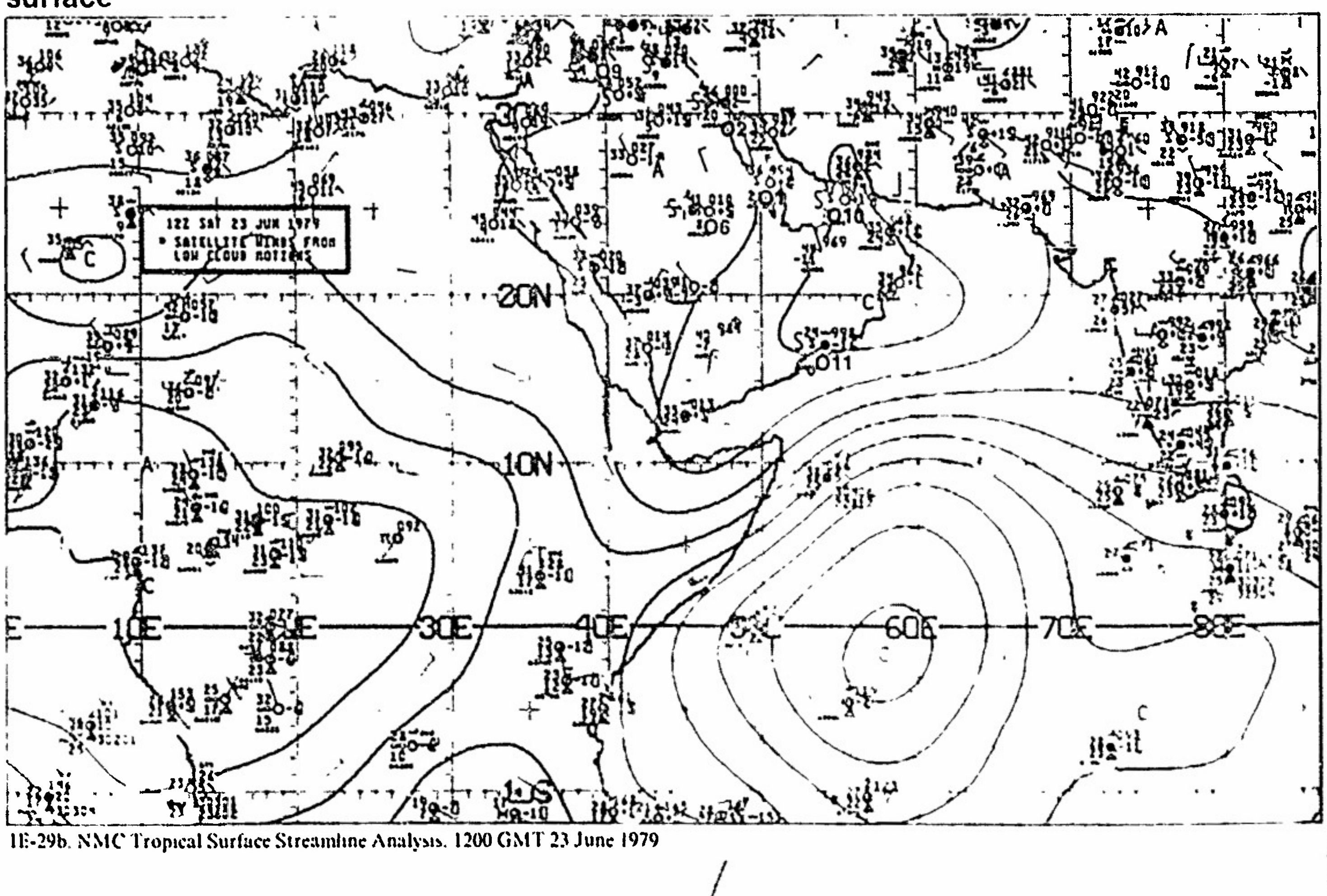


1E-29b. NMC Tropical Surface Streamline Analysis. 1200 GMT 23 June 1979


1E-29c METEOSAT, Enlarged View Visible Picture, 1155 GMT 23 June 1979

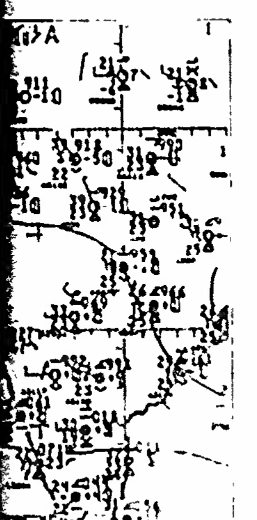


1E-29d METEOSAT Enlarged View Infrared Picture, 1155 GMT 23 June 1979.

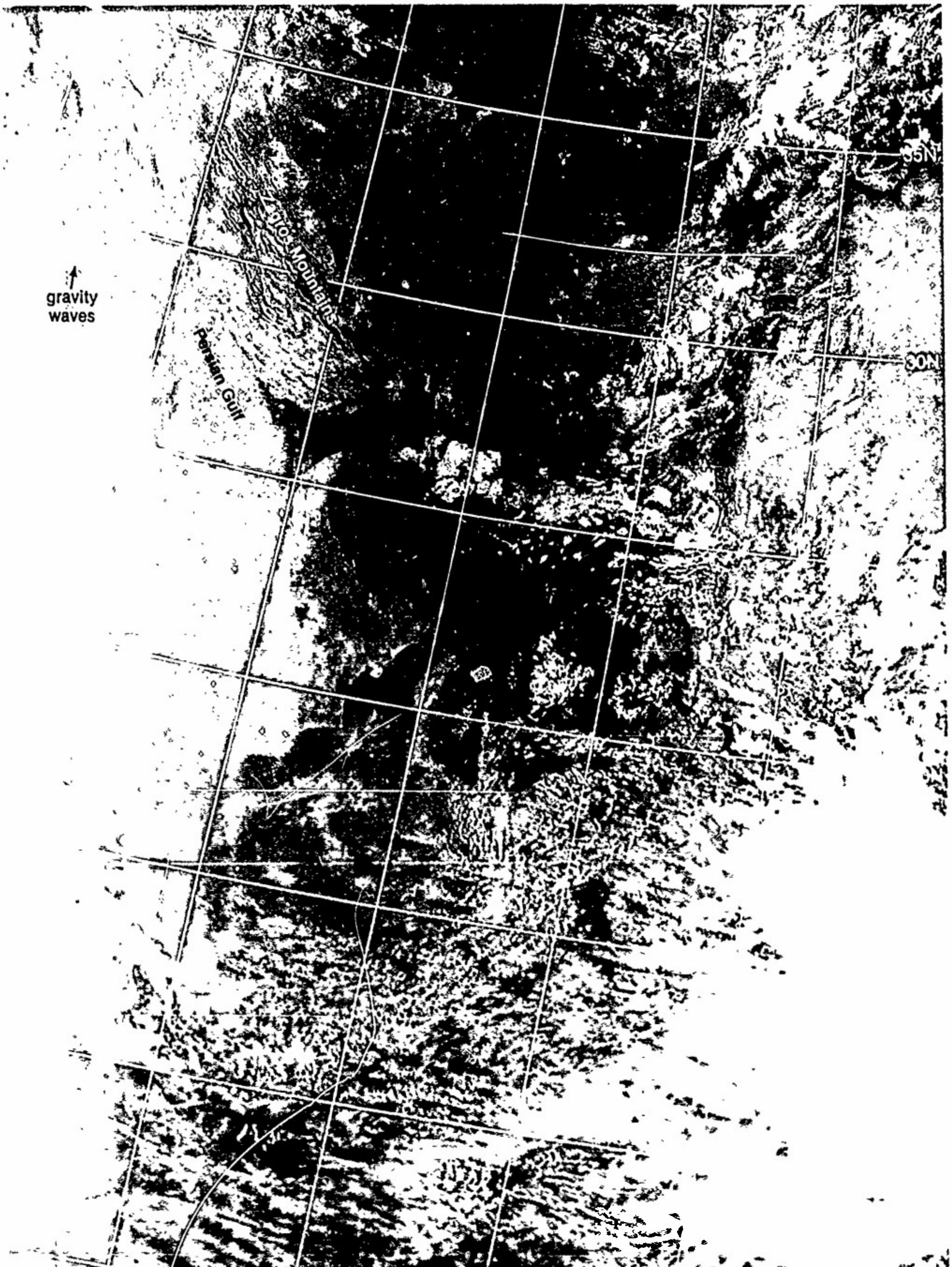


1E-30a. F-3 DMSP LF Low Enhancement 0211 GMT 24 June 1979


1E-31a F-3 DMSP FF Low Enhancement 0352 GMT 24 June 1979

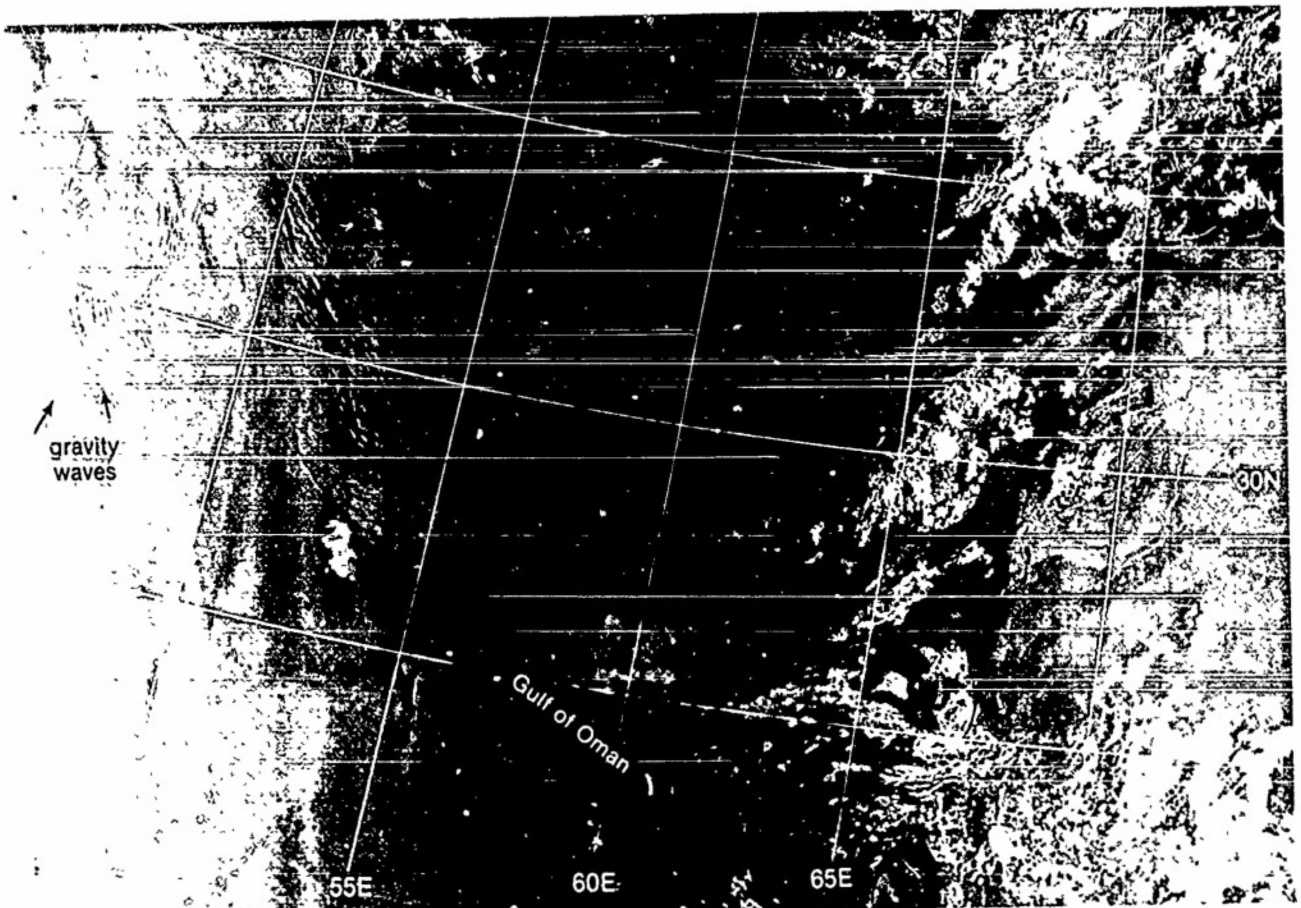


1E-32a F-3, DMSP LF Low Enhancement 0211 GMT 24 June 1979. (Note this picture is a sector of 1E-30a.)

850 mb

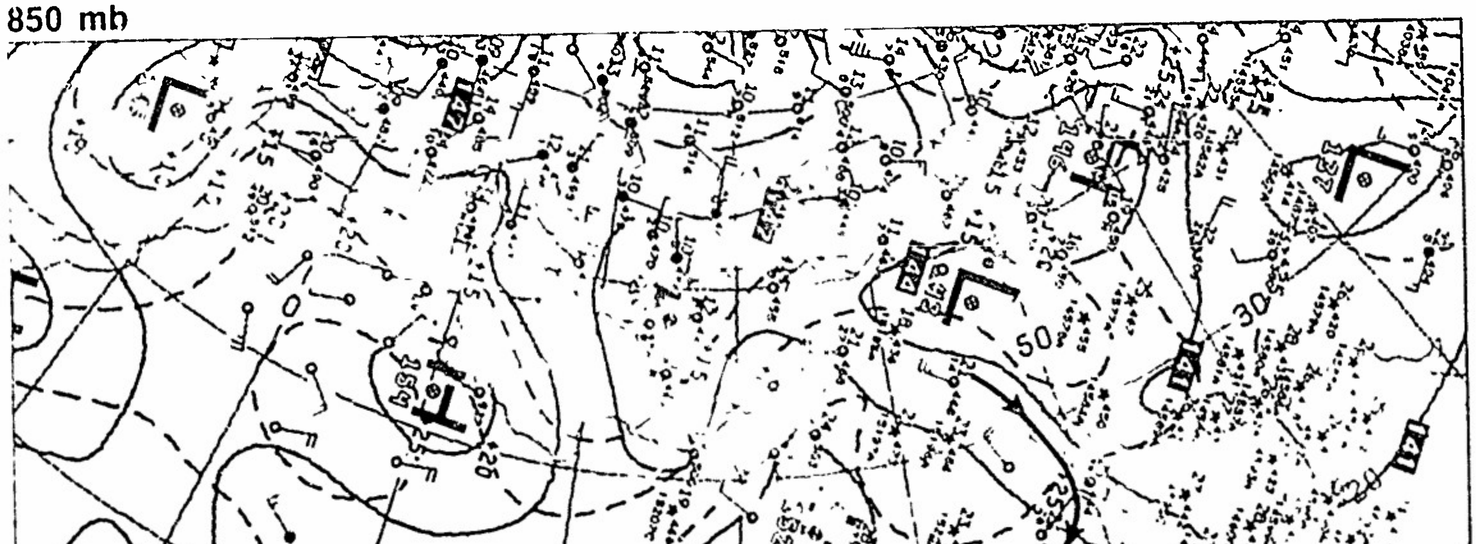

1E-32b NMC 850-mb Analysis 0000 GMT 24 June 1979

Duststorm over the Persian Gulf

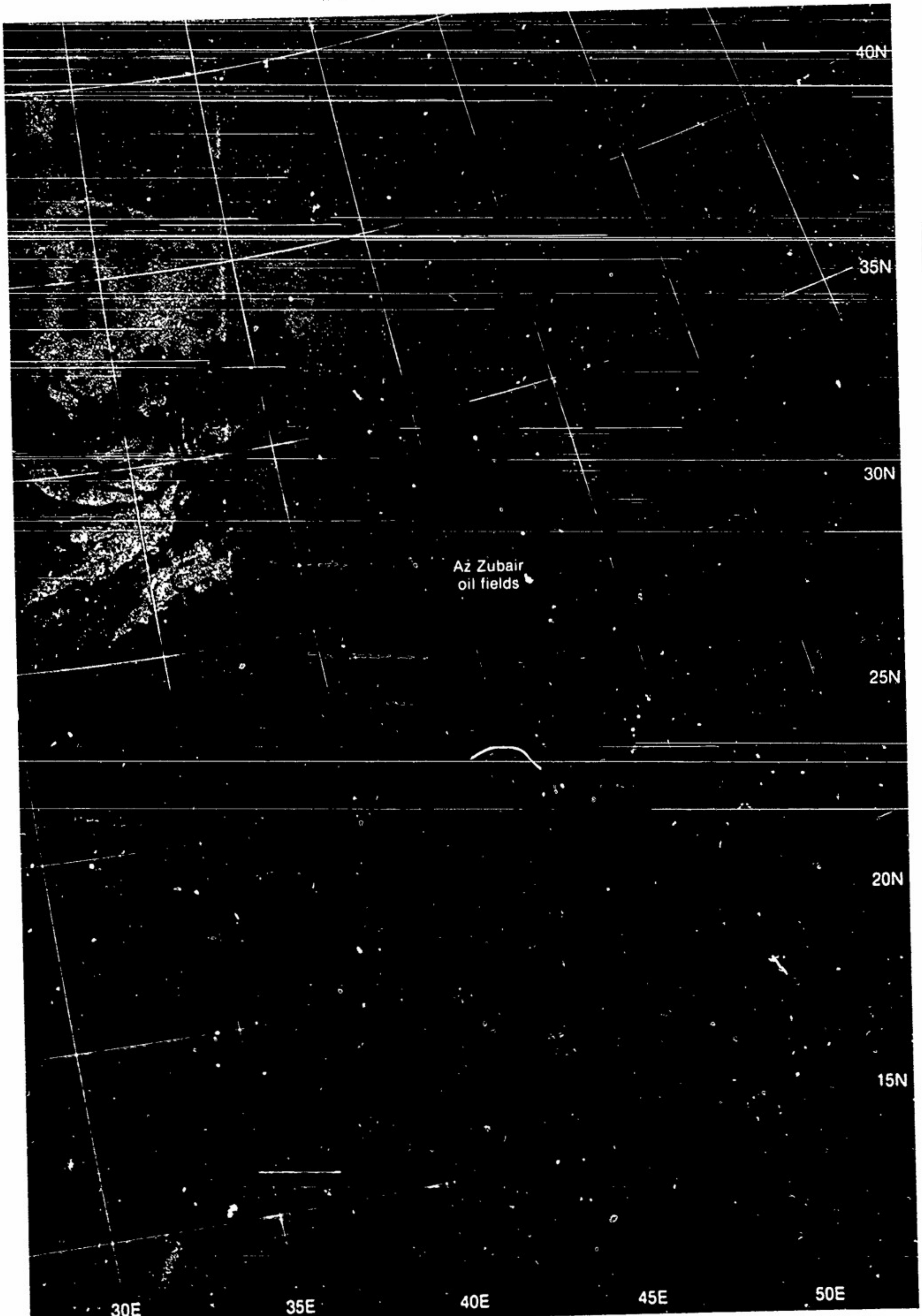


1E-33a. F-2 DMSP LS Low Enhancement. 1806 GMT 23 January 1980.

**24 June**

The METEOSAT visible picture at 1155 GMT (1E-35c) shows gray shades over the Persian Gulf and Red Sea regions associated with the duststorms. A comparison of the land area with the previous dust-free view (1E-21a) shows a degradation of contrast implying dust over portions of the land areas of Iraq, Iran, and the Arabian Peninsula. The METEOSAT infrared picture (1E-35d) is most useful at this time to delineate the areas of dust contamination. The picture reveals that the Persian Gulf is entirely obscured by dust, that dust is very heavy over the central and southern Arabian Peninsula, and that dust appears as far west as the Sudan. Perhaps more important for the area further east, dust continues to persist over the source region just southeast of the Caspian Sea, over northern Iraq and Iran. It is also apparent that the Syrian Desert east of Lebanon has ceased being a dust source, as no evidence of dust-associated cold temperatures appears evident. This suggests that the wind speed maximum has passed the area and that lighter winds now prevail over Lebanon and the Syrian Desert.

The surface streamline analysis at 1200 GMT (1E-35b) reveals widespread reports of dust in suspension over the Arabian Peninsula. Note that a duststorm is reported in progress at O6, where sustained northwest winds of 25 kt are reported. The 850-mb analysis (1E-35a) verifies that winds have diminished in speed over Lebanon and the Syrian Desert, and that they have increased somewhat over the Persian Gulf and the central Arabian Peninsula, where dust is reported being generated. The 500-mb analysis (1E-34b) shows the blocking high at mid latitudes persisting along longitude 20°E. A comparison of this analysis with the FNOC 36-hour prognosis, valid at 1200 GMT (1E-34b), shows excellent correspondence. The trough over northern Africa and the anticyclone over the northern Arabian Peninsula, following the trough over Iran, also appear precisely as forecast.

The 200-mb analysis (1E-34a) continues to show the split flow of the block and the strong jet force winds crossing the eastern Mediterranean coastline. The high-pressure cell over the Arabian Peninsula, however, has moved eastward, diverting these strong winds aloft and out of the Persian Gulf region. The block over northern Europe has also progressed eastward from near 10°E on 22 June at 1200 GMT (1E-22a), to near 30°E on this analysis. The changing upper-air pattern signals the beginning of changes in the lower atmosphere that will gradually end the duststorm phenomenon and the intense Shamal occurring over the Persian Gulf.

**25–30 June**

The METEOSAT infrared pictures for 25 June (1E-36b), 26 June (1E-37b), and 27 June (1E-37d) show heavy dust over the central Arabian Peninsula for the first two days, but none or little over that area on 27 June as the intense 3-day Shamal ended. The DMSP visible picture (1E-38a) of the central Arabian Peninsula under duststorm conditions on 25 June, as opposed to the relatively dust-free conditions on 30 June (1E-39a) demonstrate the masking effect of dust in obscuring underlying terrain features. Note in particular that the original dust source region of Syrian Desert and northern Iraq and Iran is relati... clear of dust in both figures. In the central ... northern Arabian Peninsula, however, dust obsc... terrain features (see especially the dark terrain feat... near 17°N, 48°E on 25 June, while this area app... much sharper in contrast on 30 June, under clear conditions).

The 500-mb analysis at 1200 GMT (1E-39b) shows a significant change in pattern associated with the cutoff of Shamal conditions in the Persian Gulf and the associated dust phenomenon. The block, originally established near 20°E, has moved eastward as has the anticyclone over the northern Arabian Peninsula. As a result, strong anticyclonically-turning flow no longer extends from Lebanon into the Persian Gulf, which is now "capped" by a high-pressure cell containing very weak winds (see also surface streamline analysis 1E-39c). Should the combination of the mid-latitude block and the high-pressure cell over the northern Arabian Peninsula retrogress westward, the potential for a renewed, intense Shamal with dust would again exist.

**Important Conclusions**

1. The presence of a block over northern Europe, near longitudes 20°–30°E, characterized by split flow producing a zonal branch under the block is a pattern favorable for producing the strong persistent winds associated with intense Shamal conditions.

2. The triggering effect for the storms involves an optimum position of strong zonal flow over the eastern Mediterranean, turning anticyclonically around a high-pressure cell over the northern Arabian Peninsula.

3. A cutoff of Shamal conditions and associated duststorm phenomena can be anticipated on breakdown of the block and/or movement of the high-pressure cell over the northern Arabian Peninsula in a position to shield the area from strong northerly flow.

4. Satellite infrared data, during mid-afternoon hours, are a primary tool in evaluating the presence and extent of dust, and in determining the most probable source region.

200 mb

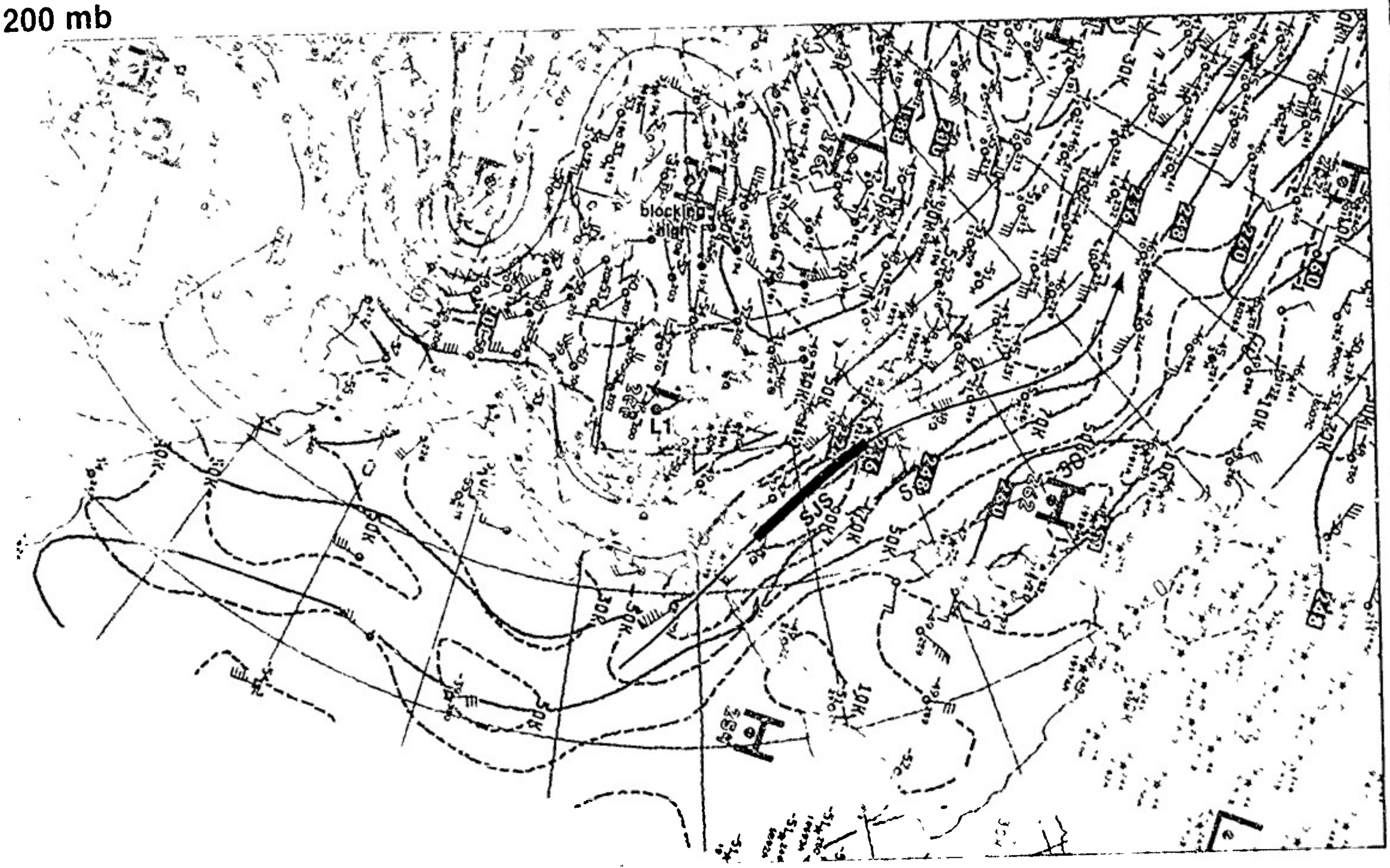


IF-34a. NMC 200-mb Analysis. 1200 GMT 24 June 1979

500 mb

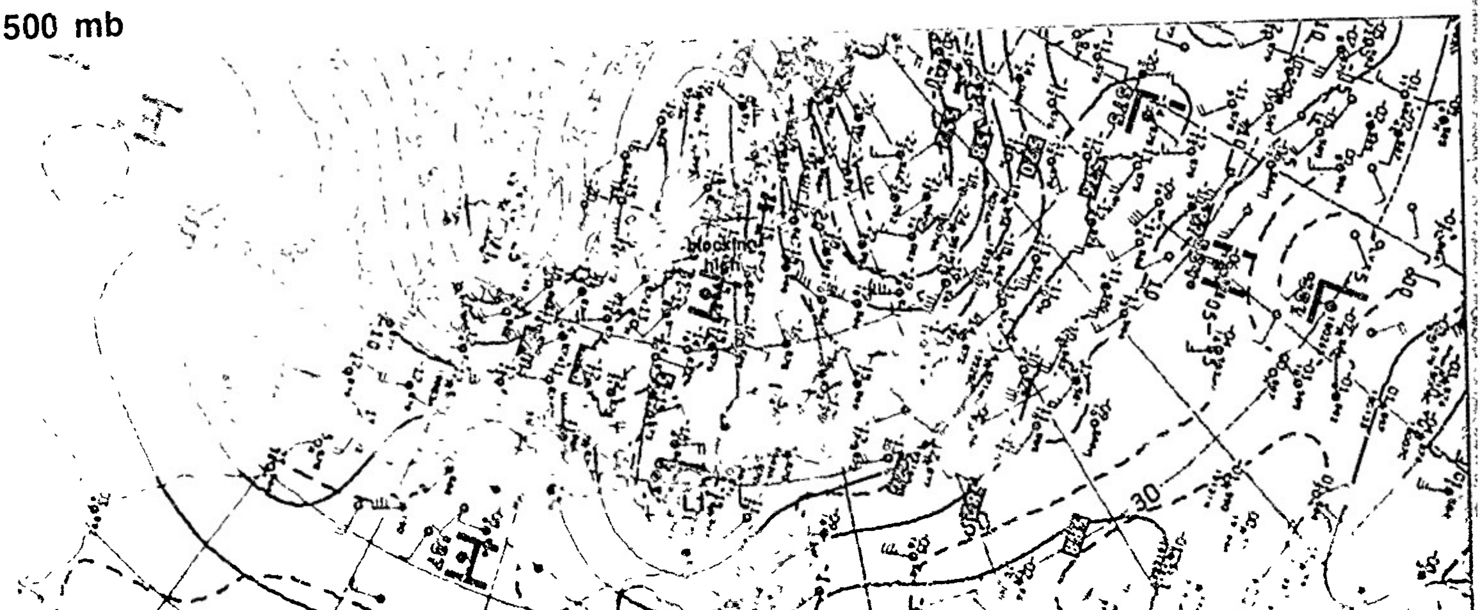


IF-34b. NMC 500-mb Analysis. 1200 GMT 24 June 1979

## 850 mb

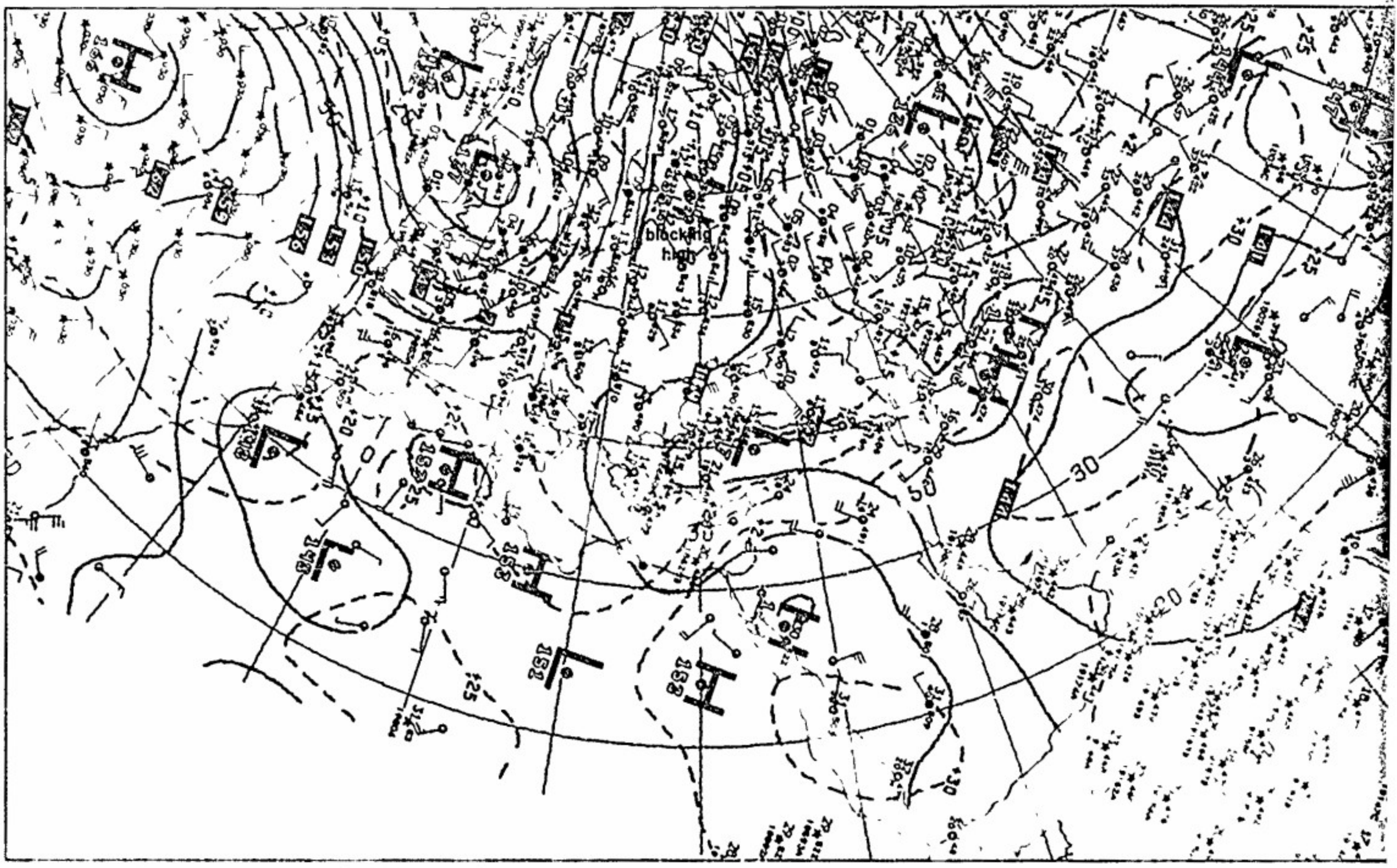


1E-35a. NMC 850-mb Analysis. 1200 GMT 24 June 1979

## surface

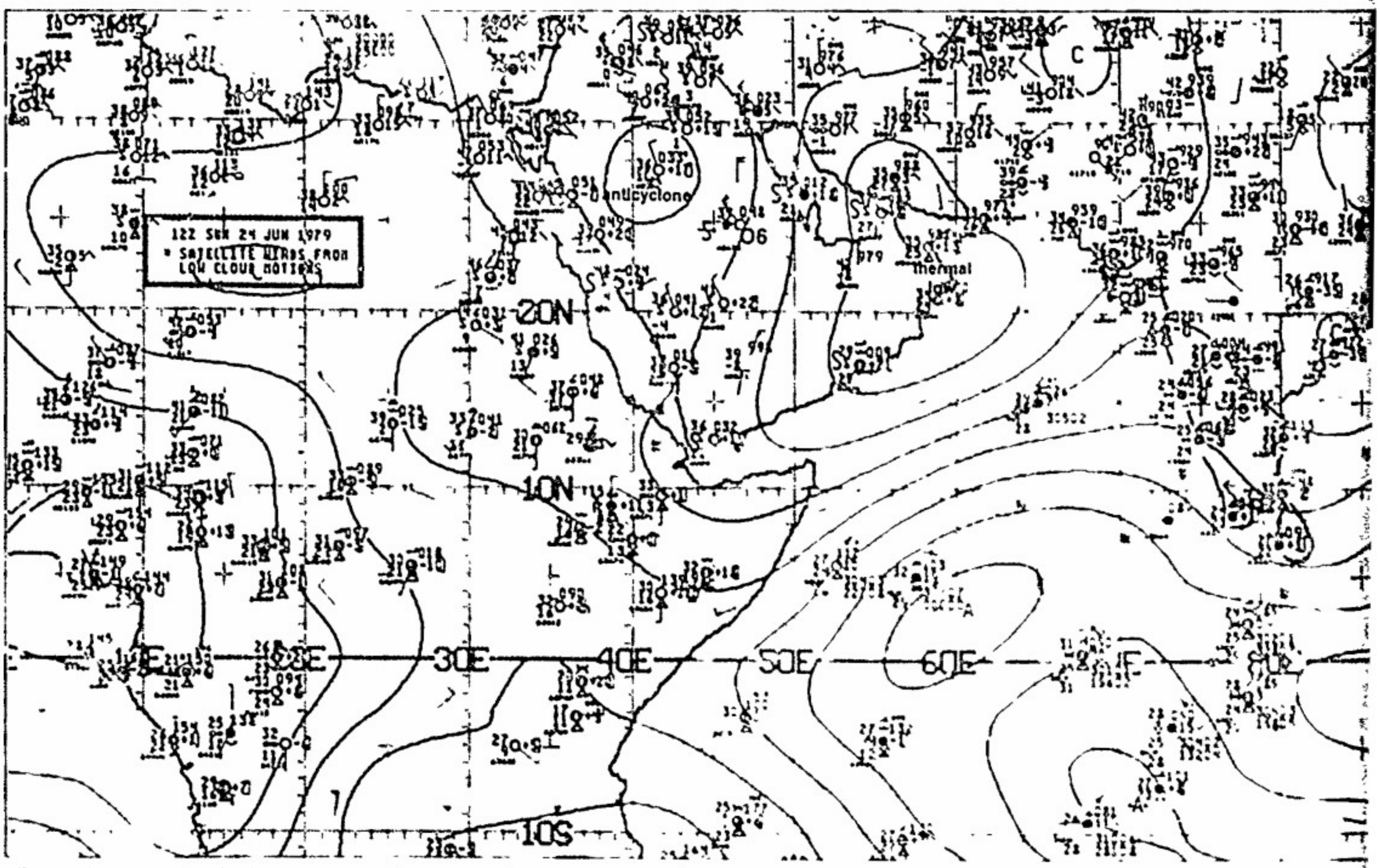


1E-35b. NMC Tropical Surface Streamline Analysis 1200 GMT 24 June 1979


1E-35c METEOSAT Enlarged View Visible Picture. 1155 GMT 24 June 1979

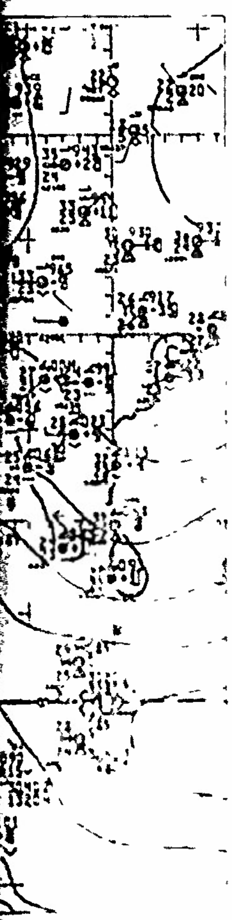

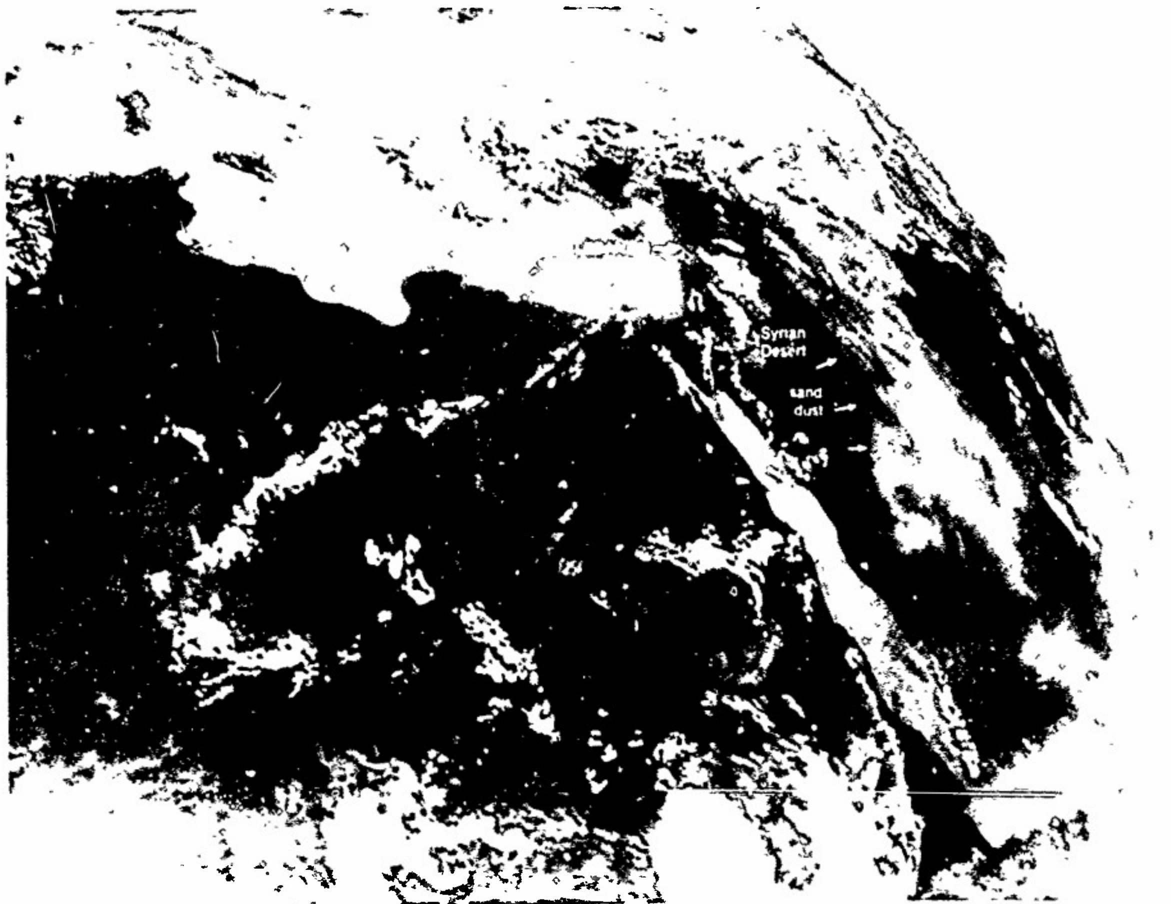


1E-35d METEOSAT Enlarged View Infrared Picture. 1155 GMT 24 June 1979.

1E-36a. METEOSAT. Enlarged View. Visible Picture. 1155 GMT 25 June 1979.

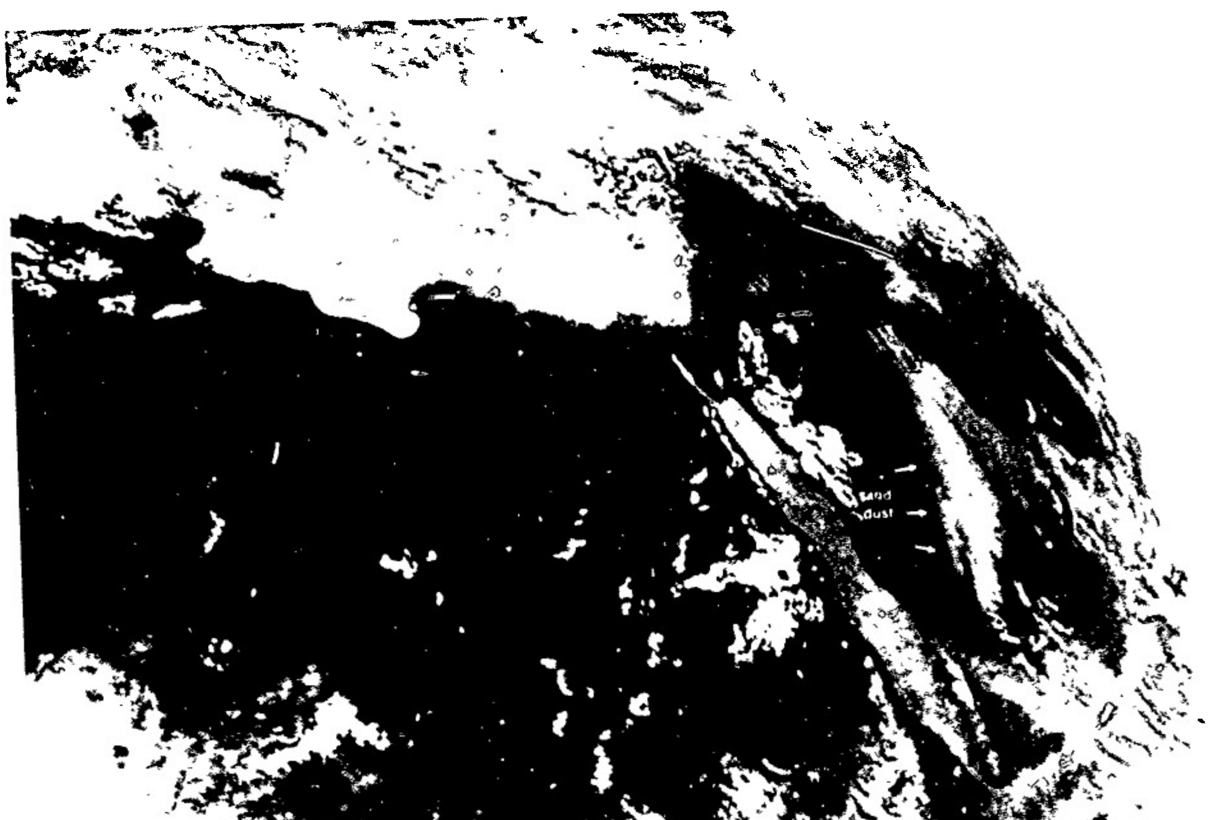


1E-36b. METEOSAT Enlarged View Infrared Picture 1155 GMT 25 June 1979.

*Duststorm over the Persian Gulf*

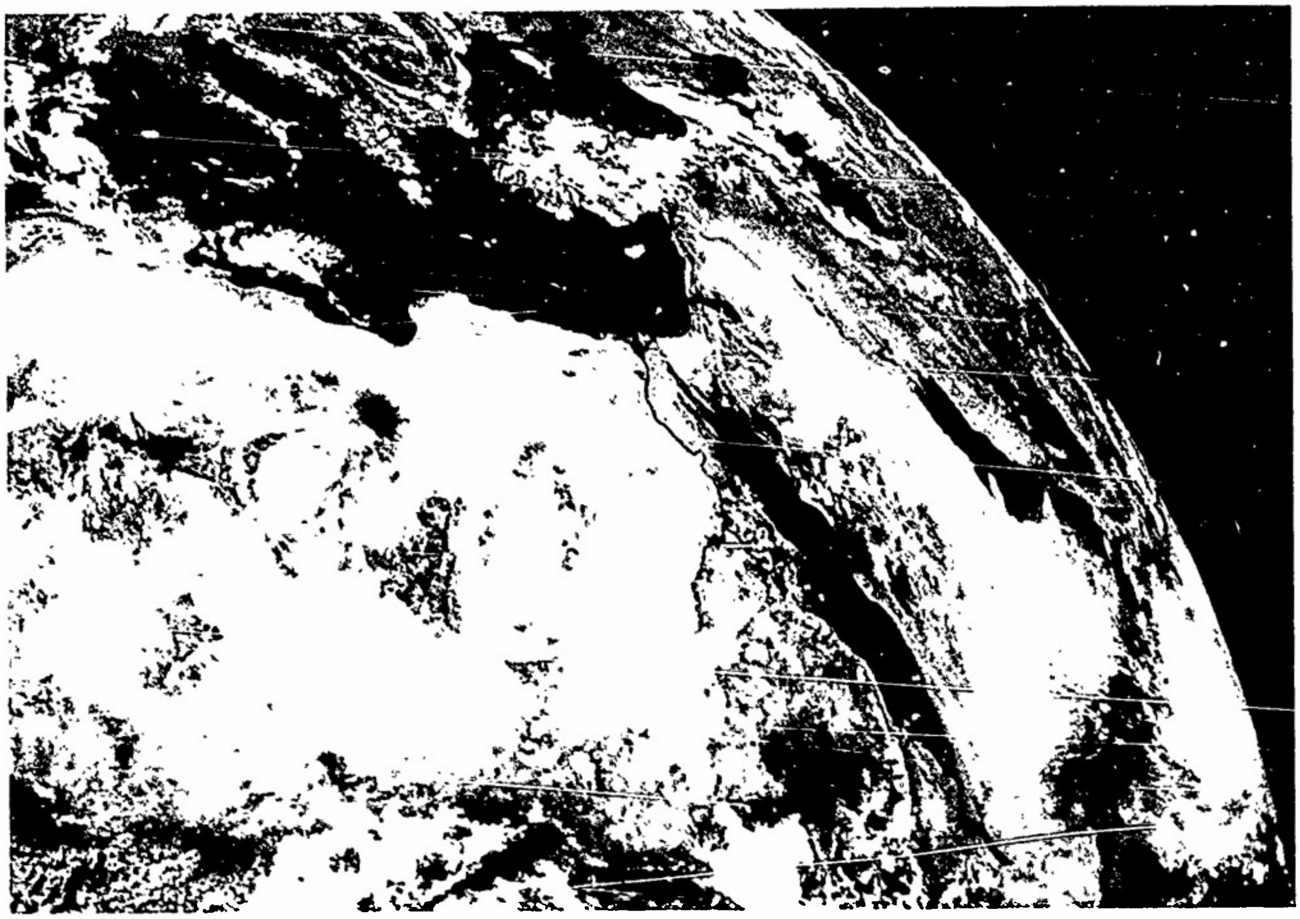

1E-37a. METEOSAT. Enlarged View Visible Picture 1155 GMT 26 June 1979.


1E-37b METEOSAT Enlarged View Infrared Picture 1155 GMT 26 June 1979

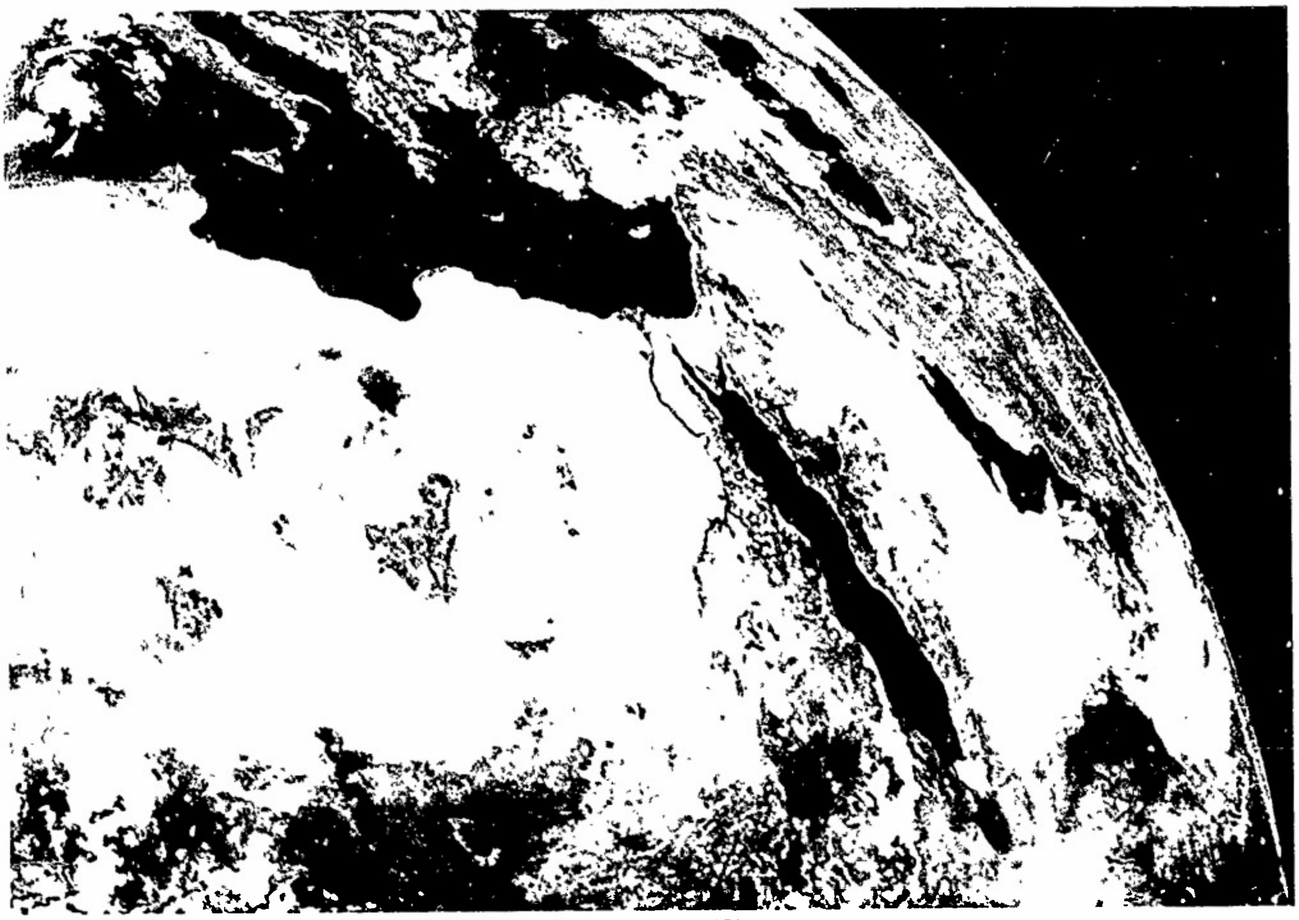

IE-37c METEOSAT Enlarged View Visible Picture, 1155 GMT 27 June 1979

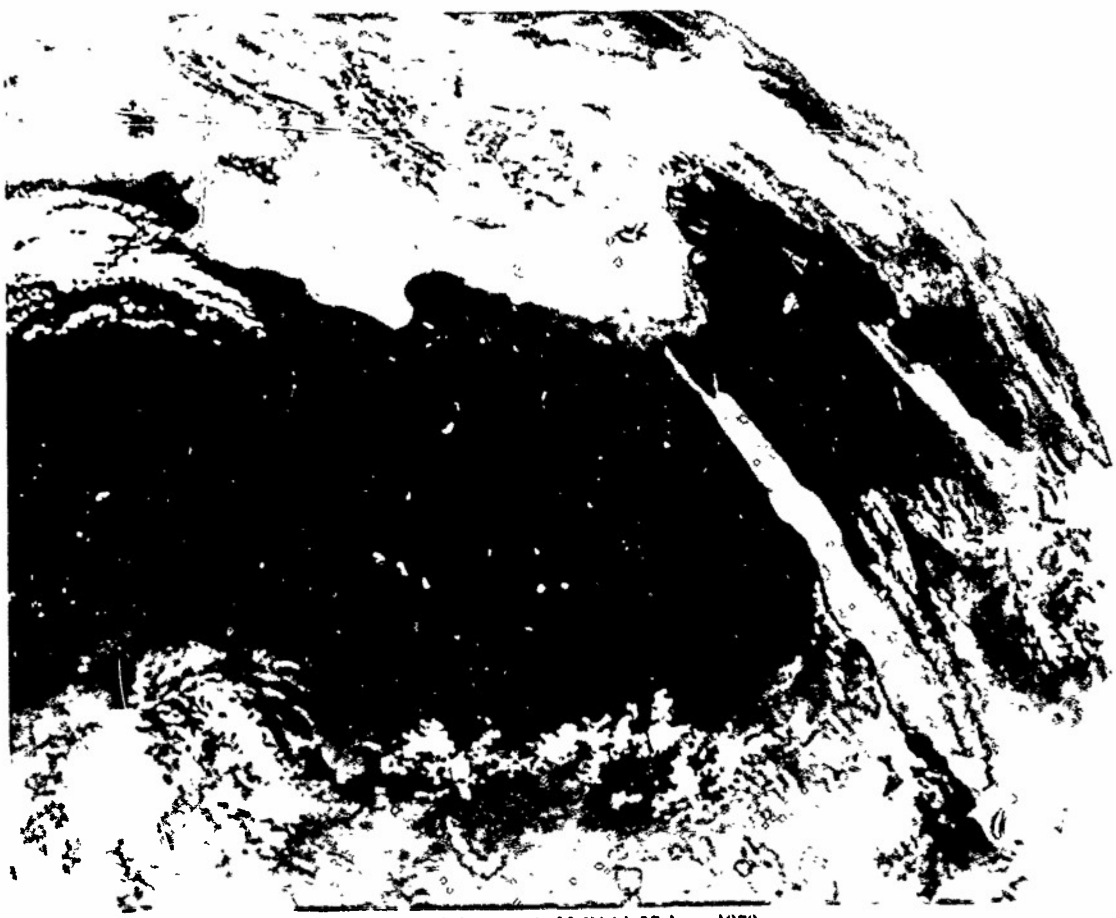

IE-37d METEOSAT Enlarged View Infrared Picture 1155 GMT 27 June 1979

1E-38a. F-1 DMSP LS Low Enhancement 0741 GMT 25 June 1979.

Duststorm over the Persian Gulf

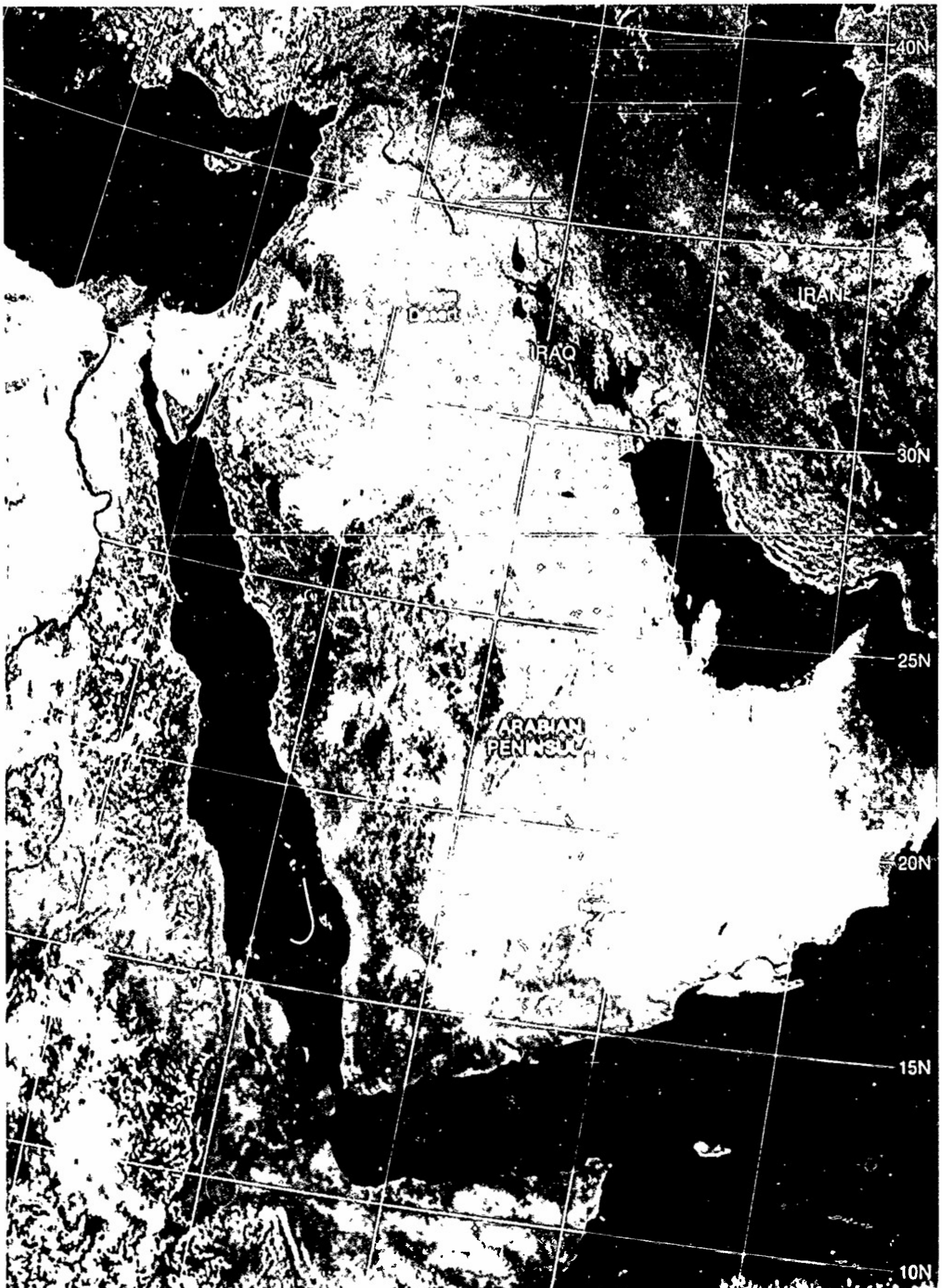


1E-39a. F-1, DMSP LS Low Enhancement 0750 GMT 30 June 1979

Gulf
se 3


50( b

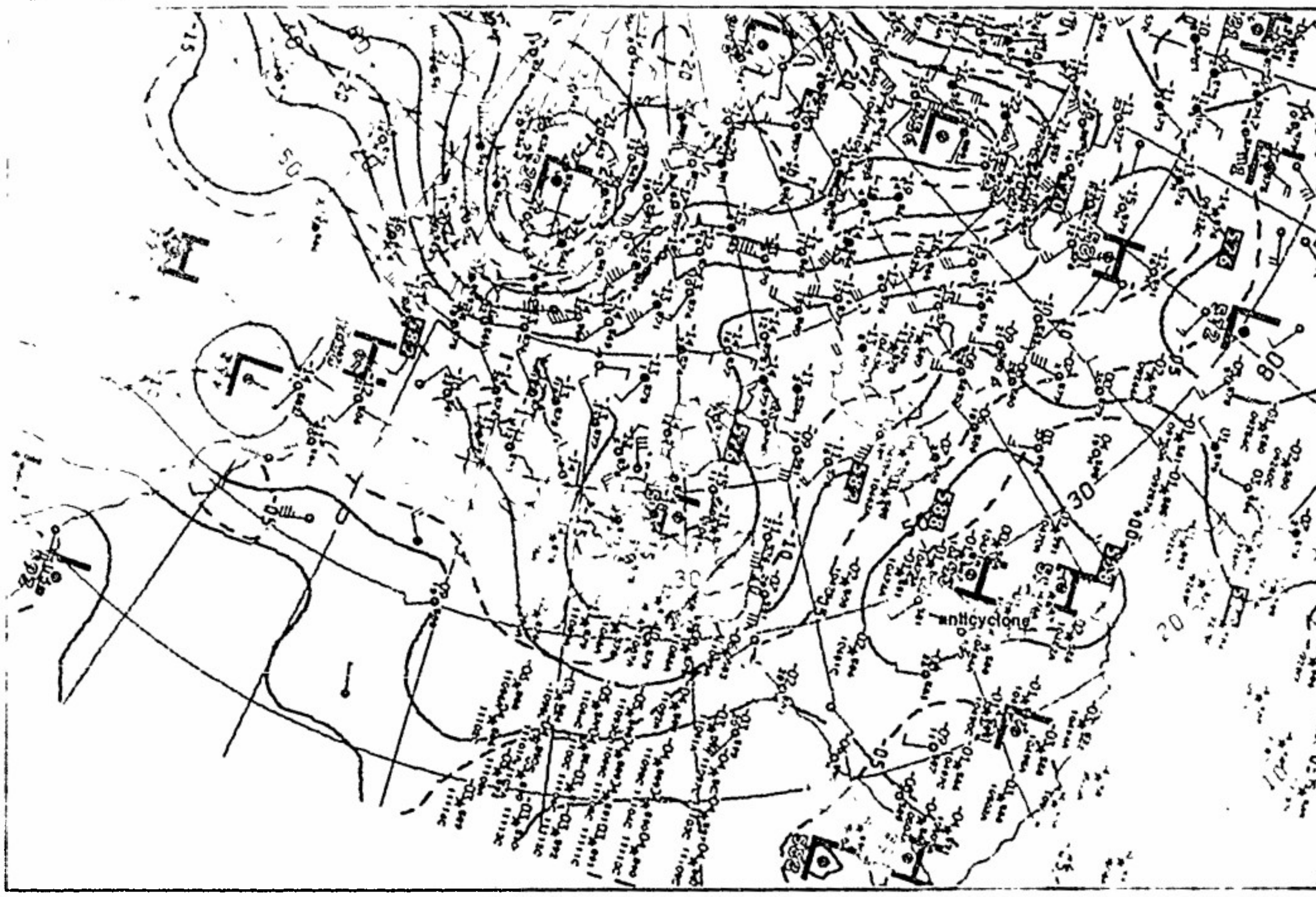


1E-39b NMC 500-mb Analysis. 0000 GMT 30 June 1979.

surface

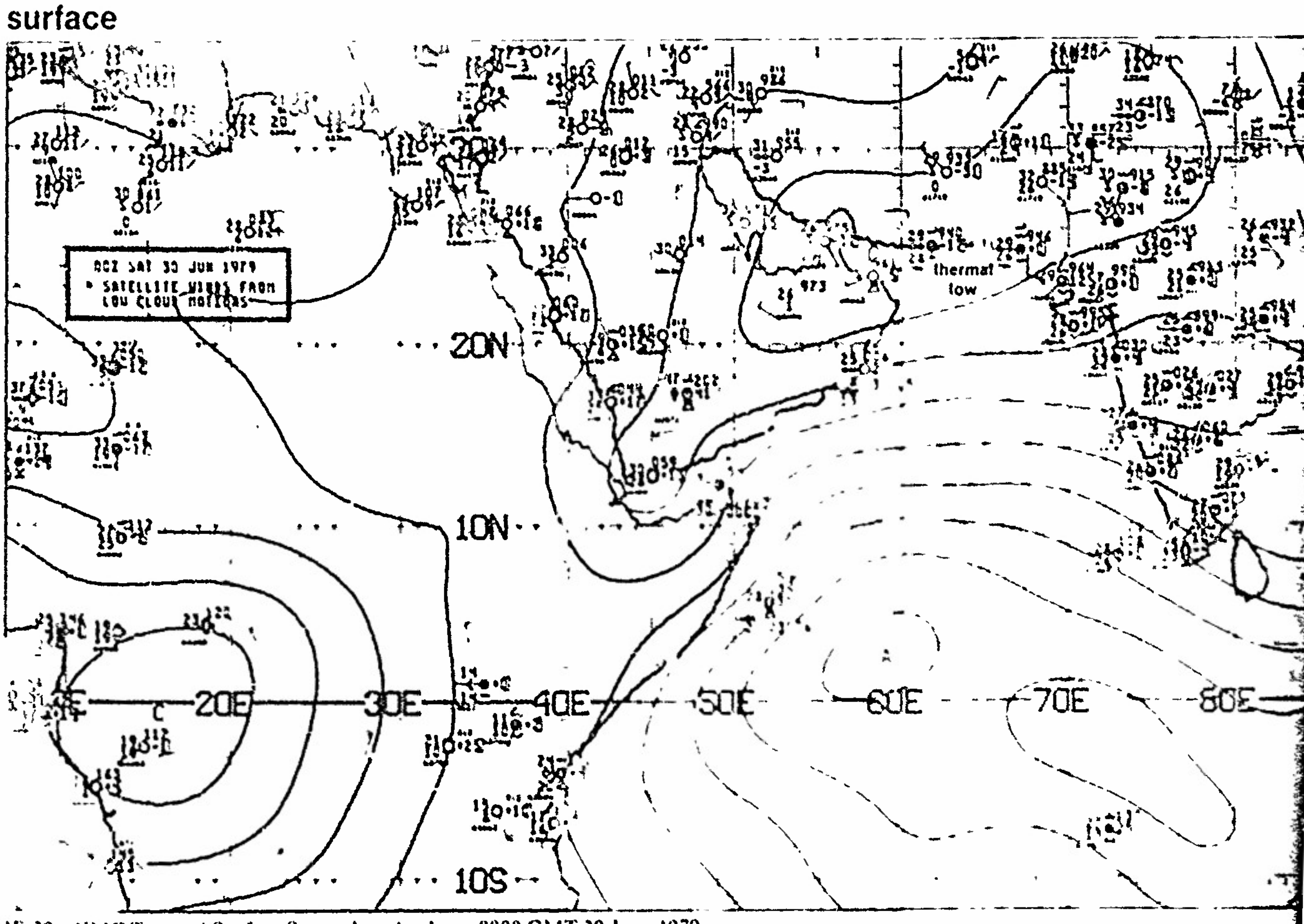


1E-39c NMC Tropical Surface Streamline Analysis. 0000 GMT 30 June 1979